CONVENTION ON LONG-RANGE TRANSBOUNDARY AIR POLLUTION
of the United Nations Economic Commission for Europe

CALCULATION AND MAPPING OF CRITICAL THRESHOLDS IN EUROPE

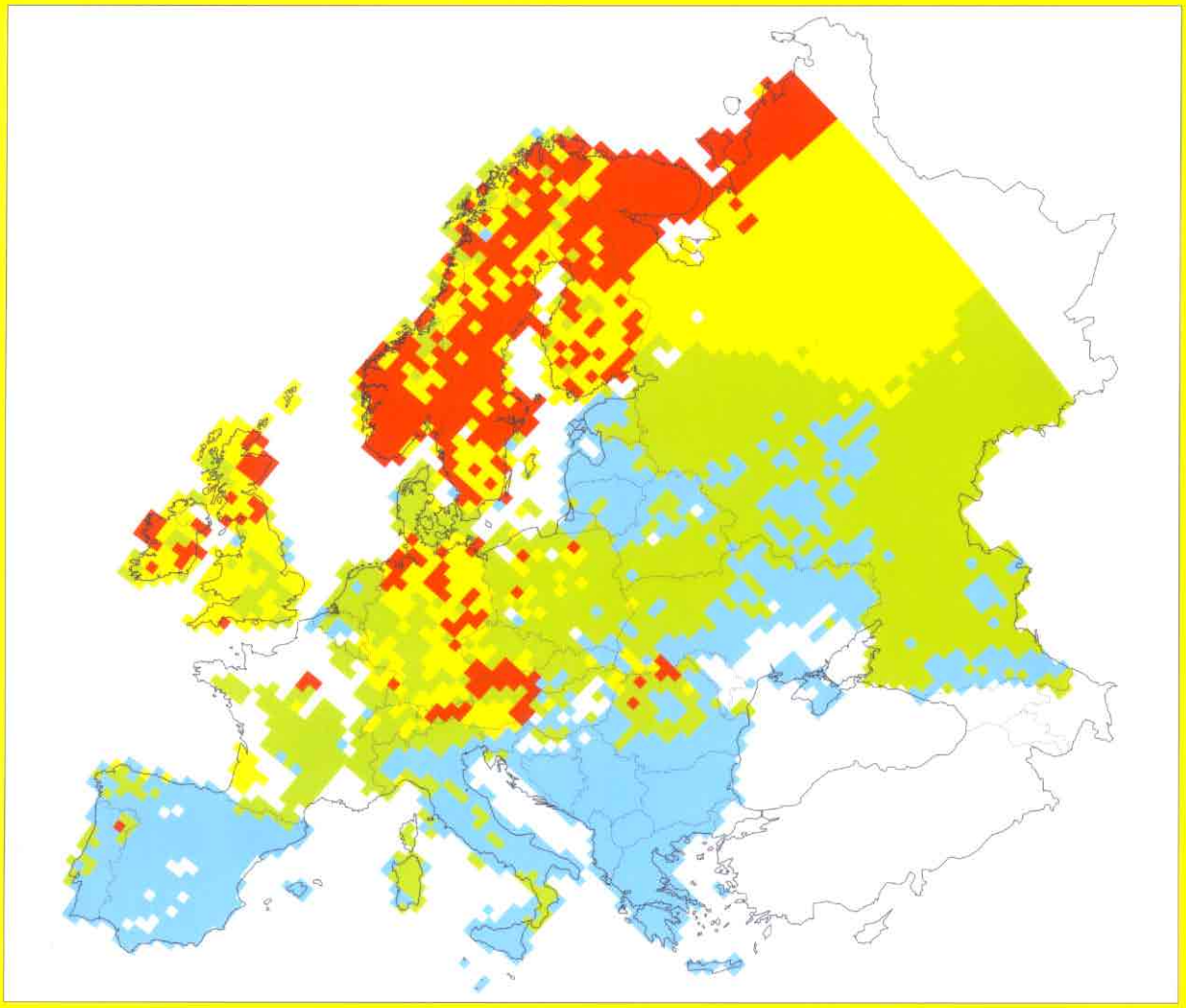

STATUS REPORT 1997
COORDINATION CENTER FOR EFFECTS

edited by

M. Posch, J.-P. Hettelingh, P.A.M. de Smet and R.J. Downing

rivm
research for
man and environment

RIJKSINSTITUUT VOOR VOLKSGEZONDHEID EN MILIEU
NATIONAL INSTITUTE OF PUBLIC HEALTH AND THE ENVIRONMENT

Calculation and Mapping of Critical Thresholds in Europe:

Status Report 1997

Edited by:

Maximilian Posch
Jean-Paul Hettelingh
Peter A.M. de Smet
Robert J. Downing

Coordination Center for Effects
National Institute of Public Health and the Environment
Bilthoven, Netherlands

RIVM Report No. 259101007

ISBN No. 90-6960-069-2

Acknowledgments

The calculation methods and resulting maps contained in this report are the product of collaboration within the Effects Program of the UN/ECE Convention on Long-range Transboundary Air Pollution, involving many individuals and institutions throughout Europe. The various National Focal Centers whose reports on their respective mapping activities appear in Part II, are gratefully acknowledged for their contributions to this work.

In addition, the Coordination Center for Effects thanks the following for their efforts:

- The Directorate of Air and Energy of the Dutch Ministry of Public Health, Physical Planning and Environment, in particular Volkert Keizer and Johan Sliggers, for funding and support of the CCE.

- Erik Berge, David Simpson and their colleagues from the EMEP/MSC-W for providing the European deposition and ozone concentration data.

- the UN/ECE Working Group on Effects, and the Task Forces on Mapping and on Integrated Assessment Modelling for their collaboration and assistance.

- The staff of Geodan B.V. for their assistance in maintaining the CCE's geographic information systems.

- Laurie Carr of Laurie Carr Graphics for assistance in graphic design.

- The staff of the RIVM graphics department for their assistance in producing this report.

Table of Contents

Introduction

J.-P. Hettelingh, M. Posch, and P.A.M. de Smet

The mandate of the Coordination Center for Effects (CCE) is to give scientific and technical support, in collaboration with the Program Centers under the Convention on Long-range Transboundary Air Pollution, to the Working Group on Effects and, as required, to the Working Group on Strategies, and their relevant Task Forces in their work related to the environmental effects of air pollution, including the practical development of critical loads/levels maps and their exceedances.

The work of the CCE is conducted in close collaboration with an extensive network of national scientific institutions (National Focal Centers). Progress on data and methodologies are reviewed annually at CCE Mapping Workshops. Eight workshops have been organized since the CCE was established in 1990: at the RIVM (1990, 1991), the Institute for the Ecology of Industrial Areas (Poland, 1992), the Research Center for Energy, Environment and Technology (Spain, 1993), the National Institute for Agricultural Research (France, 1994), the Finnish Environment Agency (Finland, 1995), in collaboration with the Hungarian Ministry of Environment (Budapest, 1996) and the Irish Environmental Protection Agency (Galway, 1997).

The work of the CCE has been described in three previous reports (Hettelingh *et al.* 1991, Downing *et al.* 1993, Posch *et al.* 1995) and in the open literature (e.g. Hettelingh *et al.* 1995). The first CCE report, published in 1991, described the critical load of acidity methodology adopted by National Focal Centers, and the alterations made to accommodate the policy requirement of identifying critical loads of sulfur. The CCE Status Report 1993 presented the final results of this approach and summarized the development of methods to compute both the critical loads of sulfur and nitrogen acidity, and the critical load for eutrophication. The critical load approach was further broadened to different kinds of impacts. In addition to the indirect effects of geochemical changes in soils and lakes, the direct effects of pollutant concentrations on vegetation and human health were also considered. These critical thresholds may be used for the scientific support of multi-pollutant protocol negotiations. The CCE Status Report 1995 introduced the application of multiple critical thresholds. This has led to the development of so-called *protection isolines*, which determine combinations of sulfur and nitrogen deposition which protect a certain percentage of ecosystems against acidification and/or eutrophication.

This report presents the current status of critical threshold mapping, incorporating the latest data available to support future negotiations of the Protocol on further reduction of nitrogen emissions. The critical thresholds considered are: (1) critical loads of acidifying nitrogen, (2) critical loads for eutrophication, (3) critical levels for nitrogen oxide and tropospheric ozone, and (4) WHO health guidelines. The focus of this report lies on the characteristics and variability of National Focal Center data and critical loads.

The report consists of three parts. Part I describes current critical threshold and exceedance maps (Chapter 1), evaluates national contributions (Chapter 2), provides a summary of the methodologies for computing conditional critical loads and protection isolines (Chapter 3), includes an analysis of the critical load and input data variability (Chapter 4), reports on the CCE land use data base used to assess stock at risk (Chapter 5) and summarizes the European background data base used to compute critical loads in regions for which no national contributions have been submitted (Chapter 6).

Part II consists of National Focal Center reports. In comparison to the last CCE Status Report in 1995, seven additional National Focal Centers: Belgium (Flanders), Croatia, France, Hungary, Ireland, Italy and Spain have submitted national results for the first time. The European map of critical loads now incorporates data of 20 National Focal Centers.

Lastly, four appendices provide details on geographical issues concerning the EMEP grid, on routines to derive protection isolines, on the CCE's anonymous FTP server, and a set of conversion tables for commonly used deposition and concentration units.

It should be noted that the application of critical thresholds is receiving increasing attention outside the framework of the UN/ECE. The World Health

Organization is incorporating critical load results as part of the update of their air quality guidelines. Critical load data have been provided to the European Union for use in the development of an acidification strategy (DG XI) and for the study on the Externalities of Energy (DG XII). Mapping Programme results are increasingly being used in other studies which address multiple stresses, e.g. the combined effects of climate change and acidification (Posch *et al.* 1996) and in the Global Environmental Outlook (UNEP 1997).

References

Downing, R.J., J.-P. Hettelingh and P.A.M. de Smet (eds.), 1993. Calculation and Mapping of Critical Loads in Europe: CCE Status Report 1993. National Institute of Public Health and Environmental Protection Rep. No. 259101003, Bilthoven, Netherlands.

Hettelingh, J.-P., R.J. Downing and P.A.M. de Smet (eds.), 1991. Mapping Critical Loads for Europe: CCE Technical Report No. 1. National Institute of Public Health and Environmental Protection Rep. No. 259101001. Bilthoven, Netherlands.

Hettelingh, J.-P., M. Posch, P.A.M. de Smet and R.J. Downing, 1995. The use of critical loads in emission reduction agreements in Europe. *Water Air Soil Pollut.* 85:2381-2388.

Posch, M., P.A.M. de Smet, J.-P. Hettelingh and R.J. Downing (eds.), 1995. Calculation and Mapping of Critical Thresholds in Europe: CCE Status Report 1995. National Institute of Public Health and the Environment Rep. 259101004, Bilthoven, Netherlands.

Posch, M., J.-P. Hettelingh, J. Alcamo and M. Krol, 1996. Integrated scenarios of acidification and climate change in Asia and Europe. *Global Environ. Change* 6(4):375-394.

United Nations Environment Programme (UNEP), 1997. Global Environmental Outlook 1997. UNEP/Oxford Univ. Press, Nairobi, Kenya.

1. Analysis of European Maps

J.-P. Hettelingh, M. Posch, and P.A.M. de Smet

Introduction

This chapter gives an overview of the critical threshold and exceedance maps produced since the last CCE Status Report (Posch *et al.* 1995). The difference between the maps described below and the maps published in 1995 is largely due to updates of national critical loads, and to the incorporation of contributions from additional National Focal Centers: Belgium (Flanders), Croatia, France, Hungary, Ireland, Italy and Spain. Between 1995 and 1997 two major updates of critical loads and input data were completed.

Critical loads have been computed for acidification and eutrophication for a large range of ecosystems in every EMEP grid square in Europe. So-called "protection isolines" have been derived to determine combinations of sulfur and nitrogen deposition which protect a certain percentage of ecosystems against acidification and/or eutrophication. The procedures to compute these isolines are described in further detail in Chapter 3.

The use of these protection isolines means that exceedances are no longer expressed as the difference between a single critical load and the deposition of a single pollutant, as was done in developing the Second Sulphur Protocol (UN/ECE 1994).

By considering two pollutants, many combinations of sulfur and nitrogen deposition can be found which provide an equal level of protection against acidification. Therefore, exceedances are expressed in terms of the proportion of ecosystems in each EMEP grid cell which is protected for a certain combination of sulfur and nitrogen deposition onto that grid cell. This chapter includes maps on the following subjects:

- Maximum critical loads for sulfur and acidifying nitrogen
- Critical loads for eutrophication (nutrient nitrogen)
- Ecosystem protection and nitrogen deposition exceedance (acidification only)
- Ecosystem protection and nitrogen deposition exceedance (acidification and eutrophication)
- Deposition reduction requirements
- Stock at risk for crops and forests due to ozone exposure
- Ozone concentrations and WHO Air Quality Guidelines

1.1 Maximum critical loads for sulfur and acidifying nitrogen

Figure 1-1 shows the 5th percentile ("pentile") and 50th percentile (median) of the maximum critical load of sulfur, $CL_{max}(S)$, and the maximum critical load of acidifying nitrogen, $CL_{max}(N)$ in every EMEP grid. (For details on percentile computations, see Chapter 3.) The maximum critical load of sulfur is equal to the critical deposition of acidity, from which (after inclusion of nitrogen uptake, immobilization and denitrification) the maximum critical load of nitrogen is derived.

The pentile maximum critical load of sulfur (top left) is very low (< 200 eq ha^{-1} yr^{-1} , i.e. lower than 320 mg S m^{-2} yr^{-1}) in Scandinavia, and central and western Europe. The median of the maximum critical load of sulfur (top right) leaves a few areas with very low critical loads in northern Europe, but results in markedly higher critical loads over the whole of Europe.

The pentile maximum critical load of nitrogen (bottom left) is low (< 700 eq ha^{-1} yr^{-1}) mostly in areas of northern Europe. These low critical load areas are significantly reduced for the median of the maximum critical load of nitrogen (bottom right).

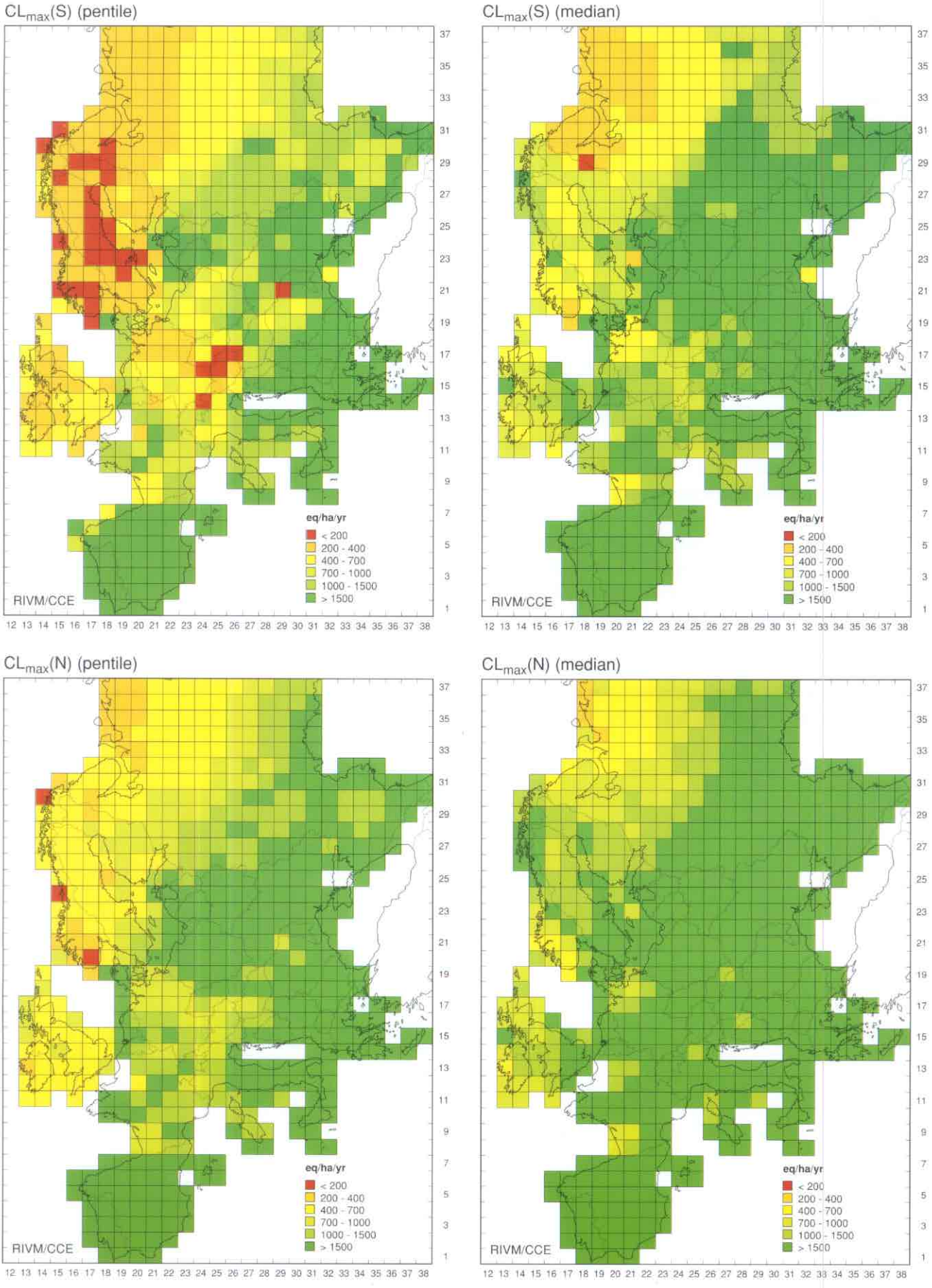

Figure 1-1. The 5th percentile (pentile) and 50th percentile (median) of the maximum critical loads for sulfur, $CL_{max}(S)$, and acidifying nitrogen $CL_{max}(N)$.

1.2 Critical loads for eutrophication (nutrient nitrogen)

Figure 1-2 shows the pentile (top) and the median (bottom) of the critical loads for eutrophication, $CL_{nut}(N)$, protecting 95% and 50% of the ecosystems against eutrophication.

The use of nitrogen immobilization values recommended in the Mapping Manual (UBA 1996) in northern Europe in general, and Finland in particular, leads to rather low pentile critical loads. Large areas of Europe show low pentile critical loads (<400 eq ha^{-1} yr^{-1}), notably in comparison to the $CL_{nut}(N)$ maps described in Posch *et al.* (1995). It should be noted that Figure 1-2 would have shown even lower $CL_{nut}(N)$ values if recommended nitrogen immobilization rates had been used by all National Focal Centers. (See Chapter 4 for an overview of national N_i distributions).

The maps of median of the critical loads of nutrient nitrogen show that values in northern, central and eastern Europe increase to more than 400 eq ha^{-1} yr^{-1}. Minor changes between pentile and median critical load values occur whenever a small variation in input data is used in computing critical loads for eutrophication. This is the case when, for example, a Level 0 approach is used, such as in France.

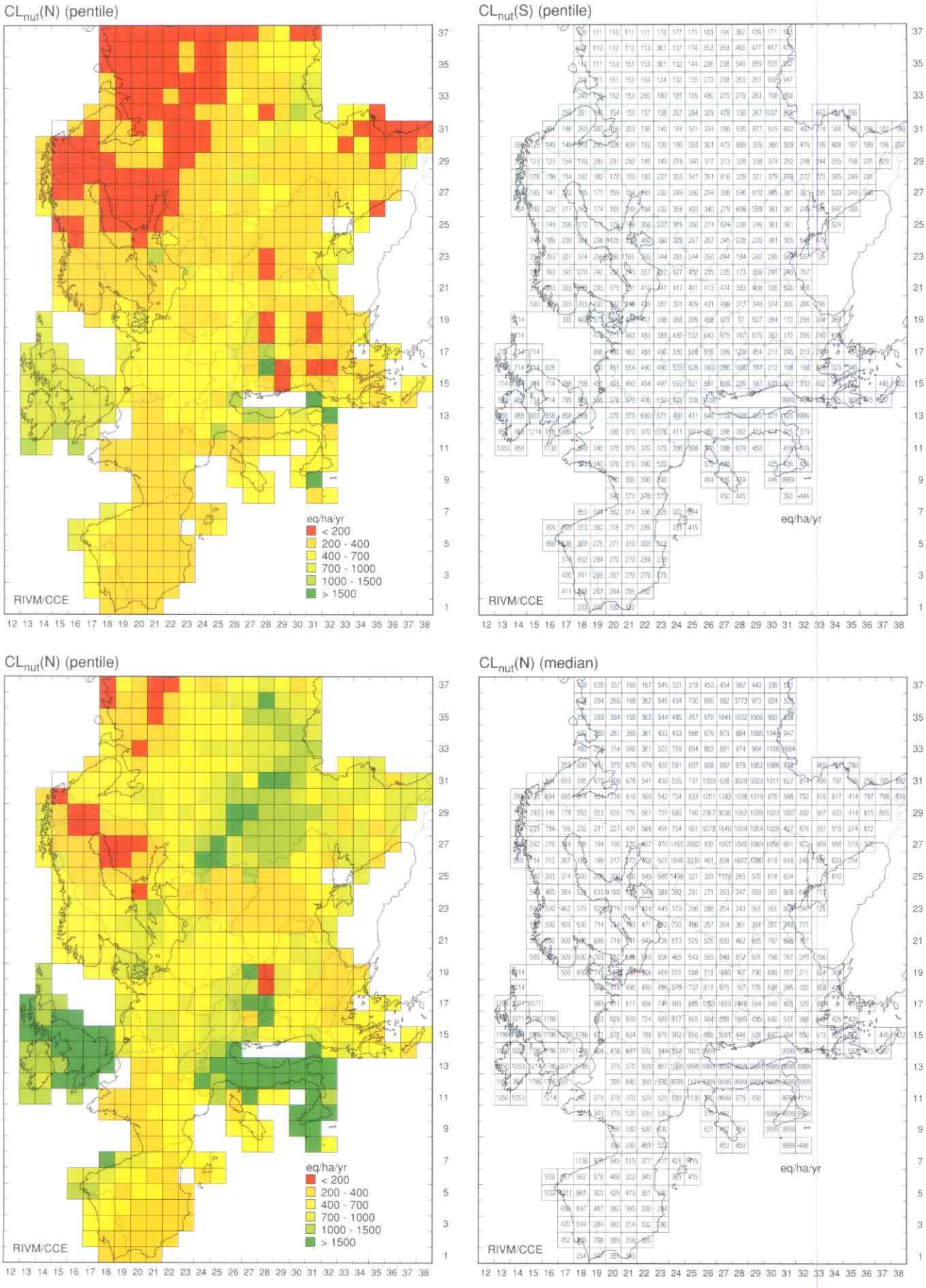

Figure 1-2. The pentile (top) and median (bottom) of the critical load for eutrophication.

1.3 Ecosystem protection and nitrogen deposition exceedance (acidification only)

An analysis of the exceedance of nitrogen-based critical loads of acidity, and the related ecosystem protection percentages, can not be carried out without specifying the sulfur deposition, since protection isolines have to be used (see also Chapter 3). These isolines characterize equal ecosystem protection for different combinations of sulfur deposition and nitrogen deposition.

Figure 1-3 shows the percentage of ecosystems protected against acidification, due to the nitrogen deposition in 1990 and the sulfur deposition in 2010 resulting from the 1994 Sulphur Protocol. A similar map using the nitrogen deposition in 2010 according to nitrogen emissions projected by Current Reduction Plans (UN/ECE 1997) is also shown (bottom left).

The exceedance of the pentile critical loads of nitrogen-based acidity is displayed for nitrogen deposition in 1990 (top right) and 2010 (bottom right), both derived by fixing the sulfur deposition to its projected level in 2010. The areas showing protection levels less than 100% coincide with areas where the critical load for nitrogen-based acidity is exceeded. The areas with the highest exceedance (lowest protection) occur in central and western Europe, although the magnitude of exceedances decreases by 2010.

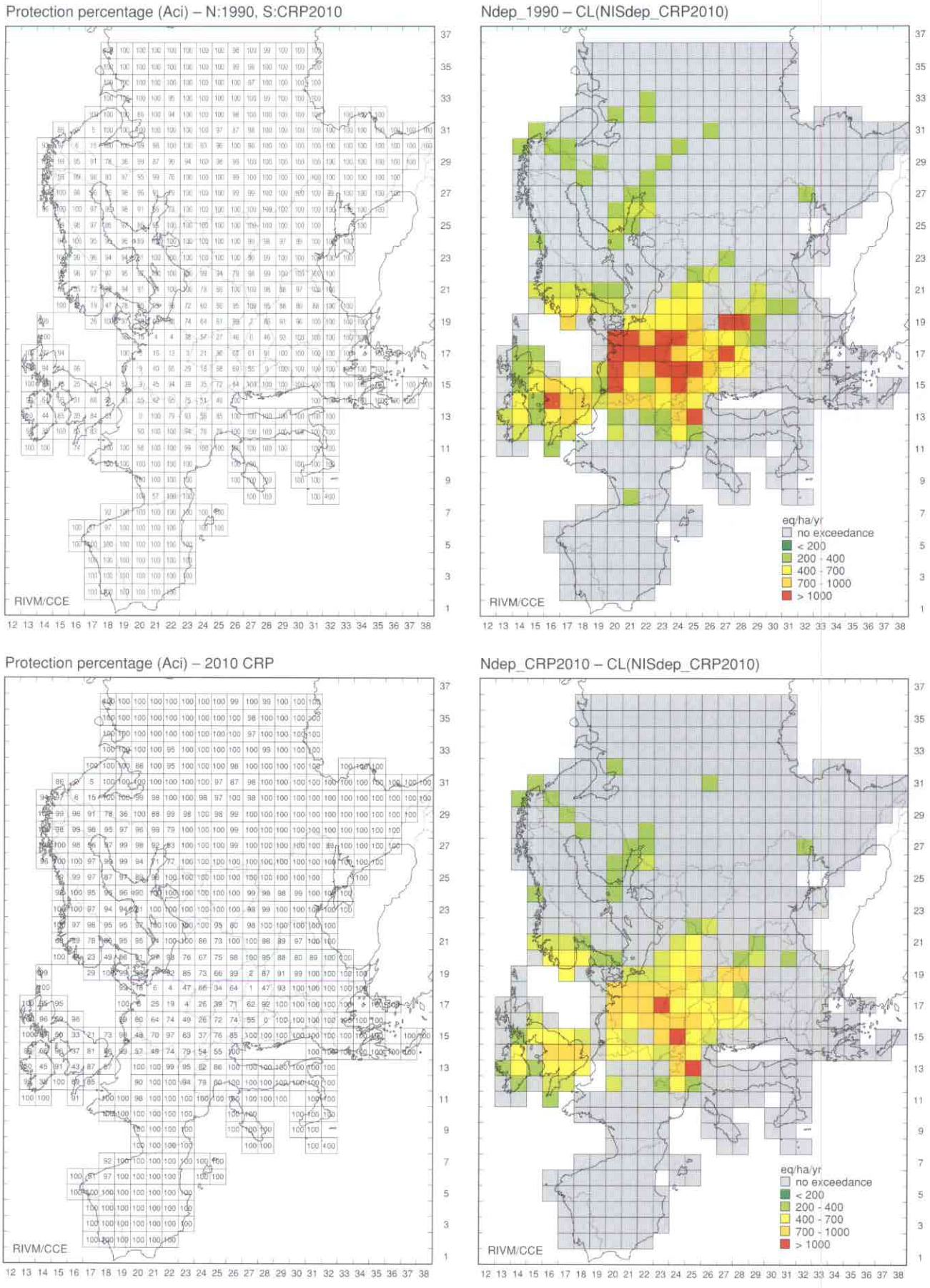

Figure 1-3. The percentage of ecosystems protected against acidification, due to the combination of the nitrogen deposition in 1990 (top left) and 2010 (bottom left). The top and bottom right maps show the exceedance of critical loads of nitrogen-based acidity in 1990 and 2010. All four maps use the projected sulfur deposition for 2010.

1.4 Ecosystem protection and nitrogen deposition exceedance (acidification and eutrophication)

Protection isolines used in Figure 1-4 reflect the combinations of sulfur and nitrogen deposition which provide protection against both acidification and eutrophication by including the critical load of nutrient nitrogen. As with Figure 1-3, sulfur deposition has been fixed to its projected 2010 value.

The top left map in Figure 1-4 shows the percentage of ecosystems protected against acidification and eutrophication due to the nitrogen deposition in 1990 and the projected sulfur deposition in 2010. A similar map (bottom left) uses the nitrogen deposition in 2010 according to nitrogen emissions as projected by Current Reduction Plans (UN/ECE 1997). The protection percentage is zero whenever nitrogen deposition exceeds $CL_{nut}(N)$.

The exceedance of the critical loads of eutrophication and nitrogen-based acidity in 1990 (top right) and 2010 (bottom right) is derived by computing the difference between the nitrogen deposition and either $CL_{nut}(N)$ or the nitrogen-based critical load for acidity (given the sulfur deposition in 2010), whichever is smaller.

The conclusions regarding ecosystem protection and exceedance are similar to those presented for Figure 1-3. The addition of the eutrophication constraint leads to a significant increase of the European area in which (a) protection is very low, and (b) exceedances are high. In large parts of central Europe, no ecosystem protection at all is achieved at nitrogen deposition at both 1990 and 2010 levels.

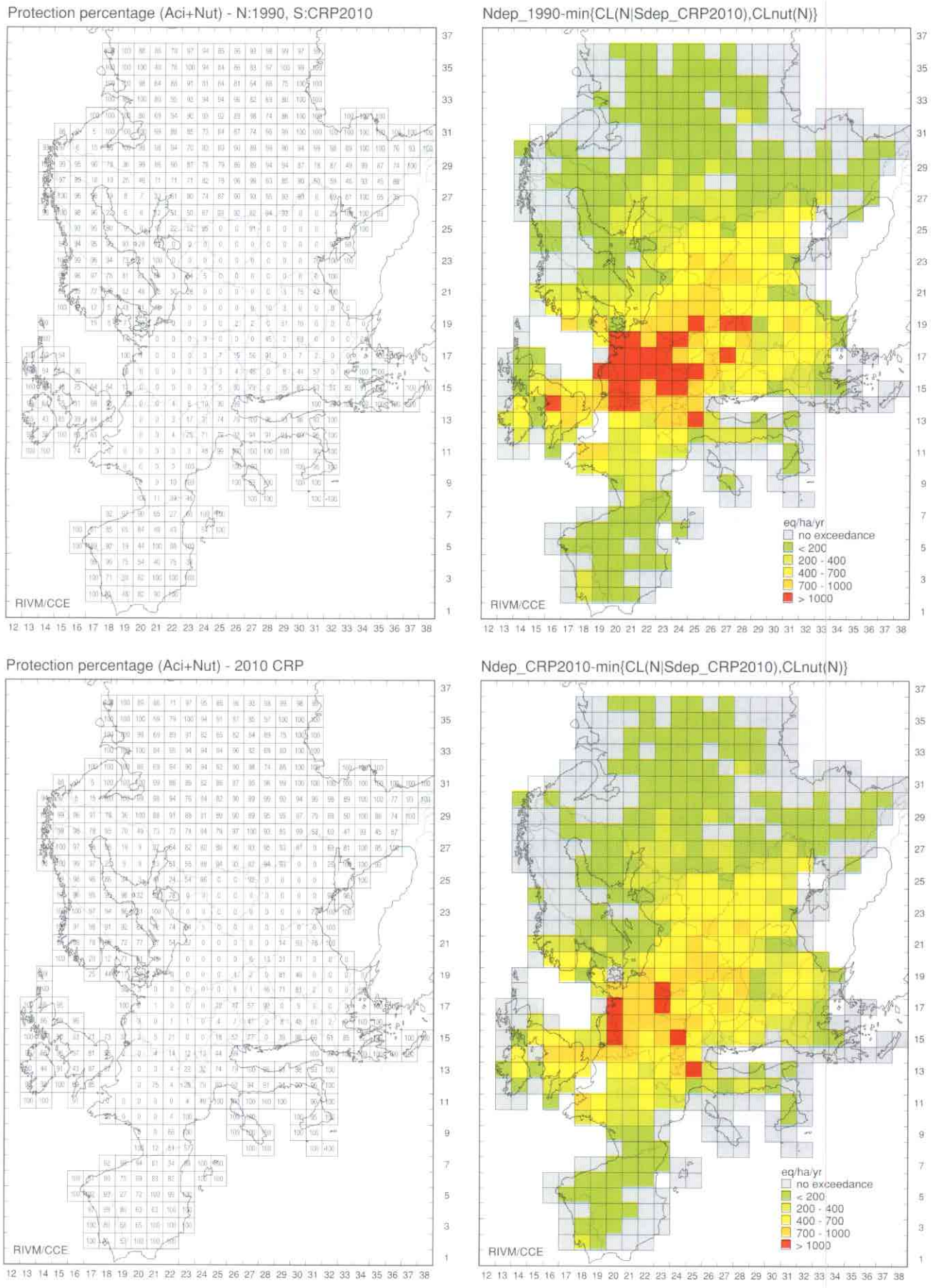

Figure 1-4. The percentage of ecosystems protected against acidification and eutrophication, due to the nitrogen deposition in 1990 (top left) and 2010 (bottom left). The top and bottom right maps show the exceedance of critical loads of eutrophication and nitrogen-based acidity in 1990 and 2010, respectively. All four maps use the projected sulfur deposition for 2010.

1.5 Deposition reduction requirements

To achieve a specified protection of ecosystems in a grid cell against acidification and/or eutrophication, five cases of reduction requirements of sulfur and/or nitrogen deposition can be distinguished:

1. No deposition reduction is required (grey shading) if the combination of sulfur and nitrogen deposition lies below the protection isoline.
2. Sulfur or nitrogen deposition reductions are fully interchangeable (blue shading) if the deposition levels lie outside the protection isoline, but within the area delimited by the maximum critical load of sulfur, $CL_{max}(S)$ and the minimum of the critical load for eutrophication, $CL_{nut}(N)$ and the maximum critical load of nitrogen, $CL_{max}(N)$.
3. A sulfur deposition reduction is mandatory (yellow shading) if the deposition level exceeds $CL_{max}(S)$, and nitrogen deposition does not exceed the minimum of $CL_{nut}(N)$ and $CL_{max}(N)$.
4. A nitrogen deposition reduction is mandatory (orange shading) if the deposition level exceeds the minimum of $CL_{nut}(N)$ and $CL_{max}(N)$, and sulfur deposition does not exceed $CL_{max}(S)$.
5. Both sulfur and nitrogen deposition reduction are mandatory (red shading) if both deposition levels lie outside the area delimited by $CL_{max}(S)$ and the minimum of $CL_{nut}(N)$ and $CL_{max}(N)$.

The figure shows the type of deposition reductions required to achieve protection against acidification in 1990 (top left) and 2010 (top right). The bottom two maps show the deposition reduction requirements to achieve protection against both acidification and eutrophication in 1990 (bottom left) and 2010 (bottom right). All four maps use the projected sulfur deposition for 2010. While protection against acidification alone requires the mandatory reduction of N in only a few grid cells (orange shading), in large areas of Europe mandatory reductions of N deposition are needed when protection against eutrophication is added as an additional requirement.

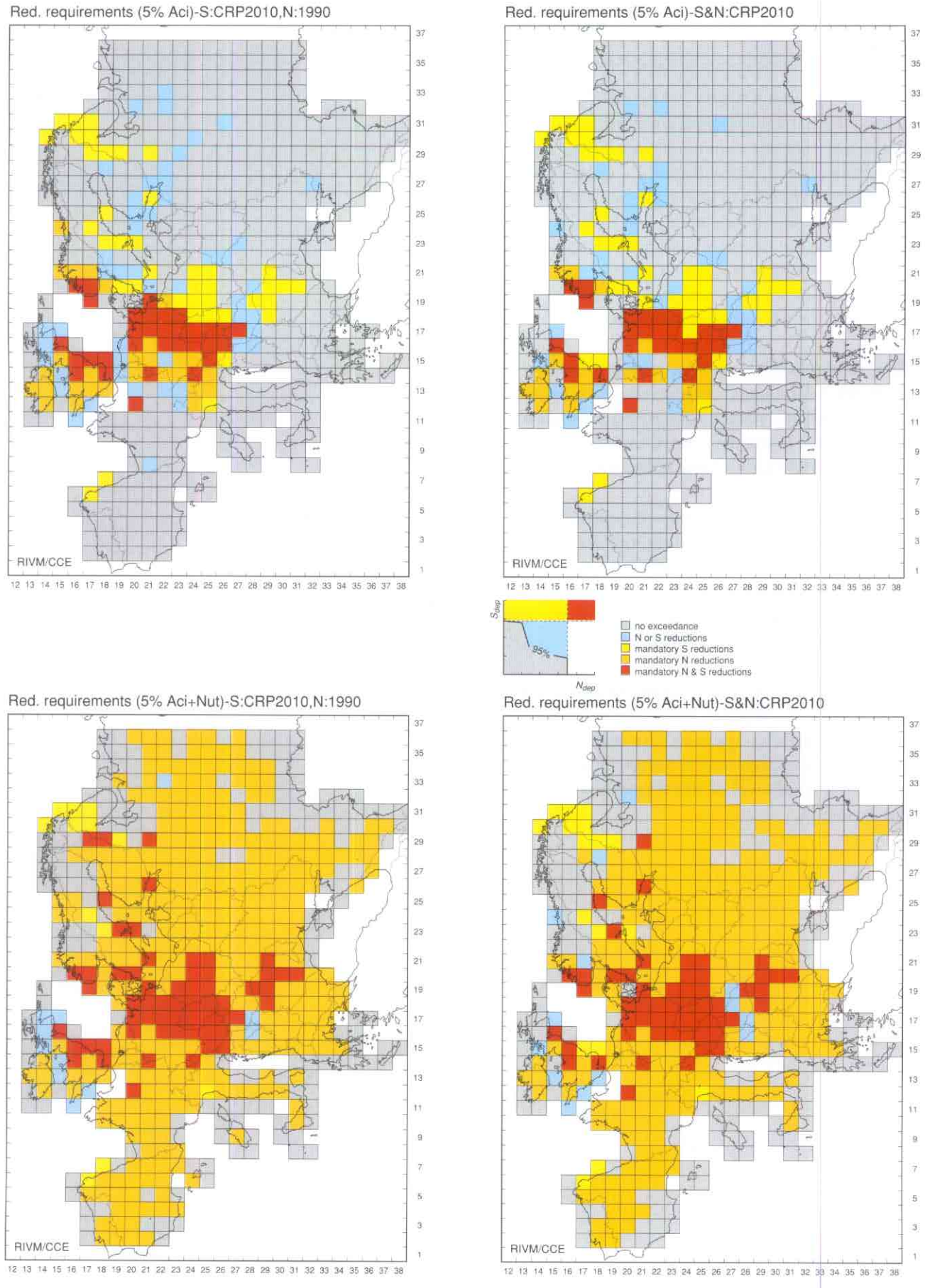

Figure 1-5. Reduction requirements for sulfur and nitrogen deposition to achieve a 5% protection level, considering critical loads of acidity alone (top), and considering both acidification and eutrophication (bottom). (See inset for explanation of color codes.)

1.6 Stock at risk for crops and forests due to ozone exposure

Land use maps (see Chapter 5) are used to assess the stock at risk of arable land and forests due to elevated tropospheric ozone concentrations (see also Hettelingh *et al.* 1996). Figure 1-6 shows the accumulated exposure to tropospheric ozone concentrations over a threshold of 40 ppb (AOT40) in 1990, compared to critical ozone levels for arable land (top) and forests (bottom). Ozone concentration data have been provided by the EMEP/ MSC-W (Barrett and Berge 1996).

Critical ozone AOT40 levels have been established at 3000 ppb·h for crops during daylight hours over the period May–July and 10,000 ppb·h for forests during daylight hours from April to September (Kärenlampi and Skärby 1996, UBA 1996).

The shadings in Figure 1-6 show the magnitude of AOT40 values. The green shading indicates grid cells where critical levels for AOT40 are not exceeded. The size of the grid cells is proportional to the area of ecosystems as the percentage of the area covered by each 50x50 km^2 EMEP grid cell.

The top map indicates that a major portion of arable land in Europe is subject to AOT40 levels which exceed 3000 ppb·h (= 3 ppm·h). The bottom map shows that in the large forested areas of northern Europe the critical level of 10000 ppb·h (=10 ppm·h) is not exceeded.

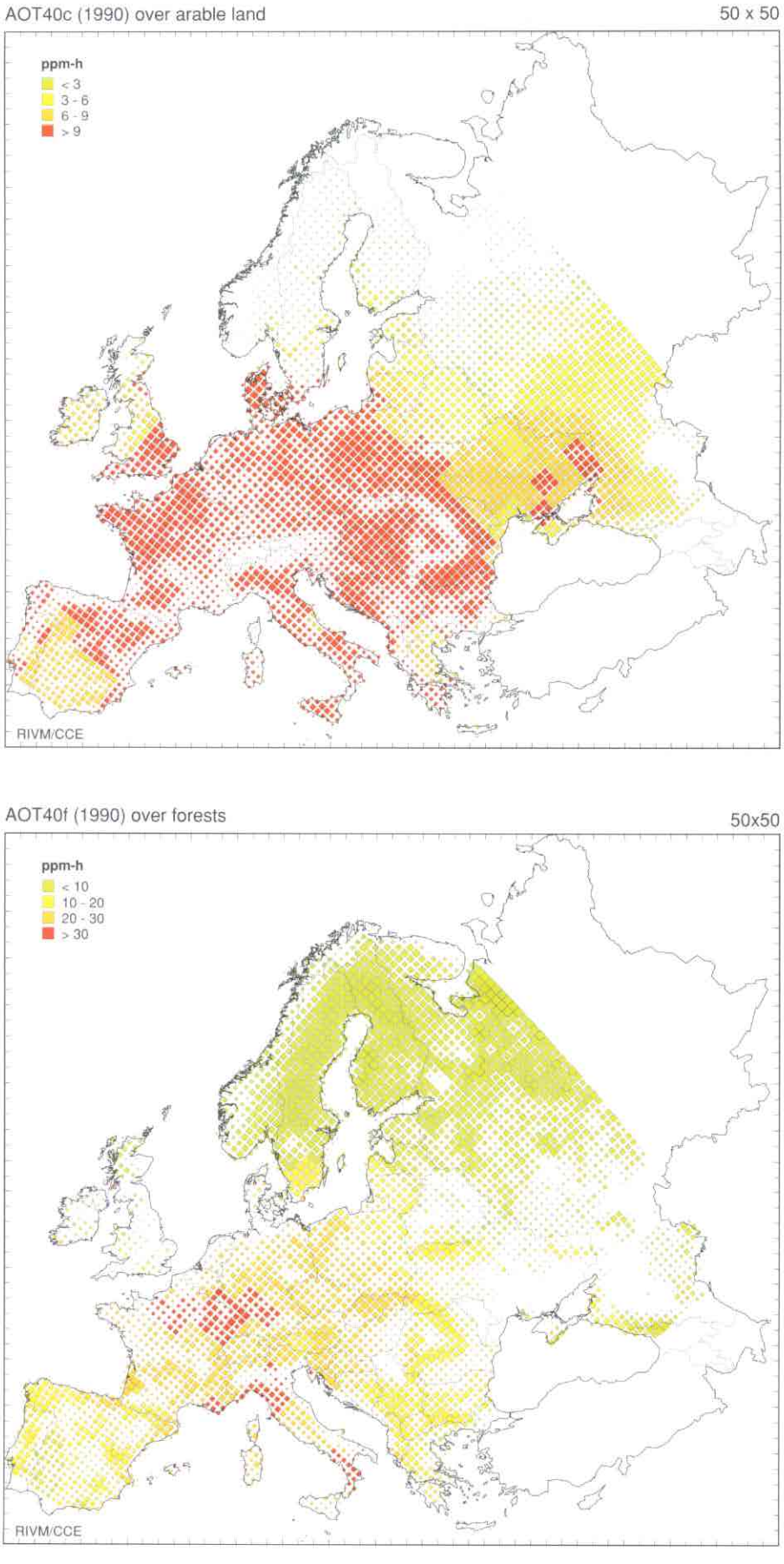

Figure 1-6. The accumulated exposure to ambient tropospheric ozone concentrations over a threshold of 40 ppb (AOT40) in 1990 for arable land (top) and forests (bottom). The green-shaded grids indicate areas where the critical AOT40 levels are not exceeded.

1.7 Ozone concentrations and WHO Air Quality Guidelines

The analysis of the exposure of population to tropospheric ozone is receiving increasing attention in the integrated assessment of air pollutants. Thus WHO Air Quality Guidelines (AQG) might be considered in addition to ecosystem-based critical loads and levels (Hettelingh *et al.* 1997). A WHO-AQG (WHO 1997) for tropospheric ozone is 60 ppb (=120 μg m^{-3}, see also Appendix D) as an 8-hour average. An AOT60 value of zero as an additional critical threshold, using 6-hourly averages of ozone model simulations, has recently been proposed as a first step to incorporate health effects into UN/ECE integrated assessments (UN/ECE-WHO 1997). Both statistics have been used in Figure 1-7 using the 6-hourly ozone concentration averages (for the period April–September) provided by EMEP/MSC-W (Barrett and Berge 1996).

The top map shows that the AOT60 value of zero is significantly exceeded in southwestern Germany and northeastern France. The bottom map illustrates the percentage of daytime (from April–September) during which the 6-hour average concentration of 60 ppb is exceeded.

Both maps show that essentially the same regions are subject to excessive ozone exposure. The interpretation in terms of health impacts requires further knowledge of the importance of accumulated exposure in comparison to episodic exposure.

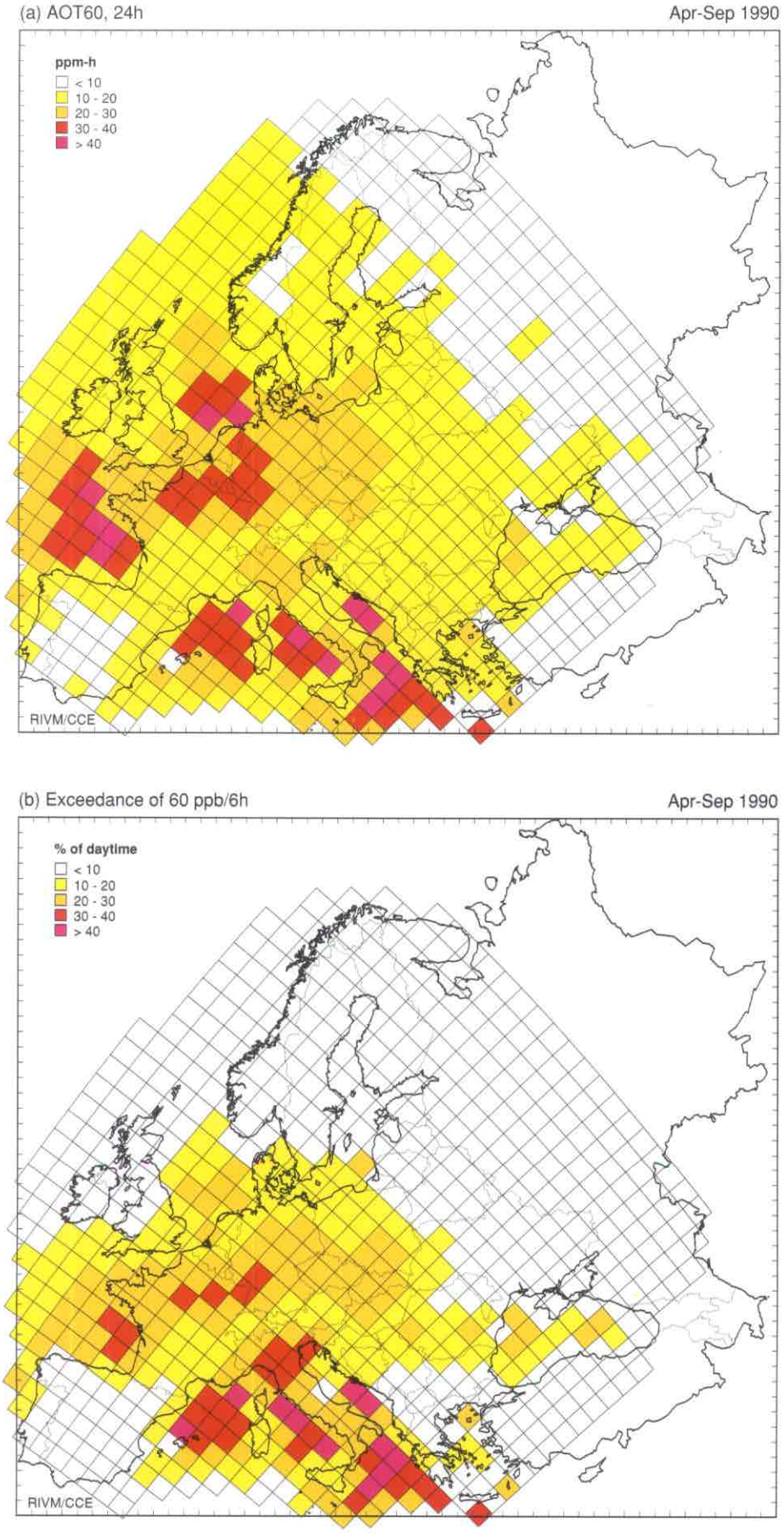

Figure 1-7. AOT60 values in 1990 derived from 6-hour average concentrations from April–September (top), and the percentage of daytime during which ozone concentrations exceed 60 ppb (bottom).

References

Barrett, K. and E. Berge (eds.), 1996. Transboundary Air Pollution in Europe. MSC-W Status Report 1996: Part One. Norwegian Meteorological Institute, Oslo, Norway.

Hettelingh, J.-P., Posch M., and P.A.M. de Smet, 1996. Mapping critical thresholds and stock at risk. *In*: L. Kärenlampi and L. Skärby (eds.), *op. cit.*, pp. 125-137.

Hettelingh, J.-P., M. Posch, and P.A.M. de Smet, 1997. Mapping critical thresholds for integrated assessment. *In*: UN/ECE-WHO, *op. cit.*, pp. 56-59.

Kärenlampi, L. and L. Skärby (eds.), 1996. Critical Levels for Ozone in Europe: Testing and Finalizing the Concepts. UN-ECE Workshop Report. Univ. of Kuopio, Dept. of Ecology and Environmental Science.

Posch, M., P.A.M. de Smet, J.-P. Hettelingh and R.J. Downing (eds.), 1995. Calculation and Mapping of Critical Thresholds in Europe: CCE Status Report 1995. National Institute of Public Health and the Environment Rep. 259101004, Bilthoven, Netherlands.

UBA, 1996. Manual on Methodologies and Criteria for Mapping Critical Levels/Loads and geographical areas where they are exceeded. UN/ECE Convention on Long-range Transboundary Air Pollution. Federal Environmental Agency (Umweltbundesamt), Texte 71/96, Berlin.

UN/ECE, 1994. Protocol to the 1979 Convention on Long-range Transboundary Air Pollution on further reduction of sulphur emissions. U.N. document ECE/EB.AIR/40. Geneva and New York.

UN/ECE, 1997. Integrated assessment modelling. UN/ECE document EB.AIR/WG.5/R.69.

UN/ECE-WHO, 1997. Health Effects of Ozone and Nitrogen Oxides in an Integrated Assessment of Air Pollution. Proceedings of a UN/ECE-WHO Workshop, Eastbourne, UK, 11-12 June 1996. Institute for Environment and Health, Univ. Leicester, Special Report 3.

WHO, 1987. Air Quality Guidelines for Europe. WHO Regional Publications, European Series No. 23, Copenhagen, Denmark, 426 pp.

2. Summary of National Data Contributions

P.A.M. de Smet and M. Posch

Introduction

Each year, the Coordination Center for Effects (CCE) requests that countries submit revised national critical load calculations, so that the integrated assessment modeling groups participating in LRTAP Convention activities may work with up-to-date critical loads data. This process gives National Focal Centers (NFCs) the opportunity to contribute their latest results, and also permits countries which have not yet been able to deliver national critical loads calculations to submit new data for incorporation into the European data bases and critical loads maps.

This chapter describes briefly the process and results of the latest round of national data updating. It lists the countries that contributed national data, and gives an overview of the ecosystem(s) selected as receptor(s), and the density (resolution) of the national data. The chapter concludes with a discussion on some items that should be addressed in future data revisions.

2.1 Overview of national contributions

The timetable for the national critical loads data contained in the European maps in Chapter 1 is as follows:

July 1996	Working Group on Effects (WGE) agrees that the CCE should make a call for data.
Sept. 1996	CCE issues formal call for data to all NFCs with a deadline of 15 Dec. 1996.
April 1997	CCE makes revised European critical loads data sets available to Task Force on Integrated Assessment Modelling (TFIAM) groups, and presents maps at its annual workshop in Galway (Ireland). Task Force on Mapping grants provisional approval of maps, pending further minor revisions before 20 May 1997.
June 1997	Revised data sets made available to TFIAM modeling groups.
August 1997	European critical loads maps to be submitted for approval by the WGE.

The number of countries which submitted data has increased to 20 (listed in Table 2-1). Countries that contributed revised data are: Czech Republic, Denmark, Estonia, Finland, France, Italy, Norway, Poland, Russian Federation, Sweden, Switzerland and the United Kingdom (excluding Northern Ireland). Four countries (Austria, Germany, Netherlands and Spain) indicated that the national data adopted by the WGE in July 1996 are still current. This year four countries contributed national data for the first time: Belgium (Flanders only), Croatia (for two 50 x 50 km^2 EMEP ("EMEP50") grid cells), Hungary and Ireland. Further details on most individual countryÌs activities can be found in Part II of this report.

At past workshops, the CCE and NFCs have agreed to the following rules concerning the application of critical load data for areas which include a national boundary:

(i) For all EMEP grid cells that do not cover a country that contributes national data, critical loads are computed using the European background data base held at the CCE. (See Chapter 6 for a description of this data base.)

(ii) For EMEP grid cells that cover part of one or more countries which has submitted national data, percentiles and isolines are based on the national critical loads data for this cell only, no matter how small the area or how few ecosystem data are supplied. For these EMEP grid cells, no background data are included.

2.2 Scope and format of national contributions

National Focal Centers have selected a variety of ecosystem types as receptors for calculating and mapping critical loads. For most ecosystem types (e.g. forests), critical loads are calculated for both acidity and eutrophication. Other receptor types (e.g. streams and lakes) have only critical loads for acidity, on the assumption that eutrophication does not occur in these ecosystems. For some receptors, like most semi-natural vegetation, only critical loads for nutrient nitrogen are computed, since the sensitivity to acidifying effects is less than eutrophication effects.

Table 2-1. Type of ecosystem (critical load) data provided by National Focal Centers.

Country	Ecosystem Type	Number of Ecosystems	Remarks	Total Ecosystems
Austria	Forest	6,444		6,444
Belgium	Deciduous forest	365		
(excl. Wallonia)	Coniferous forest	212		
	Mixed coniferous forest	51		
	Mixed deciduous forest	24		652
Croatia	Coniferous forest	18	2 EMEP 50 x 50 km^2	
	Deciduous forest	16	grids only	34
Czech Republic	Forest	29,418		29,418
Denmark	Spruce	5,463		
	Pine	1,033		
	Beech	2,814		
	Oak	447		
	Grass	9,027	acidity CLs only	18,784
Estonia	Pine-podzol	32		
	Pine-bog	22		
	Spruce-podzol	30		
	Spruce-alvar	15		
	Deciduous-podzol	12		
	Deciduous-wet	14		
	Bog	15		140
Finland	Spruce	1,004		
	Pine	1,045		
	Deciduous forest	1,034		
	Lakes	1,450	acidity CLs only	4,533
France	Coniferous forest	24	The original data base	
	Deciduous forest	48	with detailed ecosystem	
	Mixed forest	271	types has been reclassi-	
	Grassland (agricultural)	99	fied into these 4 groups.	442
Germany	Coniferous forest	44,600		
	Deciduous forest	7,550		
	Mixed coniferous forest	15,011		
	Mixed deciduous forest	27,782		94,943
Hungary	Unspecified forest	7		
	Deciduous forest	5		
	Coniferous forest	8		
	Grassland	9		
	Heath	4		
	Bog	4		
	Reed	2		
	Lakes	2		
	Marsh	1		42
Ireland	Coniferous forest	10,102		
	Deciduous forest	8,933		
	Moors/heathlands	7,348		26,383
Italy	Boreal forest	41		
	Temperate coniferous forest	22		
	Temperate deciduous forest	165		
	Mediterranean forest	110		
	Tundra	46		
	Acid grassland	118		
	Other	236		738

(continued)

Table 2-1. (continued)

Country	Ecosystem Type	Number of Ecosystems	Remarks	Total Ecosystems
Netherlands	Coniferous forest (5 species)	53,024		
	Deciduous forest (7 tree species)	74,466		127,490
Norway	Forest	720		
	Lakes/streams	2,305	acidity CLs only	
	Semi-natural vegetation	1,610	$CL_{nut}(N)$ only	4,635
Poland	Coniferous forest	1,957		
	Deciduous forest	1,957		3,914
Russian Federation	Coniferous forest	4,929		
	Deciduous forest	2,983		
	Other	6,339		14,251
Spain	Coniferous forest	2,237		
	Deciduous forest	744		
	Mixed forest	428		3,409
Sweden	Forest	1,881		
	Lakes	3,172	acidity CLs only	5,053
Switzerland	Forest	11,883	717 acidity CLs only, 29 $CL_{nut}(N)$ only	
	Alpine lakes	495	431 acidity CLs only	
	Semi-natural ecosystems	11,559	$CL_{nut}(N)$ only	23,937
United Kingdom (excluding N. Ireland)	Coniferous forest	27,120		
	Deciduous forest	65,637		
	Acid grassland	134,910	4,778 $CL_{nut}(N)$ only	
	Calcareous grassland	23,146	1,389 $CL_{nut}(N)$ only	
	Heathlands	55,355	1,545 $CL_{nut}(N)$ only	
	Fresh water (catchments)	527		306,695
TOTAL:				**671,937**

Table 2-1 shows for each country the ecosystem types and their number of records. A remark is included when not all critical loads are provided for an ecosystem type.

Table 2-2 provides details on the number, area coverage, and density of ecosystems for which NFCs have submitted critical loads of acidity and/or nutrient nitrogen. The table gives an overview of the wide variation among countries in the average size, density, and national coverage of ecosystems.

The NFCs were requested to submit files with a specific structure, with each individual ecosystem record containing the following variables:

Variable	Unit
longitude and latitude of the site or reference point of the receptor	decimal degrees
indices of the EMEP50 grid cell	i, j
ecosystem area	km^2
acidity critical loads: $CL_{max}(S)$, $CL_{min}(N)$ and $CL_{max}(N)$	eq ha^{-1} yr^{-1}
critical loads of N preventing eutrophication: $CL_{nut}(N)$	eq ha^{-1} yr^{-1}
seasalt-corrected base cation deposition: BC^*_{dep}–CL^*_{dep}	eq ha^{-1} yr^{-1}
net base cation uptake: BC_u	eq ha^{-1} yr^{-1}
weathering of base cations: BC_w or ANC_w	eq ha^{-1} yr^{-1}
critical alkalinity leaching: $Al_{le(crit)} + H_{le(crit)}$ (= $-ANC_{le(crit)}$)	eq ha^{-1} yr^{-1}
nitrogen immobilization: N_i	eq ha^{-1} yr^{-1}
net nitrogen uptake: N_u	eq ha^{-1} yr^{-1}
acceptable nitrogen leaching: $N_{le(acc)}$	eq ha^{-1} yr^{-1}
ecosystem type	text

Table 2-2. Number of critical loads and spatial density for each national contribution.

		A	B	C	D
		Acidity Critical Loads:			
Country	Area (km²)	No. of ecosystems	Area (km²)	Ecosystem cover (%)	Average ecosystem area (km²)
Austria	83,907	6,444	48,721	58.1	7.56
Belgium	30,541	652	1,588	5.2	2.44
Croatia	56,401	34	2,698	4.8	79.36
Czech Republic	79,042	29,418	26,568	33.6	0.90
Denmark	42,756	18,784	3,895	9.1	0.21
Estonia	45,651	140	18,910	41.4	135.07
Finland	334,470	4,533	322,080	96.3	71.05
France	547,828	442	136,004	24.8	307.70
Germany	356,823	94,943	86,925	24.4	0.92
Hungary	92,969	42	2,847	3.1	67.77
Ireland	69,524	26,383	6,894	9.9	0.26
Italy	301,580	738	300,235	99.6	406.82
Netherlands	36,102	127,490	3,195	8.9	0.03
Norway	317,595	3,025	221,231	69.7	73.13
Poland	311,340	3,914	178,382	57.3	45.58
Russian Federation	5,090,400	14,251	3,778,983	74.2	265.17
Spain	499,183	3,409	85,225	17.1	25.00
Sweden	444,695	5,053	396,961	89.3	78.56
Switzerland	41,263	12,349	12,349	29.9	1.00
United Kingdom	244,402	298,983	86,986	35.6	0.29

		E	F	G	H
		Critical Loads of Nutrient Nitrogen:			
Country	Area (km²)	No. of ecosystems	Area (km²)	Ecosystem cover (%)	Average ecosystem area (km²)
Austria	83,907	6,444	48,721	58.1	7.56
Belgium	30,541	652	1,588	5.2	2.44
Croatia	56,401	34	2,698	4.8	79.36
Czech Republic	79,042	29,418	26,568	33.6	0.90
Denmark	42,756	9,757	3,149	7.4	0.32
Estonia	45,651	140	18,910	41.4	135.07
Finland	334,470	3,083	195,570	58.5	63.43
France	547,828	442	136,004	24.8	307.70
Germany	356,823	94,943	86,925	24.4	0.92
Hungary	92,969	42	2,847	3.1	67.77
Ireland	69,524	26,383	6,894	9.9	0.26
Italy	301,580	738	300,235	99.6	406.82
Netherlands	36,102	127,490	3,195	8.9	0.03
Norway	317,595	2,330	139,942	44.1	60.06
Poland	311,340	3,914	178,382	57.3	45.58
Russian Federation	5,090,400	14,251	3,778,983	74.2	265.17
Spain	499,183	3,409	85,225	17.1	25.00
Sweden	444,695	1,881	182,138	41.0	96.83
Switzerland	41,263	22,789	22,789	55.2	1.00
United Kingdom	244,402	306,168	87,827	35.9	0.29

		I	J	K	L
		Both acidity *and* nutrient nitrogen CLs:		Acidity *and/or* nutrient nitrogen CLs:	
Country	Area (km²)	No. of ecosystems	Area (km²)	No. of ecosystems	Area (km²)
Austria	83,907	6,444	48,721	6,444	48,721
Belgium	30,541	652	1,588	652	1,588
Croatia	56,401	34	2,698	34	2,698
Czech Republic	79,042	29,418	26,568	29,418	26,568
Denmark	42,756	9,757	3,149	18,784	3,895
Estonia	45,651	140	18,910	140	18,910
Finland	334,470	3,083	195,570	4,533	322,080
France	547,828	442	136,004	442	136,004
Germany	356,823	94,943	86925	94,943	86,925
Hungary	92,969	42	2,847	42	2,847
Ireland	69,524	26,380	6,894	26,386	6,894
Italy	301,580	738	300,235	738	300,235
Netherlands	36,102	127,490	3,195	127,490	3,195
Norway	317,595	720	40,521	4,635	320,651
Poland	311,340	3,914	178,382	3,914	178,381
Russian Federation	5,090,400	14,251	3,778,983	14,251	3,778,983
Spain	499,183	3,409	85,225	3,409	85,225
Sweden	444,695	1,881	182,138	5,053	396,961
Switzerland	41,263	11,201	11,201	23,937	23,937
United Kingdom	244,402	298,456	86,251	306,695	88,562

National data provided for acidity critical loads is summarized in columns A through D. Column A gives the number of ecosystems for which acidity critical loads ($CL_{max}(S)$, $CL_{min}(N)$, and $CL_{max}(N)$) have been calculated. Columns B and C show the total area of these ecosytems, and the percentage of the country covered by these ecosystems, respectively. The average size of an ecosystem is given in Column D. (Col. D=B/A.) Similar information for $CL_{nut}(N)$ is provided in Columns E-H.

Columns I and J show the number and total area of ecosystems for which *both* acidity critical loads *and* $CL_{nut}(N)$ have been submitted. Columns K and L provide similar data, showing the number and total area of ecosystems for which critical loads of acidity *and/or* nutrient nitrogen have been calculated (Col. K=A + E – I).

The wide range in the number and density of ecosystems among countries can be seen from the table. For most countries, critical loads of acidity and nutrient nitrogen are computed on the same set of ecosystems, as the number and area of ecosystems are the same for both types of critical loads.

The density of critical loads mapped varies greatly among countries. For example, the Netherlands computes critical loads for only 8.9% (3195 km^2) of its land, but the density of ecosystem points is very high compared with other countries. While a few countries have used total land area to represent the ecosystem area, future updates should strive to assess more accurately the true ecosystem area (leaving out urban areas, agricultural lands, etc.).

The differences in data density is also presented in Figure 2-1, which shows the distribution of ecosystem records (for critical loads of acidity) for each EMEP 150 x 150 km^2 grid cell. The map includes critical loads from both national contributions and from the European background data base.

2.3 Points requiring attention in future updates of national data

Suitability of ecosystems: Some countries have calculated critical loads for agriculturally managed ecosystems such as arable land or pastures. Arable land is not suitable for use as a receptor for setting critical loads of acidity and eutrophication due to air pollutants because of the overwhelming influences of anthropogenic activity (fertilizers, herbicides, pesticides, etc.). Both the updated Mapping Manual and previous CCE Status Reports have explained that critical loads should only be calculated for natural ecosystems, in order to accurately assess air pollution effects. Since anthropogenic influences mask any potential impacts from long-range air pollutants, agricultural areas should be excluded from critical load calculations. Only grasslands with extensive grazing might qualify as receptors for calculating critical loads.

Preliminary checking of national data submissions: In its recent call for data, the CCE included instructions for conducting some elementary consistency checks for NFCs to apply to their data before submitting them to the CCE. More stringent application of these checks in future submissions would reduce considerably the time and effort required to incorporate national critical loads calculations into the European maps.

Input data: In several instances, NFCs have used outdated input and parameter values which have been superseded by more recent values. The CCE strongly advises all NFCs to apply input and parameter values recommended in the 1996 update of the Mapping Manual (UBA 1996)

Resolving cross-border discrepancies: The percentile maps presented in Chapter 1 include several instances in which two (or more) countries that contribute national data have large differences in the calculated values along their common borders. These differences originate in most cases from variations in chosen input values for computing critical loads. Thus the NFCs of the affected countries are encouraged to address these discrepancies on a bilateral basis.

References

Downing, R.J., J.-P. Hettelingh and P.A.M. de Smet (eds.), 1993. Calculation and Mapping of Critical Loads in Europe: Status Report 1993. RIVM Rep. 259101003. National Institute for Public Health and Environmental Protection, Bilthoven, Netherlands.

Posch, M., P.A.M. de Smet, J.-P. Hettelingh and R.J. Downing (eds.), 1995. Calculation and Mapping of Critical Thresholds in Europe: CCE Status Report 1995. RIVM Rep. 259101004. National Institute for Public Health and the Environment, Bilthoven, Netherlands.

UBA, 1996. Manual on Methodologies and Criteria for Mapping Critical Levels/Loads and geographical areas where they are exceeded. UN/ECE Convention on Long-range Transboundary Air Pollution. Federal Environmental Agency (Umweltbundesamt), Texte 71/96, Berlin.

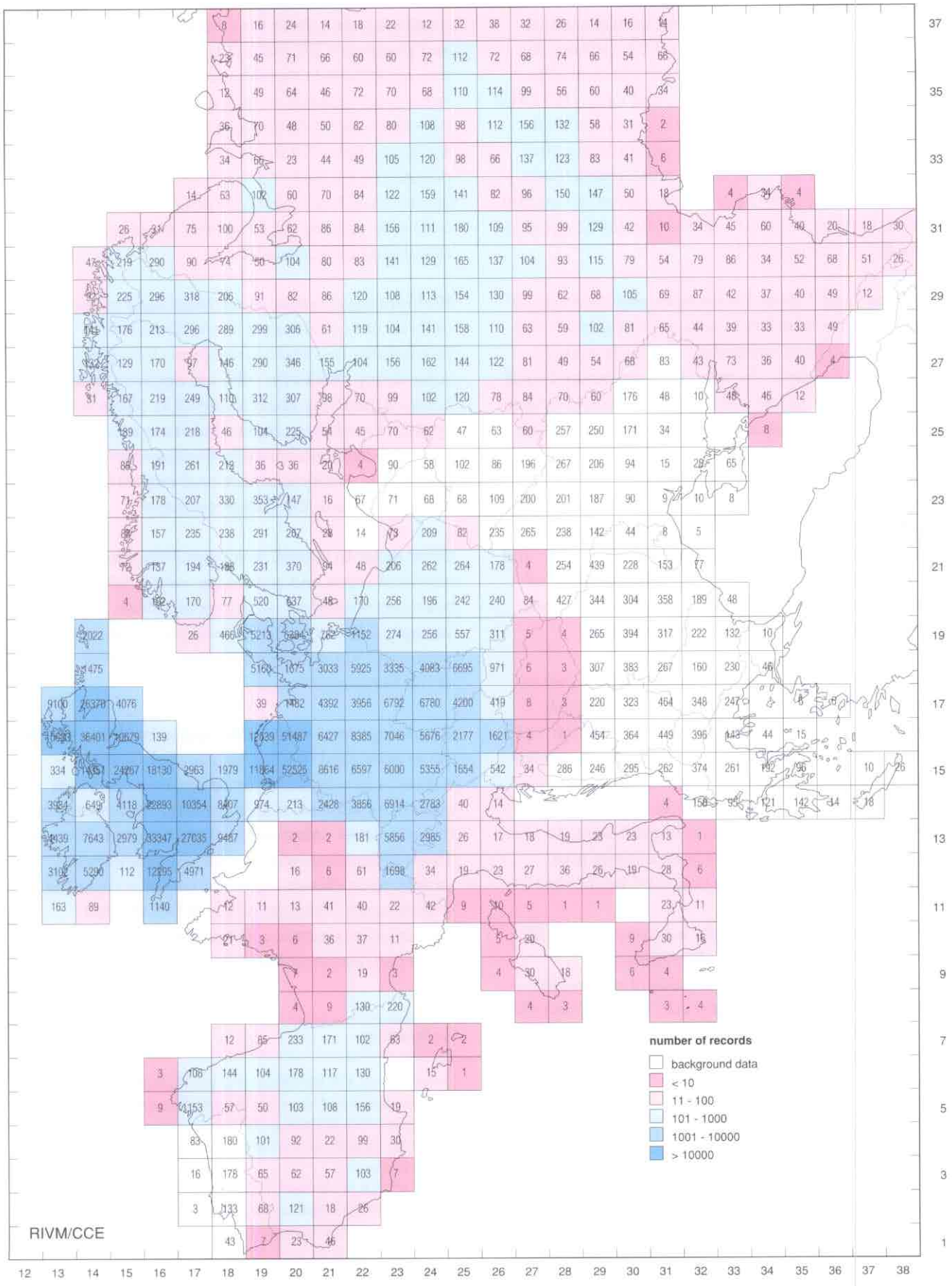

Figure 2-1. The number of ecosystems per EMEP150 grid cell with critical loads of acidity. The white grid cells denote areas for which critical loads are computed using the European background data base. (Data for $CL_{nut}(N)$ show a very similar picture.)

3. Remarks on Critical Load Calculations

M. Posch and J.-P. Hettelingh

Introduction

The methods for calculating critical loads of nitrogen (N) and sulfur (S) with the Simple Mass Balance (SMB) equation/model have been summarized in the previous CCE Status Report (Posch *et al.* 1995) and are more extensively documented in the new Mapping Manual (UBA 1996). Therefore, we will not repeat them in this chapter, but present the various possibilities for *using* the critical load information in the context of integrated assessment (comparison with deposition and their reductions).

3.1 The critical load function

Since the deposition of both S and N can contribute to the acidification of an ecosystem, no unique critical loads of sulfur or acidifying nitrogen can be specified. Rather, these critical loads are characterized by three quantities, $CL_{max}(S)$, $CL_{min}(N)$ and $CL_{max}(N)$, which define the so-called critical load function depicted in Figure 3-1. For every pair of deposition (N_{dep},S_{dep}) lying on the function or below it (the grey-shaded area in Fig. 3-1) neither critical loads of N nor S are exceeded.
Since it is impossible to define unique critical loads of N and S, it is also impossible to define a unique exceedance in the sense of quantifying the amount of S and N to be reduced. This is illustrated by the example in Figure 3-1: Let the point E1 denote the (current) deposition of N and S. By reducing N_{dep} substantially, one reaches the point Z1 and thus non-exceedance without reducing S_{dep}. On the other hand one can reach non-exceedance by only reducing S_{dep} (by a smaller amount) until reaching Z3; finally, with a smaller reduction of both N_{dep} and S_{dep} one can reach non-exceedance as well (e.g. point Z2). In practice external factors, such as the costs of emission reduction measures, will determine the path to be followed to reach zero exceedance. Note that in the above considerations we did not consider the special case $CL_{max}(N)$–$CL_{min}(N) = CL_{max}(S)$, i.e. the case of no deposition-dependent nitrogen processes, in which it is possible (within limits) to define unique critical loads and exceedances (for details see Posch *et al.* 1995).

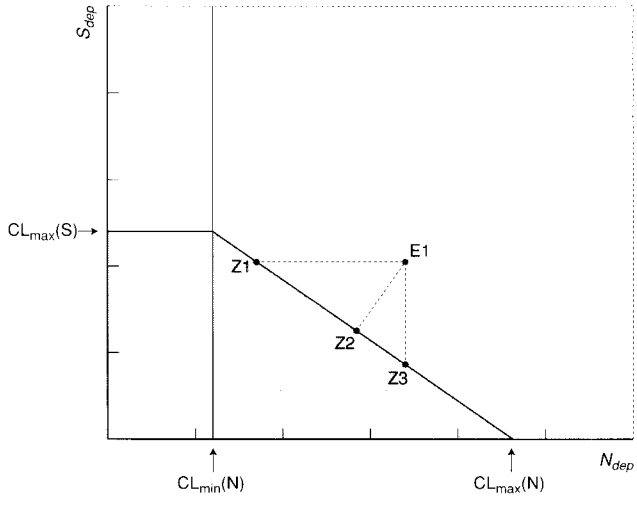

Figure 3-1. Critical load function of S and acidifying N defined by the three quantities $CL_{max}(S)$, $CL_{min}(N)$ and $CL_{max}(N)$.

3.2 Conditional critical loads of N and S

The non-uniqueness of the critical loads of N and S and their exceedances makes both their implementation into integrated assessment models and their communication to decision makers difficult. However, if one is interested in reductions of only one of the two pollutants, a unique critical load can be derived which is consistent with the above formulation.

If emission reductions deal with nitrogen only, a unique critical load of N for a *fixed* sulfur deposition S_{dep} can be derived from the critical load function. This conditional critical load of N, $CL(N \mid S_{dep})$, is computed as:

$$CL(N \mid S_{dep}) = \begin{cases} CL_{min}(N) & \text{if } S_{dep} \geq CL_{max}(S) \\ CL_{max}(N) - \alpha S_{dep} & \text{if } S_{dep} < CL_{max}(S) \end{cases} \quad (3.1)$$

with

$$\alpha = \frac{CL_{max}(N) - CL_{min}(N)}{CL_{max}(S)} \quad (3.2)$$

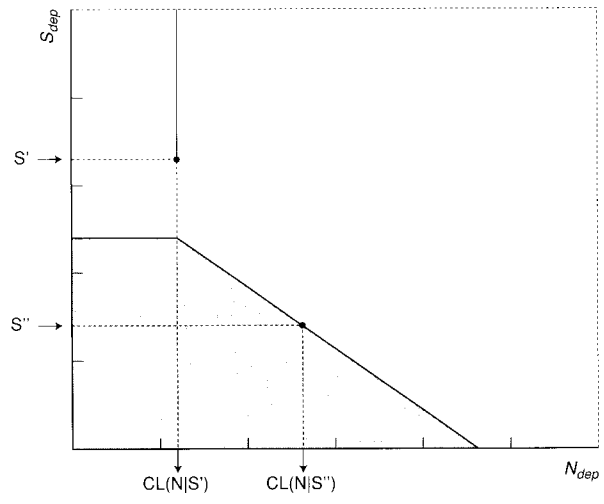

Figure 3-2. Examples of computing conditional critical loads of N for different S deposition values S' and S''.

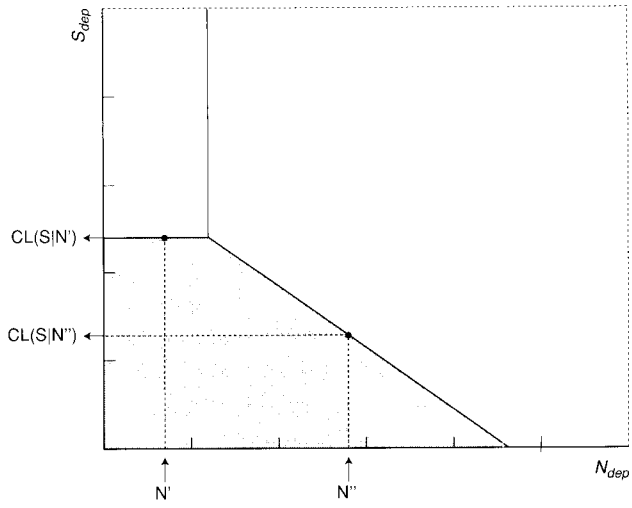

Figure 3-3. Examples of computing conditional critical loads of S for different N deposition values N' and N''.

In Figure 3-2 the procedure for calculating $CL(N \mid S_{dep})$ is depicted graphically.

If, in addition, the critical load of nutrient nitrogen, $CL_{nut}(N)$, for the same ecosystem is considered and is smaller than the computed $CL(N \mid S_{dep})$, the minimum of the two should be taken as the critical load of nitrogen.

In an analogous manner a conditional critical load of S, $CL(S \mid N_{dep})$, for a *fixed* nitrogen deposition N_{dep} can be computed according to:

$$CL(S \mid N_{dep}) = \quad (3.3)$$

$$\begin{cases} 0 & \text{if } N_{dep} \geq CL_{\max}(N) \\ \dfrac{CL_{\max}(N) - N_{dep}}{\alpha} & \text{if } CL_{\min}(N) < N_{dep} < CL_{\max}(N) \\ CL_{\max}(S) & \text{if } N_{dep} \leq CL_{\min}(N) \end{cases}$$

where α is given by Eq. 3.2. The procedure for calculating $CL(S \mid N_{dep})$ is depicted graphically in Figure 3-3.

Setting $N_{dep} = CL_{nut}(N)$, the resulting conditional critical load has been termed minimum critical load of sulfur in earlier publications (Downing *et al.* 1993): $CL_{min}(S) = CL(S \mid CL_{nut}(N))$.

Eq. 3.3 would have been the consistent procedure for calculating critical loads of S used in the negotiations of the 1994 Sulphur Protocol; however, critical loads for nitrogen – $CL_{min}(N)$ and $CL_{max}(N)$ – were not available then.

When using conditional critical loads the following caveats should be kept in mind:

(1) A conditional critical load can be considered a true critical load only when the chosen deposition of the other pollutant is kept constant.
(2) If the conditional critical loads of both pollutants are considered simultaneously, care has to be exercised. It is *not* necessary to reduce both exceedances, but only one of them to reach non-exceedance for both pollutants; recalculating the conditional critical load of the other pollutant results (in general) in non-exceedance. However, if $S_{dep} > CL_{max}(S)$ or $N_{dep} > CL_{max}(N)$, depositions have to be reduced at least to that maximum values, irrespective of the conditional critical loads.

3.3 Protection isolines

When dealing with critical loads of only one species (e.g. sulfur), their cumulative distribution functions within a grid cell and percentiles thereof are considered (see Posch *et al.* 1995 for the definition and computation of percentiles). In the case of sulfur and acidifying nitrogen, critical loads are given as functions (see above) and thus the concept of a percentile has to be generalized, leading to percentile functions or so-called protection isolines.

The (approximate) method to calculate these isolines is illustrated in Figure 3-4 (see Posch *et al.* 1995 for more details). Rays are drawn through the origin of the x-y plane (i.e. lines with a constant S:N deposition ratio) and the intersections of these rays with all critical load functions are determined (small circles in Figure 3-4b). For each ray the intersection points are sorted according to their distance from

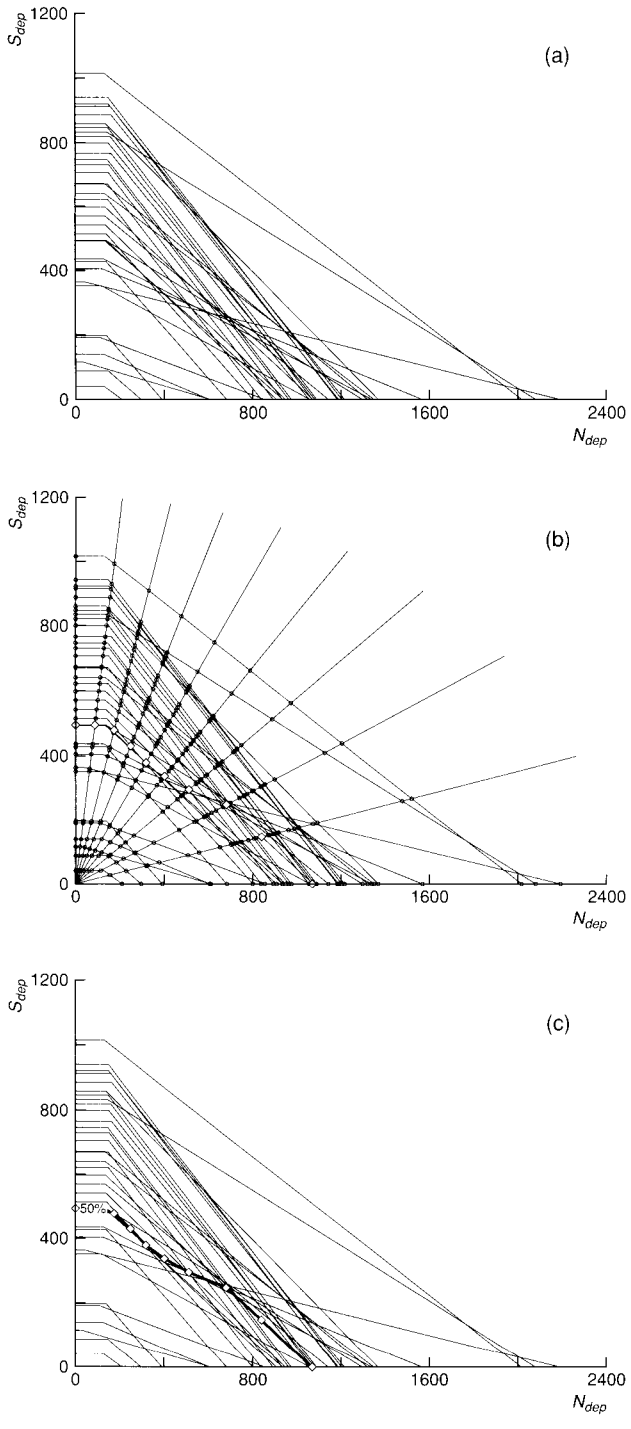

Figure 3-4. Critical load functions and the computation of a protection isoline: (a) set of critical load functions; (b) intersection of these CL functions with rays from the origin (small circles); (c) computing the percentile (50% in this case) along each ray (small diamonds) and connecting them to obtain the protection isoline (thick line).

the origin and a chosen percentile of these distances is calculated (small diamonds in Figure 3-4b,c). Finally, the resulting percentile values are connected by straight lines to form the protection isoline (Figure 3-4c). Obviously, the more rays are used in this procedure, the more accurate is the protection isoline. As the example in Figure 3-4 shows, a protection isoline is not necessarily convex.

Appendix B provides FORTRAN subroutines which can assist in the computation of protection isolines and protection percentages.

Ideally, the protection isolines computed as described above should be used in integrated assessment for determining (cost-)optimal N and S reductions. However, the non-convexity of isolines (see Figure 3-5a for examples) causes problems for many optimization programs. This can be overcome by computing the convex hull for each isoline and use it as an approximation for the true isoline (see Figure 3-5b). Note however, that some combinations of S and N deposition that lie outside the original isoline could now lie within the convex hull.

These convex hulls of the true isolines may still consist of many line segments, and each single line segment has to be translated in a constraint for the optimization programs, thus resulting in a potentially very large number of constraints.

Therefore, to further ease the optimization problem, the following approximation to the protection isolines is used, e.g., in the RAINS model: The p-th protection isoline for every grid cell is approximated by the trapezoid constructed from the three points $(0,CL_{max}(S))$, $(CL_{min}(N),CL_{max}(S))$ and $(CL_{max}(N), 0)$, where $CL_{max}(S)$, $CL_{min}(N)$ and $CL_{max}(N)$ are the $(100–p)$-th percentile of the respective cumulative distribution functions (see Figure 3-5c for an example). (Incidentally, this method was first elaborated in the 1993 Status Report (Posch *et al.* 1993), before the protection isoline concept had been developed.) Note that these trapezoids touch the N- and S-axes at the same points a the exact isolines. In addition, the percentiles of $CL_{min}(N)$ also stays explicitly available, which is not the case for the protection isolines.

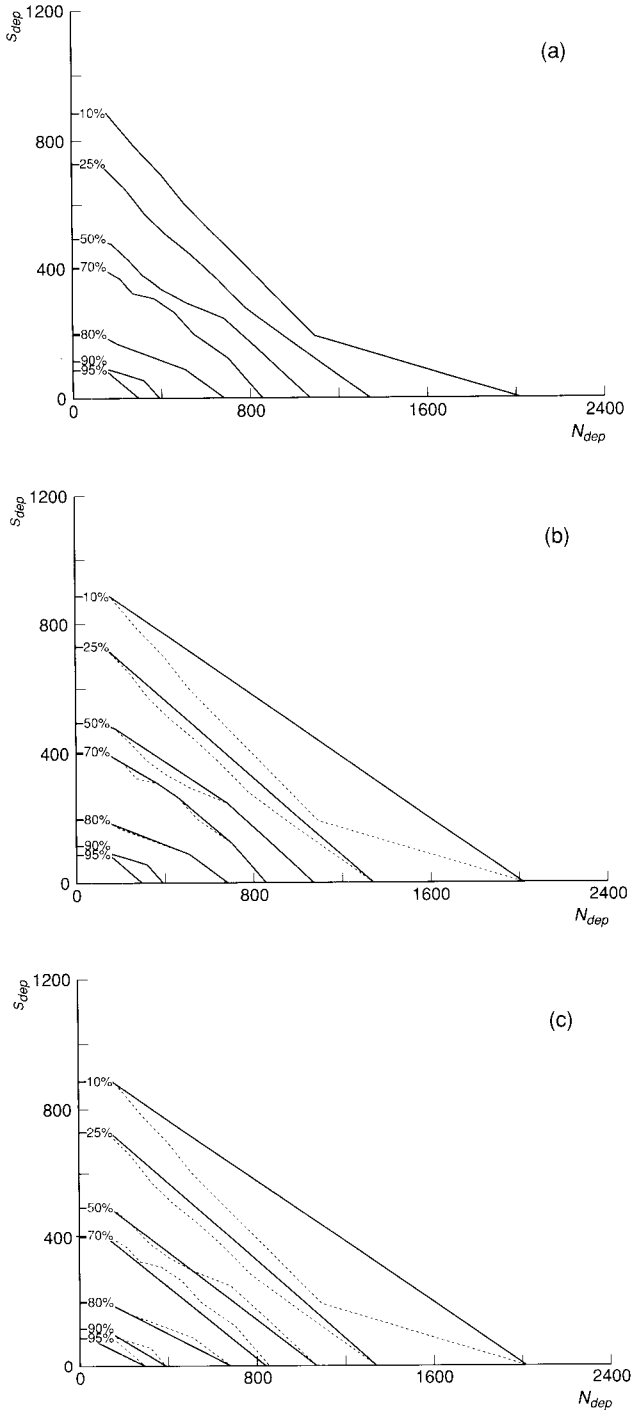

Figure 3-5. (a) Examples of protection isolines (computed from the critical load functions shown in Figure 3-4); (b) the convex hulls (solid lines) of those protection isolines (dotted lines); (c) the trapezoids (solid lines) constructed from the respective percentiles of $CL_{max}(S)$, $CL_{min}(N)$ and $CL_{max}(N)$ (protection isolines shown as dotted lines for comparison).

References

Downing, R.J., J.-P. Hettelingh and P.A.M. de Smet (eds.), 1993. Calculation and Mapping of Critical Loads in Europe: Status Report 1993. RIVM Rep. 259101003. National Institute for Public Health and Environmental Protection, Bilthoven, Netherlands.

Posch, M., J.-P. Hettelingh, H.U. Sverdrup, K. Bull and W. de Vries, 1993. Guidelines for the computation and mapping of critical loads and exceedances of sulphur and nitrogen in Europe. *In*: R.J. Downing *et al.*, 1993, *op.cit.*, pp. 25-38.

Posch, M., P.A.M. de Smet, J.-P. Hettelingh and R.J. Downing (eds.), 1995. Calculation and Mapping of Critical Thresholds in Europe: CCE Status Report 1995. RIVM Rep. 259101004. National Institute for Public Health and the Environment, Bilthoven, Netherlands.

UBA, 1996. Manual on Methodologies and Criteria for Mapping Critical Levels/Loads and geographical areas where they are exceeded. UN/ECE Convention on Long-range Transboundary Air Pollution. Federal Environmental Agency (Umweltbundesamt), Texte 71/96, Berlin.

4. An Analysis of Critical Load and Input Data Variability

J.-P. Hettelingh and M. Posch

Introduction

The reliability of critical load computations has received increasing attention recently, as the application of European critical loads is approaching the phase in which these results are used to support negotiations on a new nitrogen protocol. Critical loads and the magnitudes of their exceedances are used together with costs of emissions reductions in integrated assessment models to compare alternative policy options.

The uncertainty of critical loads is only one of the elements contributing to the varying reliability of the final outcome of such assessments. Error propagation due to emission and cost data uncertainties, and uncertainties in atmospheric transport and critical load modeling, require a cautious treatment of the quantitative results of integrated assessment modeling. Therefore, the negotiation process under the UN/ECE LRTAP Convention focuses on *relative*, rather than *absolute* assessments. When comparing different scenarios, the variability among them is primarily due to the variation in policy options in each scenario, rather than due to error propagation. The latter is independent of policy options because methodological causes of error propagation can be assumed to be fairly constant in each scenario.

Error propagation in integrated assessment is the subject of ongoing collaboration between the Coordination Center for Effects and the Task Force on Integrated Assessment Modeling (TFIAM). This chapter addresses the verification and validation of critical loads and the input data used to compute them.

Verification and validation of numerical models describing complex systems is impossible (Oreskes *et al.* 1994) because natural systems are open, i.e. subject to interactions with other systems. They write that "the terms 'verification' and 'validation' are now being used by scientists in ways that are contradictory and misleading. In the earth sciences–hydrology, geochemistry, meteorology, and oceanography–numerical models always represent complex open systems in which the operative processes are incompletely understood and the required empirical input data are incompletely known."

Similarly, one could argue that *validation* of critical loads is not possible, because it may take a long time before the appropriateness of the critical load as a risk indicator is established, i.e. before critical load exceedance leads to actual damage. Even if critical load computations were validated using measured inputs, this would still not ensure that critical load values could currently be "confirmed" as an indicator for the risk of damage due to excess deposition.

However, *verification*, i.e. the comparison of model behavior to expectations, is possible to a certain extent. This chapter provides an analysis of the variability of input data and critical load results, with focus on the Steady-state Mass Balance (SMB) approach. The SMB model was used by most of the National Focal Centers (NFCs) to compute critical loads for forest soils. Critical loads for forest soils and other ecosystems (see Chapter 2) which were derived by other, empirical approaches (including expert opinion) are difficult to subject to systematic uncertainty analysis.

The analysis presented here focuses on the variability of European critical loads, treating erroneous assumptions or errors associated with observed or estimated quantities as random events affecting the variability of critical loads. The analysis does not address the causes of uncertainty, i.e. whether uncertainty is due to inadequate representation of the processes involved or implementation failures. It is assumed that these and other causes of uncertainty which may vary among countries add randomly to the variability of critical loads. A more detailed taxonomy of uncertainties regarding critical loads can be found in Barkman (1997). This chapter is restricted to a description of the variability of input data from National Focal Centers, and describes the results of a Monte Carlo analysis using the SMB model when applied to European background and NFC data.

4.1 Background to the analysis

4.1.1 Critical load equations

The equations for the computation of critical loads can be summarized as (Posch *et al.* 1995):

$$Bc_{le} = 1.5 \cdot (x_{CaMgK} \cdot ANC_w + Bc_{dep} - Bc_u)$$

$$ANC_{le(crit)} = (Q^2 \cdot Bc_{le} / ((Bc:Al)_{crit} \cdot K_{gibb}))^{1/3} + Bc_{le} / (Bc:Al)_{crit}$$

$$CL_{max}(S) = ANC_w + Bc_{dep} - Bc_u + ANC_{le(crit)}$$

$$CL_{min}(N) = N_u + N_i$$

$$CL_{max}(N) = CL_{min}(N) + CL_{max}(S) / (1 - f_{de})$$

$$CL_{nut}(N) = N_u + N_i + N_{le(acc)} / (1 - f_{de})$$

where:

Bc_u = net base cation uptake
x_{CaMgK} = fraction of weathering as Ca+Mg+K
ANC_w = base cation weathering
Bc_{dep} = base cation deposition
$ANC_{le(crit)}$ = critical ANC leaching
Q = runoff
$(Bc:Al)_{crit}$ = critical base cation to aluminum ratio
$Cl_{max}(S)$ = maximum critical load for sulfur
$CL_{min}(N)$ = minimum critical load for nitrogen
N_u = net nitrogen uptake
N_i = nitrogen immobilization
$CL_{max}(N)$ = maximum critical load for nitrogen
f_{de} = denitrification fraction
$N_{le(acc)}$ = acceptable nitrogen leaching
$CL_{nut}(N)$ = critical load for eutrophication

4.1.2 Analyses of critical load variability

Critical load variability is investigated in two ways: one based on semi-quantitative comparisons of national data (described in point 1 below) and the other based on a systematic Monte Carlo-based approach (points 2 through 5):

1. Cumulative distributions of national data: A comparison is made among national inputs of Bc_u, N_u, N_i, $N_{le(acc)}$, ANC_w, and $ANC_{le(crit)}$, focusing on consistency checks where possible and appropriate, e.g. (a) between the data and Mapping Manual recommendations, (b) among distribution ranges of the variables submitted by each NFC and (c) of the correlation between nitrogen and base cation uptake for each country.

In the following points Monte Carlo analysis using PRISM (Gardner *et al.* 1983) is applied to the computation of $CL_{max}(S)$, $CL_{max}(N)$ and $CL_{nut}(N)$. These variables have been chosen because of their relevance to the TFIAM. Monte Carlo analysis is applied using the following input data:

2. Variability of critical loads using the European background database (EU-DB): Monte Carlo analysis is used to identify input variables which explain most of the variability of the distribution of $CL_{max}(S)$, $CL_{max}(N)$ and $CL_{nut}(N)$ using cumulative distributions of input variables taken from the EU-DB (described in Chapter 5). Figure 4-1 illustrates the cumulative distributions for Europe of base cation deposition, weathering and uptake; nitrogen uptake and acceptable N leaching; and runoff.

3. Variability of critical loads using NFC data: Again, Monte Carlo analysis is used to identify input variables which explain most of the variability of the European distribution of $CL_{max}(S)$, $CL_{max}(N)$, and $CL_{nut}(N)$ using cumulative distributions of input variables derived from the data submitted by the National Focal Centers.

4. Variability of critical loads using data from an arbitrary "binding" grid cell: A "binding" grid cell has been defined as an EMEP150 grid cell for which the cost minimization of emission reductions subject to a deposition constraint, yields a deposition value in that grid cell equal to the constraint. The set of binding grid cells across Europe can be different for each scenario. A characteristic of a binding grid cell is that the marginal costs of reducing deposition by an additional unit become significantly higher than in other grid cells. The issue of binding grid cells drew much attention in a preliminary assessment in developing an acidification strategy for the European Union (see Amann *et al.* 1996). Questions were raised about the reliability of critical load values in binding grid cells which, considering the fact that any grid cell could be binding depending on the scenario, could be generalized to the reliability of critical load values in general.

To illustrate the difference in variability of critical load values between Europe as a whole and an individual grid cell, an EMEP150 grid cell in the "Black Triangle" region (of the Czech Republic, Germany, and Poland) has been investigated in detail. This grid cell was identified in the EU study as binding when trying to reduce eutrophication. Figure 4-2 shows the cumulative distributions of the input variables in grid cell (23,18) using European background data. It is obvious that the ranges of these data are narrower than those of the European cumulative distributions shown in Figure 4-1. This difference can be seen in the cumulative distributions of most input variables in the grid cell, which are almost constant.

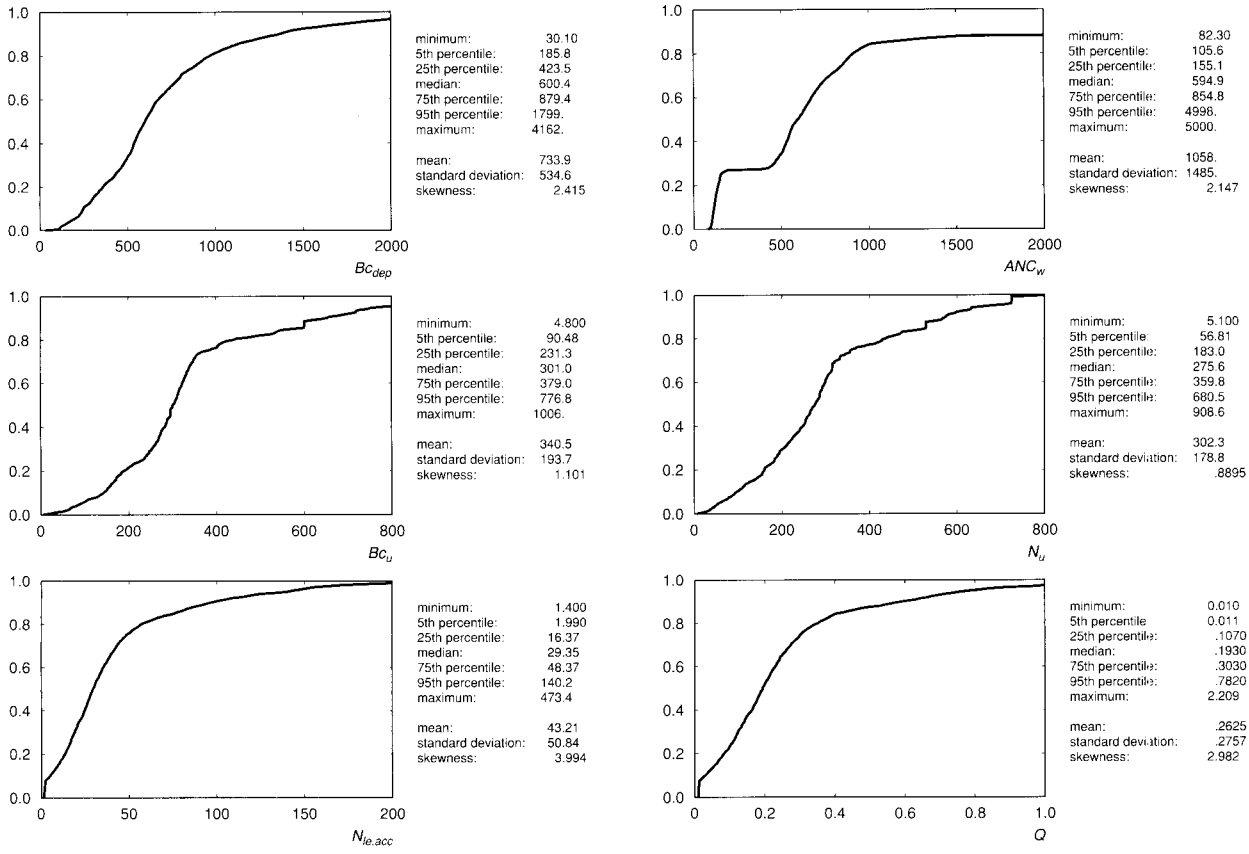

Figure 4-1. Cumulative distributions for Europe of base cation deposition, weathering and uptake; nitrogen uptake and acceptable N leaching; and runoff from the EU-DB.

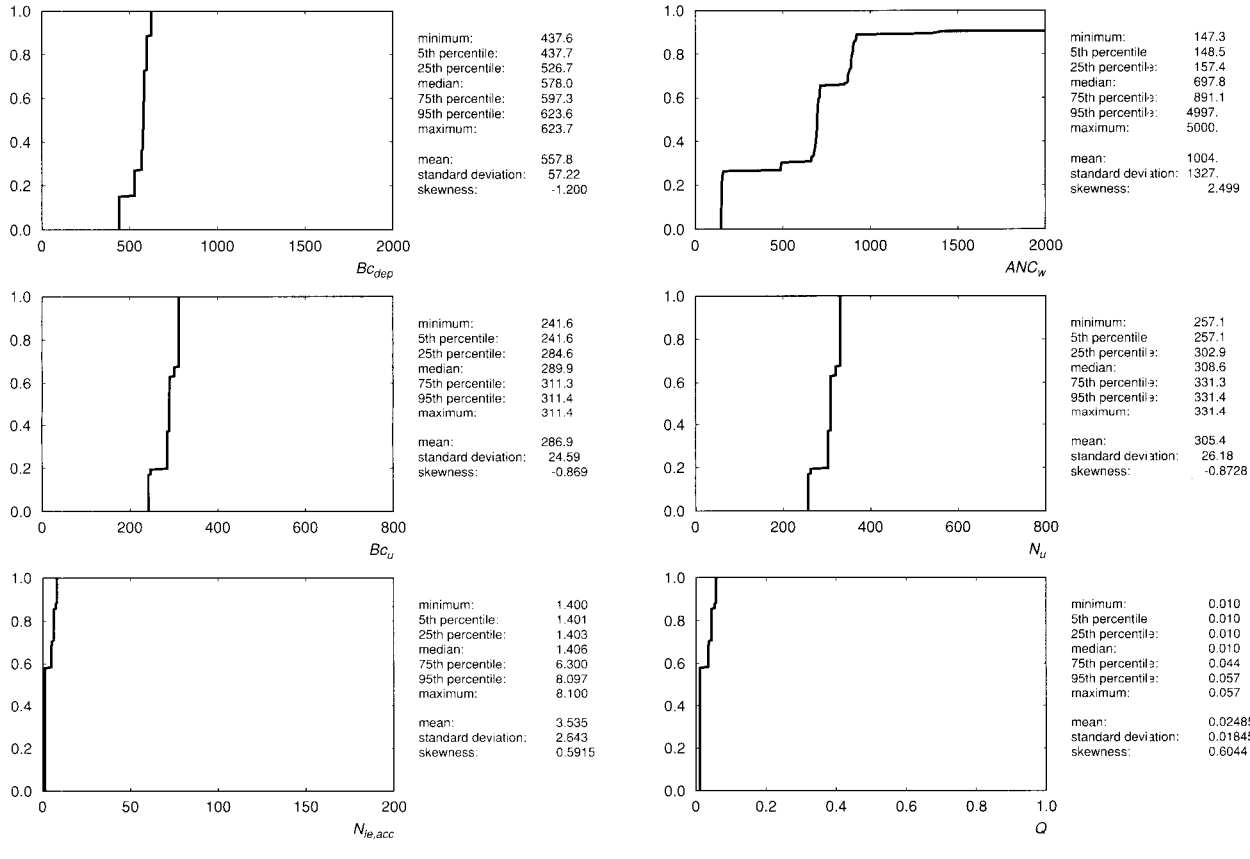

Figure 4-2. Cumulative distributions for EMEP150 grid cell (23,18) of base cation deposition, weathering and uptake; nitrogen uptake and acceptable N leaching; and runoff from the EU-DB. Note that the scales on the x-axes are the same as in Figure 4-1.

5. Variability of critical loads due to varying the critical BC/Al ratio: Recently it has been suggested that a critical BC/Al ratio of 1 may not be appropriate for assessing some critical loads at specific sites (Løkke *et al.* 1996). Here we do not discuss to what extent these results can be extrapolated to the European scale in a reliable manner. Rather, Monte Carlo analysis has been used to investigate the conditions under which a large contribution of BC/Al to the variability of $CL_{max}(S)$ and $CL_{max}(N)$ can be expected. The effect of varying BC/Al on the variability of these critical load values was tested both on the European scale and in the grid cell (23,18).

4.2 Results

4.2.1 *Cumulative distribution functions of national input data*

Cumulative distributions of the input parameters ANC_w, $ANC_{le(crit)}$, N_i, $N_{le(acc)}$, Bc_u and N_u for forest soils have been analyzed.

The weathering and critical leaching of ANC are generally soil-dependent and can be expected to vary widely among countries as shown in Figure 4-3. Countries with ANC_w and $ANC_{le(crit)}$ values exceeding 5000 eq ha^{-1} yr^{-1} contain areas with calcareous soils. Some countries (e.g. Switzerland, Denmark and Sweden) have small percentages of areas where $ANC_{le(crit)}$ is negative, suggesting that acidic deposition should be reduced below net base cation input to allow base cation replenishment. Note that Italy has used an empirical ("Level 0") approach which does not require data on ANC_w nor $ANC_{le(crit)}$ (but values of zero were submitted).

Figure 4-4 shows cumulative distribution functions of the NFCs' N_i values. The recommended values (UBA 1996) range between 0.5 and 1.0 kg N ha^{-1} yr^{-1} (35.7–71.4 eq ha^{-1} yr^{-1}). These values are based on data from Swedish forest soils, which Rosén *et al.* (1992) used to estimate the annual net nitrogen immobilization since the last glaciation. It can be seen from Figure 4-4 that, except for Finland, Ireland and the Russian Federation, many countries submitted values which lie outside the recommended range. *It should be noted that use of the recommended values would have resulted in substantially lower critical load values for nutrient nitrogen.* Some countries submitted negative values for N_i, suggesting that nitrogen fixation exceeds the sum of all other nitrogen sinks. The distribution of $N_{le(acc)}$ values shown in Figure 4-4 reflects which sensitive (indicator) system was chosen by each country, and which harmful effects are addressed.

Figure 4-5 depicts the cumulative distribution functions of national base cation and nitrogen uptake values. Countries are requested to submit net growth uptake values (corresponding to harvested biomass) and not the uptake due to element cycling. For example, uptake values of zero could be expected in a natural park where no tree harvesting is practiced. High uptake values indicate high growth or intensive harvesting.

No fixed values have been recommended for either Bc_u or N_u for computing of critical loads; however, one way to verify submitted values is the fact that tree growth requires proportional uptake of both base cations and nitrogen. This means that the ratio of base cation to nitrogen uptake should be almost constant for a given tree species, with only minor variations due to climate and site quality. The correlations between base cation uptake and nitrogen uptake for each national contribution is shown in Figure 4-6.

Figure 4-6 shows that uptake rates do not follow the expected pattern in several countries. For example, Austria submitted data for 6444 sites which shows two clusters. One subset of sites shows zero base cation uptake and non-zero nitrogen uptake. The other larger group shows combinations of increasing base cation uptake and constant nitrogen uptake. Another interesting correlation is shown for Poland, where positive base cation uptake coincides with nitrogen uptake close to zero. For some countries, such as the United Kingdom, three uptake values have been used to represent uptake in more than 90,000 sites. Constant uptake ratios are illustrated by the data of (e.g.) Denmark, Finland and the Netherlands.

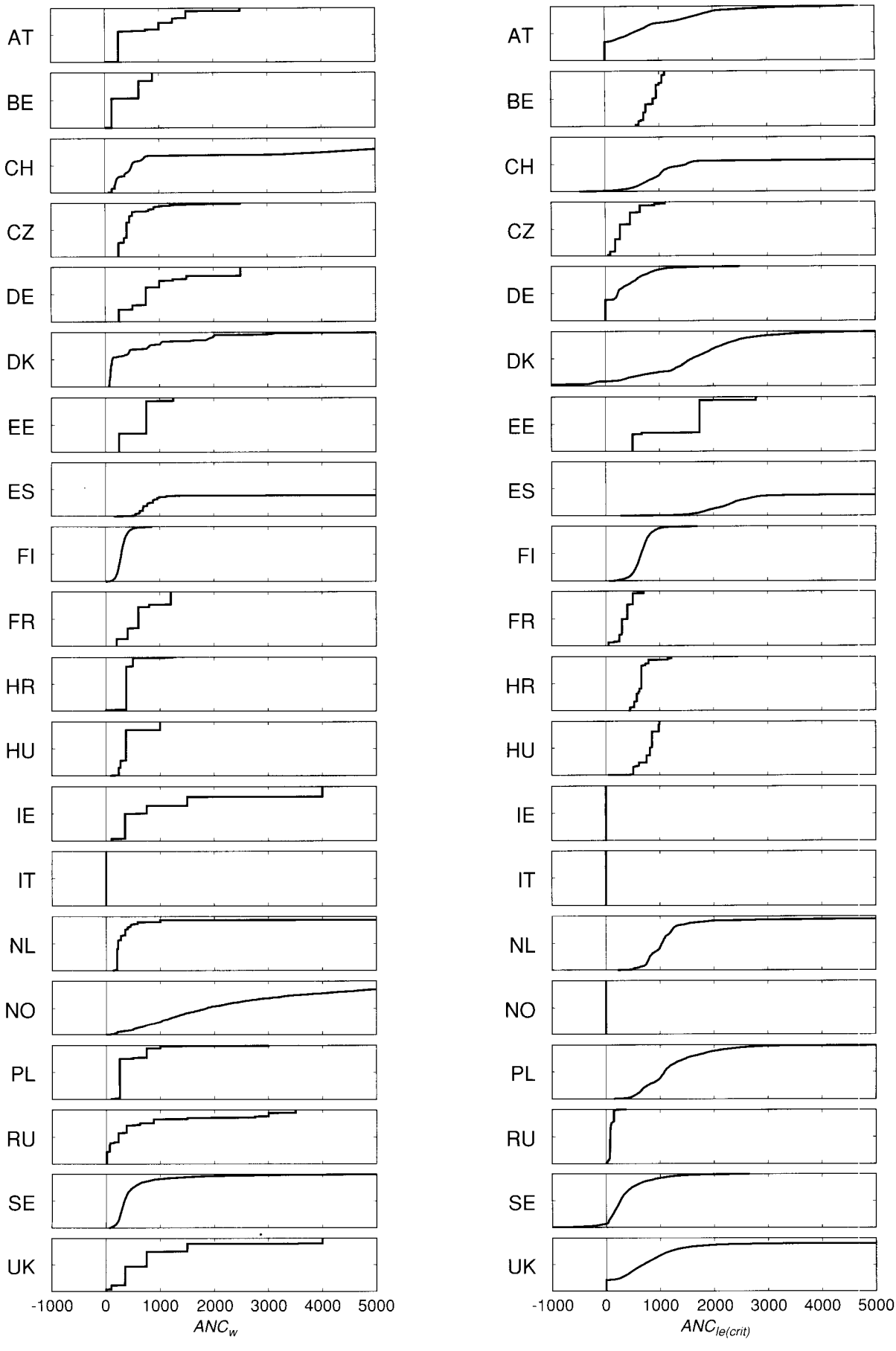

Figure 4-3. Cumulative distribution functions for critical ANC leaching and weathering (in eq ha^{-1} yr^{-1})used in the SMB calculations of critical loads for forest soils from national data contributions.

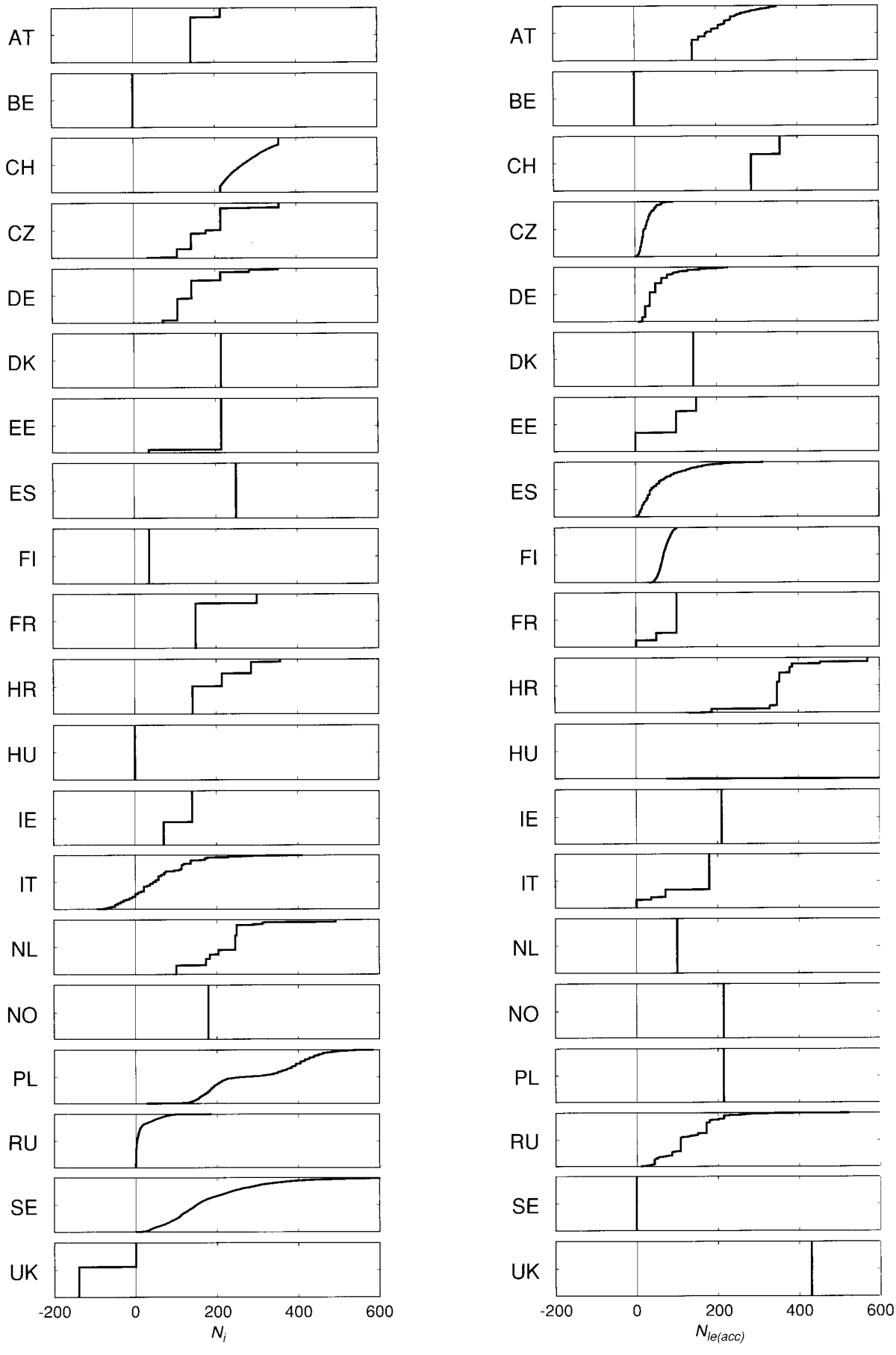

Figure 4-4. Cumulative distribution functions for nitrogen immobilization and acceptable nitrogen leaching (in eq ha^{-1} yr^{-1}) used in the SMB calculations of critical loads for forest soils from national data contributions.

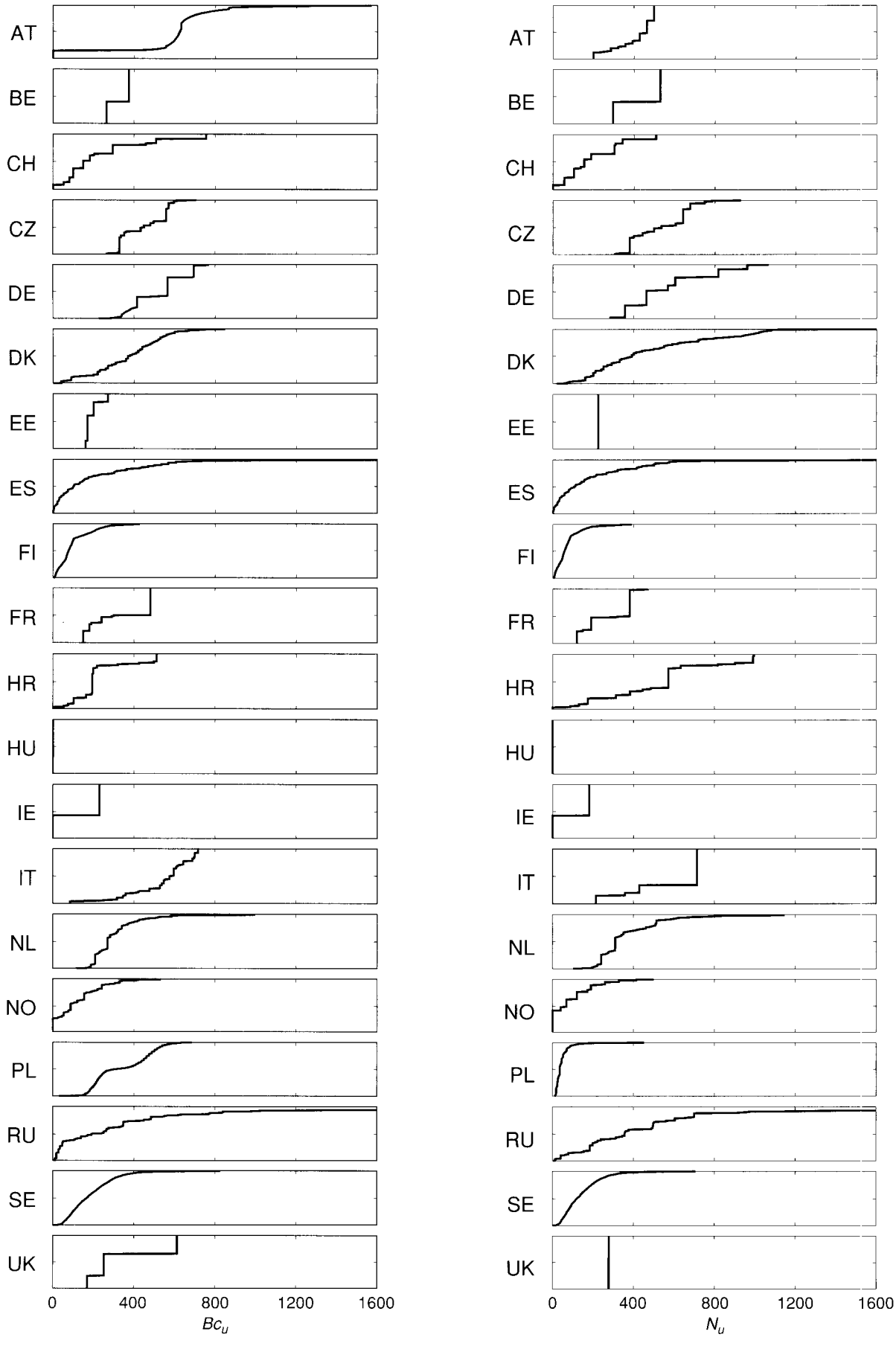

Figure 4-5. Cumulative distribution functions for base cation and nitrogen uptake (in eq ha^{-1} yr^{-1}) used in the SMB calculations of critical loads for forest soils from national data contributions.

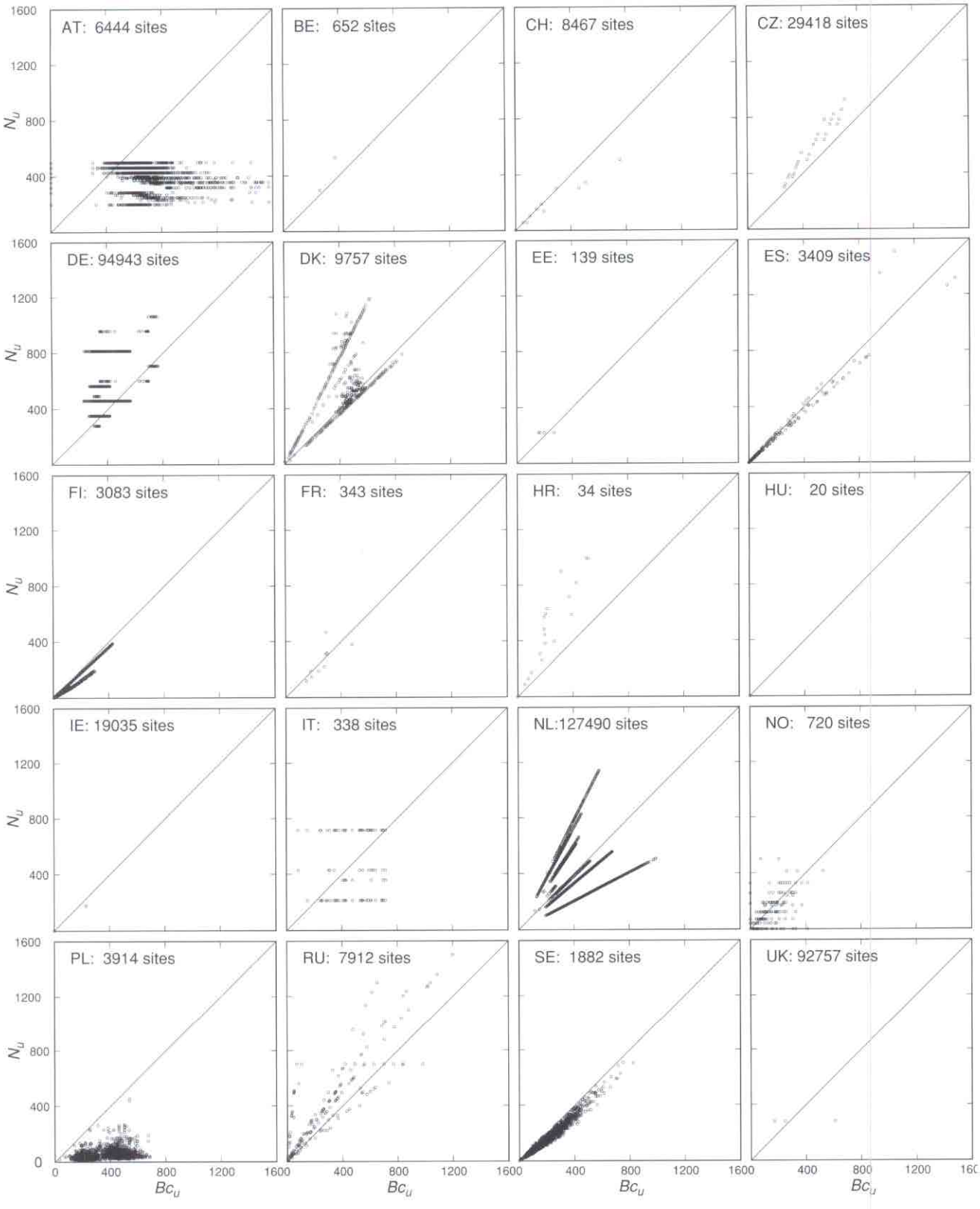

Figure 4-6. Correlation between net base cation (Ca+Mg+K) and nitrogen uptake (in eq ha^{-1} yr^{-1}) used in the SMB calculations of critical loads for forest soils from national data contributions. (See also Fig. 4-5).

4.2.2 *Variability of critical loads using data from European background and NFC data bases*

Tables 4-1 to 4-4 show the percentage of the variability of critical loads which is explained by input variables from the EU-DB and NFCs, both for Europe and grid cell (23,18). The results shown in Table 4-1 use a constant $(Bc:Al)_{crit}$ =1. Table 4-1 shows that ANC_w explains 45% of the variation of $CL_{max}(S)$ in Europe, and 97% in grid cell (23,18) when EU-DB is used. ANC_w remains the most important explanatory variable when NFC data are used, explaining 68% of $CL_{max}(S)$ variation in Europe, and 85% of the variation in grid cell (23,18). The second most important variable is base cation deposition, although it explains more of the $CL_{max}(S)$ variation in Europe compared with grid cell (23,18).

Table 4-1. Percent contributions of input variables to the variability of $CL_{max}(S)$ in Europe and grid cell (23,18) using EU-DB and NFC input data, assuming $(Bc:Al)_{crit}$ =1.

	Europe		Grid cell (23,18)	
	EU-DB	NFC	EU-DB	NFC
ANC_w	45	68	97	85
Bc_{dep}	48	18	–	6
Bc_u	2	3	–	6

Table 4-2 shows similar results for $CL_{max}(N)$.

Table 4-2. Percent contributions of input variables to the variability of $CL_{max}(N)$ in Europe and grid cell (23,18) using EU-DB and NFC input data assuming $(Bc:Al)_{crit}$ =1 and N_i=35.7 eq ha-1 yr-1 as recommended in UBA (1996).

	Europe		Grid cell (23,18)	
	EU-DB	NFC	EU-DB	NFC
ANC_w	33	60	77	63
Bc_{dep}	44	15	–	4
f_{de}	7	4	15	15
Bc_u	2	2	–	4

A tentative conclusion from Tables 4-1 and 4-2 is that ANC_w explains most of the variation of $CL_{max}(S)$ and $CL_{max}(N)$, assuming a critical BC/Al ratio of 1.

By varying the critical BC/Al ratio in a range between 0.2 and 10 (see Sverdrup and Warfvinge 1993), the percentage contributions to the variability of $CL_{max}(S)$ and $CL_{max}(N)$ change as shown in Table 4-3 and 4-4 respectively.

Table 4-3. Percent contributions of input variables to the variability of $CL_{max}(S)$ in Europe using EU-DB and NFC input data, allowing $(Bc:Al)_{crit}$ to vary between 0.2 and 10, and restricting the maximum value of ANC_w.

	EU-DB			NFC data
	full range	ANC_w <250	ANC_w <100	full range
ANC_w	33	38	9	64
Bc_{dep}	34	–	–	15
Bc_u	2	–	–	2
$(Bc:Al)_{crit}$	5	27	42	3

Table 4-4. Percent contributions of input variables to the variability of $CL_{max}(N)$ in Europe using EU-DB and NFC input data, allowing $(Bc:Al)_{crit}$ to vary between 0.2 and 10, restricting the maximum value of ANC_w, and setting N_i=35.7 eq ha^{-1} yr^{-1}.

	EU-DB			NFC data
	full range	ANC_w <250	ANC_w <100	full range
ANC_w	32	18	2	54
Bc_{dep}	31	–	–	14
f_{de}	4	16	10	5
Bc_u	1	–	–	–
$(Bc:Al)_{crit}$	4	13	8	3
N_u	–	26	62	3

Note that the explanatory power of $(Bc:Al)_{crit}$ and N_u is reversed as ANC_w decreases below 100 eq ha^{-1} yr^{-1}.

From Tables 4-3 and 4-4 it can be concluded that the explanatory power of $(Bc:Al)_{crit}$ to the variability of $CL_{max}(S)$ and $CL_{max}(N)$ increases in regions where the net base cation input is low. Nitrogen uptake tends to explain more of the variability of $CL_{max}(N)$ when net base cation input decreases to below 100 eq ha^{-1} yr^{-1}. The non-shaded grid cells in Figure 4-7 indicate areas in which net base cation input is higher than 100 eq ha^{-1} yr^{-1} for more than 95% of the ecosystem area. For these regions one could say that $ANC_{le(crit)}$ (i.e. the assumption $(Bc:Al)_{crit}$ =1) is not significant in explaining the uncertainty of $CL_{max}(S)$ and $CL_{max}(N)$. Thus, $ANC_{le(crit)}$ could be neglected in computing critical loads. In the grey-shaded regions, $ANC_{le(crit)}$ values are important for computing critical loads of sulfur and acidifying nitrogen.

Table 4-5 shows the percentage of the uncertainty of $CL_{nut}(N)$ explained by N_u, N_i, $N_{le(acc)}$ and f_{de}. Using the European background data base indicates that N_u is the most important explanatory variable. Since NFCs have used a wide range of N_i values, its importance increases accordingly.

Table 4-5. Percent contributions of input variables to the variability of $CL_{nut}(N)$ in Europe and grid cell (23.18) using EU-DB and NFC input data, using $(Bc{:}Al)_{crit}$ =1 and N_i=35.7 eq ha^{-1} yr^{-1} as recommended in UBA (1996).

	Europe		Grid cell (23,18)	
	EU-DB	NFC	EU-DB	NFC
N_u	83	87	97	39
N_i	–	6	–	19
$N_{le(acc)}$	15	6	17	24
f_{de}	3	1	1	14

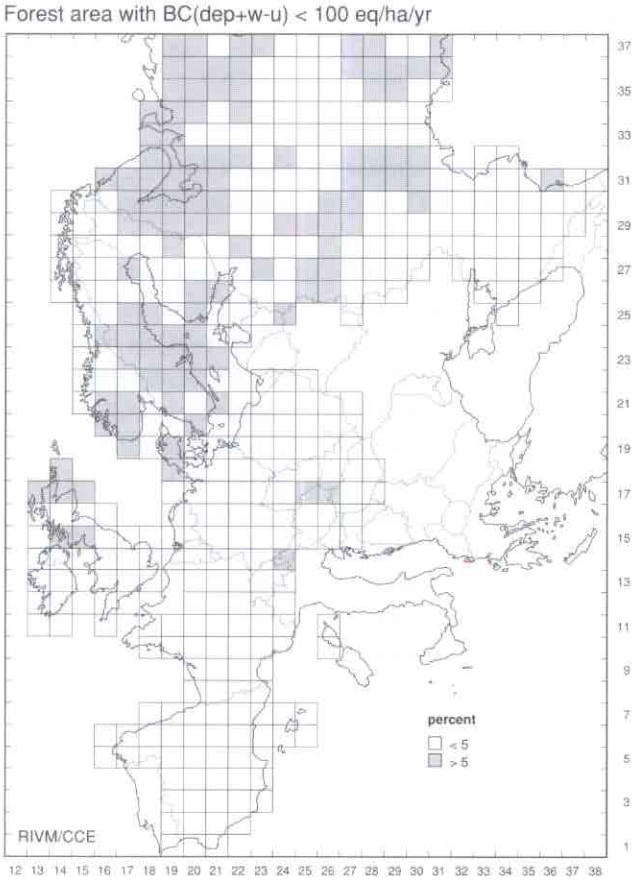

Figure 4-7. Percent of forest area in each EMEP150 grid cell with net base cation input (deposition+weathering–uptake) less than 100 eq ha^{-1} yr^{-1}.

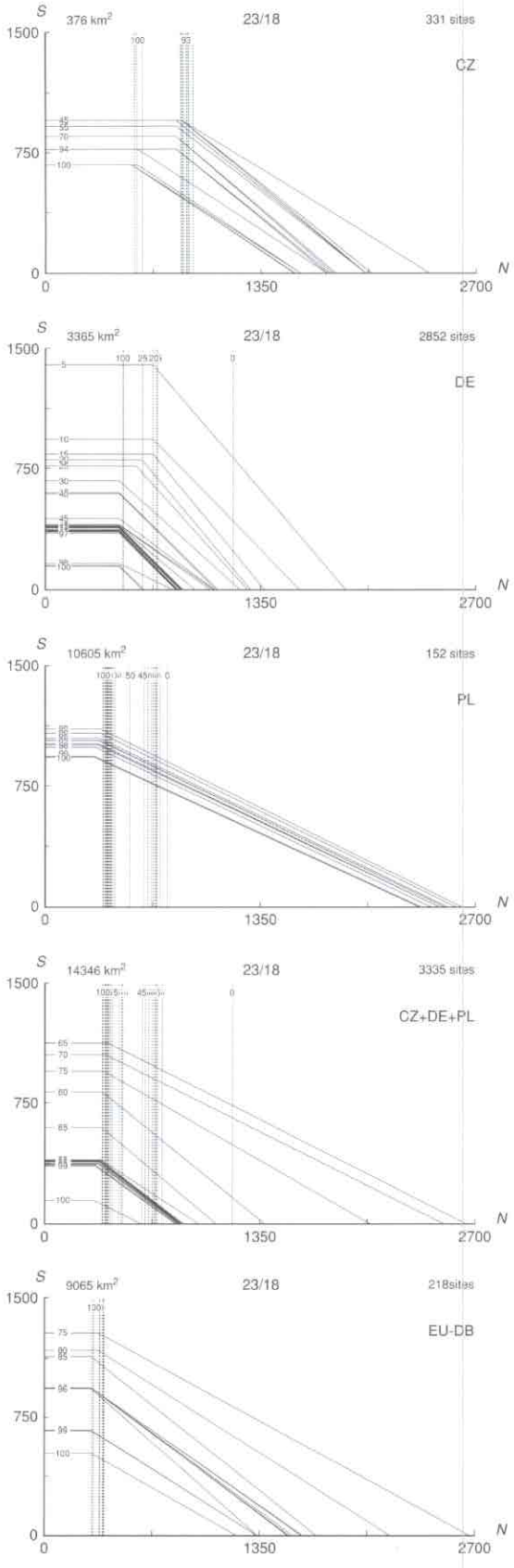

Figure 4-8. Approximated protection isolines for grid cell (23,18). Five sets of protection isolines are shown: (CZ) for the Czech portion of the grid cell, (DE) for the German portion, (PL) for the Polish portion (all of which use national data), and (CZ+DE+PL) for the three countries together. The fifth plot (EU-DB) shows protection isolines using the European background data base.

4.2.3 A closer look at the data in grid cell (23,18)

Figure 4-8 shows the approximated protection isolines for grid cell (23,18) (see Chapter 3 for details on the calculation methods). The country-to-country variation of the ranges may provide answers about the uncertainty of critical loads data in this grid cell. Five sets of protection isolines are shown: (CZ) for the Czech portion of the grid cell, (DE) for the German portion (PL) for the Polish portion (all of which use national contributions); and (CZ+DE+PL) for the three countries together. The fifth plot (EU-DB) shows protection isolines using the European background data base.

It can be seen that ranges of $CL_{max}(S)$, $CL_{max}(N)$ and $CL_{nut}(N)$ values are similar among countries, as well as with EU-DB data for this grid cell. It is concluded that there is no reason to assume that the uncertainty of critical loads in grid cell (23,18) has any greater impact on integrated assessment results than other sources of uncertainty (i.e. energy/emission data, simulated emission reduction potential and atmospheric transport) in computing exceedance.

4.3 Concluding remarks

Findings from the exercise described in this chapter can be summarized as follows:

- The variation of $CL_{max}(S)$ and $CL_{max}(N)$ is explained to a large extent by net base cation weathering.
- The influence of the critical BC/Al ratio increases when the net base cation input is low, which is predominantly the case in northern Europe.
- The lesser importance of the critical BC/Al ratio in other parts of Europe suggests that critical loads for acidity in these regions could be set equal to net base cation input, i.e. setting critical ANC leaching equal to 0.
- National Focal Centers submitted nitrogen immobilization data that are generally higher than the range recommended in the Mapping Manual (UBA 1996). The use of higher values assumes that forest soils are able to accumulate higher levels of nitrogen without increasing the risk of damage. The use of recommended values would have led to lower critical loads for eutrophication ($CL_{nut}(N)$), thus making the task of meeting optimization constraints more difficult.
- Results of Level 0 approaches do not allow for systematic uncertainty analysis, as this would require additional information on the processes by which NFCs derived national critical load values.
- The uncertainties in critical load values on a European scale as well as on a grid-cell scale is explained by the same input variables, although the magnitude of the explained variation of critical loads may vary.
- The data used to compute critical loads in a grid cell (23,18) which was identified as binding in a scenario used in an EU acidification study, do not require any adaptations.
- An analysis of error propagation involving the integration of energy and emission data, methods to assess emission reduction potentials, atmospheric transport and critical loads could be theoretically useful. However, for the exercise of supporting NO_x protocol negotiations, it is expected that the magnitude of error propagation does not vary among scenarios, thus allowing the assumption that differences among scenario results are due primarily to differences in the policy alternatives used to create them.

References

Amann, M., I. Bertok, J. Cofala, F. Gyarfas, C. Heyes, Z. Klimont and W. Schöpp, 1996. Cost-effective control of acidification and ground-level ozone. Second Interim report to the European Commission, DG XI. 120 pp.

Barkman, A., 1997. Applying the critical loads concept: constraints induced by data uncertainty. Reports in Ecology and Environmental Engineering, Rep. 1:1997. Lund University, Lund, Sweden. 64 pp.

Gardner, R.H., B. Rojder and U. Bergström, 1983. PRISM: A systematic method for determining the effect of parameter uncertainties on model predictions. Studsvik Energgiteknik AB, Studsvik/NW-83/555, Nykoping, Sweden.

Hettelingh, J.-P., M. Posch, P.A.M. de Smet and R.J. Downing, 1995. The use of critical loads in emission reduction agreements in Europe. *Water Air Soil Pollut.* 85: 2381-2388.

Løkke, H., J. Bak, U. Falkengren-Grerup, R.D. Finlay, H. Ilvesniemi, P.H. Nygaard and M. Starr, 1996. Critical loads of acidic deposition for forest soils: is the current approach adequate? *Ambio* 25(8):510-516.

Oreskes, N., K. Shrader-Frechnette and K. Belitz, 1994. Verification, validation, and confirmation of numerical models in the earth sciences. *Science* 263:641-646.

Posch, M., P.A.M. de Smet, J.-P. Hettelingh and R.J. Downing (eds.), 1995. Calculation and Mapping of Critical Thresholds in Europe: CCE Status Report 1995. RIVM Rep. 259101004. National Institute for Public Health and the Environment, Bilthoven, Netherlands.

Rosén, K., P. Gundersen, L. Tegnhammar, M. Johansson and T. Frogner, 1992. Nitrogen enrichment in Nordic forest ecosystems - The concept of critical loads. *Ambio* 21:364-368.

Sverdrup, H. and P. Warvfinge, 1993. The effect of soil acidification on the growth of trees, grass and herbs as expressed by the (Ca+Mg+K)/Al ratio. Reports in Ecology and Environmental Engineering, Rep. 2:1993. Lund University, Lund, Sweden. 177 pp.

5. Development of the European Land Use Data Base

*P.A.M. de Smet and E. Heuvelmans**
* Geodan B.V.

Introduction

In addition to mapping critical loads of sulfur and nitrogen, progress has been made on mapping critical levels of air pollutant concentrations on ecosystems. The potential quantity of biomass which might be lost due to excess pollutant concentrations, the so-called "stock at risk", can be assessed through the identification of the areas throughout Europe which are subject to pollutant excess. The accuracy of stock at risk analyses depends on the quality of European land use data.

This chapter discusses the efforts to improve the quality of the European Land Use Data Base. These efforts are designed to improve the accuracy of geographical distributions of the land use categories and their areas throughout Europe, as well as to increase consensus among National Focal Centers (NFCs) on the quality of the mapped distribution of the land use categories in the countries.

Section 5.1 describes the sources and procedures used to compile a first version of the Pan-European Land Use Data Base (PELUD). Section 5.2 covers the procedures for improving the data base, and describes the incorporation of land use data provided by the Swiss NFC. Section 5.3 describes the role of land use data in stock at risk analyses.

5.1 Synthesis of the original European Land Use Data Base

The National Institute of Public Health and the Environment in the Netherlands (RIVM) identified the need for a high-resolution land use data base for use in environmental modelling and monitoring projects on a European scale . It was decided to create a pan-European land use data base together with the Stockholm Environment Institute (SEI, United Kingdom), Geodan (Netherlands) and INENCO (Russia), as these organizations were able to provide the necessary input data on land use. The resulting data set covers the whole of Europe, including the European part of the Russian Federation, and has a resolution of 10′ × 10′ (chosen to coincide with other geographical data sets, e.g. the EPA Global Ecosystems Data Base). The first version of the data base was created in mid-1994 (Van der Velde *et al.* 1994), followed by version 2.0, which included better statistical data bases that had become available for several regions (Veldkamp *et al.* 1995). In the most recent version (2.1), the decision criteria in the calibration procedure has been improved significantly.

The Pan-European Land Use Data Base consists of two parts: a 10′ × 10′ grid cell map and an attribute table. The map is linked to the attribute table that contains data on the distribution of various land use types as a percentage of the total grid cell area. The following land use types have been included:

- deciduous forest
- coniferous and mixed forest
- arable land
- permanent crops
- grassland for agricultural use
- inland waters
- urban areas
- other (natural areas and extensive agricultural land)

Both vector and statistical sources have been used to create the data base. The vector sources are integrated in the vector data base "LuVec", and the statistical sources in the statistical data base "LuStat".

The primary vector source in LuVec is the data set of the Stockholm Environment Institute (Chadwick and Kuylenstierna 1990). Land use types not available in the SEI data set were adopted from other sources (for details see Veldkamp and Van der Velde 1995):

- Urban Areas from the Digital Chart of the World (U.S. Defense Mapping Agency 1992)
- Inland Waters from World Databank II (ESRI 1993)
- Permanent Crops from Land Use Map of Europe (FAO-Cartographia 1980)

Since the SEI polygon data have a very low level of detail in eastern Russia compared with the rest of the Europe, the Digital Land Use Map of the USSR (1993) replaced the SEI polygons for that part of Russia.

The statistical data base LuStat contains land use statistics at a variety of spatial levels, ranging from national level to NUTS 3 (counties) level.

The following data sources are incorporated:

- Eurostat (1991): Table *agri2landuse*; NUTS regions 0,1,2,3 scale.
- FAO-Agrostat (1991): FAO-Agrostat computerized information series; national scale.
- Eurostat (1993): Pan-European Questionnaire Eurostat; national scale.
- Regional statistical information from national statistics departments of Austria (1992), Norway (1989), Switzerland (1985) and Finland (1992).
- Inventory East Europe: National statistical yearbooks/reports from Ukraine, Latvia, Czech Republic, Belarus, Estonia, Slovakia, Lithuania, Poland, Hungary, Romania; national scale, collected by Geodan Polska 1993.
- INENCO (1993): Inventory of statistical land use figures for Russia; regional scale.

LuVec and LuStat are integrated into the Pan-European Land Use Database (PELUD) by an iterative calibration procedure which compares the regional land use from LuVec with the statistical figures from LuStat. The resolutions vary throughout Europe from national level to NUTS3 level. The resulting data base LuGrid consists of the area percentages of each land use type per land area in each 10′ × 10′ grid cell.

More detailed descriptions of sources and procedures is given in the CCE Status Report 1995 (Posch *et al.* 1995) and in van de Velde *et al.* (1994) and Veldkamp *et al.* (1995).

5.2 Revisions to the data base

Due to limitations in data sources, the vector and statistical sources contained in the first version of the European map were sometimes incomplete, at a low resolution, or contained significant uncertainties. A revised version (2.0) was created shortly thereafter, which contained major improvements in the calibration criteria and increased the resolution of some of the statistical data bases (Veldkamp et al. 1995). LuGrid version 2.1, which is published on a limited number of CD-ROMs, is not used due to later discovered inconsistencies in some countries. We use the European land use map version 2.0 with fixing of a known bug in the German Bundesländer Schleswig-Holstein and Lower Saxony. The resulting version is presented in this chapter and also includes comments from National Focal Centers and others.

In discussions of the data base at CCE Mapping Workshops, several countries noted that the data base was not sufficiently accurate. Therefore, in mid-1995 the CCE sent maps of land use types *coniferous and mixed forest, deciduous forest, arable land* and *permanent crops* to all NFCs and requested that they verify and correct the land use information where necessary. It is planned to update the land use data base to include national data on classifications and resolution. As with the critical loads mapping procedure, this will result in a European data base that includes NFC contributions wherever possible. The resulting version will be used only for tasks defined by the Working Group of Effects.

All NFC comments on the data base have been incorporated in the data base as far as possible. Land use information for Switzerland has been replaced by a national statistical land use data base submitted by the Swiss NFC. The classification scheme for presenting land use area percentages per grid cell have also been modified to incorporate suggestions from Scandinavian countries. The first class (<10%) in previous maps has been subdivided into classes <1%, 1–5% and 5–10%. The revised classification scheme allows cells with relatively small but (economically) important land use areas (e.g. arable land) to now be adequately reflected in the maps.

Incorporating Swiss land use data:
Data submitted by the Swiss NFC is based on data bases created by the Federal Office of Statistics (GEOSTAT/BFS, Berne) and the National Forest Inventory (NFI), and is derived from aerial photographs using visual stereographic interpretation. For a regularly spaced grid with a 100-meter interval, 3966 aerial photographs were interpreted to create 4.1 million sample points. The Swiss NFC extracted from these points a subset on a 1km interval, such that this value is simply the sample at that specific location and not the dominant land use in the 1 km square.

The following steps were conducted to incorporate the Swiss data into the European data base:
1. The Swiss sample points at a 1km interval are transformed to 10′ × 10′ grid, and the map layers of the two data bases are overlaid in a geographic information system (GIS). In each 10′ × 10′ cell (about 16 × 16 km^2 in Switzerland), the number of sample points per land use type and the total number of sample points in the cell are counted.

Land use percentages are calculated by dividing the number of points per land use type by the total number of points in the cell and multiplying the result by 100.

2. To incorporate the Swiss land use values in the European database, the country borders are overlaid with the 10′ × 10′ map of Europe. All cells intersected by country borders are split, and a country code and unique identification number are is assigned to each section. For all intersecting points in Switzerland, the data are substituted by the results from Step 1 above. The Swiss National Focal Center has reviewed and approved the resulting data base.

Figures 5-1 to 5-4 show maps from the presently used version of the data base on the 10′ × 10′ resolution. The dominant land use (Figure 5-1) is derived from a comparison of the eight land use types, with some adjustments for urban areas. The land use type with the highest percentage is considered dominant in a cell. Figures 5-1 through 5-3 are presented here for comparison with the maps in CCE Status Report 1995, since (e.g.) the distribution of the Swiss land use types and percentages differ significantly.

5.3 Land use data for stock at risk analysis

The European land use data base is used in assessing the impacts of direct air pollution on ecosystems and crops by overlaying the land use categories with maps of SO_2 concentrations, NO_x concentrations and AOT40 levels for O_3. Note that critical levels vary among land use categories, e.g. the AOT40 for ozone for forests differs from that for crops.

Chapter 1 includes maps of the stock at risk for forests and crops related to the exceedances of their specific AOT40 for ozone, on the EMEP50 grid. These maps use land use data from version 2.0 of the European land use data base. To assess the stock at risk of crops, the land use type *arable land* was selected for the distribution and density of crops over Europe. Figure 5-5 shows the result of converting the 10′ × 10′ arable land map (Figure 5-4) to the EMEP50 grid resolution. This data on the EMEP50 grid resolution is superimposed with exceedances of the critical levels for crops to produce Figure 1-6 (top) in Chapter 1. The second example is the stock at risk of forests (Figure 1-6 (bottom)). The forest data applied on the EMEP50 resolution consist of both the *deciduous* and *coniferous and mixed forest* land use types, because the critical level for ozone (AOT40) is set the same for all forest types.

5.4 Conclusions

The substitution of land use data in Switzerland by the Swiss national data in a first step to improve the accuracy of geographical distributions of land use categories and their areas in Europe. Further updating the European land use data base with national updates should increase consensus among NFCs on the quality of the mapped distribution of the land use categories in the countries. Other NFCs have noted that small areas of land use types can be of significant importance, thus grid cells with relatively small but (economically) important land use areas (e.g. arable land) should be identified in the maps by adapting the legend classes so that these small areas are represented in the maps.

Since the European land use data base will be used in LRTAP Convention assessments of the risk of damage by air pollutants, it is necessary to improve the data base whenever possible. Thus additional national data contributions from NFCs are welcome.

References

Chadwick, M.J. and J.C.I. Kuylenstierna, 1990. The relative sensitivity of ecosytems in Europe to acidic depositions. A preliminary assessment of the sensitivity of aquatic and terrestrial ecosystems. Perspectives in Energy, vol. 1, pp. 71-93.

ESRI, 1993. World Data Bank II, 1989-1993, Country Boundaries. Vector-based data set (Scale 1:3,000,000). Environmental System Research Institute, Redlands, California.

FAO-Cartographia, 1980. Land use map of Europe (Scale 1:2,500,500). Budapest.

U.S. Defense Mapping Agency, 1992. Digital chart of the world (Scale 1:1,000,000). Washington, DC.

Veldkamp and van der Velde, 1995. Mapping land use and land cover for environmental monitoring on a European scale. *In*: Posch, M., P.A.M. de Smet, J.-P. Hettelingh and R.J. Downing (eds.), 1995. Calculation and Mapping of Critical Thresholds in Europe: CCE Status Report 1995. RIVM Rep. 259101004. National Institute for Public Health and the Environment, Bilthoven, Netherlands.

Velde, R.J. van de, W.S. Faber, V.F. van Katwijk, J.C.I. Kuylenstierna, H.J. Scholten, T.J.M. Thewessen, M. Verspuij and M. Zevenbergen, 1994. The preparation of a European Land Use Data Base. RIVM report number 712401001. RIVM, Bilthoven, Netherlands, 63 pp.

Veldkamp, J.G., W.S. Faber, V.F. van Katwijk and R.J. van de Velde, 1995. Enhancements of the 10 × 10 minutes Pan-European Land Use Data Base. Report No. 724001001. RIVM, Bilthoven, The Netherlands. 62 pp.

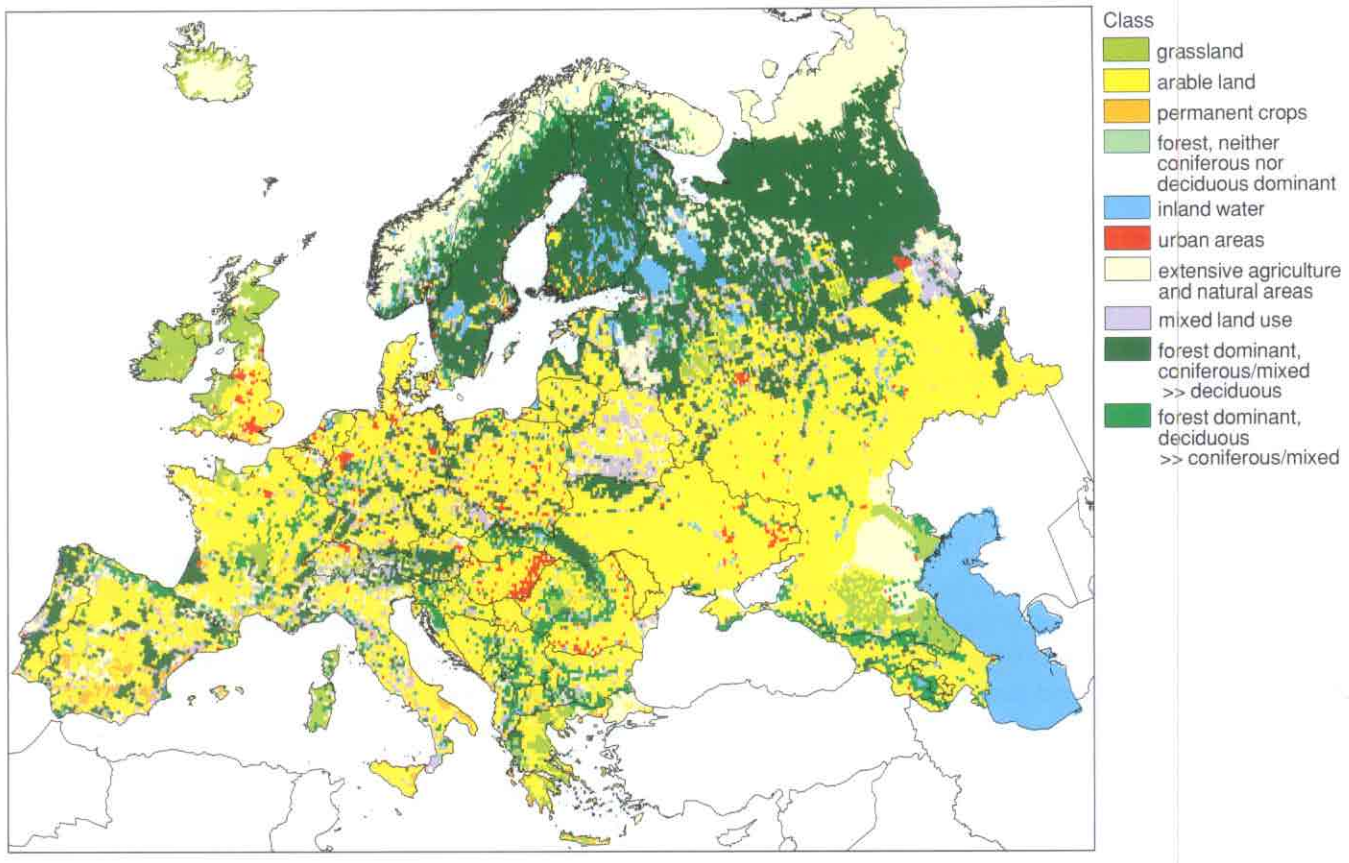

Figure 5-1. The dominant land use class per 10′ × 10′ grid cell.

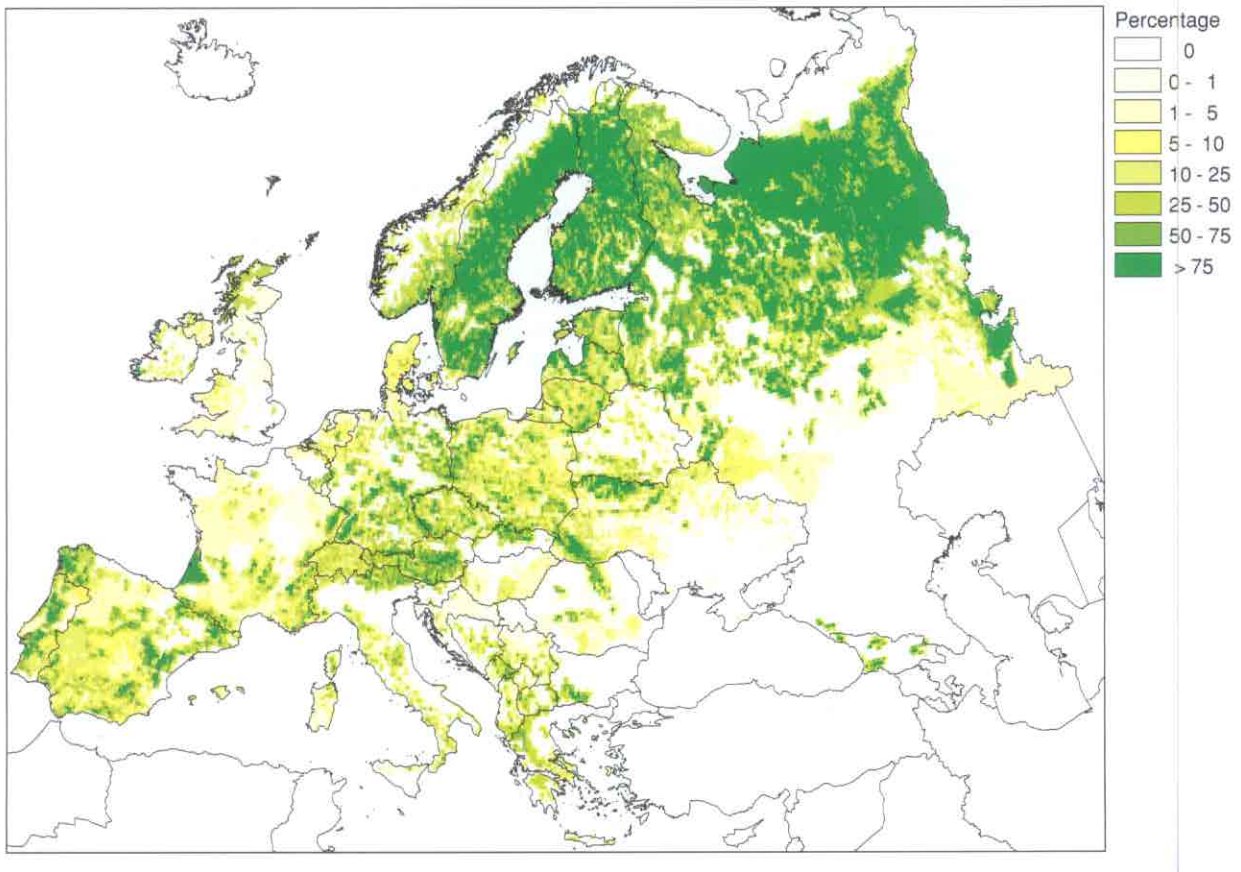

Figure 5-2. Percentage of mixed and coniferous forest per 10′ × 10′ grid cell.

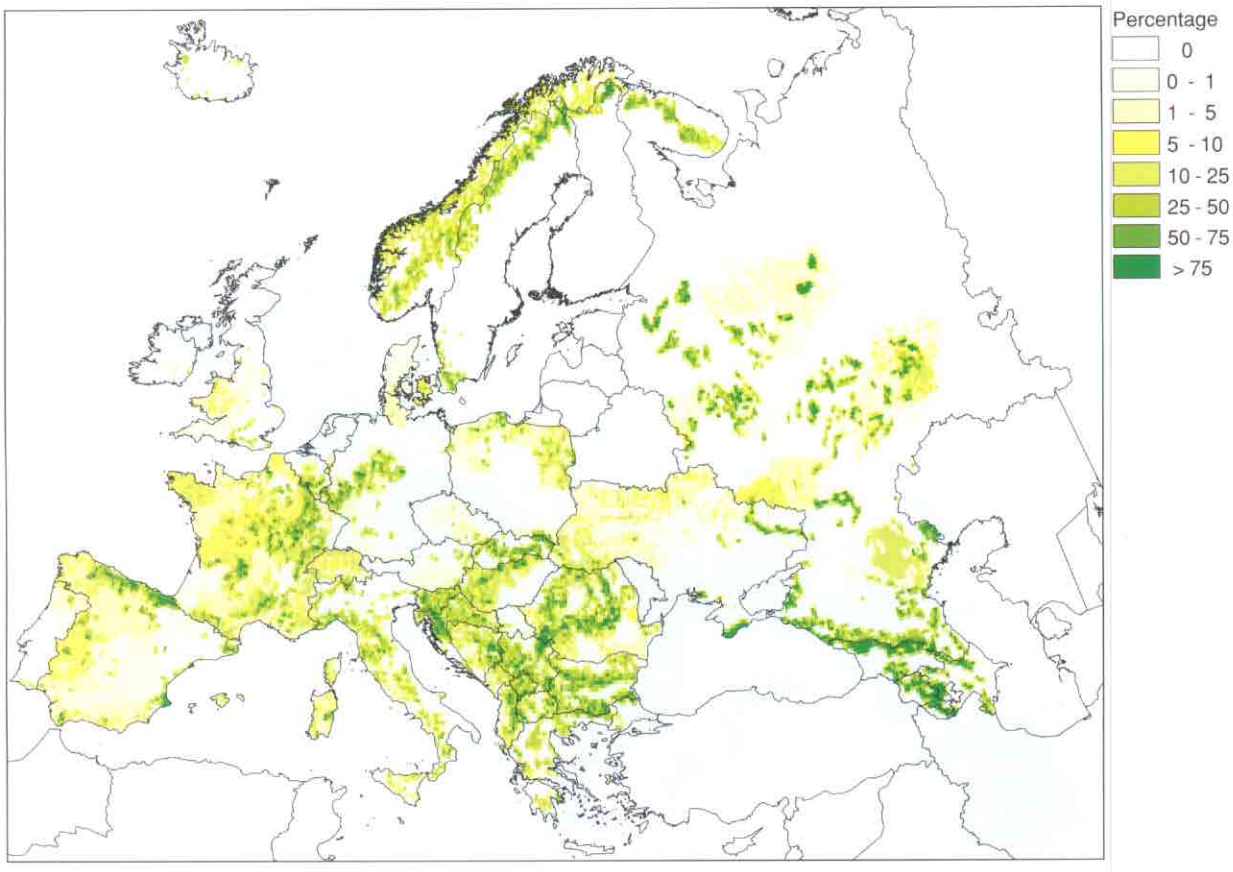

Figure 5-3. Percentage of deciduous forest per 10′ × 10′ grid cell.

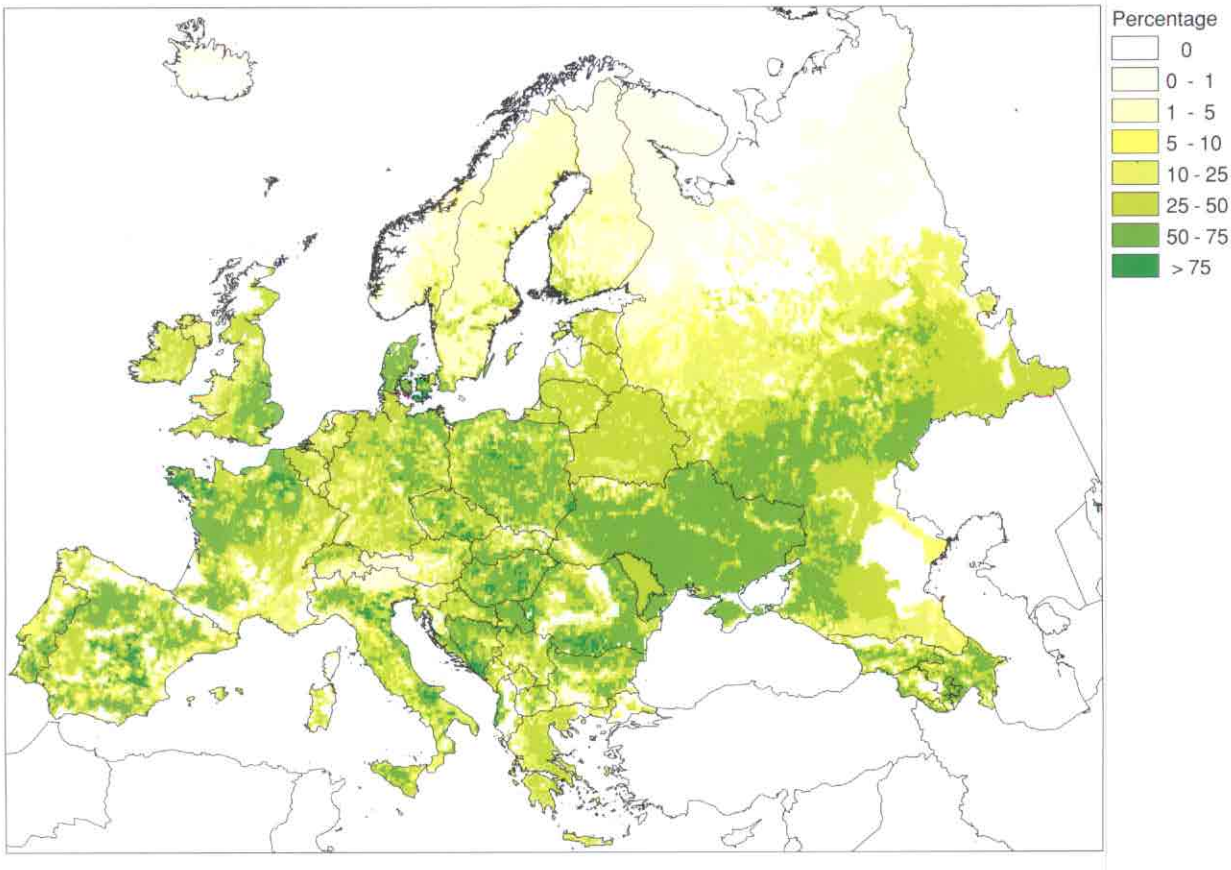

Figure 5-4. Percentage of arable land per 10′ × 10′ grid cell.

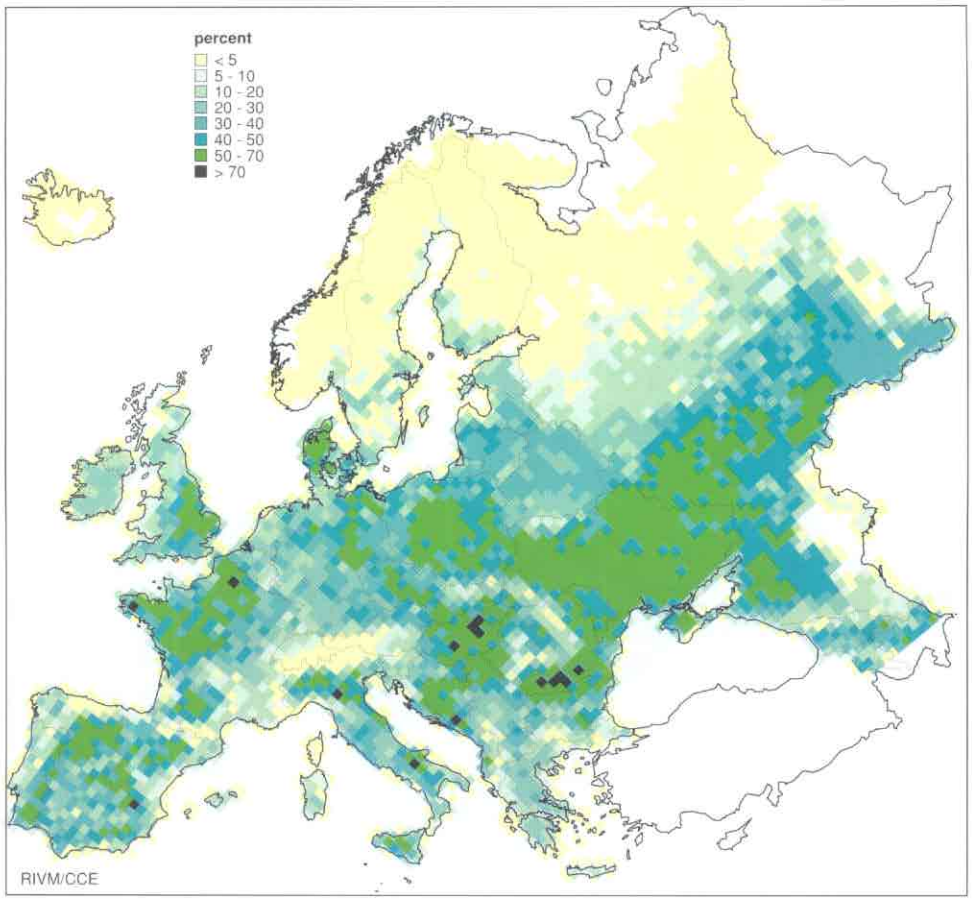

Figure 5-5. Percentage of arable land per EMEP50 grid cell.

6. The European Background Data Base for Critical Loads

P.A.M. de Smet, J. Slootweg and M. Posch

Introduction

One of the activities of the Coordination Center for Effects (CCE) is to provide European critical load maps and data bases to the relevant bodies under the UN/ECE LRTAP Convention. Ideally, the critical load and exceedance maps are based on national data submissions from all European countries. However, when a country does not contribute national critical loads data, the CCE uses for that area values from its own European background data base (EU-DB) for critical loads.

The European background data base discussed in this chapter is based primarily on published sources. The data base can easily be updated when new information becomes available. The EU-DB consists of data from: (a) the 1994 digital FAO Soil Map (FAO 1994), (b) the forested areas of version 2.0 of the 10′ × 10′ gridded RIVM-European Land Use Map (Veldkamp *et al.* 1995), (c) the 50 km (50 km EMEP grid map (see Appendix A in this report) and (d) the WDB II Country Border map (ESRI 1993). For forest-soil ecosystems resulting from the overlay of these data sources, critical loads of sulfur, acidifying nitrogen and nutrient nitrogen are computed.

This chapter explains the technicalities on how the data base is produced. It describes the geographic data sources of the map layers (Sections 6.1 to 6.4) and their resulting overlay (Section 6.5). Section 6.6 describes how the attributes of the original data sources are related to the overlay, and Section 6.7 shows how these culminate in the EU-DB. All digital geographic-based sources are imported into and manipulated in ArcInfo, and data base processing is done with the INGRES relational data base. Section 6.8 mentions forthcoming improvements of the critical load data in the European background data base.

6.1 The EMEP50 grid map layer

Each EMEP150 grid cell contains a 3 × 3 subdivision (the so-called "EMEP50"grid), which will eventually become the grid resolution used in the deposition and integrated assessment models within the LRTAP Convention (see Appendix A).

The longitude and latitude coordinates for the EMEP50 grid are first generated as an ASCII file containing the lower left corner points of the grid cells (i,j) from (1,1) to (117,126), and the file is then imported into INGRES. The attributes i and j are the unique horizontal and vertical coordinate identifiers (integers) of each EMEP50 grid cell. (The grids around the North Pole are excluded to avoid problems with some inconsistencies at the North Pole in the Lambert azimuthal equal-area projection definitions for Europe in ArcInfo.)

Using INGRES report scripts and ArcInfo AML scripts respectively, a map of the EMEP50 grid cell polygons and an attribute table is generated in ArcInfo. This polygon attribute table contains geographical information on all grids in the map, such as grid cell lines, polygons, coordinates of the lower-left corner and center of the grid cell, and grid label points. This information is used to relate other grid attributes to the correct grid cell in the map and is also stored in INGRES. Finally, the EMEP50 grid coverage is converted from a longitude/latitude (geographic) projection onto the Lambert azimuthal equal-area projection, in which the other map layers are presented.

6.2 The FAO Soil Map layer

The FAO Soil Map of the World (FAO 1994) is available on CD-ROM. The polygon and soil attribute files for the European part of the map have been extracted, and the polygon coverage attributes and some soil attributes are included in seven separate ArcInfo export files (EUSNTLL.E01 to EUSNTLL.E07) and are the "first-level attributes". A separate "expansion" ASCII database (WORLDEXP.DAT) contains extensive "second-level attributes" which represent more qualitative and quantitative information on the soil mapping units. Details are given in the notes accompanying FAO (1994).

The seven ArcInfo export files containing polygons and the necessary first-level attributes are first imported into the ArcInfo system. Next, a European soil polygon coverage and a related polygon attribute table is built in the Lambert azimuthal

equal-area projection. Each polygon is represented in this table and has its FAO Soil Mapping Unit identified by a unique number. This number is the relational attribute between the polygon attributes of the first- and the second-level attribute codes of WORLDEXP.DAT. This attribute table contains a record for each soil mapping unit. Every record includes the dominant, co-dominant, associated and inclusion soil types (up to 8 types per record), together with their area percentage within the mapping unit and the percentages of their texture and slope. All first- and second-level attribute codes are imported into INGRES as a set of tables, and serve as look-up tables for collecting information from the FAO Soil Map.

6.3 European country border map layer

A country border map of the world in ArcInfo export E00-format is maintained at RIVM for general purposes within the institute. This file is imported into ArcInfo and the country border polygon coverage is generated for European countries. The country attributes table from the World Data Bank II, ArcWorld 1:3M (ESRI 1993) is imported into INGRES.

6.4 European Land Use grid map layer

A European Land Use Data Base (version 2.0) has been developed (Veldkamp *et al.* 1995, Posch *et al.* 1995) by RIVM. The map and related data are stored as polygons on a 10′ × 10′ resolution. A map coverage of these polygons is generated in ArcInfo using the ArcInfo export file format. The attribute table for each grid cell contains the total land area in the grid cell, the eight land use classes *(deciduous forest, mixed and coniferous forest, grassland, permanent crops, arable land, urban, water and other)* including their areas as percentage of the total land in the grid cell. These percentages are translated into square kilometers, and the table is imported into a set of INGRES relational tables.

6.5 Overlay of the four map layers

Using ArcInfo, a polygon intersections coverage is created by overlaying the four single-item polygon map layers described above. The resulting coverage contains only those polygon intersections at which polygons exist in each of the four single map layers. Figure 6-1 shows a small section of the map resulting from the overlay, giving an impression of the density of polygon intersections of the four individual map layers. Country borders are shown as black lines, while the 10′ × 10′ land use grid polygons are shown as purple lines, and the soil type polygons in red, with the dominant soil type code. The EMEP150 grid (21,14) and its subdivision into nine EMEP50 grid cells are yellow polygons, with grid identifiers in black numbers (e.g. 63,40).

Together with this coverage, a polygon attribute table is created containing all the key attributes of the four original single map layers for every intersection polygon. Subsequently, the coverage is converted from the Lambert azimuthal equal-area projection to the longitude/latitude projection, and the center points of the intersections are added to the coverage. Its longitude and latitude coordinates (in decimal degrees) are added to its attributes table. This polygon attribute table is then imported into INGRES, and can also be used as a data base in any desired geographic projection or geographic information system (GIS).

6.6 Linking map overlay attributes in a relational data base

Once the four separate map layers have been overlaid, the necessary attributes are stored in a series of tables in INGRES, such that they form a link between the source map polygons and attributes, and the intersection polygons of the resulting overlay. This linkage permits the combination of information from the source maps with each other at the level of the polygon intersections. In addition, it allows other scientific characteristics to be associated with the intersections. This combining of attributes from different sources is the basis for computing critical loads for every intersection. This is done with SQL look-up procedures within INGRES.

6.7 Deriving the final European background data base for critical loads

To produce a pan-European set of critical loads, we select only the intersection polygons with the forest land use types *deciduous forests* and *mixed and coniferous forests.*

From the INGRES relational tables, an ASCII output table (see Figure 6-2) is created containing all unique

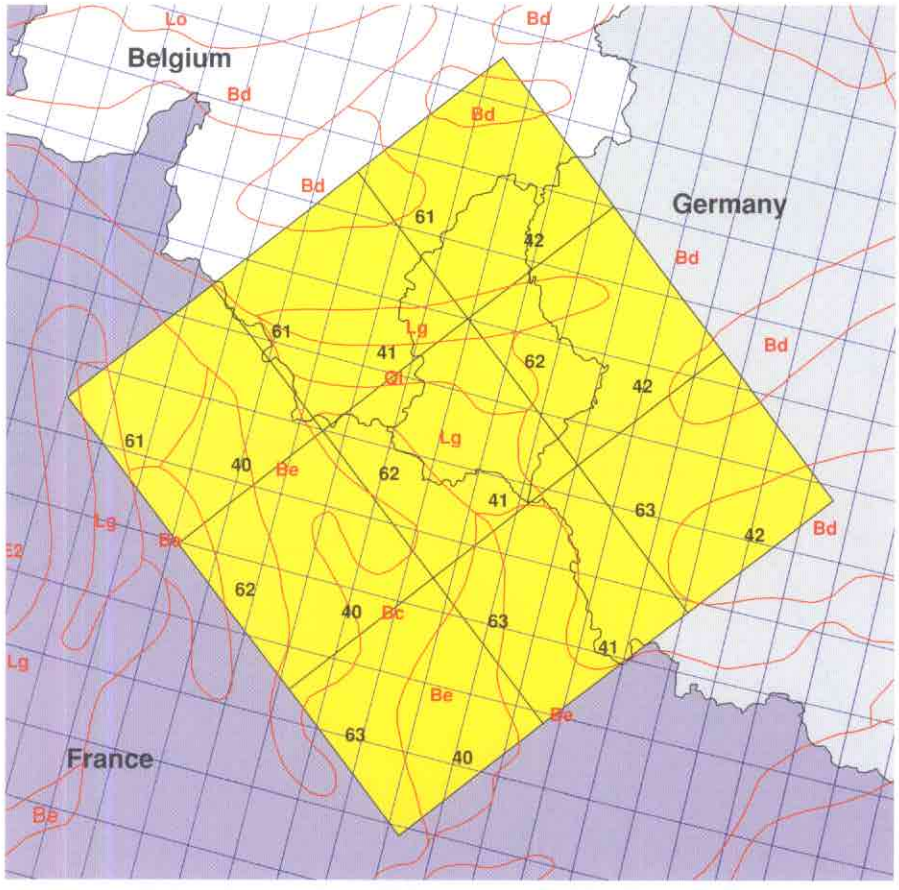

Figure 6-1. A small section of the map resulting from overlaying four maps: (FAO Soil Map, EMEP50 grid map, European Land Use grid, and country border map).

combinations of the country, the soil type, texture/slope, deciduous and coniferous forest land use type and EMEP50 (*i,j*) grid cell. All intersection polygons in the same EMEP50 grid cell with exactly the same set of attribute values are grouped into one data record. The output table consists of the following attributes: the EMEP50 (*i,j*) coordinates, an average longitude/ latitude coordinate, the country code, the soil type code, the texture/slope code, and the areas (in km^2) of both mixed/ coniferous and deciduous forests. Where the areas of both mixed/coniferous and deciduous are smaller then 1 ha, the record is considered spurious and thus not written to the output file. This procedure reduces the number of output records significantly with no essential loss of the total area.

A FORTRAN program developed by the CCE collects relevant attributes for all intersection polygons and computes critical loads, following UBA (1996). These attributes include:

- soil type characteristics (e.g. parent material) for 94 soil types (de Vries *et al.* 1993)
- climate characteristics (temperature, precipitation and evapotranspiration) in a 0.5° × 0.5° gridded data set updated from Leemans and Cramer (1991)
- forest growth characteristics (e.g. growth rates) for deciduous and coniferous forests throughout Europe from 1.0° × 0.5° latitude gridded data sets (de Vries *et al.* 1993)
- 1990–1992 average base cation deposition (wet/ bulk) interpolated to a 50 × 50 km^2 grid from Pedersen *et al.* (1992) and Schaug *et al.* (1993, 1994).

Linking these attributes with the overlay attributes in the ASCII table is done by assigning the average longitude/latitude coordinates of the (grouped) intersection polygons to the grid index of each of the other data sets. For areas in which polygons exist but no growth and climate data are available, the program extrapolates existing growth and climate grid data until it covers the same area as the intersection polygons. The program also defines all necessary attribute values for nutrient element

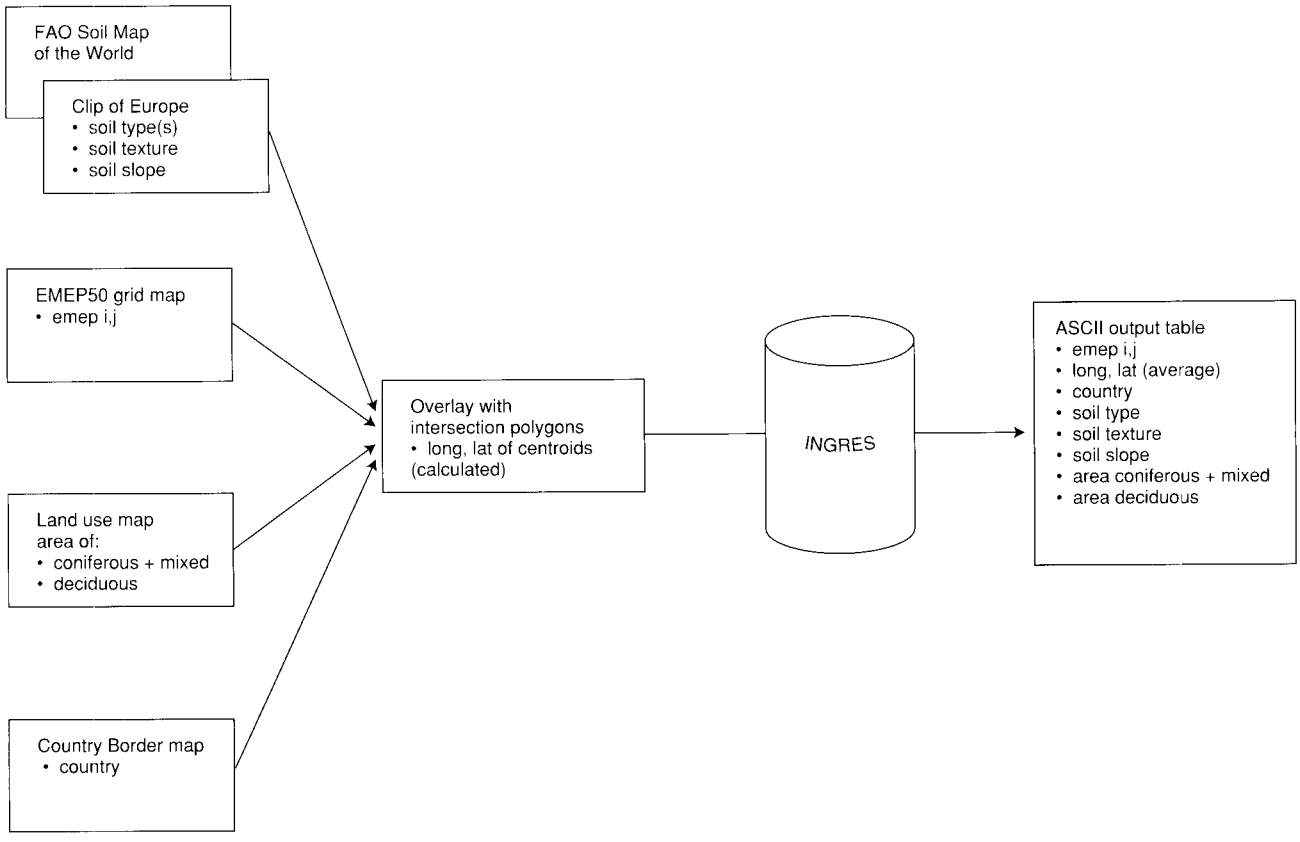

Figure 6-2. The process of overlaying the four single-item map layers and their most important polygon attributes (bullets). The resulting ASCII data base contains all attributes of the intersection polygons necessary to calculate critical loads for forest soil ecosystems.

contents (N, Ca+K+Mg) present in stems and branches of tree types at different latitudes in Europe (de Vries *et al.* 1993). The total nutrient content of forests as well as nutrient uptake in coniferous and deciduous forests at different latitudes is then computed. In addition, the program computes the precipitation surplus, the denitrification fraction and the base cation weathering for each soil type depending on the parent material and texture (UBA 1996). For every record containing grouped forest intersection polygons, the program computes:

- the maximum critical load of sulfur, $CL_{max}(S)$
- minimum critical load of nitrogen, $CL_{min}(N)$
- maximum critical load of nitrogen, $CL_{max}(N)$ and
- critical load of nutrient nitrogen, $CL_{nut}(N)$.

Finally, the program writes out for every record critical loads values and relevant parameters: longitude and latitude (in decimal degrees), the related EMEP50 grid index (i,j), the forest type (coniferous or deciduous) and its area (in km^2), the four critical loads listed above, BC^*_{dep}–Cl^*_{dep}, BC_u, BC_w, $ANC_{le(crit)}$, N_i, N_u, $N_{le(acc)}$, soil type, texture class, runoff, and $ANC_{le(crit)}$ (= $-Al_{le(crit)}$–$H_{le(crit)}$).

6.8 Future improvements

All the maps and attributes discussed in the previous sections have been synthesized with widely available software tools. All procedures have been documented and allow for simple reproduction. Revised input data can easily be incorporated, and updated critical load calculations can be made by simply executing the procedures again. In future updates of European critical loads maps, it is planned to improve the critical load calculations of the European background data base. The improvements will most likely include:

- incorporation of the latest version of the land use data base (described in Chapter 5),
- new interpolations of base cation deposition based on more recent NILU data, and
- inclusion of updated forest growth data.

The European background data base for critical loads will continue to provide the basis for critical load computations in cases where countries cannot provide national data. Uncertainty and sensitivity analysis on computed critical load values can be performed and might even lead to improvements in the other data sources.

References

De Vries, W., M. Posch, G.J. Reinds and J. Kämäri, 1993. Critical loads and their Exceedance on Forest Soils in Europe. The Winand Staring Centre for Integrated Land, Soil and Water Research, Rep. 58 (revised version), Wageningen, Netherlands, 116 pp.

ESRI, 1993. World Data Bank II, 1989-1993, Country Boundaries. Vector-based data set (Scale 1:3,000,000). Environmental System Research Institute, Redlands, California.

FAO, 1994. The Digital Soil Map of the World, version 3.0. (10 May 1994, Scale 1:5,000,000.) Land and Water Development Division, FAO, Rome, Italy.

Leemans, R. and W. Cramer, 1991. The IIASA database for mean monthly values of temperature, precipitation and cloudiness on a global terrestrial grid. IIASA Research Report RR-91-18. International Institute of Applied Systems Analysis, Laxenburg, Austria, 61 pp.

Pedersen, U., J. Schaug and J.E. Skjelmoen, 1992. Data Report 1990. Part 1: Annual summaries. EMEP/CCE Rep. 2/92. Norwegian Institute for Air Research, Lillestrøm, Norway.

Posch, M., P.A.M. de Smet, J.-P. Hettelingh and R.J. Downing (eds.), 1995. Calculation and Mapping of Critical Thresholds in Europe: CCE Status Report 1995. RIVM Rep. 259101004. National Institute for Public Health and the Environment, Bilthoven, Netherlands.

Schaug, J., U. Pedersen, J.E. Skjelmoen and I. Kvalvågnes, 1993. Data Report 1991. Part 1: Annual summaries. EMEP/CCE Rep. 4/93. Norwegian Institute for Air Research, Lillestrøm, Norway.

Schaug, J., U. Pedersen, J.E. Skjelmoen, K. Arensen and A. Bartonova, 1992. Data Report 1992. Part 1: Annual summaries. EMEP/CCE Rep. 4/94. Norwegian Institute for Air Research, Lillestrøm, Norway.

Pedersen, U., J. Schaug and J.E. Skjelmoen, 1992. Data Report 1990. Part I: Annual summaries. EMEP/CCE Rep. 2/92. Norwegian Institute for Air Research, Lillestrøm, Norway.

Veldkamp, J.G., W.S. Faber, V.F. van Katwijk and R.J. van de Velde, 1995. Enhancement of the 10×10 minutes Pan-European Land Use Data Base. RIVM Rep.724001001. RIVM, Bilthoven,
The Netherlands.

UBA, 1996. Manual on Methodologies and Criteria for Mapping Critical Levels/Loads and geographical areas where they are exceeded. UN/ECE Convention on Long-range Transboundary Air Pollution. Federal Environmental Agency (Umweltbundesamt), Texte 71/96, Berlin.

Part II: National Focal Center Reports

Part II consists of reports on national input data and critical threshold calculations submitted by National Focal Centers. A total of 20 countries now collaborate in the Mapping Program by submitting critical loads data to the CCE. Countries which report on their national mapping activities for the first time are Belgium (Flanders), Croatia, France, Hungary, Ireland, Italy and Spain. National Focal Center reports have been submitted by nearly all countries (for France, see the CCE Status Report 1995).

In comparison to the 1995 CCE Status Report, more attention has been given to the assessment of stock at risk due to tropospheric ozone exposure. In addition, some NFCs present preliminary results of the computation and mapping of critical loads for heavy metals. The latter work could be used as input to a workshop on critical loads for heavy metals and POPs organized by the Task Force on Mapping in November 1997.

AUSTRIA

National Focal Center/Contact
Jürgen Schneider
Federal Environment Agency
Spittelauer Lände 5
A-1090 Vienna
tel: +43-1-313 04 5863
fax: +43-1-313 04 5400
email: schneiderj@uba.ubavie.gv.at
Home page of Federal Environment Agency:
http://www.ubavie.gv.at

Collaborating Institutions/Contacts
Wolfgang Loibl
Austrian Research Centre Seibersdorf
Environmental Planning Department
A-2444 Seibersdorf
tel: +43-2254-780 3875
email: loibl@arcs.ac.at

A. Critical Loads

There have been no major revisions of nationwide critical loads data since the 1995 CCE Status Report. Currently, there is some work being done on small-scale deposition mapping by the Federal Environment Agency. Critical loads of acidity and nitrogen have been modelled by the Research Centre Seibersdorf as part of a case study for forest soils in the Tyrolean Limestone Alps using the steady-state mass balance (SMB) model, soil data and tree data for soil inventory sites (Knoflacher and Loibl, 1996).

To generate SMB model results from the irregularly distributed sample points that do not show any regional trends, a special interpolation model was used. Several non-linear response functions with predictor variables reflecting the influence of location (relative to the emission sources), morphology and precipitation were approximated for the two main bedrock types. The model results were combined to generate critical loads at a resolution of 1×1 km^2. The results (shown in the CCE Status Report 1995) show that the highest critical loads for forest soils along the slopes near alpine valley floors (e.g., the Inn Valley and the Ziller Valley).

B. AOT40 Values

To map the spatial distribution of ozone exposure in hourly steps, the measurements carried out at discrete points are interpolated using rather sophisticated models.

Increases and decreases of ozone are very much dependent on the concentration and mix of precursors, as well as the presence and intensity of solar radiation. The spatial pattern of valleys and ridges leads to different patterns of precursors and ozone concentrations, due to the concentration of emission sources in the valley floors. Thus in mountainous regions there is a large variation in ozone concentrations (and therefore a large variation in AOT40 values) within small distances.

The ozone interpolation model considers relative altitude as reference of spatial influence on precursor and ozone concentrations, and time of day as reference of the temporal influence on the ozone production–depletion cycle. In the model, hourly ozone concentration maps are calculated by an statistical function reflecting the time-of-day and elevation dependence of ozone using a digital elevation model, the actual time of day, and hourly monitoring data. The function is fitted to the season- and day-specific general ozone concentration dependence on altitude and time to generate day-specific ozone concentration surfaces for every hour (Loibl *et al.* 1994, Schneider *et al.* 1996).

The spatial distribution of AOT40 values at a resolution of 2.5×2.5 km^2 was calculated starting from the ozone measurements conducted at approximately 120 monitoring stations located throughout Austria. First, the measured ozone concentrations were interpolated over the whole territory. These calculations were carried out for every hour (i.e. every one-hour mean). In a second step the AOT40 was determined for each grid point by summing the calculated ozone concentration depending on the receptor type (forest and agricultural areas) corresponding to the recommendations of the Kuopio Workshop (Kärenlampi and Skärby, 1996).

Figure AT-1 shows the ozone AOT40 for forest ecosystems as an average of the years of 1993 and 1994. Only forested areas are shown on the map. Table AT-1 shows the frequency distribution of AOT40 values for forest areas in Austria. Only the first class (<10 ppm·h) is below the critical load.

Table AT-1. Frequency distribution of AOT40 values for forest areas in Austria.

Range (ppm·h)	1993–94 Averages (%)
< 10	1.33
10 – 20	25.71
20 – 30	42.04
30 – 40	24.53
40 – 50	6.34
> 50	0.05

Additionally, AOT40 values for crops and natural vegetation were calculated. Table AT-2 provides information on the percentage of areas affected by various classes of ozone levels. The data are given for two separate years, since crops have a one-year growing season. Only the first class (< 3 ppm·h) is in compliance with the critical level.

Table AT-2. Percentage of areas affected by various classes of ozone levels.

Range (ppm·h)	1993 (%)	1994 (%)
< 3	0.09	0.04
3 – 6	4.43	3.39
6 – 9	42.44	34.82
9 – 12	36.40	41.40
12 – 15	9.80	12.93
> 15	6.76	7.41

Comments and Conclusions

Generally, AOT40 levels are quite high in Austria. As can be seen in Figure AT-1, ozone levels have a very heterogeneous distribution. In particular, areas at higher altitudes tend to have AOT40 levels which can be significantly higher than those in nearby valleys. As these small-scale variations cannot be modelled within large-scale models, small-scale results can be seen as a supplement to European models.

References

Kärenlampi, L. and L. Skärby (eds.), 1996. Critical Levels for Ozone in Europe: Testing and Finalizing the Concepts. UN-ECE Workshop Report. Univ. of Kuopio, Dept. of Ecology and Environmental Science.

Knoflacher, H.M. and W. Loibl, 1996. Flächenbezogene Abschätzung des Risikos durch Protonen und Stickstoff-Einträge für Waldböden des Tiroler Kalkalpen. FBVA-Bericht 94, Wien.

Loibl, W., W. Winiwarter, A. Kopcsa, J. Züger and R. Baumann, 1994. Estimating the spatial distribution of ozone concentrations in complex terrain using a function of elevation and day time and Kriging techniques. *Atmos. Environ.* 28:2557-66.

Schneider, J., W. Loibl and W. Spangl, 1996. Kumulative Ozonbelastung der Vegetation in Österreich. Berechnung und Darstellung nach dem Konzept der kritischen Belastungsgrenzen ('Critical Levels'). Report UBA-96-127, Umweltbundesamt Wien.

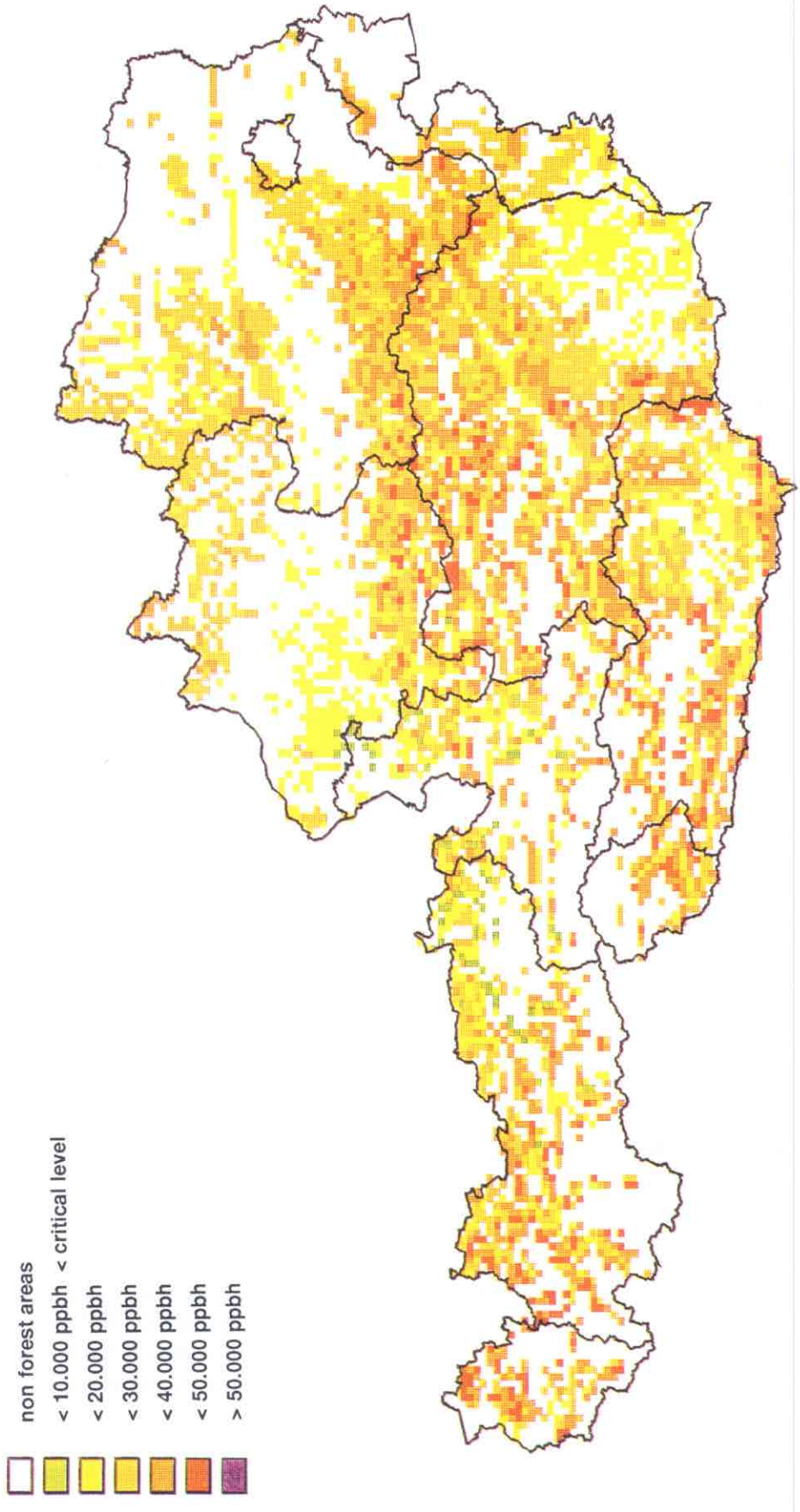

Figure AT-1. Ozone AOT40 values for forest ecosystems averaged over 1993 and 1994. Vegetation period: April - September, daylight hours only.

BELGIUM (Flanders)

National Focal Center/Contacts
M. Van Steertegem
Eddie Muylle
Flemish Environment Agency
Environmental Reporting
Van Benedenlaan 34
B-2800 Mechelen
tel: +32 -15-451467
fax: +32-15-433280
email: m.vansteertegem@vmm.be

Collaborating Institutions/Contacts
H. Craenen
E. Van Ranst
University of Ghent
Laboratory of Soil Science
Krijgslaan 281 (S8)
B-9000 Ghent
tel: +32-9-264 4629
fax: +32-9-264 4997
email: hilde@zadeh.rug.ac.be

F. Tack
M. Verloo
Lab. of Analytical Chemistry
and Applied Ecochemistry
Coupure Links 653
B-9000 Ghent
tel: +32-9-264 5990
fax: +32-9-264 6232

Calculation Methods

Critical loads and their exceedances for forest soils were calculated according to the Steady-state Mass Balance (SMB) method as described in Posch *et al.* (1993):

$$CL(A) = ANC_w - ANC_{le(crit)} \quad (1)$$

$$ANC_{le(crit)} = PS \cdot [Alk] \quad (2)$$

The alkalinity is calculated as the sum of critical hydrogen and critical aluminum leaching. Two criteria were used to determine the critical aluminum leaching $[Al^{3+}]_{crit}$:

1. The Al concentration criterion:
Exact limits for Al concentrations in soils which have a visible negative influence on growth and vitality are fixed at 0.0002 eq l^{-1} (de Vries 1988).

2. The Al/Ca ratio criterion:

$$[Al^{3+}]_{crit} = (RAl/Ca \cdot BC_u) \; / \; PS \quad (3)$$

$$CL_{nut}(N) = N_{u(crit)} + N_{i(crit)} + N_{le(crit)} \; / (1-f_{de}) \quad (4)$$

$$N_{le(crit)} = [N]_{crit} \cdot PS \quad (5)$$

$$CL_{max}(S) = CL(A) + BC_{dep} - BC_{u(crit)} \quad (6)$$

$$BC_{u(crit)} = BC_{dep} + ANC_w - PS \cdot [BC]_{crit} \quad (7)$$

$$CL_{min}(N) = N_{u(crit)} + N_{i(crit)} \quad (8)$$

Table BE-1. Constants used in critical loads calculations.

Constant	Value and unit
$N_{i(crit)}$	213 eq ha^{-1} yr^{-1}
$[BC]_{crit}$	0.01 eq m^{-3}
$[Al]_{crit}$	0.0002 eq l^{-1}

Data Sources

Soils: The Flemish soil profile inventory "Aardewerk" (Van Orshoven and Vandenbroucke, 1993) was used to derive information on soil types. A digitized map with the profile locations was overlaid with the Flemish forest inventory map. Four major forest types were considered: coniferous, mixed coniferous, deciduous and mixed deciduous stands. All profiles situated in forested areas were selected as receptor points for which critical loads were calculated. The digitized map with a total of 653 receptor points was then overlaid with a 5 × 5 km^2 grid to produce the resulting grid maps. As the number of receptor points per cell was rather small, the calculation of percentiles was impossible. Therefore the lowest critical load and the highest exceedance within every grid cell were attributed to the whole cell.

Deposition: Calculated values for present wet and dry deposition of SO_2, NO_x and NH_x on a 5 × 5 km^2 grid were provided by VMM (Flemish Environment Agency). Filtering factors were derived from Erisman (1990) and from Ivens *et al.* (1988) and were used to account for the increased capture by forest filtering. Recent data on dry and wet base cation deposition in Flanders were not available. De Vries (1994) stated that in the Netherlands total deposition of Cl^- is in equilibrium with deposition of Mg^{2+}, K^+

and Na^+ and that BC_{dep} can be approximated by the total Ca^{2+} deposition. Therefore, one-year measurements (February 1988–February 1989) of mean total deposition (dry + wet) of Ca^{2+} in open field near 10 forest plots were used (Van Den Berghe *et al.* 1991). For each receptor point the value of the nearest plot was taken.

Precipitation surplus: Data on mean annual precipitation were derived from precipitation data registered in 5 climatic stations in Flanders over a period of 10 years (1986-1995). The value for each receptor point was set equal to the value registered in the nearest climatic station. Values for interception fractions were derived from Hootsmans and van Uffelen (1991). Mean annual evapotranspiration was fixed at 320 mm yr^{-1}, according to Van Miegroet and Dua (1985).

Weathering rate: In the absence of more specific data on the production of basic cations through mineral weathering for the Flemish region, weathering rates were calculated according to the method proposed by Hettelingh and de Vries (1992). Base cation release rates were attributed to each weathering class on the basis of mineralogy according to Sverdrup and Warfvinge (1988).

Biomass uptake: Due to the lack of specific information, data from a Dutch literature study were used in which growth rates are deduced from yield tables based on soil suitability classes for tree species (de Vries 1990 a,b). Mean nitrogen uptakes of 300 and 500 eq ha^{-1} yr^{-1} were derived for coniferous and deciduous wood respectively. Base cation uptake amounts to 300 and 350 eq ha^{-1} yr^{-1} for coniferous and deciduous forest respectively.

Results

Calculation of *CL(A)* resulted in the highest values for calcareous soils under deciduous forests. The estimated base cation release rate from mineral weathering processes is high in these areas, and thus provides a high long-term buffering capacity against soil acidification. The lowest critical loads (836 eq ha^{-1} yr^{-1}) occur in the Campine and the north of Limburg where the ecosystems largely consist of very sensitive coniferous forests on poor sandy soils. The dominance of coniferous forest types in the Campine is also responsible for the low $Cl_{nut}(N)$ in this region. Calculated values vary between 536 and 971 eq ha^{-1} yr^{-1}.

The highest values for *Ex(A)* (Figure BE-2) mounted up to 6630 eq ha^{-1} yr^{-1} in most sensitive areas mainly concentrated in the northwest of the Flemish region. In 158 of the 652 receptor points the critical load for acidity was not exceeded. Calculated values for $Ex_{nut}(N)$ shown in Figure BE-4, vary between 153 and 3501 eq ha^{-1} yr^{-1} for all points considered. Black points with exceedances above 2000 eq ha^{-1} yr^{-1} are situated mainly in the west of Flanders, where high NH_x deposition (due to intensive animal husbandry) were measured.

Comments and Conclusions

It can be concluded that the data sets presently available for Flanders are too limited to enable accurate determination of specific critical values for the Flemish region. Nevertheless, the calculated values give a good initial indication of the spatial variability of ecosystem sensitivity to acidification and eutrofication in Flanders. Future activities will seek to extend and complete available data bases and to update computation methods. Moreover, use of the steady-state mass balance method for forest soils causes difficulties in the Flemish region where forested areas are relatively few and strongly fragmented.

References

Boxman, A.W., H.F.G. Van Dijk, A. Houdijk and J.G.M. Roelofs, 1988. Critical loads for nitrogen with special emphasis on ammonium. *In*: Nilsson, J. and P. Grennfelt (eds.), Critical loads for sulphur and nitrogen. Miljorapport 1988; 15. Nordic Council of Ministers, Copenhagen, Denmark. pp. 295-322.

de Vries, W., 1988. Critical deposition levels for nitrogen and sulphur on Dutch forest ecosystems. *Water Air Soil Pollut.* 42:221-239.

de Vries, W., 1990a. Methodologies for the assessment and mapping of critical acid loads and of the impact of abatement strategies on forest soils in the Netherlands and in Europe. Winand Staring Centre Rep., Wageningen, Netherlands, 91 pp.

de Vries, W., 1990b. Philosophy, structure and application methodology of a soil acidification model for the Netherlands. *In*: J. Kamari (ed.), Environmental Impact Models to Assess Regional Acidification, Kluwer Academic Publishers, Dordrecht, Netherlands. pp. 3-21.

de Vries, W., 1990b. Soil reponse to acid deposition at a different regional scale: field and laboratory data, critical loads and model predictions. Ph.D. dissertation, Univ. Wageningen, Netherlands. 487 pp.

Erisman, J. W., 1990. Atmospheric deposition of acidifying compounds onto forests in the Netherlands: throughfall measurements compared to deposition estimates from inference. National Institute of Public Health and Environmental Protection, Bilthoven, Netherlands, 29 pp.

Hettelingh, J.P. and W. de Vries, 1992. Mapping Vademecum. National Institute of Public Health and Environmental Protection Rep. 259101002. Bilthoven, Netherlands, 39 pp.

Hootsmans, R.M. and J.G. van Uffelen, 1991. Assessment of input data for a simple mass balance model to map critical acid loads for Dutch forest soils. Interne mededeling Nr. 133, Winand Staring Centre, Wageningen, Netherlands. 98 pp.

Ivens, W. P. M. F., G.P.J. Draaijers, M.M. Bos and W. Bleuten, 1988. Dutch forests as pollutant sinks in agricultural areas. A case study in the central part of the Netherlands on the spatial and temporal variability of atmospheric deposition to forests. Dep. Physical Geography, State Univ. of Utrecht, Netherlands. Dutch Priority Programme on Acidification Rep. 37-09, 43 pp.

Ministerie van de Vlaamse Gemeenschap, 1992. Boskartering van het Vlaamse Gewest, Kaartblad 18/6-2, OC-GIS Vlaamse Landmaatschappij, Brussel.

Posch, M., J.-P. Hettelingh, H.U. Sverdrup, K. Bull and W. de Vries, 1993. Guidelines for the computation and mapping of critical loads and exceedances of sulfur and nitrogen in Europe. *In*: R.J. Downing, J.-P. Hettelingh and P.A.M. de Smet (eds.), Calculation and Mapping of Critical Loads in Europe: CCE Status Report 1993. National Institute of Public Health and Environmental Protection Rep. No. 259101003, Bilthoven, Netherlands, pp. 25–38.

Sverdrup, H.U. and P.G. Warfvinge, 1988. Assessment of critical loads of acid deposition on forest soils. *In*: Nilsson, J. and P. Grennfelt (eds.), Critical loads for sulphur and nitrogen. NORD 1988:97, Nordic Council of Ministers, Copenhagen, Denmark: 81-129.

Van Den Berghe, K., D. Maddelein, B. De Vos B. and P. Roskams, 1991. Analyse van de luchtverontreiniging en de gevolgen daarvan op het bosecosysteem. Voorlopige versie eindrapport project nummer 87.60.BL.001.0, Labo voor bosbouw, RUG.

Van Miegroet, M. and V. Dua, 1985. Bossterfte en luchtverontreiniging. Rapport nummer 9, Labo voor bosbouw, RUG.

Van Orshoven, J. and D. Vandenbrouck, 1993. Aardewerk, databestand van bodemprofielgegevens. Rapport 18 A, Katholieke Universiteit Leuven.

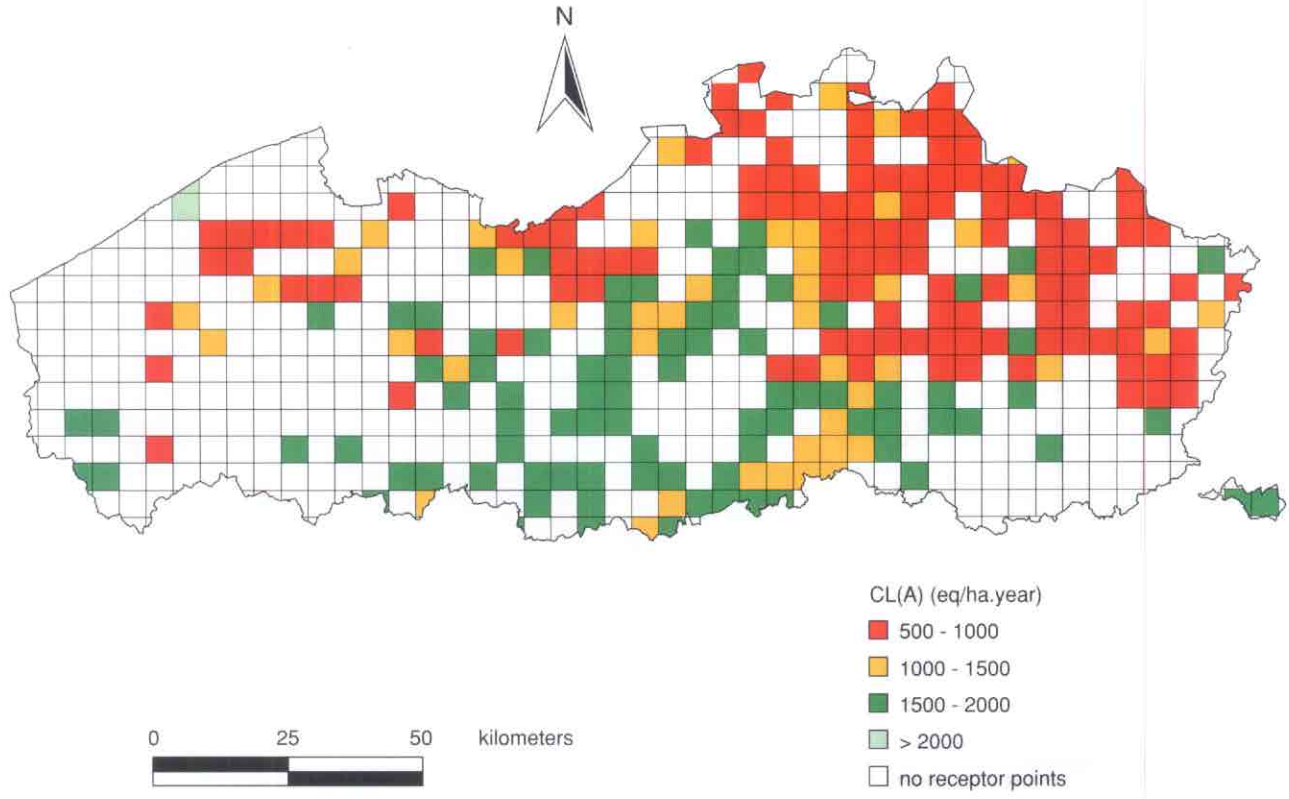

Figure BE-1. Critical load of acidity, *CL(A)*.

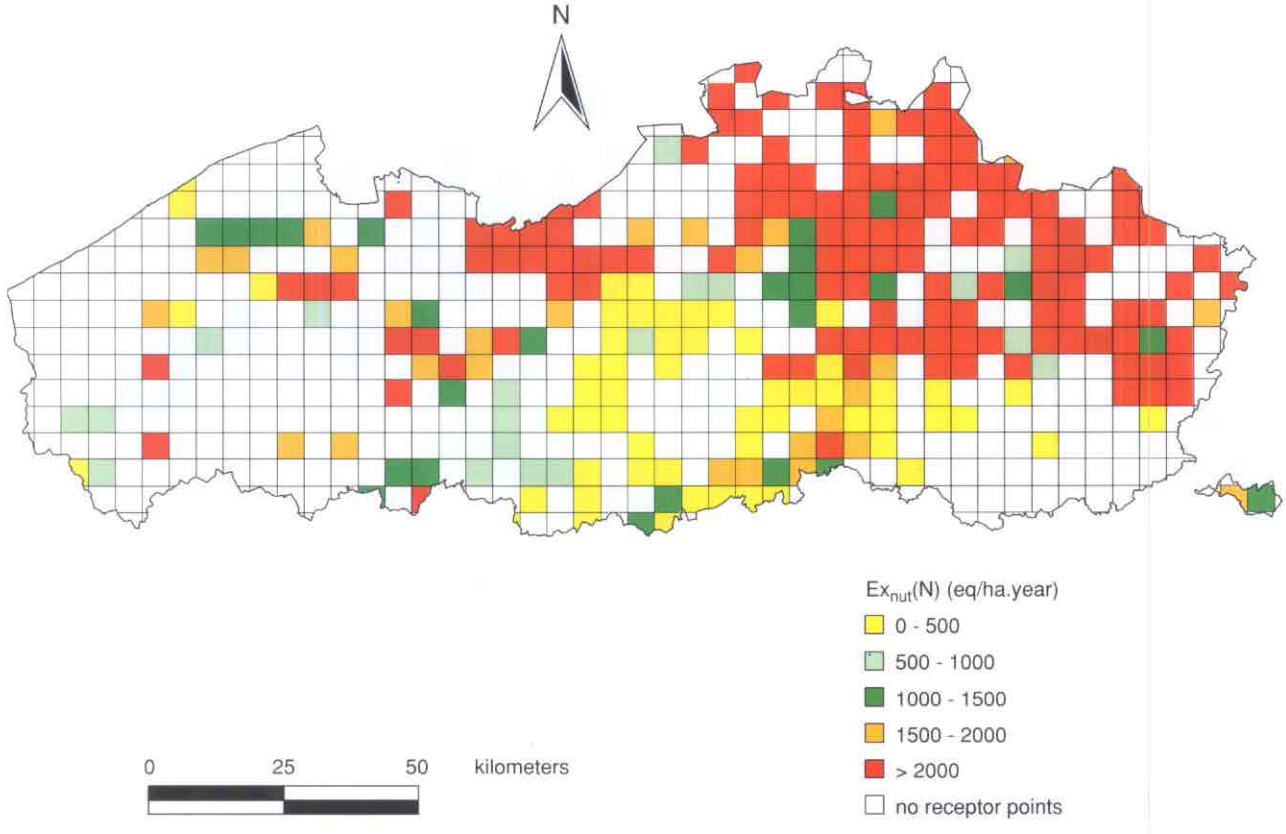

Figure BE-2. Exceedance of critical load of acidity, *Ex(A)*.

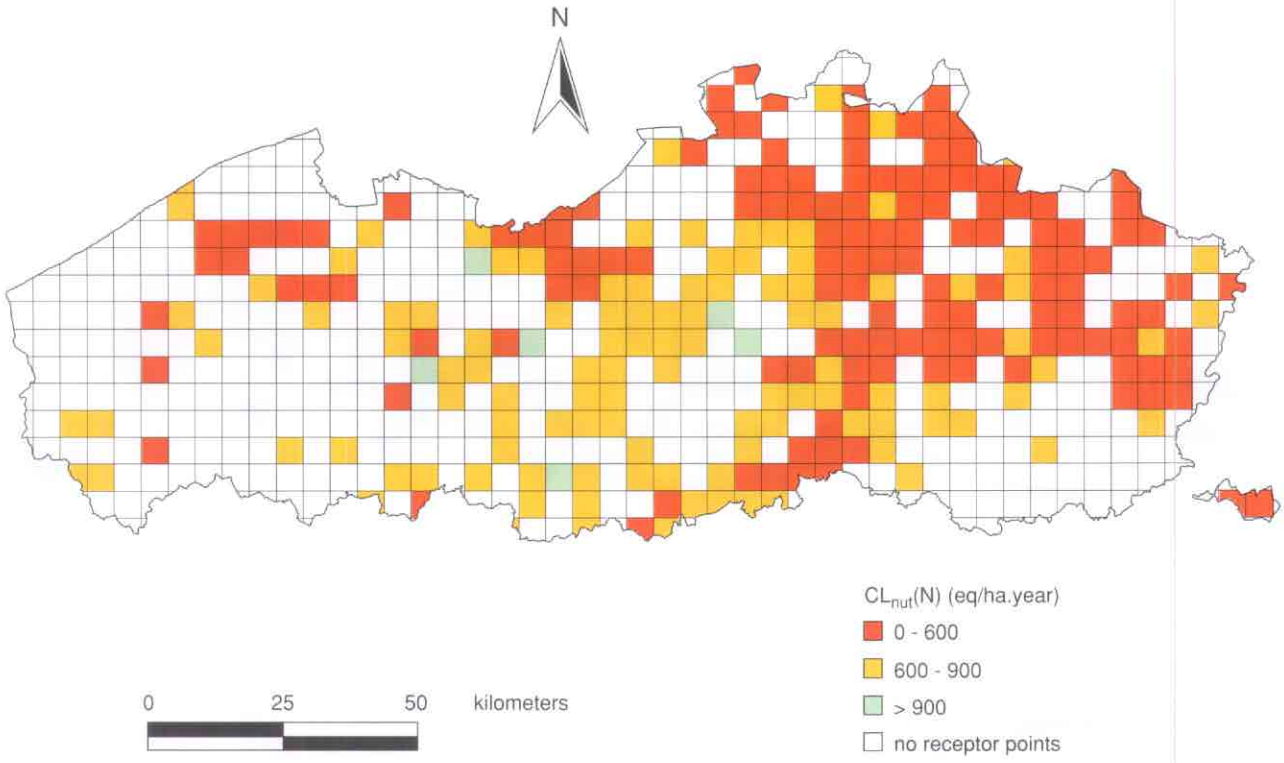

Figure BE-3. Critical load of nutrient nitrogen, $CL_{nut}(N)$.

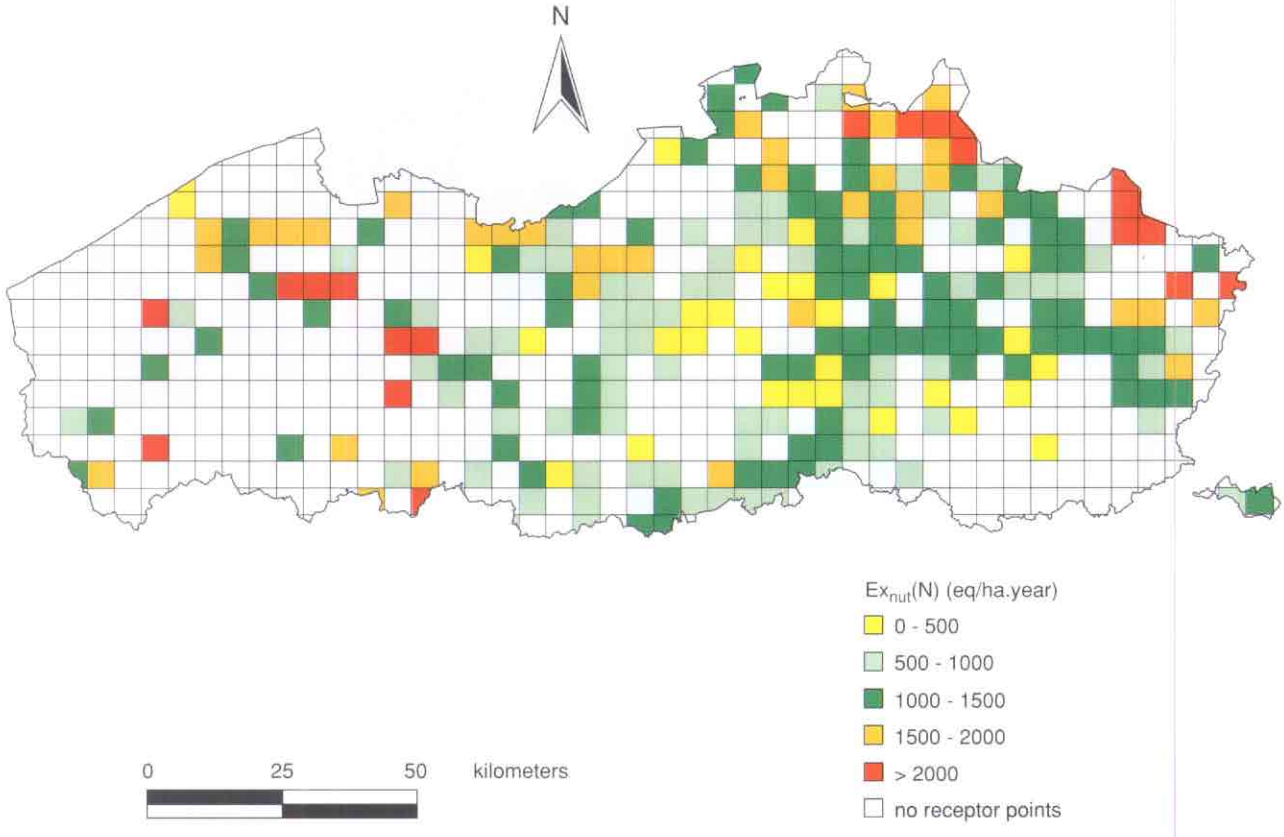

Figure BE-4. Exceedance of the critical load of nutrient nitrogen, $Ex_{nut}(N)$.

CROATIA

National Focal Center/Contact
Stella Dolenec
State Directorate for Environment
Ulica grada Vukovara 78
10000 Zagreb
tel: +385-1- 6133 444/2343
fax: +385-1-537 203
email: sdolenec@duzo.tel.hr

Collaborating Institutions/Contacts
Vladimir Jelavic
Coordinator EKONERG - Zagreb
Ulica grada Vukovara 37
10000 Zagreb
tel: +385-1-6115 189
fax: +385-1-530 604
email: vjelavic@open.hr

Working Group
Vladimir Jelavic, Co-ordinator
Stella Dolenec
Jakob Martinovic
Andrija Vrankovic
Nikola Pernar
Ankica Krznar
Vladimir Lindic

Calculation Methods

The application of the Steady-state Mass Balance Method (SMB) for critical load mapping of soils in Gorski kotar (the central-western mountainous part of Croatia) is complicated by great site variety and numerous combinations of parent rock, soil and vegetation. In two 50 km × 50 km EMEP grid cells, 24 soil–vegetation combinations were identified. Soils with alkaline reaction were not included into the critical load calculations. Grid cell data are based on 218 forest soil profiles.

Weathering: Since the chemical weathering of hard pure limestone is very slow and products of weathering do not have impact on soil acidity, a value of zero was chosen. BC_w and ANC_w values have been calculated according to the Mapping Vademecum (Hettelingh and deVries 1992, pp. 34-37). When dolomites and dolomite-limestone appear together with limestone, the suggested BC_w values have been multiplied by a factor of 0.3.

$Alk_{le(crit)} = -Q\,(([Al_i]_{crit} + [H]_{crit})$
where $[Al_i]$ = inorganic Al

Input data (from de Vries 1991)

	$[Al_i]_{crit}$ (mol$_c$ m^{-3})	$[H]_{crit}$ (mol$_c$ m^{-3})
pH > 4.0	0.2	0.1
pH < 4.0	0.4	0.2

Interception: The mean annual interception evaporating has been defined as:
$I = P \cdot a$
where P = precipitation

Values for a from de Vries (1991): pine 0.25, spruce 0.45, fir 0.40 (species composition: fir 60%, beech 40%, thus a = 0.34), beech 0.25 and oak 0.15.

Base cation uptake: Elements: Annual volume increment m^3 ha^{-1} and wood cut were taken for normally managed forests. Mean values of volume density (kg m^{-3}) and Ca, Mg, K and Na contents were taken from de Vries (1991). For receptors 1, 4 and 9, BC_u and N_u were determined to be zero, as these receptors are treated as virgin forests (no utilization).

Critical nitrogen leaching: $= Q \cdot [N]_{crit}$
$[N]_{crit}$has been defined within the ranges from Posch *et al.* (1993):

Tree species	$[N]_{crit}$ (mg N l^{-1})
mugho pine	0.1
spruce and fir	0.15
beech and fir	0.35
oak	0.35

Nitrogen immobilization: The range of N immobilization (2–5 kg N ha^{-1} yr^{-1} , from Posch *et al.* 1993) was assigned to receptors on the basis of the total N content in the A soil layer:

N content (%)	$N_{i(crit)}$ (kg N ha^{-1} yr^{-1})
< 0.40	2
0.40 – 0.50	3
0.50 – 0.60	4
> 0.60	5

Denitrification:
$N_{de} = f_{de}\,(N_{dep} - N_u - N_i)$ if $N_{dep} > N_u + N_i$
$N_{de} = 0$ otherwise

f_{de} is a denitrification function dependent on soil type and degree of aeration (Posch *et al.* 1993). Overly high values were obtained for Mediterranean soils, and thus adjustments to categories was necessary to achieve more realistic relations. The range of N_{de} values, obtained by a control method based on water regime and soil type (pH), was 0.0–1.0 kg N ha^{-1} yr^{-1}. These values were more realistic, but were not included in further calculations.

Data Sources

- Receptor map 1:100,000 (Martinovic and Vrankovic 1996). Mapping units were defined by the sequence of soil-vegetation forest types. Alkaline soils have not been included in calculating critical loads.
- Soil data: Land data base of northeastern Croatia (Martinovic and Vrankovic 1996).
- Precipitation: data on climatic zones of forest vegetation (Bertovic 1983).
- Base cation (BC_{dep}) and chlorine (Cl) deposition: Meteorological and Hydrological Service of Croatia, data of Ogulin station, for the period 1981–1994.
- NO_3^- deposition: EMEP/MSC-W, Report 1/96, p. C:83, 694 mg(N) m^{-2}
- Base cation (BC_u) and nitrogen (N_u) uptake by harvesting: local data on normal wood volume increment and harvest, the average timber quantity in last 20 years.
- Drainage water (Q): Data on measuring of main receptors, $Q = (P–I)\cdot 0.15$.

Comments and Conclusions

Results are presented in Table HR-1. Computation and mapping of critical loads have been started in the Republic of Croatia. Two 50 × 50 km^2 EMEP grid cells (79,43 and 80,43), located within the 150 × 150 km^2 grid cell 27,15, have been mapped. The most complex soil-vegetation relationship in Croatia can be found in this region, which also has most valuable coniferous forests. It is planned to implement the SMB model for other parts of Croatia. The grid cells already mapped will be analysed by more complex models (e.g. SMART and PROFILE).

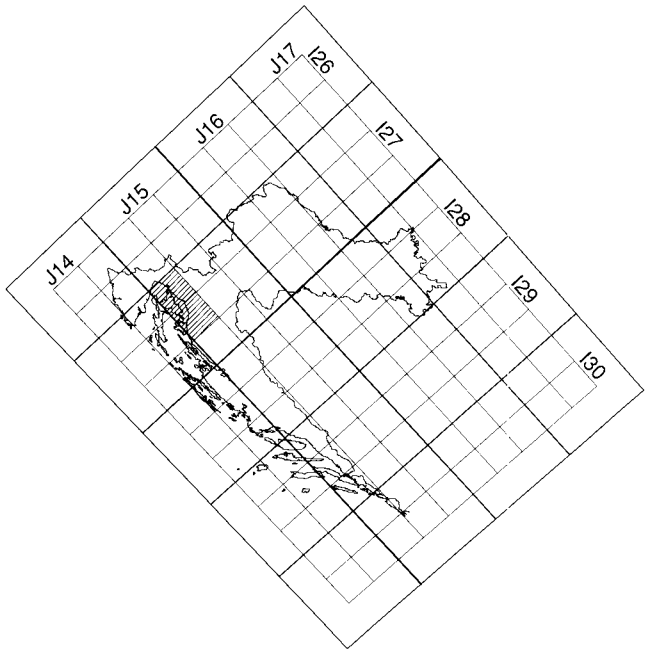

Figure HR-1. Location of the two EMEP 50 km × 50 km grid cells for which critical loads have been calculated.

References

Bertovic, S., 1983. Klima i klimatologija, Šumarska enciklopedija 2, 257, Zagreb.

de Vries, W., 1991. Methodologies for the assessment and mapping of critical loads and the impact of abatement strategies on forest soils. DLO The Winand Staring Centre, Wageningen, Netherlands, Rep. 46, 109 pp.

Downing, R.J., J.-P. Hettelingh and P.A.M. de Smet (eds.), 1993. Calculation and Mapping of Critical Loads in Europe: CCE Status Report 1993. National Institute of Public Health and Environmental Protection Rep. No. 259101003, Bilthoven, Netherlands.

Hettelingh, J.-P. and W. de Vries, 1992. Mapping Vademecum. National Institute of Public Health and Environmental Protection Rep. No. 259101002, Bilthoven, Netherlands.

Martinovic, J. and A. Vrankovic, 1996. Stojbinska baza podataka sjeverozapadnog dijela Hrvatske.

Posch M., J.-P. Hettelingh, H.U. Sverdrup, K. Bull and W. de Vries, 1993. Guidelines for the Computation and Mapping of Critical Loads and Exceedances of Sulfur and Nitrogen in Europe. *In*: Downing *et al.*, 1993. *op. cit.*

Table HR-1. Calculated values of critical loads (in eq ha^{-1} yr^{-1}) for different soil-vegetation forest types.

No.	Receptor combinations	$CL_{max}(S)$	$CL_{min}(N)$	$CL_{max}(N)$	$CL_{nut}(N)$
1	*Lonicero-Pinetum mugi, Eutric Lithosols*	2650	357	3007	506
2	*Homogyno-alpinae-Fagetum, Calcic Cambisols*	2492	526	3018	910
3	*Piceetum subalpinum, Calcic Cambisols*	2315	620	2935	763
4	*Calamagrostio-Piceetum, Eutric Lithosols*	2574	357	2931	524
5	*Calamintho-Abieti-Fagetum, Calcic Cambisols (shallow and moderately deep)*	2836	714	3550	1061
6	*Calamintho-Abieti-Fagetum, Calcic Cambisol (deep)*	2813	846	3659	1193
7	*Calamintho-Abieti-Fagetum, Eutric Lithosols*	2838	771	3609	1118
8	*Calamintho-Abieti-Fagetum fac. Seslerio autumnalis, Calcic Cambisol*	2901	731	3632	1184
9	*Calamagrostio-Abietetum, Eutric Lithosols*	2976	357	3333	543
10	*Blechno-Abietetum, Dystric Cambisols-Orthic Podzols (Brunipodzols)*	3387	1043	4430	1229
11	*Abietetum dolomiticum, Calcic Cambisol and rendzinas*	3649	954	4603	1140
12	*Lamioorvale-Fagetum, Calcic Cambisol (shallow)*	2023	1102	3125	1455
13	*Lamioorvale-Fagetum, Calcic Cambisol (moderately deep)*	1936	1132	3068	1485
14	*Blechno-Fagetum sylvaticae, Dystric Cambisols (Brunipodzols)*	2648	1209	3857	1562
15	*Luzulo-Fagetum sylvaticae, Dystric Cambisols*	2771	862	3633	1215
16	*Helleboro-Fagetum, Rendzinas*	2857	1251	4108	1604
17	*Piceetum montanum, Dyistric Cambisols-Orthic Podzols (Brunipodzols)*	3158	805	3963	979
18	*Piceetum dolomiticum, Rendzinas*	2905	756	3661	886
19	*Helleboro-Pinetum, Rendzinas*	2533	626	3159	756
20	*Seslerio-Fagetum sylvaticae, Calcic Cambisol*	3050	596	3646	1166
21	*Ostryo-Quercetum pubescentis, Calcic Cambisol*	2128	460	2588	838
22	*Ostryo-Quercetum pubescentis, Rendzinas*	2405	344	2749	1604
23	*Querco-Carpinetum orientalis, Calcic Cambisol*	1798	416	2214	745
24	*Querco-Carpinetum orientalis, Chromic Cambisols (Terra rossa)*	1444	301	1745	630

(Note: Receptors No. 16, 19 and 22 are not included in the critical load computations due to calcareous soil.)

CZECH REPUBLIC

National Focal Center/Contacts
Irena Skorepová and
Šárka Roušarová
Czech Environmental Institute
Vršovická 65
CZ-10010 Prague 4
tel: +42-2-6712 2195
fax: +42-2-741695
email: skorepa@ceu.cz

Collaborating Institutions/Contacts
Tomás Paces
Czech Geological Institute
Geologická 6
CZ-152 00 Prague 5

Miloslav Zapletal
Ekotoxa - Opava
Horní nám. 2
CZ-746 01 Opava

National Maps Produced

National maps on the 50 km x 50 km EMEP grid were produced using ArcInfo. The following maps (averages and 5-percentile) were produced:

- maximum critical loads of sulfur
- minimum critical loads of nitrogen
- maximum critical loads of nitrogen
- critical loads of nutrient nitrogen
- exceedances of critical loads of sulfur
- exceedances of critical loads of nutrient nitrogen

Calculation Methods

The simple mass balance method summarized in CCE Technical Report No. 1 (Hettelingh *et al.* 1991) and CCE Status Report 1995 (Posch *et al.* 1995) was used to calculate sulfur and nitrogen critical loads. The values of weathering rates were derived from the soil type, parent material and soil texture provided in Hettelingh and de Vries (1992). The values of the critical uptake of base cations and nitrogen for forest ecosystems were calculated as shown in Tables CZ-1 and CZ-2 (see NFC report of Germany, pp. 123-130 in Posch *et al.* 1995). The rates of nitrogen immobilization were obtained from Table CZ-3. The exceedance maps for nitrogen and sulfur are based upon critical load calculations and average annual atmospheric deposition from the period of 1991–1994 for sulfur, and from 1994 for nitrogen. The calculations of critical loads include these equations:

- $CL(A) = ANC_w + 0.09 \cdot Q + 0.2 \cdot Q$
- $CL_{max}(S) = CL(A) + BC_{dep} - Bc_{u(crit)}$
- $CL_{min}(N) = N_{u(crit)} + N_{i(crit)}$
- $CL_{max}(N) = CL_{min}(N) + CL_{max}(S) \; / \; (1-f_{de})$
- $CL_{nut}(N) = N_{u(crit)} + N_{i(crit)} + N_{le(crit)} \; / \; (1-f_{de})$
- $N_{le(crit)} = Q \cdot [N]_{crit}$

ANC_w = alkality from weathering at critical load
Q = runoff below root zone (groundwater runoff was used)
$N_{u(crit)}$ = uptake of nitrogen at critical load
$N_{i(crit)}$ = immobilization of nitrogen at critical load
$N_{le(crit)}$ = leaching of nitrogen at critical load
f_{de} = denitrification fraction
BC_{dep} = atmospheric deposition of basic cations
$Bc_{u(crit)}$ = uptake of basic cations at critical load
$[N]_{crit}$ = N concentration in soil solution at critical load

Table CZ-1. Critical uptake classes base on critical weathering rate, annual temperature and precipitation surplus.

	ANC_w (eq ha^{-1} yr^{-1})									
	200–500					> 500				
T (° C)	8	7	6	5	<5	8	7	6	5	<5
PS (mm):										
> 1000		I	II	III	IV		I	I	II	IV
800–1000		I	II	III	IV	I	I	I	II	IV
600–800	I	I	II	III	IV	I	I	I	II	IV
400–600	I	II	II	III	IV	I	I	I	II	
200–400	II	III	III	III		II	II	II	III	
< 200	III	IV	IV			III	III	III		

Table CZ-2. Rates (in eq ha^{-1} yr^{-1}) of critical uptake of base cations and nitrogen for coniferous and deciduous forests for the yield classes in Table CZ-1.

	Coniferous		Deciduous	
Class	N_u	BC_u	N_u	BC_u
I	607	546	964	675
II	464	420	821	575
III	357	321	571	400
IV	285	257	500	350

Table CZ-3. Rates of nitrogen immobilization in forest soils.

Annual temperature (° C)	N immobilization (kg N ha^{-1} yr^{-1})
5	4.0
6	3.0
7	2.0
8	1.5

Parameters used in the calculations of critical loads:

Parameter	Symbol	Value (eq m^{-3})
critical N concentration	$[N]_{crit}$	0.0157
critical proton concentration	$[H^+]_{crit}$	0.09
critical Al^{3+} concentration	$[Al^{3+}]_{crit}$	0.2

Data Sources

Hydrological and meteorological data in the forest stands were derived from hydrogeological maps (scale of 1:200,000) issued by the Czech Geological Institute (1981). Soil types and soil texture characteristics were taken from maps with a scale of 1:500,000. The modelled data of atmospheric deposition provided by Ekotoxa–Opava were used for the atmospheric input of sulfur and total nitrogen. The data on the basic cation deposition were provided by the CCE from the European background database.

Comments and Conclusions

In contrast to the previous evaluation of critical loads for a 37.5km × 37.5km grid, these calculations of critical loads are based on the assessment of critical weathering rates derived from soil types and texture classes. Changes were made in the assessment of base cation critical uptake, nitrogen critical uptake, and in the derivation of nitrogen immobilization rates.

References

Downing, R.J., J.-P. Hettelingh and P.A.M. de Smet (eds.), 1993. Calculation and Mapping of Critical Loads in Europe: CCE Status Report 1993. National Institute of Public Health and Environmental Protection Rep. No. 259101003, Bilthoven, Netherlands.

Hettelingh, J.-P., R.J. Downing and P.A.M. de Smet (eds.), 1991. Mapping Critical Loads for Europe: CCE Technical Report No. 1. National Institute of Public Health and Environmental Protection Rep. No. 259101001. Bilthoven, Netherlands.

Hettelingh J.-P. and W. de Vries, 1992. Mapping Vademecum. National Institute of Public Health and Environmental Protection Rep. No. 259101002, Bilthoven, Netherlands.

Posch, M., P.A.M. de Smet, J.-P. Hettelingh and R.J. Downing (eds.), 1995. Calculation and Mapping of Critical Thresholds in Europe: CCE Status Report 1995. National Institute of Public Health and the Environment Rep. 259101004, Bilthoven, Netherlands.

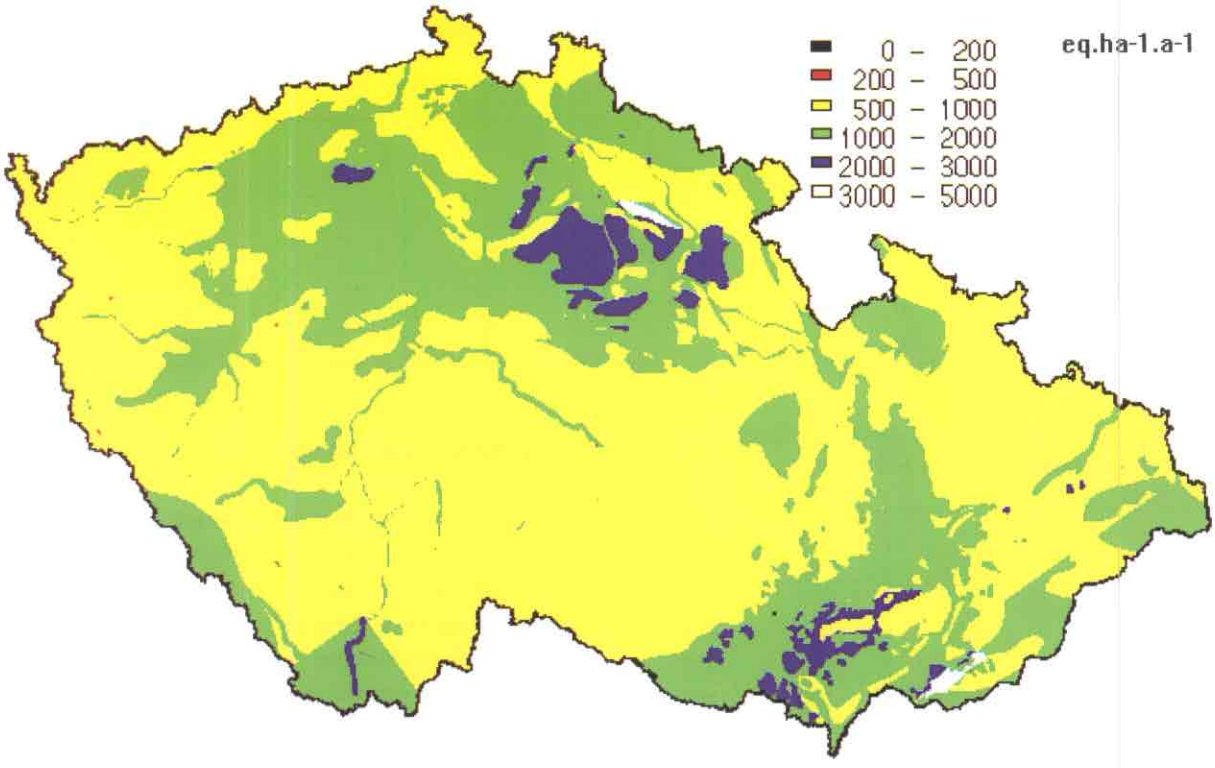

Figure CZ-1. Maximum critical loads of sulfur.

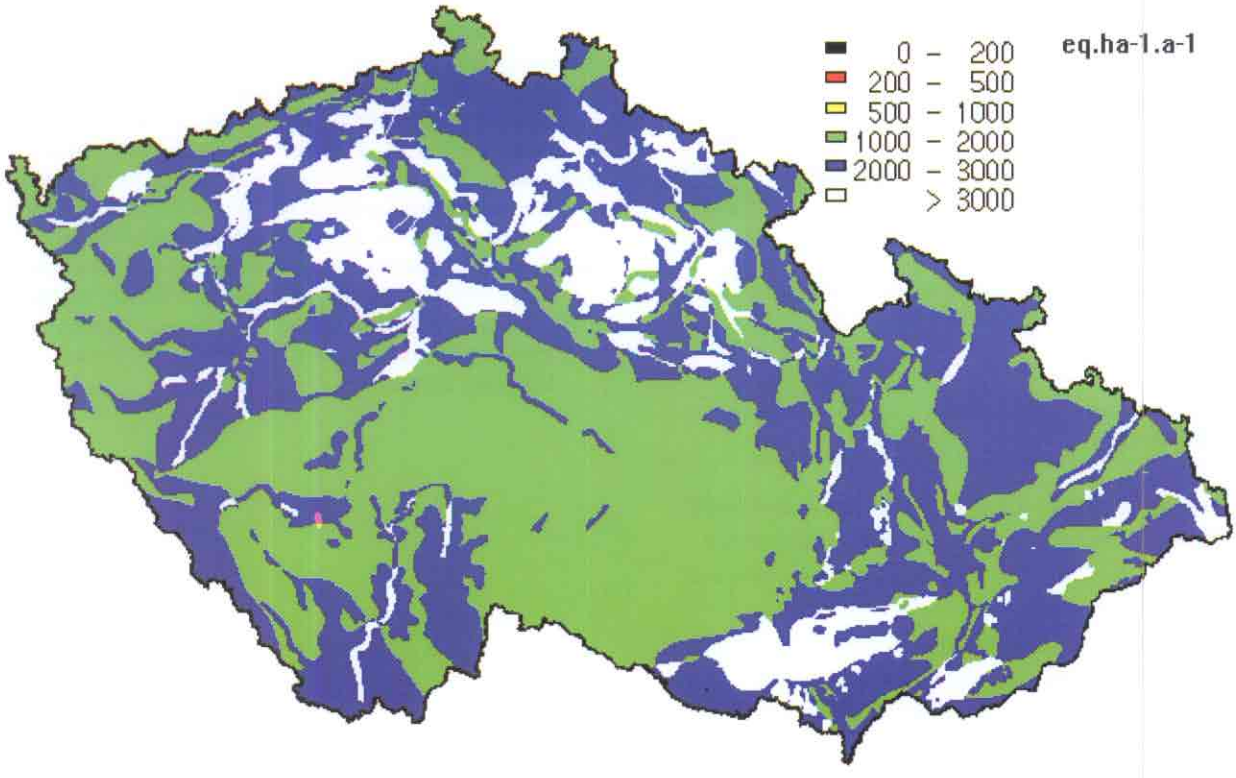

Figure CZ-2. Maximum critical loads of nitrogen.

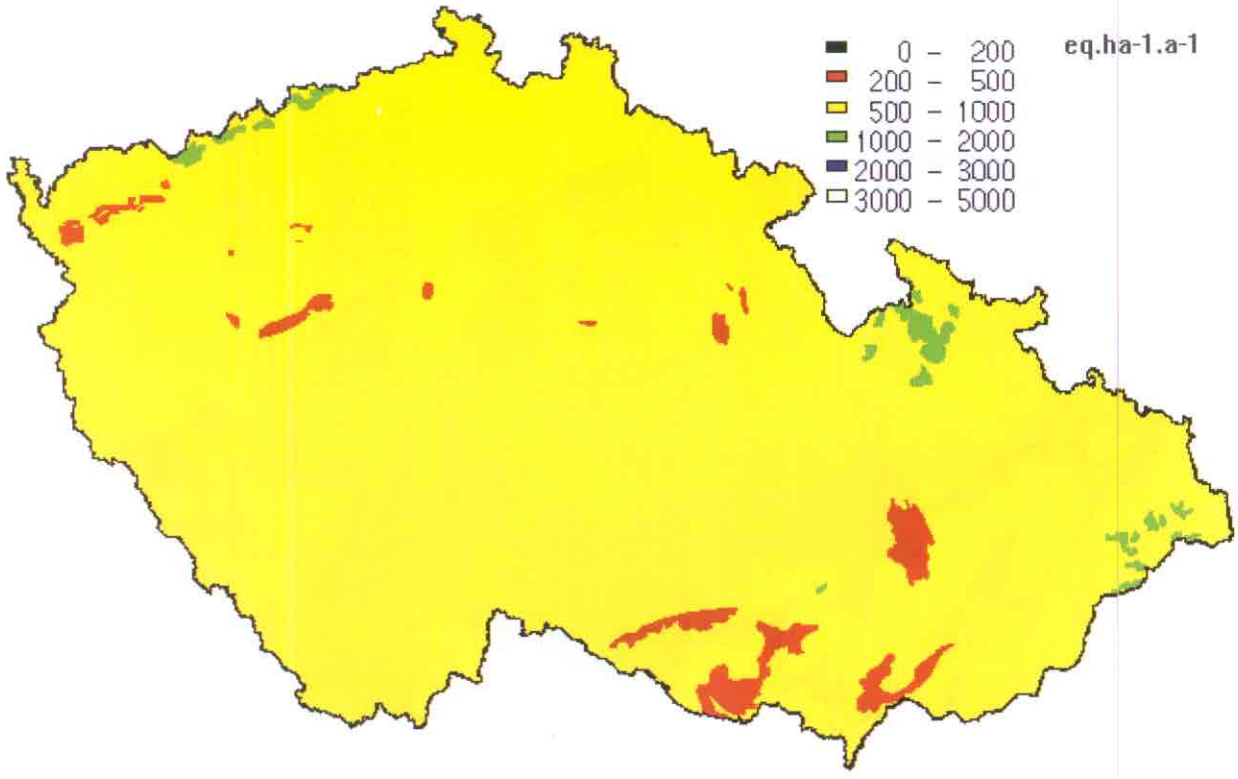

Figure CZ-3. Minimum critical loads of nitrogen.

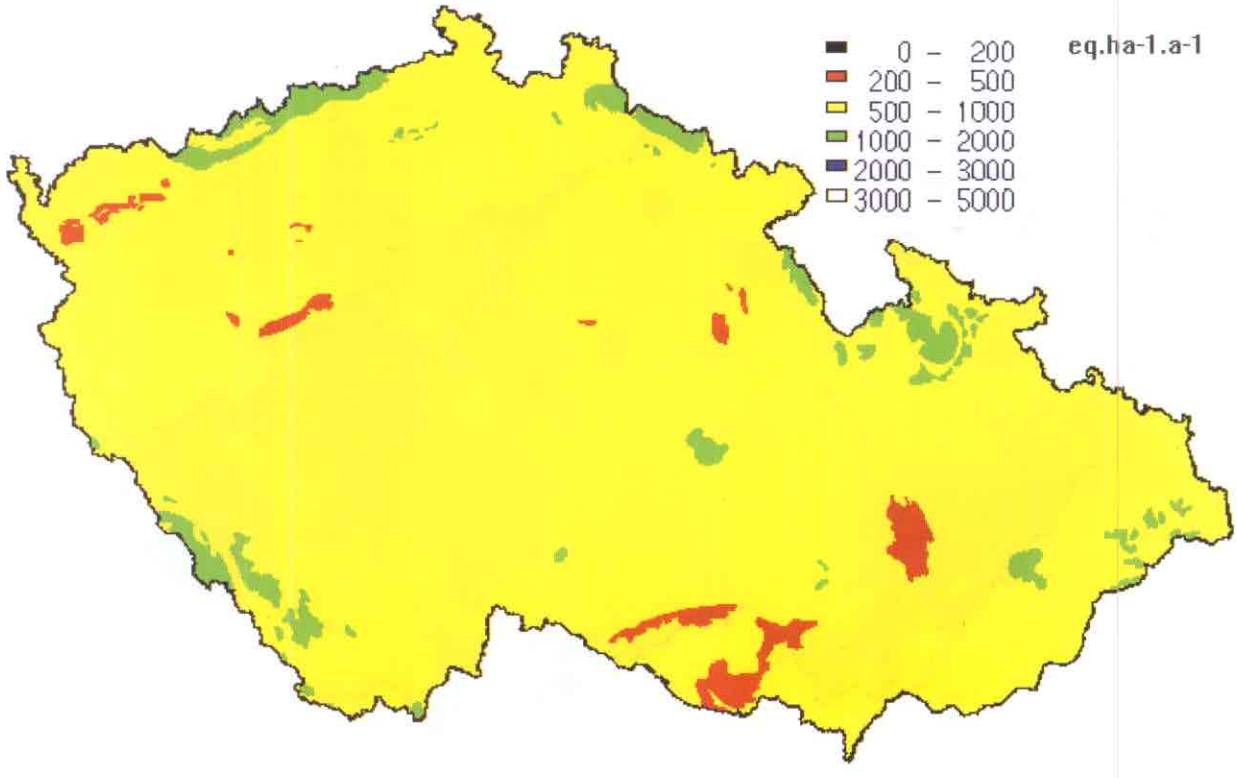

Figure CZ-4. Critical loads of nutrient nitrogen.

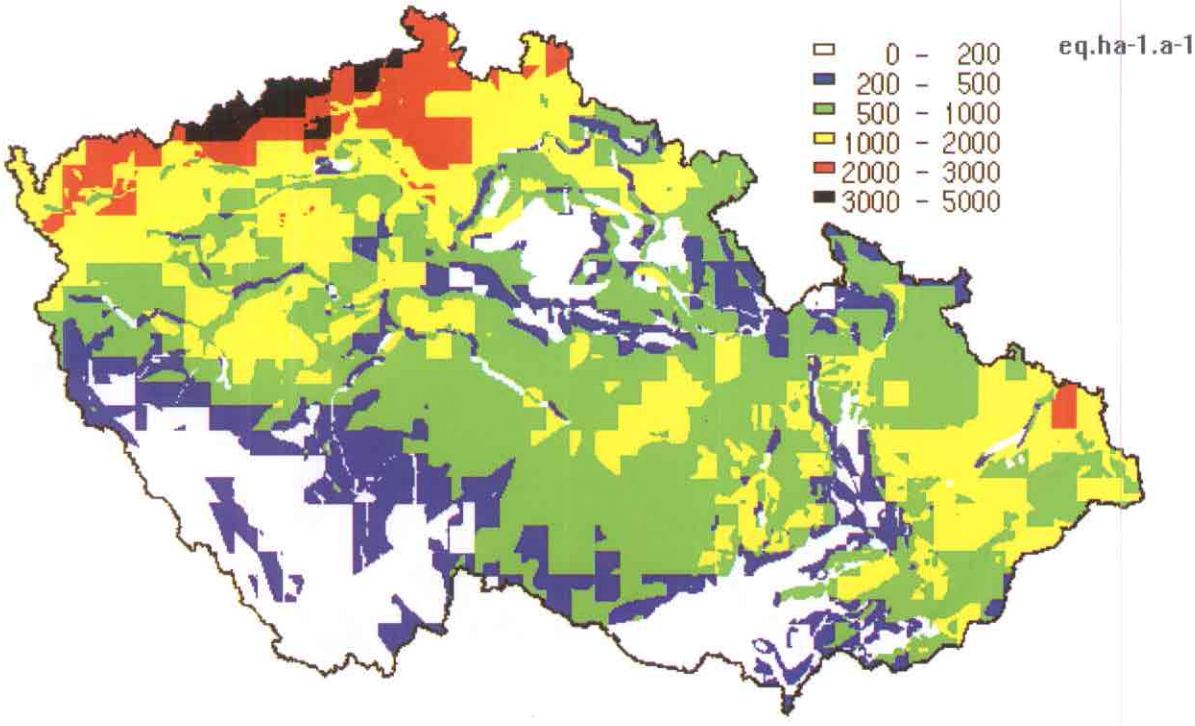

Figure CZ-5. Exceedance of critical loads of sulfur.

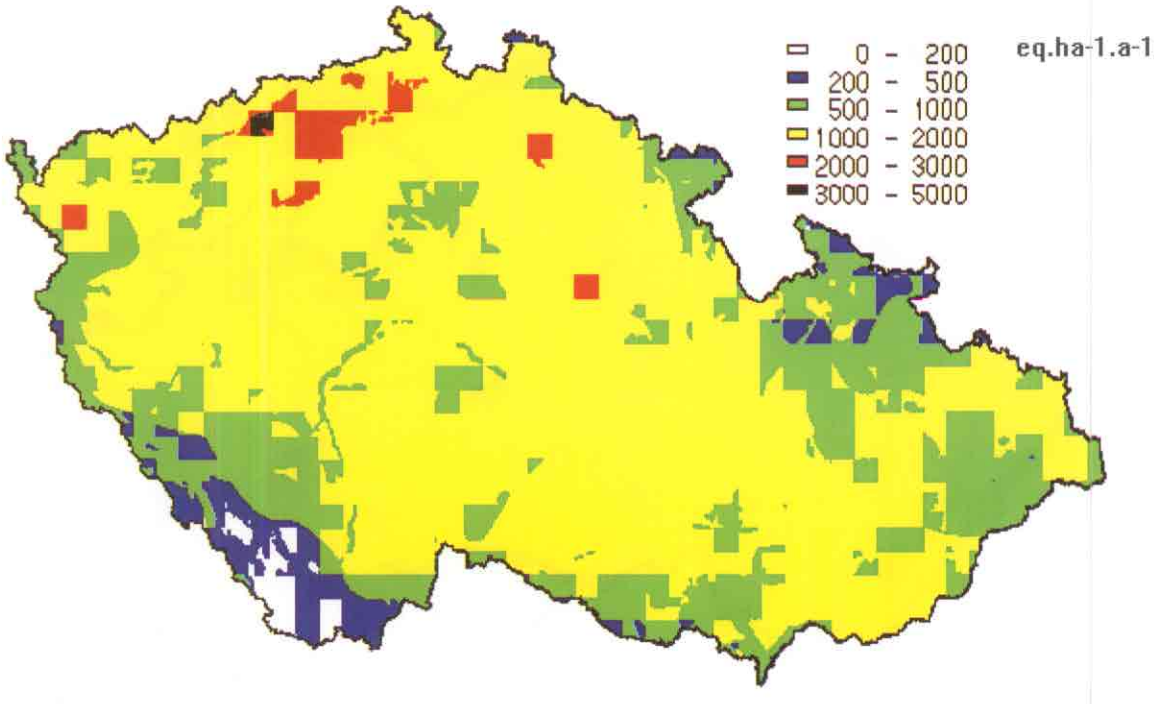

Figure CZ-6. Exceedances of critical loads of nutrient nitrogen.

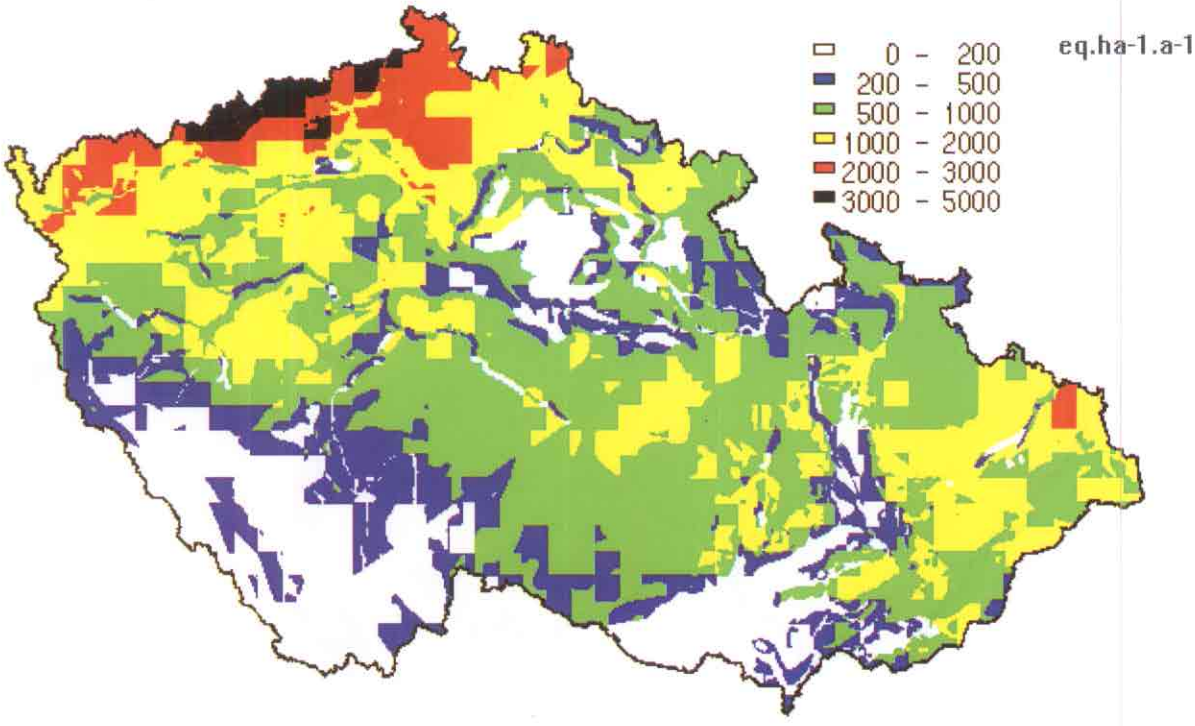

Figure CZ-5. Exceedance of critical loads of sulfur.

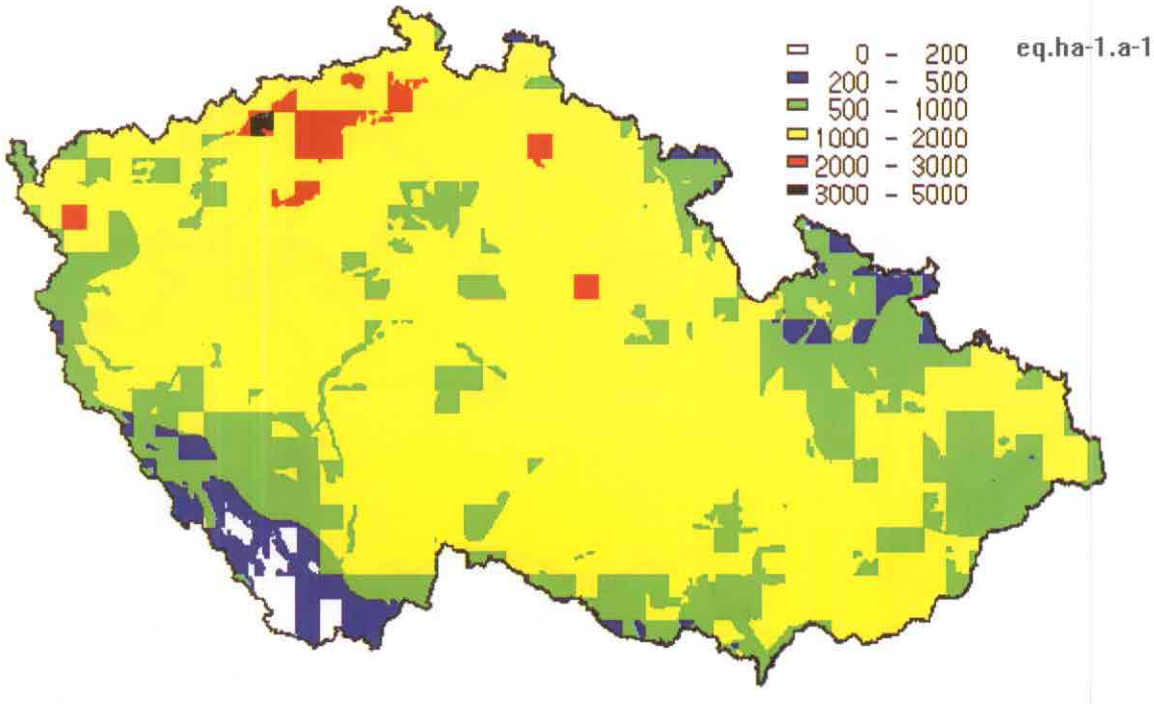

Figure CZ-6. Exceedances of critical loads of nutrient nitrogen.

DENMARK

National Focal Center/Contacts
Jesper Bak and Hans Løkke
National Environmental Research Institute
Dept. of Terrestrial Ecology
25 Vejlsøvej
DK-8600 Silkeborg
tel: +45-89-201400
fax: +45-89-201414
email: jlb@dmu.dk

National Maps Produced

- Critical loads and exceedances of acidity for forest soils and extensively managed, permanent grasslands calculated with PROFILE, and calculated with the SMB model for grasslands.
- Critical loads and exceedances of nutrient nitrogen for production forests calculated with PROFILE.
- National deposition maps of NH_x and NO_y on a 5 × 5 km^2 grid.
- National deposition map of SO_x on a 20 × 20 km^2 grid.
- Yield losses as a result of exceedances of the critical level for ozone calculated on a 25 × 25 km^2 grid.

Calculation methods

Critical loads of acidity and nutrient N: The PROFILE model has been used to calculate the critical load of acidity and nitrogen eutrophication, and the values of BC_u, N_u, BC_w, and $ANC_{le(crit)}$. From this calculation, the values of $CL_{min}(S)$, $CL_{max}(S)$, $CL_{min}(N)$, and $CL_{max}(N)$ have been derived. In calculating the critical load for grasslands, the weathering rate for 11 classes of mineralogy were calculated at 1000 points with the PROFILE model. The calculation of critical loads for grasslands were performed with the SSMB model (UBA 1996). The total number of calculations and the calculated critical loads and exceedances for the different vegetation types are summarized in Table DK-1.

A BC/Al ratio of 1 was used as the chemical criterion for both forest soils and grasslands. To calculate critical loads of nutrient nitrogen, a critical N leaching, $N_{le(crit)}$, of 2 kg N ha^{-1} yr^{-1} and an immobilization, $N_{i(crit)}$, of 3 kg N ha^{-1} yr^{-1} were applied. For the model calculations, the root zone has been stratified in a 5-cm thick A/E horizon, and a soil-dependent B and C horizon. A total root depth of 50 cm was applied for spruce and pine, 70 cm was applied for beech, 90 cm for oak, and 25 cm for grasslands, respectively.

National deposition maps: Wet and dry deposition of NH_x and dry deposition of NO_y have been calculated with the TREND model on a 5 × 5 km^2 grid (Asman 1992). The calculated values are within an expected uncertainty range of 30-40% compared to measured values. While the accuracy for modeled values of NO_y wet deposition is poorer, the total variation in NO_y wet deposition within Denmark is less than 30% (estimated from measured data). An average value from measured data has been used to calculate critical load exceedances.

Wet and dry deposition of SO_x has been calculated with the TREND model on a 20 × 20 km^2 grid. The uncertainty of this calculation is within a range of 30-40%. For SO_x, transport matrices between grids and between receptor grids and major Danish sources have been calculated for use in integrated assessment modelling (Asman *et al.* 1996).

Yield losses as a result of exceedances of the critical level for ozone: A Level I approach has been used in a first attempt to map yield losses as a result of exceedances of the critical level for ozone. The calculation has been performed for wheat, pasture, deciduous forest and coniferous forest. Values from three Danish measuring stations have been used to calculate an average value of AOT40 for crops and trees for the period 1991–1994. For crops the AOT40 value has been calculated for the period May–July, while the period April–September was used for forests. The spatial distribution of crops and forests have been adapted from the CORINE land-use data base, while the relations between AOT40 values and yield losses were adopted from Fuhrer and Achermann (1994). The yield loss for pasture has been based on clover. The average AOT40 values are presented in Table DK-2 and the calculated yield losses in Table DK-3. A map of calculated total yield losses is displayed in Figure DK-1.

Table DK-1. Calculated critical loads and exceedances for acidification and for nitrogen eutrophication for various ecosystems. All values are given in keq ha^{-1} yr^{-1} as the range between the 5th and the 95th percentiles.

	beech	oak	spruce	pine	grass
No. calculations	2825	448	5480	1035	18178
CL(A)	0.9 – 2.7	0.8 – 2.2	1.4 – 4.1	1.4 – 2.4	0.9 – 2.4
Exc(A)	-0.9 – 0.6	-0.8 – 0.8	-1.5 – 1.3	-0.7 – 1.3	-1.1 – 0.7
$CL_{nut}(N)$	1.2 – 1.9	1.2 – 2.0	0.6 – 1.1	0.5 – 0.7	–
$Exc_{nut}(N)$	-0.3 – 0.6	-0.3 – 0.7	0.4 – 1.2	0.3 – 1.2	–

Table DK- 2. Ozone AOT40 for crops and forests in Denmark.

AOT40	crops	forests
minimum	3381	5994
average and (s.d.)	7029 (3600)	9926 (3649)
maximum	11899	14496

Table DK-3. Estimated annual yield loss as a result of exceedances of the critical level for ozone.

Receptor	loss (mil. DKK)
wheat	724
pasture	307
deciduous forest	16
coniferous forest	46
Total	1,094

Data Sources

The main sources of data have not been changed since the 1995 and 1993 CCE Status Reports. The main changes in available data is that the CORINE land use map has been finalized, and a new national calculation of SO_x deposition has been performed. The sources and resolution of data are shown in Table DK-4.

Table DK-4. Sources of data.

parameter	resolution	source
soil mineralogy	60 points	DLD, literature
soil texture	1:500,000	DLD
geological origin	1:500,000	DLD
crop yields	county	DSO
forest production	1:500,000	DLD, DSO
ecosystem cover	25 ha	NERI
deposition (S, N)	5×5, 20×20	NERI
meteorology	1:1,000,000	DMI

DLD: National Institute of Soil Science, Dept. of Land Data
DSO: Danish Statistical Office
NERI: National Environmental Research Institute
DMI: Danish Meteorological Institute

Comments and Conclusions

The main focus of the Danish NFC in the past two years has been:

- The development of methods and preparation of data to calculate critical loads of nutrient nitrogen for sensitive, natural or seminatural terrestrial ecosystems, primarily raised bogs and heathlands.
- The development of methods for, and a first attempt to map yield losses due to exceedances of the critical level for ozone.
- A first attempt to map critical loads of heavy metals.
- Estimation of the uncertainties in the current calculations for NHX.

As indicated, only minor progress has been made in the availability of data for calculating critical loads and deposition. The critical load calculations have been updated according to the revised mapping manual (UBA 1996), but the revision has only caused minor changes to the mean value and spatial distribution of the calculated critical loads of acidity and nitrogen. Maps of $CL(A)$ and $CL_{nut}(N)$ are displayed in Figure DK-2. The current development of methods and preparation of data for calculating critical loads of nitrogen for raised bogs and heathlands will result in data by the end of 1997.

Critical loads of the heavy metals Hg, Pb, and Cd will be available by the end of 1997. In 1996 the results from a Danish monitoring program on heavy metals were reported. The monitoring program, initiated in 1992, includes the heavy metals Pb, Cd, Ni, Zn, Cu, Cr, Hg, and As, monitored at 393 sites covering arable land and nature areas. As part of this project, models to calculate soil concentrations of heavy metals have been developed, and the relationships between soil concentrations and the current load of heavy metals as well as other biotic and abiotic factors have been assessed. Additional calculations of critical loads of Ni, Zn, Cu, and Cr are planned before 1999.

Consequences of adapting the EMEP50 grid: The calculation of critical load exceedances implies in general the combination of critical load data at high spatial resolution with deposition data at a much coarser spatial resolution. Usually the exceedance is calculated as the difference between a deposition value and a percentile of the critical load values calculated within each grid. The total uncertainty of the calculated exceedance can thus be divided among: i) the uncertainty of the calculated critical loads, ii) the uncertainty of the calculated deposition for the grid, and iii) the spatial variation in the deposition within the grid. The spatial variability within the grids will be smaller when going to a higher resolution grid if the gradients in deposition have a spatial scale larger than the grid. This will be the case for NO_y and SO_x, but not necessarily for NH_x in high-deposition areas. The trade-off in going to a higher resolution is higher uncertainty in the calculated percentiles of critical loads, and more uncertain deposition estimates.

The Danish critical load calculations are performed at a maximum resolution of 25 ha, reflecting the accuracy of the basic data available with the highest resolution. Critical loads of nitrogen have been calculated for a total of 16,229 data points. The highest number of calculations on a EMEP50 grid cell is 773, the lowest is 30. The uncertainty of the calculated percentile values of critical loads is mainly dependent on the distribution function and the number of samples. Figure DK-3 shows the estimated relative uncertainty of the 5, 10, 25, 50 and 95 percentile of *CL(N)* as a function of the number of samples. The distribution function is estimated from all calculation points. Assuming a similar distribution function in each EMEP50 grid, the added uncertainty introduced by going from the EMEP150 to the EMEP50 grid can be estimated to be in the range between 2 and 25% for the Danish grids. This extra uncertainty is reasonably low compared to other uncertainties in the calculation process.

Local variation of NH_x deposition: The spatial variation of the NH_x deposition is to a high degree governed by the spatial pattern of local sources, topography, microclimate, etc. Even with the higher spatial resolution of the EMEP50 grid, there will still be large variation within the grid, especially in high-deposition areas. Figure DK-4 illustrates the values of different percentiles of critical load exceedance as a function of the local variation in NH_x deposition. If the variation in NH_x deposition within the individual grids is 25%, the 95 percentile exceedance will on average be underestimated by 16%.

References

Asman, W., 1992. Estimated nitrogen depositions for Denmark for use in critical load computations. NERI internal report.

Asman, W. *et al.* 1996. MeMos: Udvikling af en konsekvensmodel for svovldeposition for Sydskandinavien, Faglig rapport fra DMU, nr 149.

Fuhrer, J. and B. Achermann (eds.), 1994. Critical Levels for Ozone: a UN-ECE workshop report. FAC-Liebefeld.

UBA, 1996. Manual on Methodologies and Criteria for Mapping Critical Levels/Loads and geographical areas where they are exceeded. UN/ECE Convention on Long-range Transboundary Air Pollution. Federal Environmental Agency (Umweltbundesamt), Texte 71/96, Berlin.

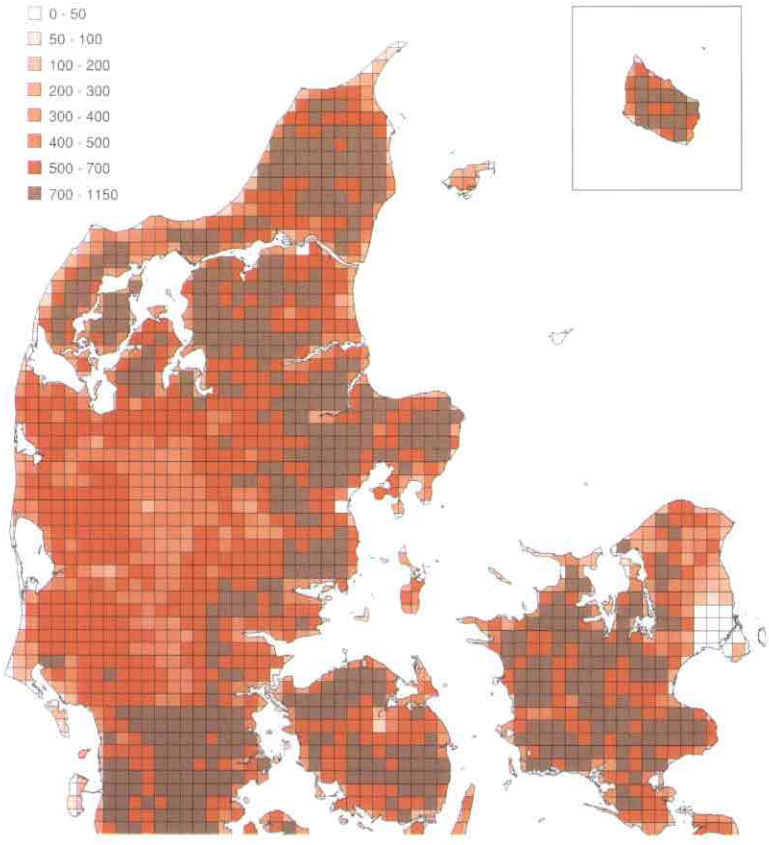

Figure DK-1. Calculated average yield losses as a result of exceeding the critical limit for ozone.

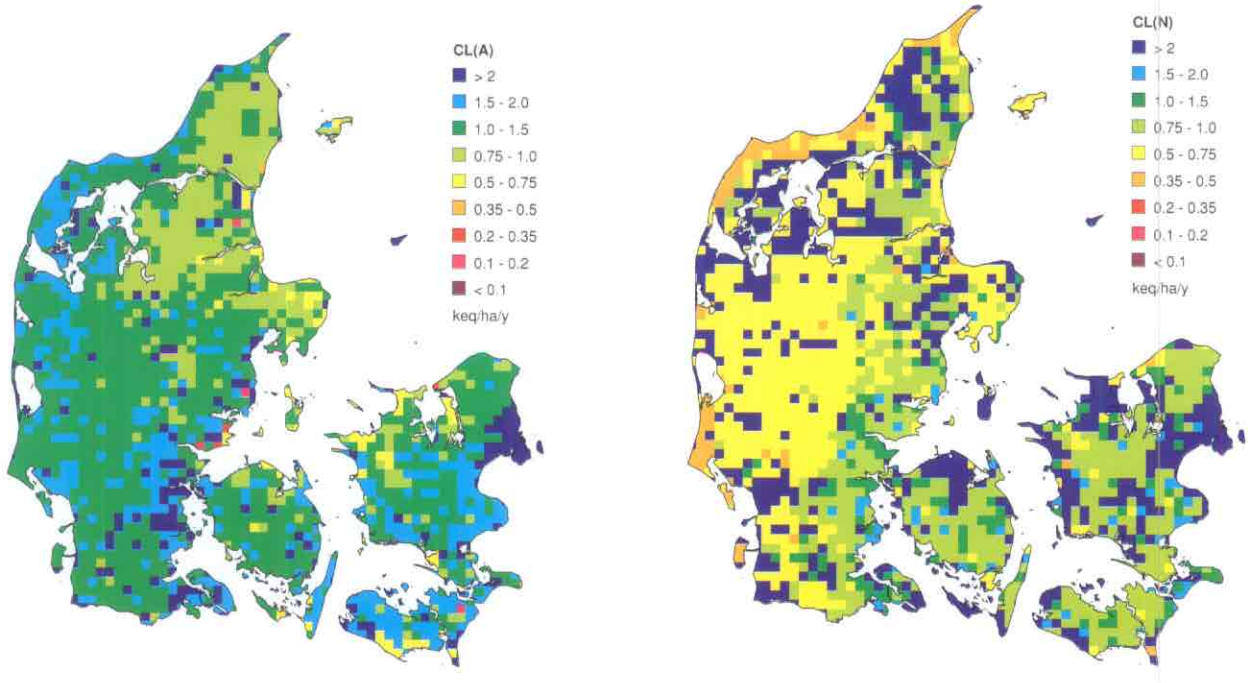

Figure DK-2. Critical loads of acidity and nutrient nitrogen, 5 percentile.

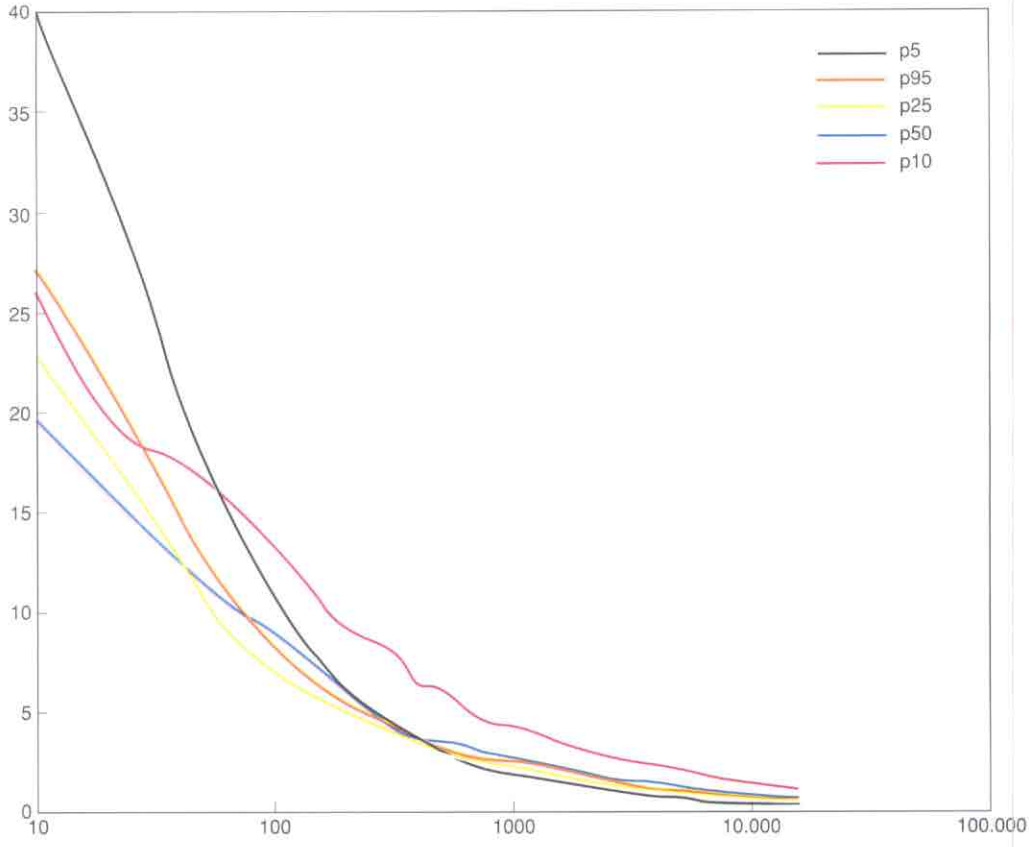

Figure DK-3. Estimated uncertainty (in %) of the calculated values of the 5, 10, 25, 50, and 95 percentile *CL(N)* values, with various numbers of samples.

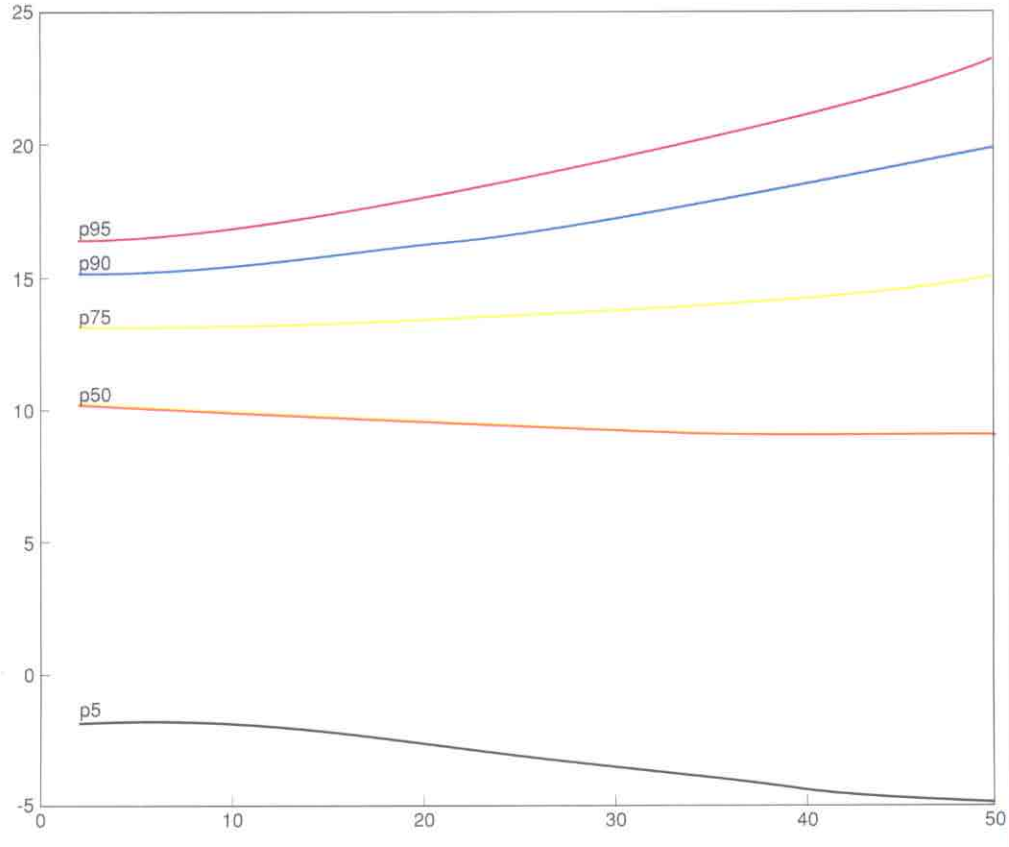

Figure DK-4. Percentiles of critical load exceedance as a function of local variation of NH_x.

ESTONIA

National Focal Center/Contact
Leo Saare
Estonian Environmental Information Center
Mustamäe tee 33
EE-0006 Tallinn
tel: +372-6-565373
fax: +372-6-564071
email: eeic@ciesin.ee

Collaborating Institution/Contact
Tõnu Oja
Institute of Geography
University of Tartu
EE-2400 Tartu
tel: +372-7-465819
fax: +372-7-465825
email: toja@ut.ee

National Maps Produced

Critical loads of nitrogen (minumum, maximum, and nutrient); sulfur (minimum and maximum); and exceedances of nutrient nitrogen and total acidity (N+S).

Calculation Methods

Two methods have been used to calculate critical loads: the empirical method for raised bogs, and steady-state mass balance calculations for forested areas (UBA 1996). After implementing the more detailed EMEP 50 × 50 km^2 grid, the differentiation of ecosystems mapped was substantially increased, which is particularly important for the cells only partly covering Estonia.

A change has been made in the rates of base cation deposition (BC_{dep}). In preliminary calculations, measured base cation deposition data were used, which are substantially higher than natural background in northeastern Estonia (due to industrial emissions). Recently, sulfate and nitrate deposition as well as base cation deposition have shown decreases in this area. Although the still-elevated base cation deposition buffers a large part of the impact of acidic ions, this is not be considered in calculating critical loads. In the new calculations, base cation deposition in Estonia were considered equal to those in northwest Estonia, a region with similar natural background conditions.

To estimate exceedances of critical loads, actual deposition of sulfate and nitrate/ammonia were compared to critical load calculations. Deposition data from earlier measurements were used together with measurements for 1994/95 (Kört and Roots 1996, Kört *et al.* 1996, Aguraijuja 1996, Nilson 1996, Frey *et al.* 1996). Nutrient nitrogen impact and the acidifying impact of sulfur/nitrogen ($CL_{max}(S)$ + $CL_{min}(N)$) were analyzed separately.

Comments and Conclusions

Maps of $CL_{nut}(N)$, $CL_{min}(N)$, $CL_{max}(N)$, and $CL_{max}(S)$ are shown in Figure EE-1. Exceedances for nutrient nitrogen and the combined acidifying impact of N+S are presented in Figure EE-2. The grid cells with light vertical stripes are ones where actual deposition is equal to critical loads or slightly (by not more than 20%) exceed them. The more intensive color denotes the cell where actual deposition clearly exceeds the critical loads for natural background (by about 1000 $mol_c\ ha^{-1}\ yr^{-1}$). As the deposition measurements do not cover the Estonian territory densely enough, it is impossible to determine the exceedances precisely. Exceedances of critical loads of nutrient nitrogen can be expected in those parts of sensitive cells where extra nitrogen might start to influence the plant communities in bogs. However, the exeedances found remain within the limits of calculation and measurement error, and thus we should probably speak about critical loads being achieved rather than being exceeded. Further increases in nitrogen deposition will clearly lead to critical load exceedances.

The situation regarding acidifying impact is similar in that many cells have actual deposition equal to critical loads. Only one cell (63,76) shows deposition clearly exceeding critical loads (figure EE-2, right). The critical load is exceeded when calculated with natural background base cation levels. However, due to the increased base cation deposition, the area does not actually suffer from acidification, but rather from alkalinization. Comparing two different regions with deposition equal to critical loads, all of northeastern Estonia is characterized by substantially increased base cation deposition which fully buffers the acidic

deposition. Southern Estonia differs in that base cation deposition here corresponds to that of natural background. Thus deposition exceeding critical loads in some of the more sensitive areas will have an acidifying impact.

References

Aguraijuja, K. 1996. Kompleksseire. Keskkonnaseire 1995. Eesti Vabariigi Keskkonnaministeerium, Info- ja tehnokeskus, Tallinn, lk. 114-117.

Frey, T., J. Frey and P. Kask, 1996. Saarejärve kompleksseire. Keskkonnaseire 1995. Eesti Vabariigi Keskkonnaministeerium, Info- ja tehnokeskus, Tallinn, lk. 119 - 122.

Kört, M. and O. Roots, 1996. Õhu saasteainete kauglevi seire. Keskkonnaseire 1995. Eesti Vabariigi Keskkonnaministeerium, Info- ja tehnokeskus, Tallinn, lk. 12 - 15.

Kört, M., O. Roots and I. Kirjanen, 1996. Sademete keemia. Keskkonnaseire 1995. Eesti Vabariigi Keskkonnaministeerium, Info- ja tehnokeskus, Tallinn, lk. 15 - 19.

Nilson, E., 1996. Vilsandi kompleksseireala. Keskkonnaseire 1995. Eesti Vabariigi Keskkonnaministeerium, Info- ja tehnokeskus, Tallinn, lk. 117 - 119.

Roots, O., L. Saare, M. Kört and E. Otsa, 1994. Wet deposition of airborne pollutants in Estonia.

UBA, 1996. Manual on Methodologies and Criteria for Mapping Critical Levels/Loads and geographical areas where they are exceeded. UN/ECE Convention on Long-range Transboundary Air Pollution. Federal Environmental Agency (Umweltbundesamt), Texte 71/96, Berlin.

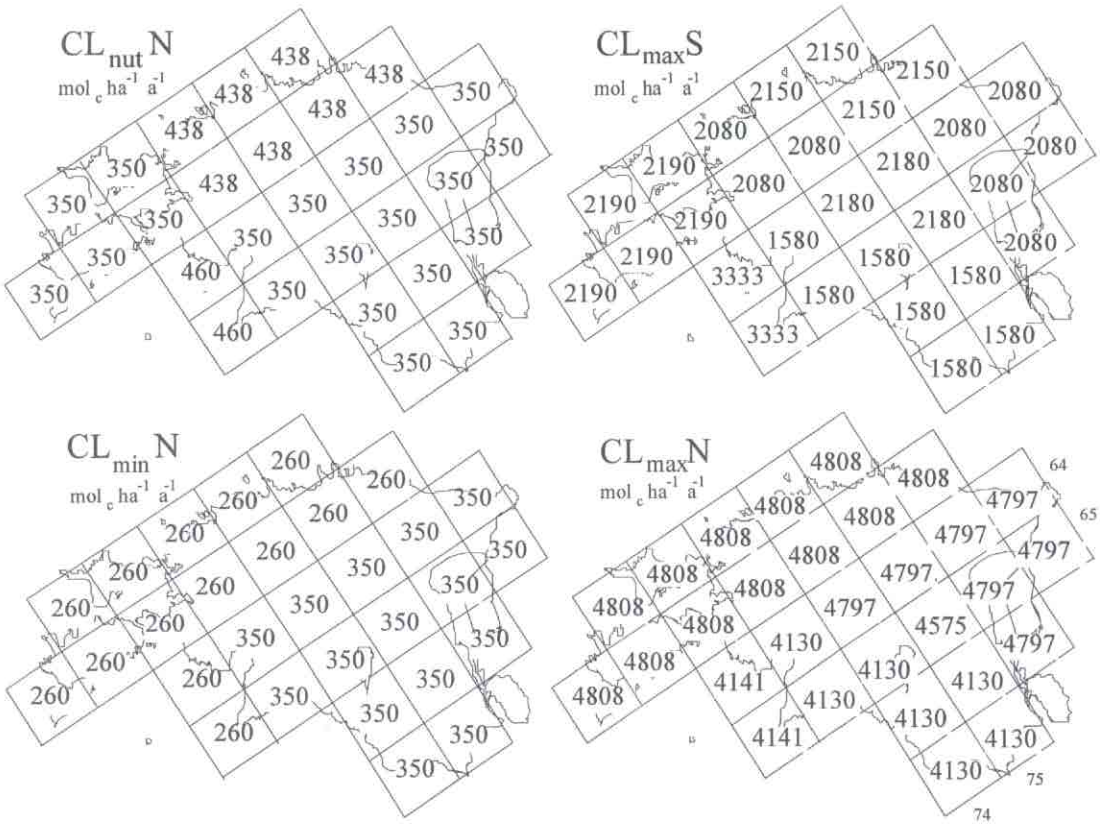

Figure EE-1. $CL_{nut}(N)$, $CL_{min}(N)$, $CL_{max}(N)$ and $CL_{max}(S)$ in eq ha^{-1} yr^{-1}.

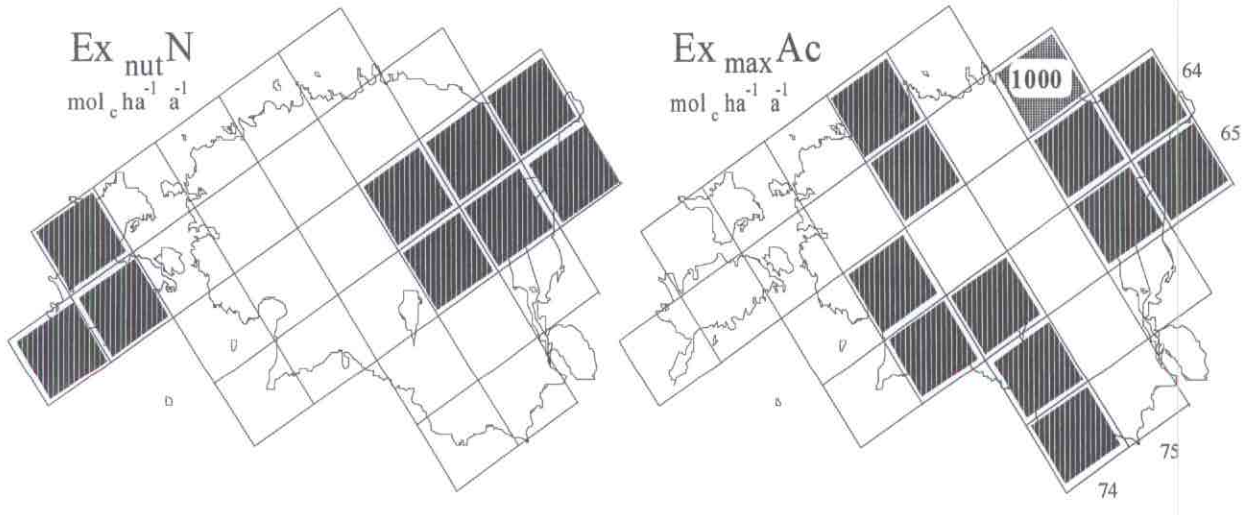

Figure EE-2. Exceedance of critical loads of nutrient nitrogen (left) and of acidic N+S (right).

FINLAND

National Focal Center/Contacts
Matti Johansson
Sanna Syri
Martin Forsius
Juha Kämäri
Jaakko Mannio
Jussi Vuorenmaa
Finnish Environment Institute
P.O. Box 140
FIN-00251 Helsinki
tel: +358-9-403000
fax: +358-9-40300390
email: matti.johansson@vyh.fi

Collaborating Institutions/Contacts
Tuomas Laurila
Juha-Pekka Tuovinen
Virpi Lindfors
Finnish Meteorological Institute
Sahaajankatu 20 E
FIN-00810 Helsinki
tel: +358-9-19291
fax: +358-9-19295403
email: tuomas.laurila@fmi.fi

Timo Tarvainen
Geological Survey of Finland
P.O.Box 96
FIN-02151 Espoo
tel: +358-205502399
fax: +358-2055012
email: timo.tarvainen@gsf.fi

National Maps Produced

The required reductions of sulfur and nitrogen can be defined with the position of the current or future deposition pair in relation to the ecosystem protection isoline. The S-N plane is divided into five areas: one where there is no exceedance at all and four with a combination of mandatory or exchangeable S and N reductions. We have presented the five cases for reduction requirements of critical load exceedances to achieve protection of 95% of Finnish lakes and forest soils against acidification in each 50km x 50km grid cell at present (1995) total sulfur and nitrogen deposition (see Figure FI-1).

Critical levels for ozone have been mapped according to the recommendations from the UN/ECE workshop in Kuopio (Kärenlampi and Skärby 1996). In Figure FI-2 the measured AOT40 (accumulated hourly exposure above the threshold of 40 ppb, displayed in ppm·h) values for agricultural crops and forests are displayed for the years 1989-95.

Calculation Methods

Critical loads of acidity of N and S for surface waters and forest soils are derived the following acidity balance for the sum of N and S deposition (described more fully in Posch *et al.* 1997):

$$N_{dep} + S_{dep} = fN_u + (1-r)(N_i+N_{de}) + rN_{ret} + rS_{ret} + BC_{le} - ANC_{le} \quad (1)$$

where the base cation (BC) leaching is given by

$$BC_{le} = BC_{dep} + (1-r)BC_w - fBC_u \quad (2)$$

where f is the fraction of forested land in the catchment area, r is the lake:catchment area ratio, N_u and BC_u are the net growth uptake of N and BC, N_i is the immobilization of N in soils, N_{de} is N denitrified in soils, N_{ret} and S_{ret} are the in-lake retention of N and S, BC_w is the BC weathering, and ANC_{le} is the alkalinity leaching. For lake catchments the term $(1-r)$ limits the influence of N_i, N_{de} and BC_w to the terrestrial area, and f limits the uptake to the forested area only. For forest soils one has to set f=1 and r=0.

Inserting the deposition-dependent expressions for soil denitrification and in-lake N and S retention into Eq. 1, one obtains:

$$a_N N_{dep} + a_S S_{dep} = b_1 N_u + b_2 N_i + BC_{le} - ANC_{le} \quad (3)$$

where the dimensionless constants a_N, a_S, b_1 and b_2 are all smaller than one and depend on ecosystem properties only: denitrification fraction (f_{de}), net mass transfer coefficients for S and N (s_S and s_N), and runoff (Q). For soils, BC_{le} at critical load is computed from Eq. 2.

For lakes the net base cation leaching at critical load is computed from water quality data:

$$BC_{le(crit)} - ANC_{le(crit)} = Q([BC]^*_0 - [ANC]_{limit}) \quad (4)$$

where $ANC_{le(crit)}$ is ANC_{le} at critical load, $Q([BC]^*_0$ is the pre-acidification leaching of base cations from the catchment area, and $Q[ANC]_{limit}$ is the critical alkalinity leaching. By prescribing an acceptable leaching of N, the critical load of nutrient nitrogen can be computed for soils, using the mass balance:

$$CL_{nut}(N) = N_u + N_i + N_{de} + N_{le(acc)} \quad (5)$$

Data Sources

Forest soils: Information is needed for BC_{dep}, BC_w, BC_u, N_{dep}, N_u, N_{de}, N_i, $N_{le(acc)}$ and $ANC_{le(crit)}$. BC_{dep} is interpolated from the data from the years 1993-95 of a nationwide network of stations measuring monthly bulk deposition (Järvinen and Vänni 1990), and seasalt correction is made where necessary. The long-term average BC_w was estimated by applying the results of the field studies of Olsson and Melkerud (1993) and using the effective temperature sum (ETS) and the total element content of Ca and Mg in the C-horizon as input data. Total analysis data on the < 2.0 mm fraction of till required by the method were obtained for 1057 plots from the Geological Survey of Finland (Johansson and Tarvainen 1997). N_u and BC_u refer to the long-term average net uptake of nutrients in the stem and bark biomass removed from forest via harvesting. They are estimated from annual forest growth, calculated for each tree species based on ETS, and the element contents (Rosén, pers. comm.) in biomass. N_{de} was assumed to be proportional to the net incoming N, and the denitrification fractions were related to the soil type by linearly interpolating between a low value of 0.1 for podzolic mineral soils and a value of 0.8 for peat soils, depending on the soil type fractions (de Vries *et al.* 1993). For N_i, including N_{fix}, a value of 0.5 kg N ha^{-1} yr^{-1} as a long-term average was used for Finnish forest soils (Rosén *et al.* 1992). For $[BC]_{min}$ a limiting concentration, below which trees can no longer extract nutrients from soil solution, is set to a precautionary value of 2 μeq l^{-1} (UBA 1996). $ANC_{le(crit)}$ is calculated by adding the critical aluminum leaching, obtained from the molar Al/BC ratio of 1.0, to the hydrogen leaching, calculated from a gibbsite equilibrium ($K_{gibb} = 10^{8.3}$). Acceptable nitrogen leaching is derived with runoff using the concentration criterion 0.3 mg N l^{-1} (Downing *et al.* 1993). The runoff values needed to convert concentrations to fluxes were obtained from a digitized runoff map for 1961-1975 (Leppäjärvi 1987). Sulfur and nitrogen deposition is calculated with the DAIQUIRI (Deposition, AIr QUality and Integrated Regional Information) model, employing long-range and mesoscale transfer matrices from EMEP/MSC-W and the Finnish Meteorological Institute (Syri *et al.* 1997).

Lakes: Additional information is needed for f, r, S_{ret}, N_{ret}, $[BC]^*_0$ and $[ANC]_{limit}$. The data for lakes were mostly obtained from a national statistically based lake survey of 970 lakes conducted in 1987. The spatial distribution of the lake data set reflects the actual lake density in different regions. Both lake and catchment areas, as well as the forest fraction, were measured from topographic maps. S_{ret} and N_{ret} were computed from kinetic equations (Kelly *et al.* 1987). The mass transfer coefficients s_S and s_N were taken from retention model calibrations in North-America (Baker and Brezonik 1988, Dillon and Molot 1990). $[BC]^*_0$ was estimated using the so-called F-factor, which relates the change over time in the leaching of base cations to long-term changes in inputs of strong acid anions in a lake, estimated as a function of the present base cation concentration. $[SO_4]^*_0$ was estimated from the relationship between present sulfate and base cation concentrations from 251 lakes located in northern Fennoscandia receiving very low acidic deposition. An $[ANC]_{limit}$ value of 20 μeq l^{-1} was selected as the chemical criterion based on results of a fish status survey conducted in Norway (Lien *et al.* 1996).

Based upon experience gained from extensive lake surveys in Finland, Norway and Sweden (Henriksen *et al.* 1992), a joint Nordic Lake Survey was conducted in fall 1995. The cooperation was expanded to adjacent areas in Denmark, Russian Kola and Karelia, and Scotland and Wales. This integrated approach included harmonizing the lake selection criteria and sampling procedures (Henriksen *et al.* 1996). The key objectives of the integrated survey were to assess the status of the lakes with respect to: 1) general water quality, 2) occurrence and large-scale variation of acidification, 3) creation of a new chemical data baseline to follow up the future effects of the second sulfur protocol of UN/ECE, 4) establishing the effects of nitrogen deposition on lake water chemistry in connection with the development of critical loads of nitrogen and 5) the eutrophication status, and 6) levels of heavy metals.

In Finland, 873 lakes were selected separately by regions covering the whole country. From each region, statistical sampling was conducted on five lake size classes. Water samples (one sample per lake) were collected during the autumn overturn, and major and minor elements (25 variables) were analyzed from each lake. The lake data base also includes background information on catchment characteristics for individual lakes, such as lake and catchment area, proportion of different land use classes, forest and soil types, long-term annual mean value for runoff and annual deposition of sulfur, nitrogen and base cations.

The description of the chemical characteristics of the total lake populations and calculations of critical loads of acidity and exceedance of sulfur acidity applied by the steady state water chemistry (SSWC) method, will be published in 1997 (Henriksen *et al.* 1997). Some initial results of the survey are presented in the Norwegian NFC report in this volume; however, the data was not yet ready to incorporate into the final critical load calculations. In the future, there will be also an integrated evaluation of the heavy metals in the lakes.

Tropospheric ozone: The accumulated ozone exposure index, AOT40, has been evaluated by the Finnish Meteorological Institute (FMI) for eight background monitoring stations (e.g. Laurila and Tuovinen 1996). These results are shown in Figure FI-2 for crops and forests, calculated according to the definitions adopted in 1996 at the UN/ECE workshop in Kuopio. Exposure maps based on earlier definitions have been published recently as a result of the Nordic mapping project (Lövblad *et al.* 1996). The monitoring results have also been used for studying the variability and the origin of the near-surface ozone in Finland (Laurila 1996, Laurila and Hakola 1996, Rummukainen *et al.* 1996). In addition, the role of biogenic emissions in the photochemical processes related to ozone formation have been assessed by emission and atmospheric modelling combined with measurements of ambient VOC concentrations (Lindfors *et al.* 1996).

The fact that in northern Europe ozone episodes are more frequent at the beginning of the growing season than later in the summer emphasizes the importance of the choice of the first date of the exposure period. If the growing season for forests is defined as the period for which daily average temperatures exceed 5°C, the exposures are much less than for the April-September period used in the UN/ECE definition (Laurila and Tuovinen 1996). A more specific definition for birch, i.e. the actual period between leaf emergence and leaf fall, was shown to give the shortest exposure period and the lowest AOT40. For agricultural crops, a similar sensitivity is observed.

The relationship between the exposure to ozone and the actual ozone dose received by the vegetation has also been studied at the FMI. These studies are based on the scientific campaigns conducted to directly measure the ozone flux to vegetation (e.g. Aurela *et al.* 1996, Tuovinen *et al.* 1996, 1997). Measurements above pine forest indicate a clear difference between the diurnal variation of the accumulation of AOT40 and the flux. Due to the relatively inefficient night-time deposition, these data support limiting the definition of the AOT40 index for forests to daylight hours (Kärenlampi and Skärby 1996).

In addition to direct measurements, the exposure-flux relationship has been addressed by modelling the ozone deposition to an agricultural field (Tuovinen and Laurila 1996). The results demonstrate the need for correcting the near-surface concentration gradient which becomes important when AOT40 is evaluated from concentrations measured or modelled above the exposed vegetation. This profile effect may be partly compensated for, however, by the correlation in the diurnal cycle of the concentration and stomatal conductance.

Comments and Conclusions

The critical load calculations have been refined in Finland with improvements in input data and suggestions in the mapping manual and guidelines. The uncertainties are still considerable for the nitrogen processes. Further improvements are underway, especially through new data on critical loads for surface waters and mapping of stock at risk for tropospheric ozone. Work has been initiated to study the relations between results from critical load calculations and dynamic acidification models.

References

Aurela M., T. Laurila and J.-P. Tuovinen, 1996. Measurements of O_3, CO_2 and H_2O fluxes over a Scots pine stand in Eastern Finland by the micrometeorological eddy correlation method. *Silva Fennica* 30:97-108.

Baker, L.A. and P.L. Brezonik, 1988. Dynamic model of in-lake alkalinity generation. *Wat. Resour.* Res. 24:65-74.

de Vries, W., M. Posch, G.J. Reinds and J. Kämäri, 1993. Critical loads and their exceedance on forest soils in Europe, Report 58 (revised version), DLO The Winand Staring Centre for Integrated Land, Soil and Water Research, Wageningen, Netherlands. 77 pp.

Dillon, P.J., and L.A. Molot, 1990. The role of ammonium and nitrate in the acidification of lakes and forested catchments. *Biogeochem.* 11:23-43.

Downing, R.J., J.-P. Hettelingh and P.A.M. de Smet (eds.), 1993. Calculation and Mapping of Critical Loads in Europe: CCE Status Report 1993. National Institute of Public Health and Environmental Protection Rep. No. 259101003, Bilthoven, Netherlands.

Henriksen, A., J. Kämäri, M. Posch and A. Wilander, 1992. Critical loads of acidity: Nordic surface waters. *Ambio* 21:356-363.

Henriksen, A., B.L. Skjelkvåle, L. Lien, T.S. Traaen, J. Mannio, M. Forsius, J. Kämäri, I. Mäkinen, A. Berntell, T. Wiederholm, A. Wilander, T. Moiseenko, P. Lozovik, N. Filatov, R. Niinioja, R. Harriman and J.P. Jensen, 1996. Regional Lake Surveys in Finland - Norway - Sweden - Northern Kola - Russian Karelia - Scotland - Wales 1995. Coordination and Design. Acid Rain Research Report 40/1996. Norwegian Institute for Water Research, Oslo, Norway. 30 pp.

Henriksen, A., B.L. Skjelkvåle, A. Wilander, J. Mannio, T. Moiseenko, J.P. Jensen, R. Harriman, E. Fjeld, J. Vuorenmaa, T.S. Traaen and P. Kortelainen, 1997. Regional Lake Surveys 1995 in Finland, Norway, Sweden, Denmark, Russian Kola, Russian Karelia, Scotland and Wales - Results. Acid Rain Research Report 46/1997. Norwegian Institute for Water Research, Oslo, Norway. (In press.)

Johansson, M. and T. Tarvainen, 1997. Estimation of weathering rates for critical load calculations in Finland. *Environ. Geology* 29(3/4): 158-164.

Järvinen, O. and T. Vänni, 1990. Bulk deposition chemistry in Finland. *In*: P. Kauppi, P. Anttila and K. Kenttämies (eds.), Acidification in Finland. Springer, Berlin, pp. 151-165.

Kärenlampi, L. and L. Skärby (eds.), 1996. Critical Levels for Ozone in Europe: Testing and Finalizing the Concepts. UN-ECE Workshop Report. Univ. of Kuopio, Dept. of Ecology and Environmental Science.

Kelly, C.A., J.W.M. Rudd, R.H. Hesslin, D.W. Schindler, P.J. Dillon, C.T. Driscoll, S.A. Gherini and R.H. Heskey, 1987. Prediction of biological acid neutralization in acid sensitive lakes. *Biogeochem.* 3:129-140.

Laurila T. and J.-P. Tuovinen, 1996. Monitored data in relation to exceedances of AOT40. *In:* L. Kärenlampi and L. Skärby, *op. cit.* pp. 115-124.

Laurila T., 1996. Effects of environmental conditions and transport on surface ozone concentrations in Finland. *Geophysica* 32:167-193.

Laurila T. and H. Hakola, 1996. Seasonal cycle of C_2–C_5 hydrocarbons over the Baltic Sea and Northern Finland. *Atmos. Environ.* 30:1597-1607.

Leppäjärvi, R. (ed.) 1987. Hydrological Yearbook 1981-1983. Publications of the Water Research Institute Finland 66, 238 pp.

Lien, L., G.G. Raddum, A. Fjellheim and A. Henriksen, 1996. A critical limit for acid neutralizing capacity in Norwegian surface waters, based on new analyses of fish and invertebrate responses. *Sci. Total Environ.* 177:173-193.

Lindfors V., H. Hakola and T. Laurila, 1996. Boundary layer photochemistry of light hydrocarbons in Finland; measurements and model studies. *In*: P.M. Borrell, K.K. Cvitas and W. Seiler (eds.), Proceedings of EUROTRAC Symposium '96, Vol 1. Computational Mechanics Publications, Southampton, UK, pp. 1019-1022.

Lövblad G., P. Grennfelt, L. Kärenlampi, T. Laurila, L. Mortensen, K. Ojanperä, H. Pleijel, A. Semb, D. Simpson, L. Skärby, J.-P. Tuovinen and K. Tørseth, 1996. Ozone Exposure Mapping in the Nordic Countries. *TemaNord* 1996:528. Nordic Council of Ministers, Copenhagen, 67 pp.

Olsson, M., K. Rosén and P.-A. Melkerud, 1993. Regional modelling of base cation losses from Swedish forest soils due to whole-tree harvesting. *Applied Geochemistry, Suppl. Issue* 2:189-194.

Posch, M., J. Kämäri, M. Forsius, A. Henriksen and A. Wilander, 1997. Exceedance of critical loads for lakes in Finland, Norway, and Sweden: reduction requirements for acidifying nitrogen and sulfur deposition. *Environ. Manage.* 21:291-304.

Rosén, K., P. Gundersen, L. Tegnhammar, M. Johansson and T. Frogner, 1992. Nitrogen enrichment of Nordic forest ecosystems. *Ambio* 21:364-368.

Rummukainen M., T. Laurila and R. Kivi, 1996. Yearly cycle of lower tropospheric ozone at the Arctic Circle. *Atmos. Environ.* 30:1875-1885.

Syri, S., M. Johansson and L. Kangas, 1997. Application of nitrogen transfer matrices for integrated assessment. *Atmos. Environ.* (In press.)

Tuovinen, J.-P., M. Aurela and T. Laurila, 1997. Resistances to ozone deposition to an arctic aapa mire. *Annales Geophysicae* 15, Suppl. II, C443.

Tuovinen J.-P. and T. Laurila, 1996. Corrections for the vertical concentration gradient and flux in estimating surface exposure to ozone. *In*: L. Kärenlampi, L. and L. Skärby (eds.), *op. cit.*, pp. 330-336.

Tuovinen J.-P., M. Aurela and T. Laurila, 1996. The relationship between ozone exposure and the flux measured above a pine forest. *In*: L. Kärenlampi, L. and L. Skärby (eds.), *op. cit.*, pp. 325-329.

UBA, 1996. Manual on Methodologies and Criteria for Mapping Critical Levels/Loads and geographical areas where they are exceeded. UN/ECE Convention on Long-range Transboundary Air Pollution. Federal Environmental Agency (Umweltbundesamt), Texte 71/96, Berlin.

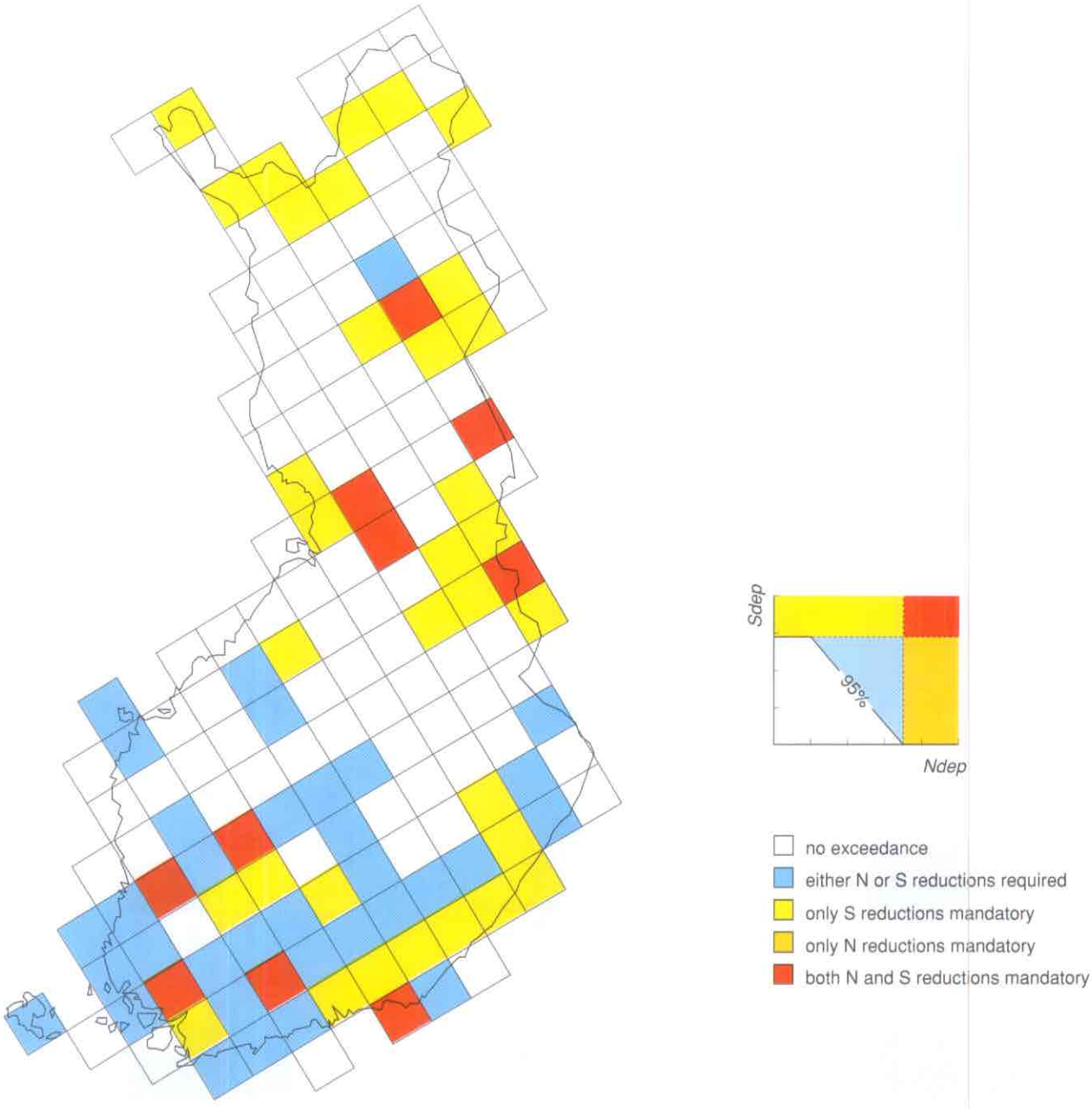

Figure FI-1. Five cases for reduction requirements of critical load exceedances to achieve protection of 95% of Finnish lakes and forest soils against acidification in each 50 km × 50 km grid cell at present (1995) total sulfur and nitrogen deposition.

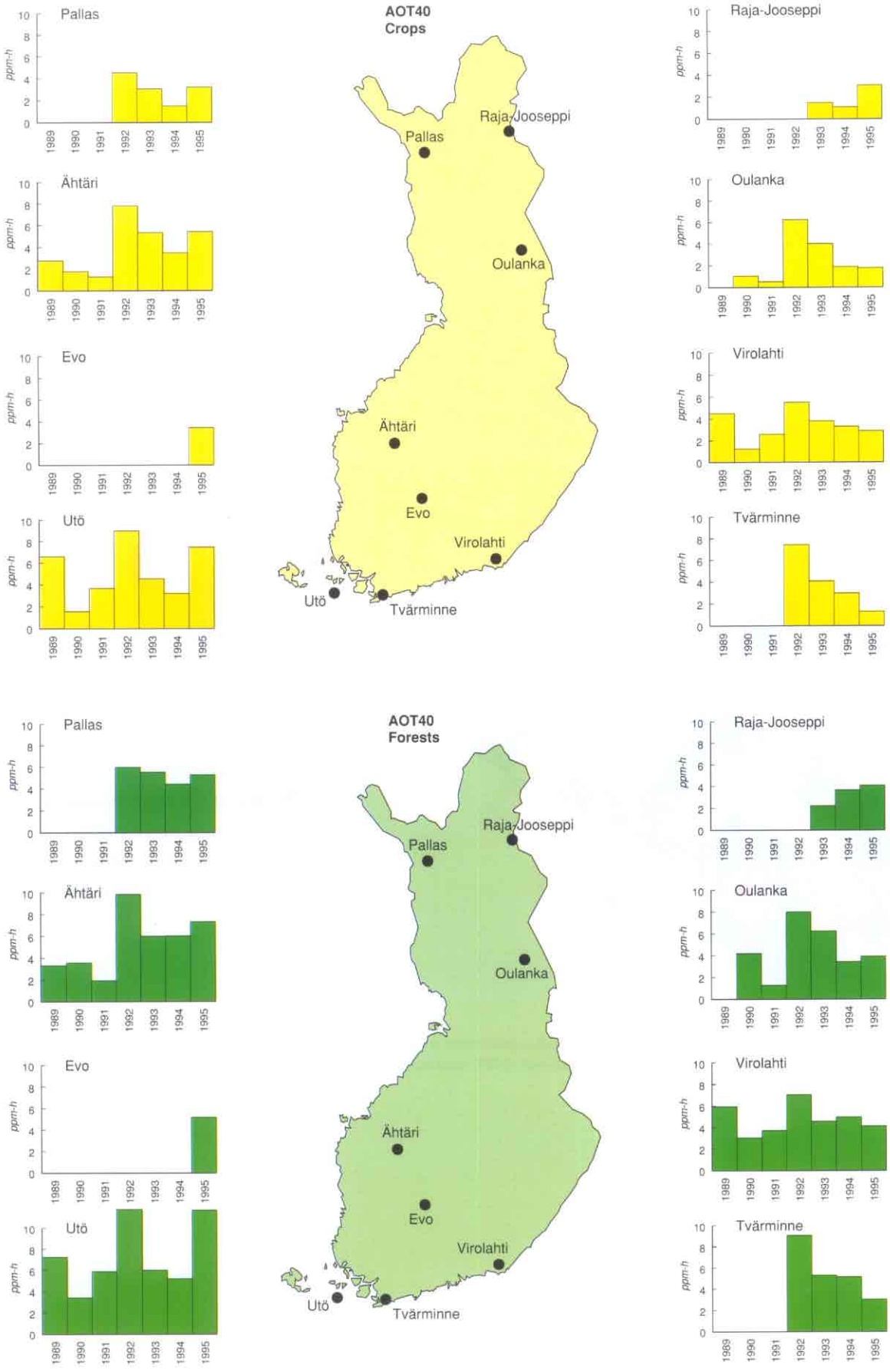

Figure FI-2. The measured yearly AOT40 (accumulated exposure above the threshold of 40 ppb) values, displayed in ppm·h, for agricultural crops and forests, as defined at the UN/ECE workshop in Kuopio.

GERMANY

National Focal Center/Contacts
Heinz D. Gregor
Beate Werner
Federal Environmental Agency
P.O. Box 330022
Bismarckplatz 1
D-14193 Berlin
tel: +49-30-8903 2846
fax: +49-30-8903 2285
email: heinz-detlef.gregor@uba.de
email: beate.werner@uba.de

Collaborating Institutions
Hans-Dieter Nagel
ÖKO-DATA GmbH
Am Annaflieβ 4D
D-15344 Strausberg
tel: +49-3341-31864
fax: +49-3341-31866
email: hans.dieter.nagel@t-online.de

Renate Köble
Institute of Navigation
Stuttgart University
Geschwister-Scholl-Str. 24
D-70174 Stuttgart
tel: +49-711-121 3412
fax: +49-711-121 2755
email: renate.koeble@nav.uni-stuttgart.de

Dry deposition data provided by
Erik van Leeuwen
Jan-Willem Erisman
RIVM Air Research Laboratory
P.O. Box 1
NL-3720 BA Bilthoven, Netherlands

National Maps Produced

Critical loads of nitrogen:
Projection: Lambert Conformal Conic
Grid size: 1 × 1 km^2
Grid origin: Forest Distribution Map (satellite image)
- Net uptake of nitrogen (N_u)
- Nitrogen immobilization (N_i)
- Acceptable leaching of nitrogen ($N_{le(acc)}$)
- Denitrification (N_{de})
- Critical loads of nutrient nitrogen ($CL_{nut}(N)$)

Critical loads of acidity:
Projection: Lambert Conformal Conic
Grid size: 1 × 1 km^2
Grid origin: Forest Distribution Map (satellite image)
- Net uptake of base cations (BC_u)
- Weathering rate of base cations (BC_w)
- Critical leaching of acid neutralizing capacity ($ANC_{le(crit)}$)
- Base saturation (BS)
- Critical loads of acidity ($CL(Ac_{act})$)

Deposition:
Projection: Lambert
Grid size: 2.1 × 2.1 km^2
Grid origin: Land Use Map of Germany (6 classes from satellite imagery: urban area, coniferous, deciduous and mixed forests, agriculture, waters).

Total (sea-salt-corrected*) deposition (1989 and 1991/93) of: SO_x*, NO_y, NH_x, Na, Base Cations* (Ca, Mg, K), potential acidity (SO_x* + NO_y + NH_x + Cl*), and net potential acidity (SO_x* + NO_y + NH_x – BC* + Cl*).

Exceedances:
Projection: Lambert Conformal Conic
Grid size: 2.1 × 2.1 km^2
Grid origin: Forest Distribution Map (satellite image)
- Exceedance of critical loads of nutrient nitrogen ($Ex(N)$)
- Exceedance of critical loads of acidity ($Ex(Ac_{pot})$)

Ozone AOT40:
Projection: Lambert
Grid size: 1/6 degree × 1/6 degree
Grid origin: Interpolation of measurements
- AOT40 Maps for forest ecosystems 1992–94
- AOT40 Maps for crops 1992–94

Ozone critical level exceedances:
Projection: Lambert
Grid origin: Land cover information from the Forest Map of the Federal Environmental Agency.
- Exceedance of critical levels of ozone for the years 1992–94.

Calculation Methods

In general critical loads are calculated for the CCE data set in accordance to the methods in the

Mapping Manual (UBA 1996). $CL_{max}(S)$, $CL_{min}(S)$, $CL_{max}(N)$, $CL_{min}(N)$ and $CL_{nut}(N)$ have been calcuated; national approaches are also elaborated.

Critical loads of acidity: To calculate critical loads of acidity for forest soils equation 5.15 in UBA (1996) was used:

$$CL(Ac_{act}) = BC_{w} - ANC_{le(crit)}$$

The calculation method of this approach is valid for acid forest soils. To take into account base soils as occur in Germany the base saturation was integrated into the estimation of critical loads. The base saturation was assigned to the FAO soil units as shown in the following table:

Base saturation [%]	FAO soil type
0 – 20	Bd, Bds, Dd, Gd, Jd, Od, Pg, Ph, Phf, Pl, Po
20 – 40	Dg, Oe, Rd, U
40 – 80	Be, Bea, Bec, Bg, Bh, Bv, Bvc, Bvg, De, Ge, Gm, Jc, Jcf, Jcg, Jeg, Lc, Le, Lg, Lgs, Lo, Rc
> 80	Bk, Bkf, Ch, Ck, Eo, Hc, Hh, Hl

For all soils with a base saturation > 20%, $ANC_{le(crit)}$ is set to 0, in this case the critical load of acidity is equal to the weathering of base cations. The resulting map is shown in Figure DE-1 (left).

Critical loads of nitrogen: The methods of calculating critical loads of nitrogen are described in detail in the Mapping Manual (UBA 1996). The map of critical loads of nutrient nitrogen is presented in Figure DE-1 (right).

Total deposition: Total deposition in Germany was mapped by combining interpolated wet deposition measurements and inferential modelling of dry deposition (van Leeuwen *et al.* 1996, Köble *et al.* 1997). Figure DE-2 shows the German deposition maps 1991/93 for potential acidity (left) and nitrogen (right). The procedure for producing deposition maps is described in the following diagram:

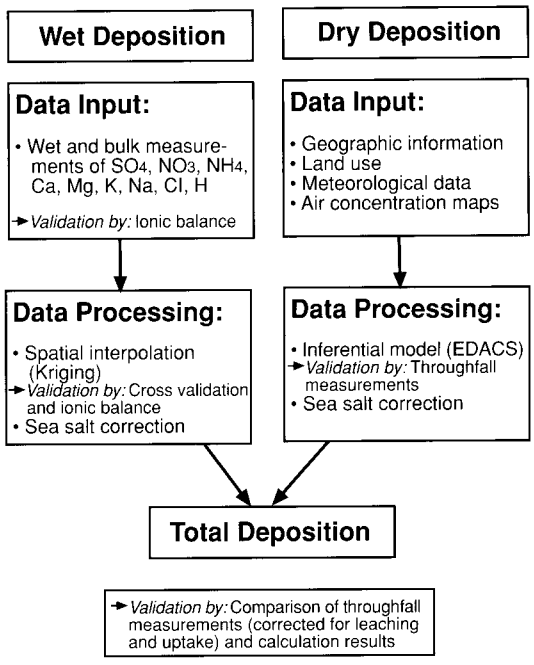

Exceedances: The exceedance of critical loads by the deposition are mapped in Figure DE-3 for acidity (left) and nutrient nitrogen (right).

Ozone AOT40 values and exceedance of critical levels of ozone: Ozone AOT40 maps have been compiled by calculating the AOT40 for forests and crops at each rural measurement site. The results were interpolated for forests and crops separately. By intersecting both maps with the forest map of the Federal Environmental Agency, the AOT40 values have been related to the corresponding receptor. AOT40 calculations conform to the Kuopio Workshop guidelines (see UBA 1996).

Daylight hours are defined as the time period with a solar radiation above 50 W m^{-2}, in Germany from about 0600–1800 as an average over the summer months (April-September). Comparisons of AOT40 calculations using the constant time approach versus the time periods with solar radiation values >50 W m^{-2} showed an average deviation below 3%. At the Kuopio Workshop in April 1996, the calculation period of AOT40 for forest ecosystems was changed from a total day to daylight hours only. This revision leads to a 5% to 55% reduction of the AOT40 values at rural measurement sites. Maximum reductions in Germany occur at high altitudes; nevertheless, for most parts of Germany, critical levels of ozone are exceeded to a large extent. Figure DE-4 shows AOT40 exceedances (AOT40 minus critical level) for 1993 (left) and 1994 (right) in forest and agricultural areas.

References

Köble, R., T. Gauger and G. Smiatek, 1997. Kartierung kritischer Belastungskonzentrationen und -raten für empfindliche Ökosysteme in der Bundesrepublik Deutschland und anderen ECE-Ländern. Teil 1: Deposition Loads, Teil 2: Critical Levels, Teil 3: Informationssystem CANDIS. Endbericht des FE-Vorhabens 106 01 061 im Auftrag des Umweltbundesamtes. In press.

Nagel *et al.*, 1996. Modellgestützte Bestimmung der ökologischen Wirkungen von Emissionen. Texte des Umweltbundesamtes, 79/96.

UBA, 1996. Manual on Methodologies and Criteria for Mapping Critical Levels/Loads and geographical areas where they are exceeded. UN/ECE Convention on Long-range Transboundary Air Pollution. Federal Environmental Agency (Umweltbundesamt), Texte 71/96, Berlin.

Van Leeuwen *et al.*, 1996. Mapping dry deposition of acidifying components and base cations on a small scale in Germany. Rijksinstituut voor Volksgezondheid en Milieu, Report no. 722108012.

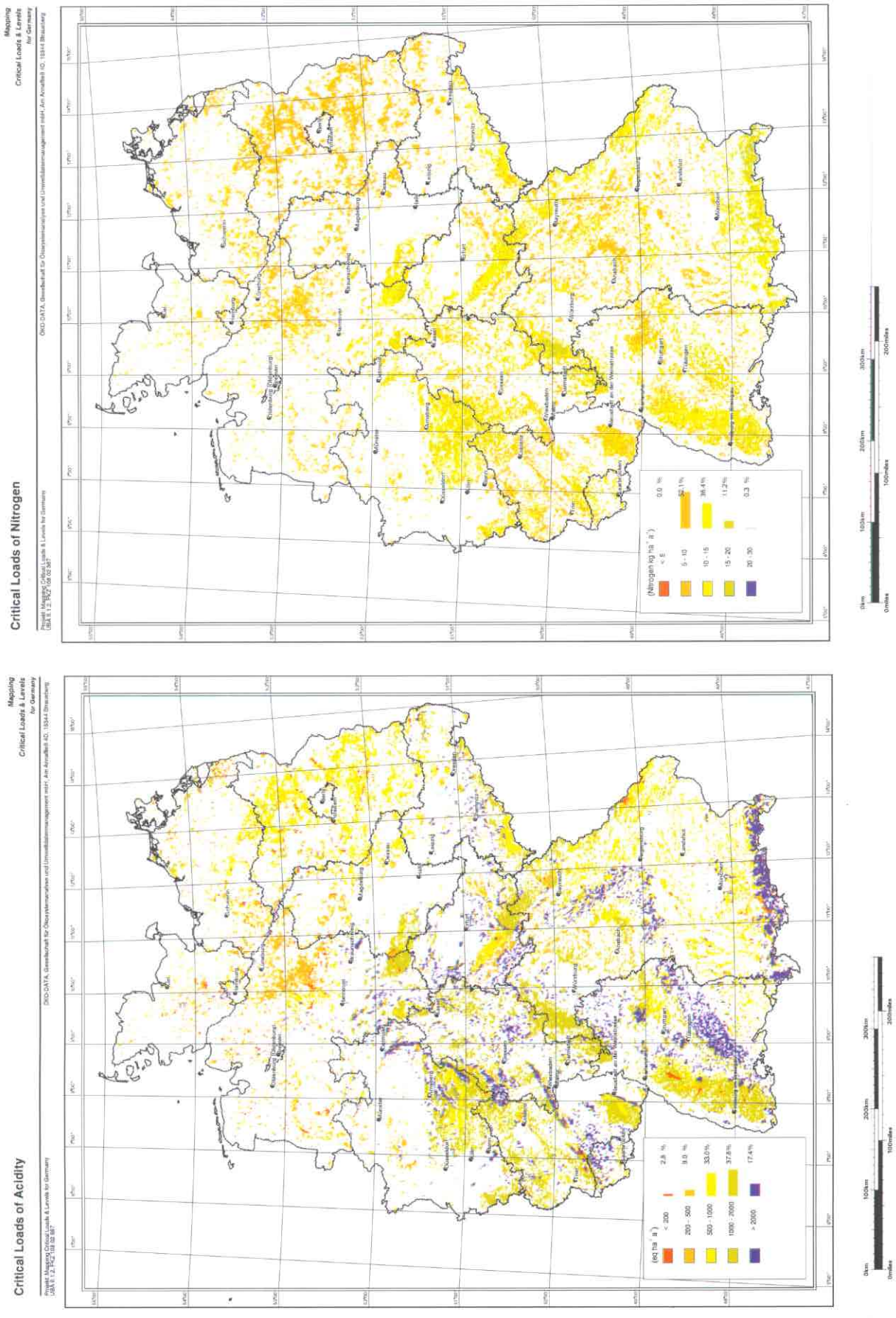

Figure DE-1. Critical loads of acidity (left, in eq ha^{-1} yr^{-1}) and of nutrient nitrogen (right, in kg N ha^{-1} yr^{-1}) for forest ecosystems.

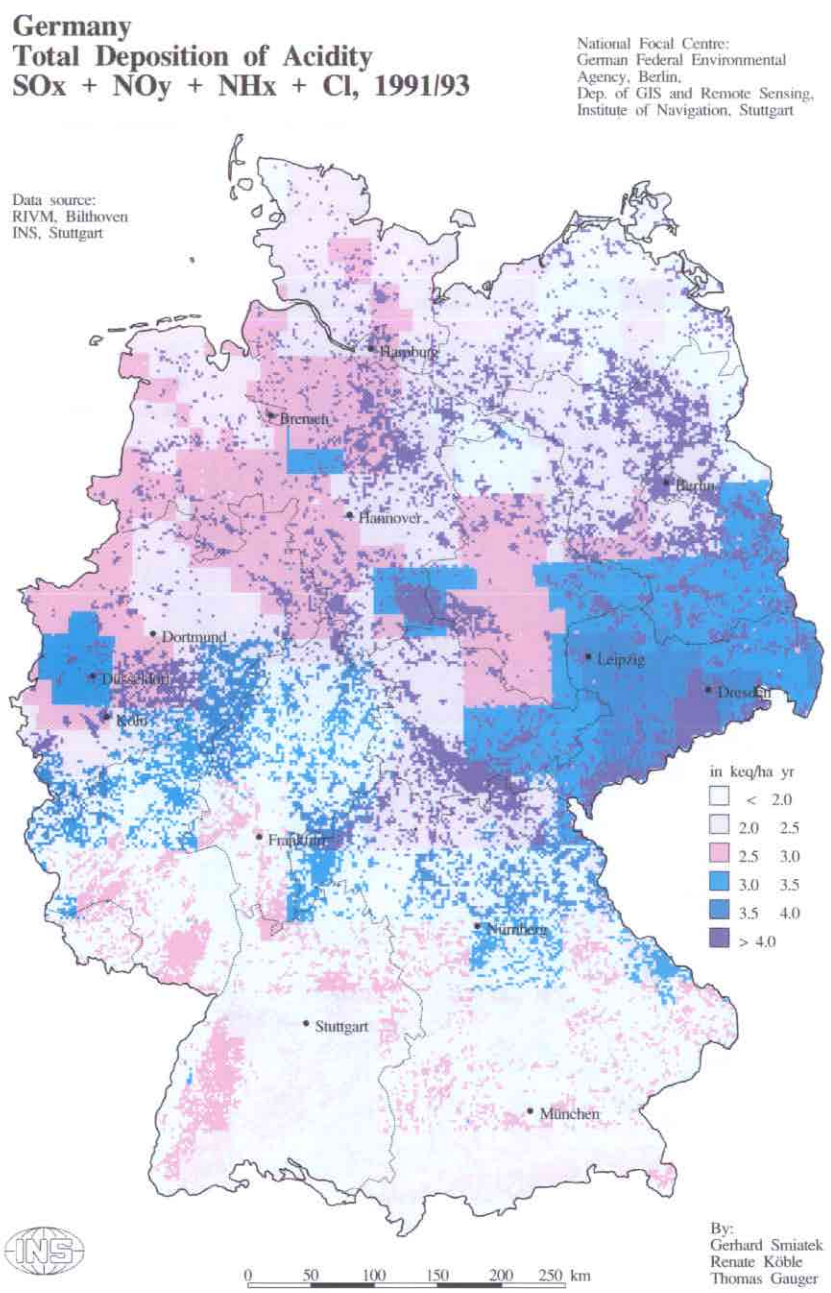

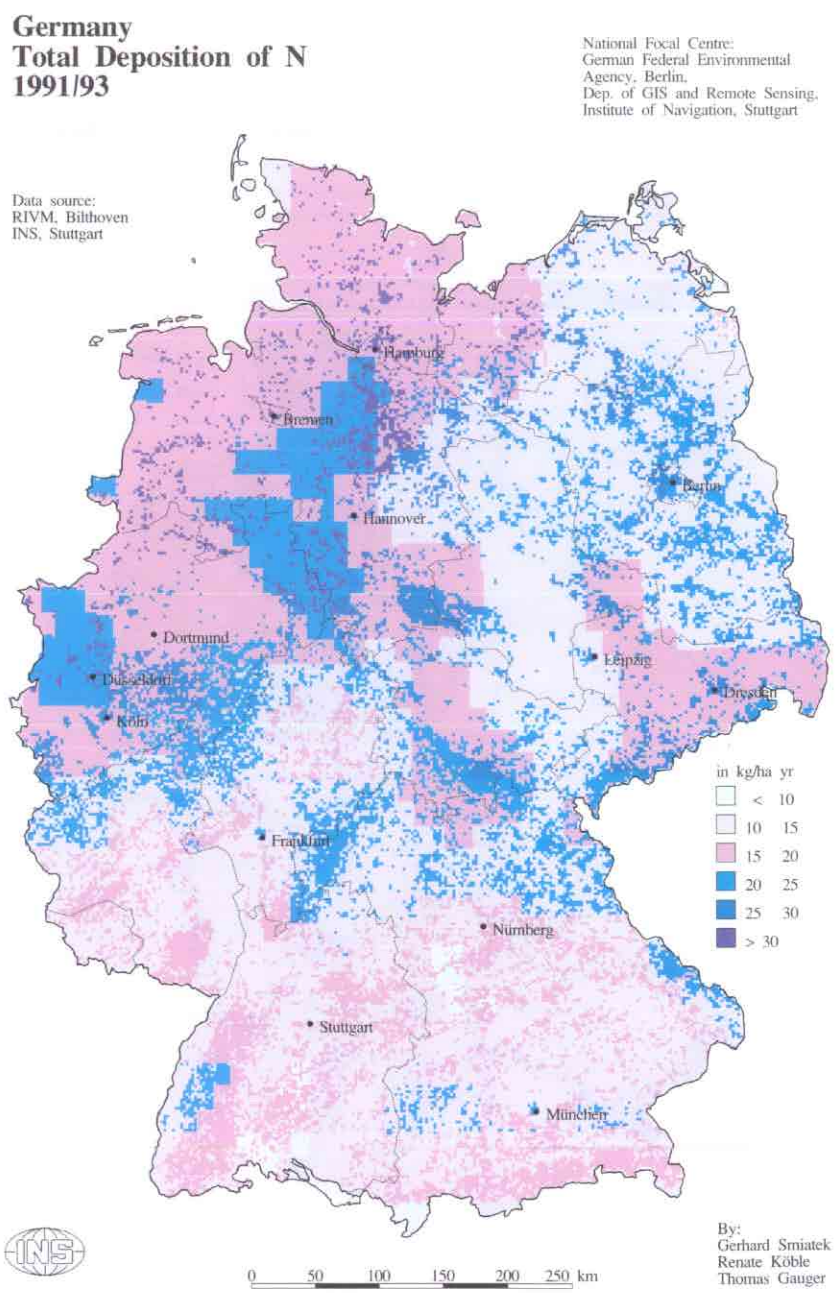

Figure DE-2. Total deposition of acidity (left, in keq ha^{-1} yr^{-1}) and of nitrogen (right, in kg N ha^{-1} yr^{-1}).

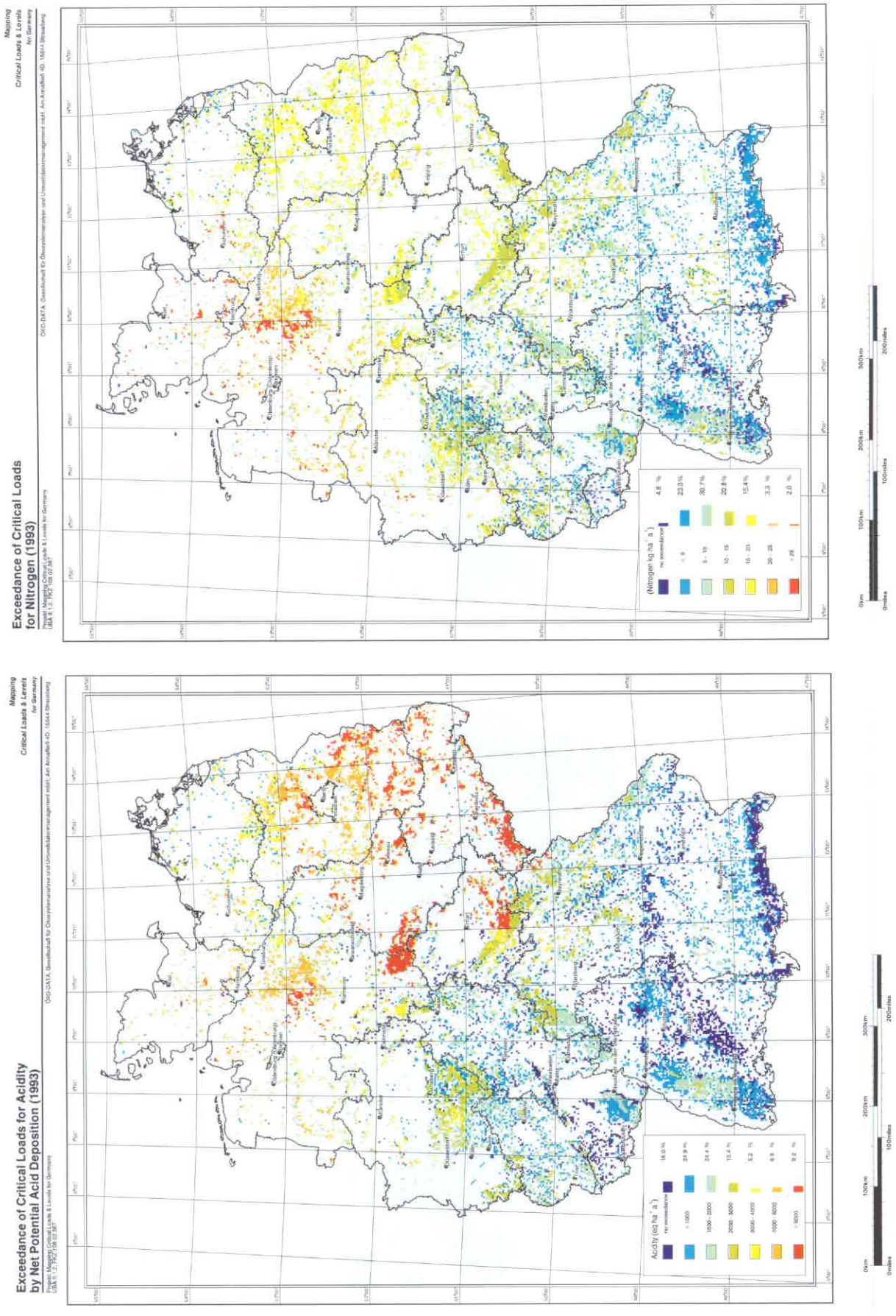

Figure DE-3. Exceedance of critical loads of acidity (left, in eq ha^{-1} yr^{-1}) and of nitrogen (right, in kg N ha^{-1} yr^{-1}) for forest ecosystems.

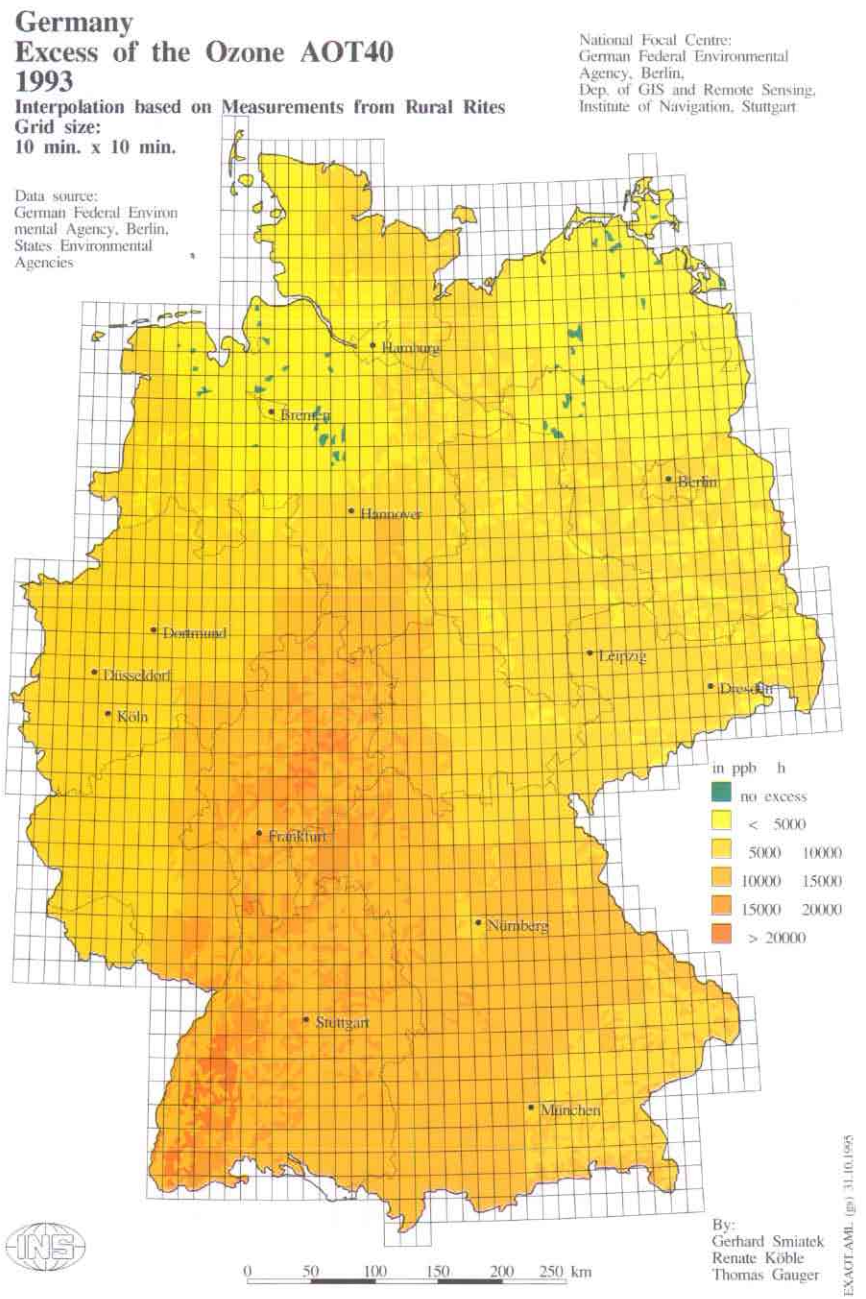

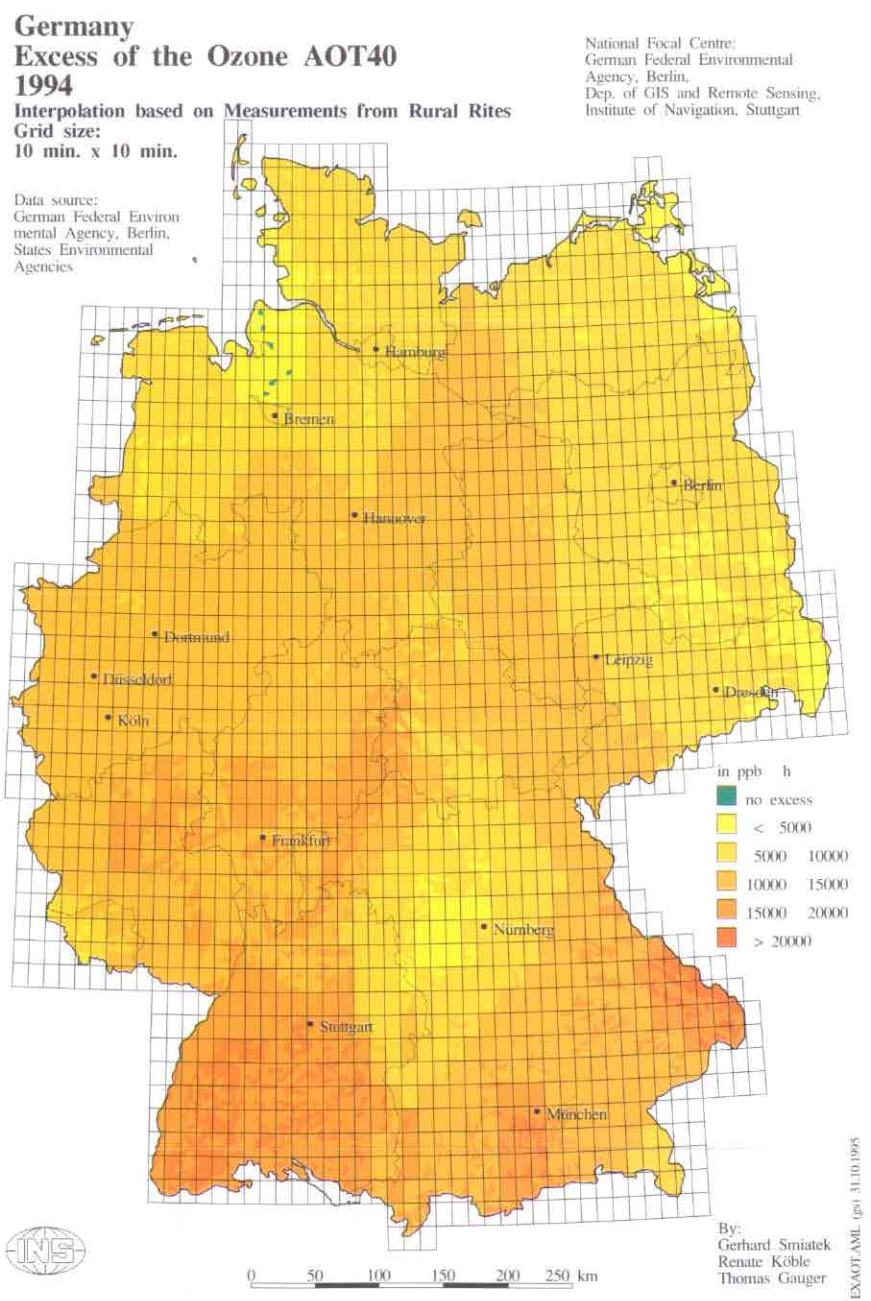

Figure DE-4. Exceedance of ozone AOT40 values for forest and crops (in ppb-h) for 1993 (left) and 1994 (right).

HUNGARY

National Focal Center/Contacts
Tamás Németh
Zsuzsanna Flachner
Research Institute for Soil Sciences and Agriculture
Hungarian Academy of Sciences
Hermann Ottó utca 14.
1022 Budapest
tel: +36-1-1564644
fax: +36-1-1558839
email: flaci@enviro.bke.hu

Collaborating Institutes/Contacts
Róbert Rakics
Róbert Tóth
Ministry for Environment and Regional Policy

Interdisciplinary Team
József Szabó, László Pásztor and Diana Sári
Research Institute for Soil Sciences and Agriculture,
Hungarian Academy of Sciences

László Bozó, Györgyi Barankai, László Horváth and
Katalin Nárai Feketéné
Hungarian Meteorological Institute (HMI)

Katalin Török and László Horváth
Institute for Botany, Hungarian Academy of Sciences

György Büttner
Institute for Remote Sensing

Szabina Török
Central Institute for Physics

Róbert Maninger
Institute for Forest Management

Tibor László
Office for the State of the Environment Survey

National Maps Produced

Due to the lack of digital information, a set of basic maps had to be produced quite recently, with partial support of international programs such as Phare.

1. Soil Map for Hungary (1: 50,000),RISSAC
2. Soil degradation areas for Hungary, (1:50,000), RISSAC
3. Maximum critical load of sulfur
4. Maximum critical load of acidifying nitrogen

Calculation Methods

The Steady-state Mass Balance approach has been applied (Downing *et al.* 1993). For some grids, limit values have been drawn from research data. Problems occurred in obtaining appropriate weathering rate data, since the published parameters given for more humid and colder climates are not suitable. Maps have been produced for the EMEP50 grid, and efforts are now underway to improve and prepare maps on 1km x 1km resolution; although deposition data is not yet available at this scale.

Data Sources

In 1996 an interdisciplinary team was established by the NFC to collect and assess data and information from different sources, research programs and institutes.

Soil data: Digital soil maps (1:50,000) have been used, as well as some of the results of studies for particular regions (HUNSOTER, RISSAC 1996)

Meteorological data: For modelling purposes daily measurement data from HMI have been used.

Forest data: Forest data were provided from the Forest Management Institute based on the 16 km x 16 km monitoring network. CORINE land cover data have also been used to have an accurate map for the areas (Corine Land Cover for Hungary 1990-91, MERP 1996.)

Ecosystem data: Due to the importance of the protection of natural landscapes without forest cover, detailed information has been gathered and matched with field research results on the sensitivity of these ecosystems in Hungary. Due to the large variation of habitat types in each cell, the most sensitive habitat has been selected as a receptor. The CORINE Biotop program has also provided a large portion of information.

Land Cover Data: The 1:50,000 Corine Land Cover map compiled in late 1996 for Hungary has been used.

Deposition data: Official model calculations are available from the MERP on 150 km × 150km scale for the year 1993, besides new estimations are available for 1994 for 50km × 50km grid resolution from MERP.

Comments and Conclusions

First steps to map critical loads have been made with the help of the participating institutions and the CCE. Further work is required to improve information on deposition loads and levels of relevant pollutants as a function of surface cover and roughness.

It can be concluded that the basic data on nutrient uptake and weathering rates, as well as the sensitivity classification of natural and important agricultural areas, are insufficient. Since some important programs (e.g. CORINE Land Cover, Biotop) are now complete, further progress can be made in preparing exceedance maps. The identification of areas where critical loads are exceeded will help indicate where additional field work and monitoring activities should be conducted, in conjuction with further assessment and mapping activities.

While further improvements of the Hungarian critical load calculations can be made, the critical load concept should be introduced in regional decision making processes.

Acknowledgments

The maps, data, and information provided by all collaborating institutions are gratefully appreciated, as is the support of the Ministry of Environment and Regional Policy. The CCE is acknowledged for its assistance in producing the first Hungarian national maps.

IRELAND

National Focal Center/Contact
Michael McGettigan
Environmental Protection Agency
St. Martins House
Waterloo Road
Dublin 4
tel: + 353-1-667 4474
fax: +353-1-660 5848
email: m.mcgettigan@epa.ie

Collaborating Institutions
Julian Aherne
E.P. Farrell
Forest Ecosystem Research Group
Dept. of Environmental Resource Management
University College
Belfield
Dublin 4
tel: + 353-1-706 7081 / 7716
fax: + 353-1-706 1102
email: julian.aherne@ucd.ie
email: ted.farrell@ucd.ie

National Maps Produced

All maps are on the 1 x 1 km^2 Irish national grid:

- Critical loads of acidity for soils (empirical).
- Maximum critical loads of sulfur for coniferous woodland, deciduous woodland and heathland ecosystems.
- Minimum critical loads of nitrogen for coniferous woodland, deciduous woodland and heathland ecosystems.
- Critical loads of nutrient nitrogen (empirical).
- Deposition of sulfur, nitrogen and base cations.

Calculation Methods

The critical loads of acidity for soils (empirical) is based on the Skokloster classification (Nilsson and Grennfelt 1988; Hornung *et al.* 1995a). The maximum critical loads of sulfur and minimum critical loads of nitrogen were calculated using:

$$CL_{max}(S) = CL(A) + BC_{dep} - BC_u$$
$$CL_{min}(N) = N_u + N_i$$

The critical loads of nutrient nitrogen (empirical) were estimated by assigning critical load ranges (UBA 1996) to selected land cover types. Deposition values for the major ions in precipitation were produced by combining interpolated average annual precipitation chemistry concentrations for approximately 30 point measurements, with interpolated long-term average annual precipitation volume for approximately 600 points.

Data Sources

Soils: 1:575,000 General Soil Map of Ireland and the accompanying Soil Survey Bulletin (Gardiner and Radford, 1980).

Land cover: 1:100,000 CORINE land cover project, Ireland (Ordnance Survey of Ireland 1993).

Precipitation: Interpolation (kriging) of long-term average annual precipitation volume for approximately 600 sites between the period 1951-1980 (Fitzgerald 1984).

Deposition: Combination of precipitation with interpolated (kriging) average annual bulk precipitation chemistry concentrations for approximately 30 sites between the period 1985-1994. The minimum sampling period is not less than 3 years.

Base cation deposition: Combination of interpolated point source bulk concentration measurements and interpolated rainfall volumes. A filtering factor of 1.5 was used to scale from bulk deposition to total deposition.

Weathering rate: Estimated using the Skokloster classification ranges which were assigned to the principal soil of each soil association on the General Soil map of Ireland. The mid-value of each of the five classes was used to define soil weathering, except for the final (non-sensitive) class which was set at 4000 eq ha^{-1} yr^{-1}.

Uptake: Estimated only for coniferous ecosystems. Potential uptake was calculated using average yield class (m^3 ha^{-1} yr^{-1}), density of wood of (kg m^{-3}) and stem concentrations (mol$_c$ kg^{-1}). Actual uptake was assumed to be equal to 75% of the average yield class.

Immobilization: Based on literature values (Hornung 1995b, UBA 1996).

Comments and Conclusions

Since the Irish critical load mapping program began in 1996, considerable advances have been made in the application of the critical load concept to Ireland. The improvement of methods for the calculation and mapping of critical loads, levels and exceedences is continually ongoing. Presently work is being carried out on:

- Validation of the "Level 0" Skokloster map.
- Calculation and mapping critical loads of freshwaters.
- Calculation and mapping of critical levels of ozone.

References

Fitzgerald, D., 1984. Monthly and annual averages of rainfall for Ireland 1951-1980. Irish Meteorological Service, Climatological Note No. 7. Dublin.

Gardiner, M. and J. Radford, 1980. Soil associations of Ireland and their land use potential. An Foras Taluntais, Soil Survey Bulletin No. 36. Dublin.

Hornung, M., K.R. Bull, M. Cresser, J. Hall, S.J. Langan, P. Loveland and C. Smith, 1995a. An empirical map of critical loads of acidity for soils in Great Britain. *Environ. Pollut.* 90:3, 301-310.

Hornung, M., M.A. Sutton and R.B. Wilson (eds.), 1995b. Mapping and modelling of critical loads for nitrogen: Proceedings of the Grange-Over-Sands Workshop. Institute of Terrestrial Ecology (UK), 207 pp.

Nilsson, J., and P. Grennfelt (eds.), 1988. Critical loads for sulfur and nitrogen. Miljörapport 1988:15. Nordic Council of Ministers, Copenhagen.

Ordnance Survey of Ireland, 1993. 1:100,000 CORINE land cover project (Ireland).

UBA, 1996. Manual on Methodologies and Criteria for Mapping Critical Levels/Loads and geographical areas where they are exceeded. UN/ECE Convention on Long-range Transboundary Air Pollution. Federal Environmental Agency (Umweltbundesamt), Texte 71/96, Berlin.

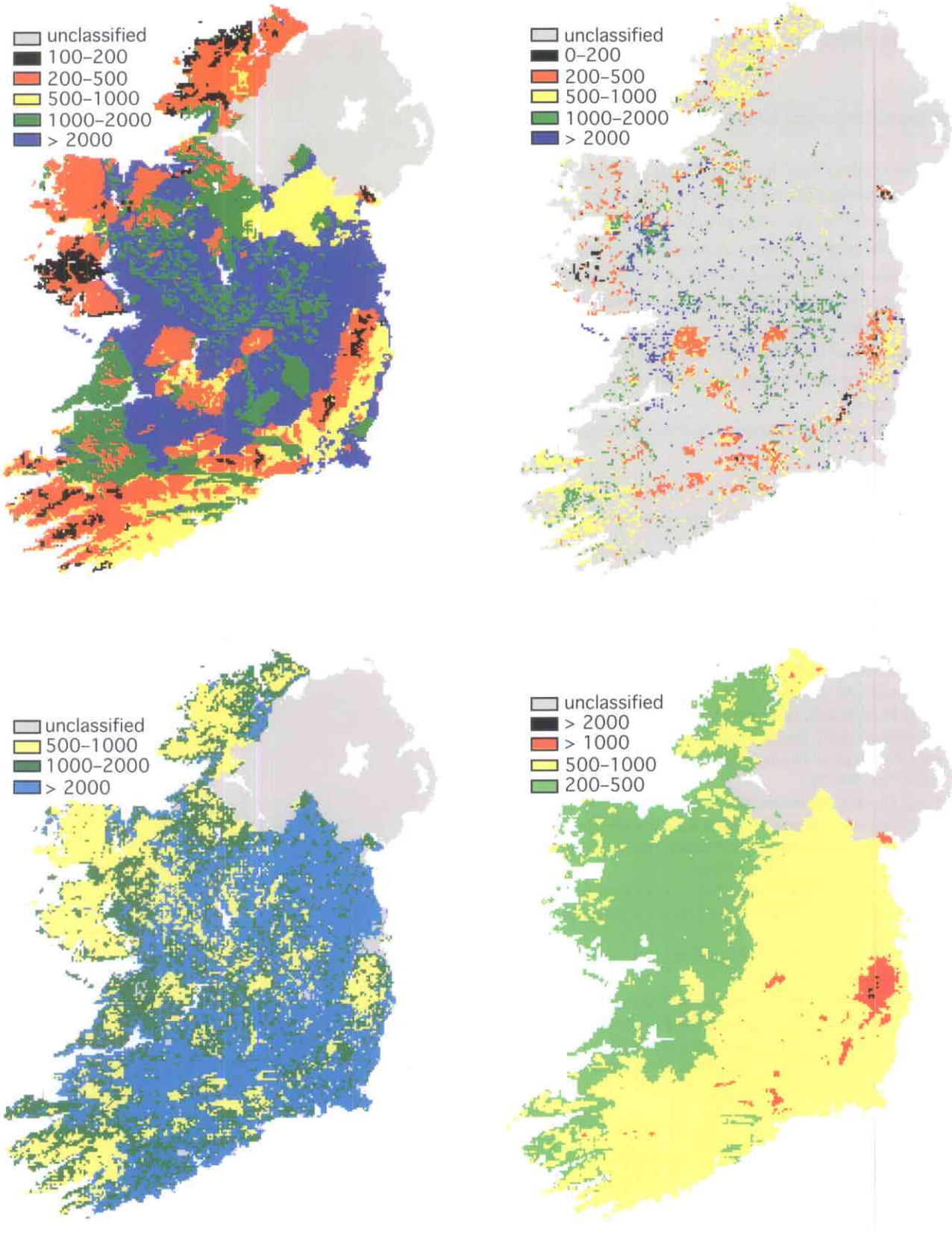

Figure IE-1. From top left, moving clockwise:
(a) Critical load of acidity for soils, empirical approach ($mol_c\ ha^{-1}\ yr^{-1}$).
(b) Maximum critical load of sulfur for coniferous, deciduous and heathland ecosystems ($mol_c\ ha^{-1}\ yr^{-1}$).
(c) 5 percentile critical load of nutrient nitrogen, empirical approach ($mol_c\ ha^{-1}\ yr^{-1}$).
(d) Deposition of acidity ($mol_c\ ha^{-1}\ yr^{-1}$).

ITALY

National Focal Center/Contacts

Silvia Brini
Patrizia Bonanni
Giusy Vetrella
ENEA - Italian Agency for New Technology, Energy and Environment - C.R. Casaccia
Environment Department
Via Anguillarese 301
I-00060 Santa Maria di Galeria (Rome)

tel:	+39-6-3048 4564	(SB)
	+39-6-3048 4673	(PB)
	+39-6-3048 3745	(GV)
fax:	+39-6-3048 4318	(SB)
	+39-6-3048 4318	(PB)
	+39-6-3048 4925	(GV)
email:	brini@casaccia.enea.it	(SB)
	bonanni@casaccia.enea.it	(PB)
	safcont@casaccia.enea.it	(GV)

Collaborating Institutions/Contacts

Pietro Bacci
Romano Ambrogi
Armando Buffoni
ENEL DSR/ CRAM
Via Rubattino 54
I-20134 Milan
tel: +39-2-7224 3061
fax: +39-2-7224 3915

Rosario Mosello
CNR - National Research Council
Italian Institute of Hydrobiology
Largo V. Tonolli, 50
I-28048 Verbania - Pallanza
tel: +39-323-556 571
fax: +39-323-556 513

National Maps Produced

- Critical load of acidity
- Critical load of nitrogen (nutrient, minimum and maximum)
- Maximum and minimum critical load of sulfur
- Critical load of sulfur and nitrogen

All maps are produced are for the 5th percentile, on the 50 x 50 km^2 EMEP grid resolution.

A. Critical Loads of Acidity

Calculation methods

The ecosystems considered include: coniferous forest, rough grazing, deciduous forest, and arable land. The "Level 0" method (Kuylenstierna and Chadwick 1988, Chadwick and Kuylenstierna 1990), has been used to determine sensitivity to acid deposition. The method has been modified to address some Italian characteristics.

The four ecosystem characteristics (bedrock lithology, soil type, land use and precipitation) have been assigned to categories and combined using a weighting procedure to obtain five broad classes of relative sensitivity. In particular, the percentage of territory within each category for each of the four factors has been evaluated for every cell. For each factor, a parameter is obtained through the linear combination of each factor's and each category's weight, multiplied by the percentage of soil corresponding to the determinate category.
The values obtained lie within the range 0-7 (continuous), and are assigned to one of the five critical load classes of sensitivity. The critical load of acidity, *CL(A)*, has been estimated by a linear interpolation of the range of the critical load class on the basis of the actual parameter value.

Data sources

Bedrock lithology: Geological map of Italy (1:1,000,000).

Soil types: Thematic maps and literature data: FAO-UNESCO (1981) Soil Map of the World (1:5,000,000) and CEE (1985) Soil Map of the European Communities (1:1,000,000).

Land Use: Map of the Italian vegetation (1:1,000,000) of Ministry of Environment, including 54 different vegetation types.

Precipitation: Map of Italian annual average precipitation for the years 1921–1950 (1:1,000,000) of Ministry of Public Works and RIDEP data from Italian Institute of Hydrobiology of Pallanza.

B. Other Critical Loads

Calculation methods

Forest soils were mapped. The ecosystems considered are: tundra, boreal forest, temperate coniferous, temperate deciduous, Mediterranean forest, acid grassland and other (moors, mountain shrubs, basophilous grasslands, zonal vegetation, area with poor or no vegetation). Using the methodology suggested at the Grange-Over-Sands Workshop (Hornung 1995), the SMB method has been used. This approach balances inputs and outputs of S and N at equilibrium, and is based on the following equations:

$CL_{nut}(N) = N_{le} + N_i + N_{re} + N_{de} - N_{fix} + N_{burn} + N_{vol}$

$CL_{min}(N) = N_i + N_{re} + N_{de} - N_{fix} + N_{burn} + N_{vol}$

$CL_{max}(N) = CL_{min}(N) + CL_{max}(S)$

$CL_{max}(S) = CL(A) + BC_{dep} - BC_u$

$CL(S+N) = CL(S) + CL(N)$

Since $CL_{nut}(N) < CL_{max}(N)$ for all of Italy, we define $CL(N)$ as $CL_{nut}(N)$ and $CL(S)$ as $CL_{min}(S)$.

Data sources

Land use: The Map of Italian vegetation (1:1,000,000) (Ministry of Environment), including 54 different vegetation types. Total ecosystem area has been calculated for each grid cell.

N_{le} and N_i: The central value of the range defined in Hornung *et al.* (1995; Ch. 4, Table 1), has been applied.

N_{re} and N_{de}: Data on vegetation growth and soil moisture were provided by experts of the Italian Ministry of Agriculture and Forests.

N_{fix} and N_{burn}: Precipitation data have been derived by overlaying the 1:1,000,000 Map of Annual Average Precipitation for 1921–1950 (provided by the Ministry of Public Works) to the Map of Italian Vegetation. Data on the frequency of fires are from an assessment of the total burned surface for 1982–1993 carried out by the Italian Ministry of Agriculture and Forests.

N_{vol}: For temperate coniferous and Mediterranean forests, a value of 0.25 was used. All other areas have been assigned a value of zero.

BC_{dep} and BC_u: Data have been taken from EMEP data (in Downing *et al.* 1993, Figs. A.2.2.-A.2.3.).

Deposition: Data on sulfur and nitrogen deposition are provided by the Politecnico of Milan. Deposition data have been calculated by RAINS model based on Italian CORINAIR 90 emissions data. Deposition data for the year 1990 have been applied in the critical load calculations.

References

Carniello, A., 1984. Notes on the origins of ground waters and on their distribution on the rocks. Hydrology Course, Univ. Naples. Naples, Italy.

CEE, 1985. Soil Map of the European Communities (1:1,000,000). Directorate-General for Agriculture, Commission of the European Communities. Luxembourg.

Chadwick, M.J. and J.C.I. Kuylenstierna, 1990. The relative sensitivity of ecosystems in Europe to acid depositions. Stockholm Environment Institute, Stockholm, Sweden.

de Vries, W., 1991. Methodologies for the assessment and mapping of critical loads and impacts of abatement strategies on forest soils. Report 46. Winand Staring Center. Wageningen, The Netherlans.

Downing, R.J., J.-P. Hettelingh and P.A.M. de Smet (eds.), 1993. Calculation and Mapping of Critical Loads in Europe: CCE Status Report 1993. National Institute of Public Health and Environmental Protection Rep. No. 259101003, Bilthoven, Netherlands.

ENEA-Ministry of Environment, 1995. Map of Critical Load of Acidity for Italy. ENEA-Environment Department, Rome.

FAO, 1982. Micronutrients and the nutrient status of soils: a global study. FAO, Rome.

FAO-UNESCO, 1981. Soil Map of the World. Volume V:Europe (1:5,000,000). UNESCO, Paris.

Hornung, M., M.A. Sutton and R.B. Wilson (eds.), 1995. Mapping and modelling of critical loads for nitrogen: Proceedings of the Grange-Over-Sands Workshop. Institute of Terrestrial Ecology (UK), 207 pp.

Ministry of Environment, 1992. Report on the state of the environment in Italy. Map of the Italian Vegetation (1:1,000,000). Rome

Ministry of Public Works. Map of annual average precipitation for the years 1921-1950 (1:1,000,000).

Mosello, R., 1993. The Italian network for the study of the acidic depositions (RIDEP). Report on the RIDEP network activity in the five-year period 1988- 1992, Appendix B.3. Verbania (Pallanza).

Nilsson, J. and P. Grennfelt (eds.), 1988. Critical Loads for Sulfur and Nitrogen. Nord 1988:15, Nordic Council of Ministers, Copenhagen, Denmark, 418 pp.

Posch, M., P.A.M. de Smet, J.-P. Hettelingh and R.J. Downing (eds.), 1995. Calculation and Mapping of Critical Thresholds in Europe: CCE Status Report 1995. National Institute of Public Health and the Environment Rep. 259101004, Bilthoven, Netherlands.

Sverdrup, H. and P. Warfvinge, 1988. Weathering of primary silicate minerals in the natural soil environment in relation to a chemical weathering model. *Water Air Soil Pollut.* 38:387-408.

Tomaselli, R., A. Balduzzi and S. Filipello, 1972. Bioclimatic Map of Italy. Univ. Pavia, Institute of Botany. Ministry of Agriculture and Forests, Pavia, Italy.

Trade and Industry Ministry, 1961. Geological service. Geological Map of Italy (1:1,000,000). Rome.

UBA, 1996. Manual on Methodologies and Criteria for Mapping critical Levels/Loads and Geographic Areas where they are exceeded. Convention on Long-Range Transboundary Air Pollution. Task Force on Mapping. Geneva. Federal Environmental Agency. Berlin, Germany. Texte 25/93.

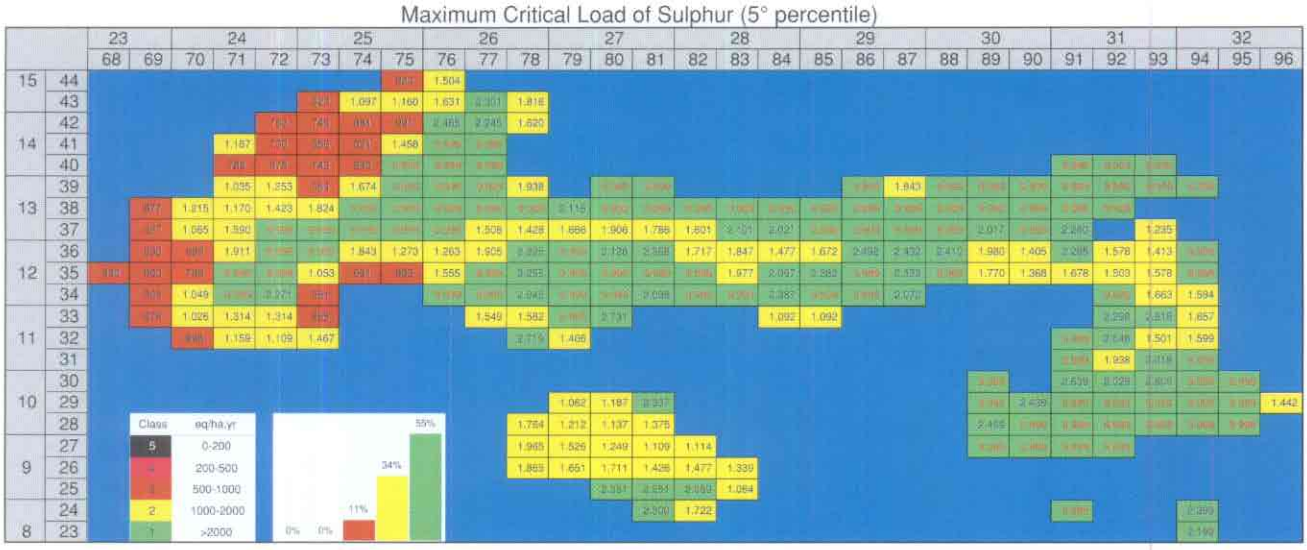

Figure IT-1. Maximum critical load of sulfur (5th percentile).

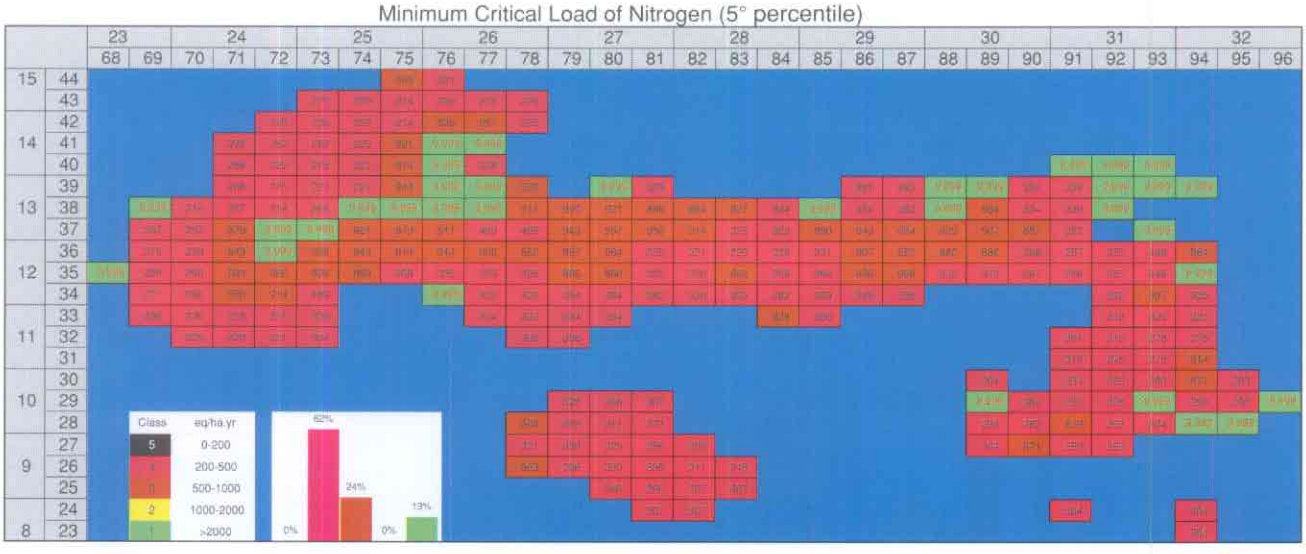

Figure IT-2. Minimum critical load of nitrogen (5th percentile).

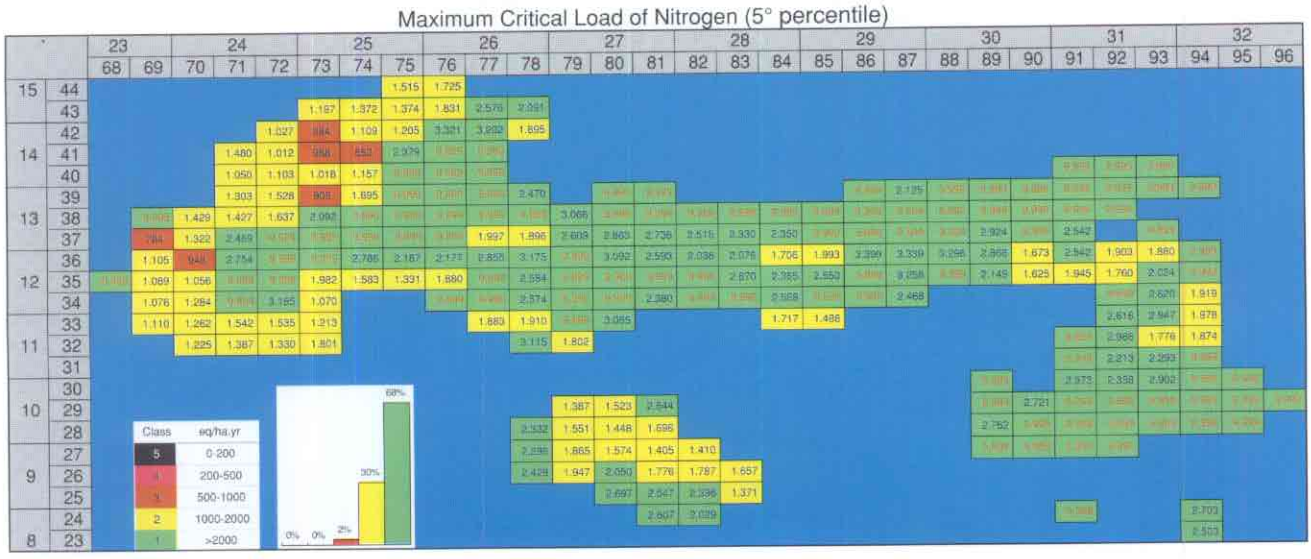

Figure IT-3. Maximum critical load of nitrogen (5th percentile).

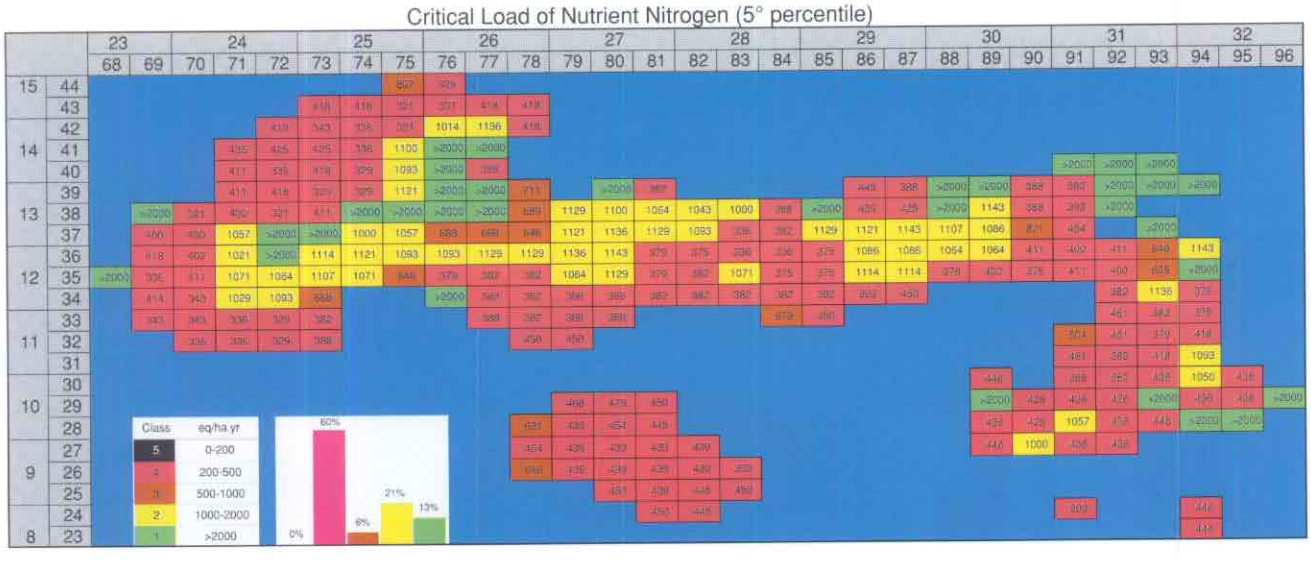

Figure IT-4. Critical load of nutrient nitrogen (5th percentile).

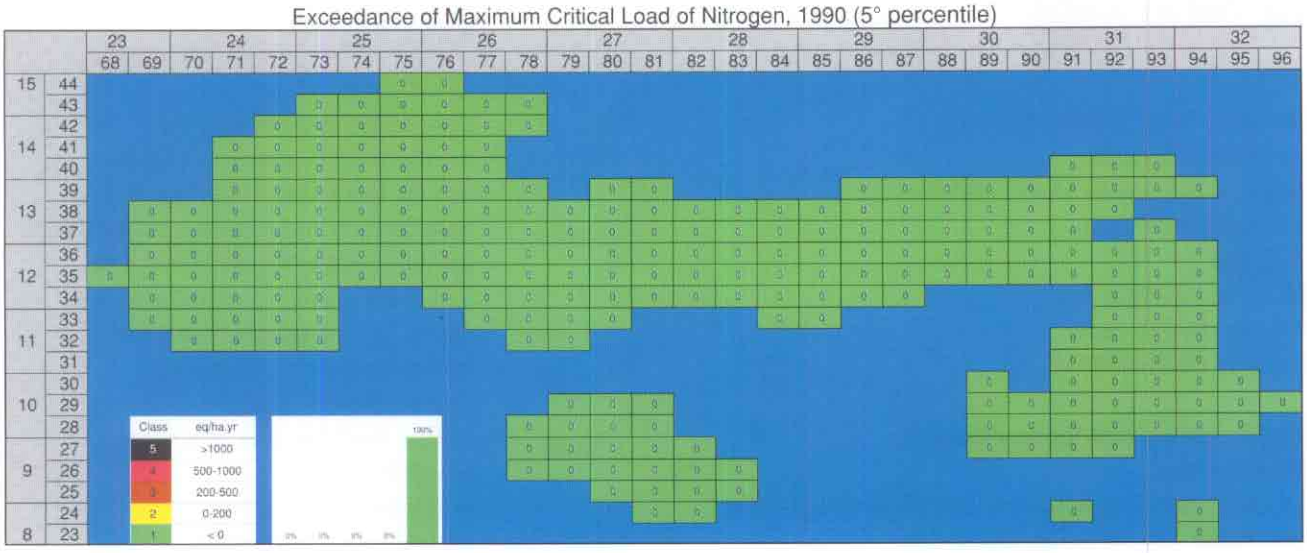

Figure IT-5. Exceedance of the maximum critical load of nitrogen, 1990 (5th percentile).

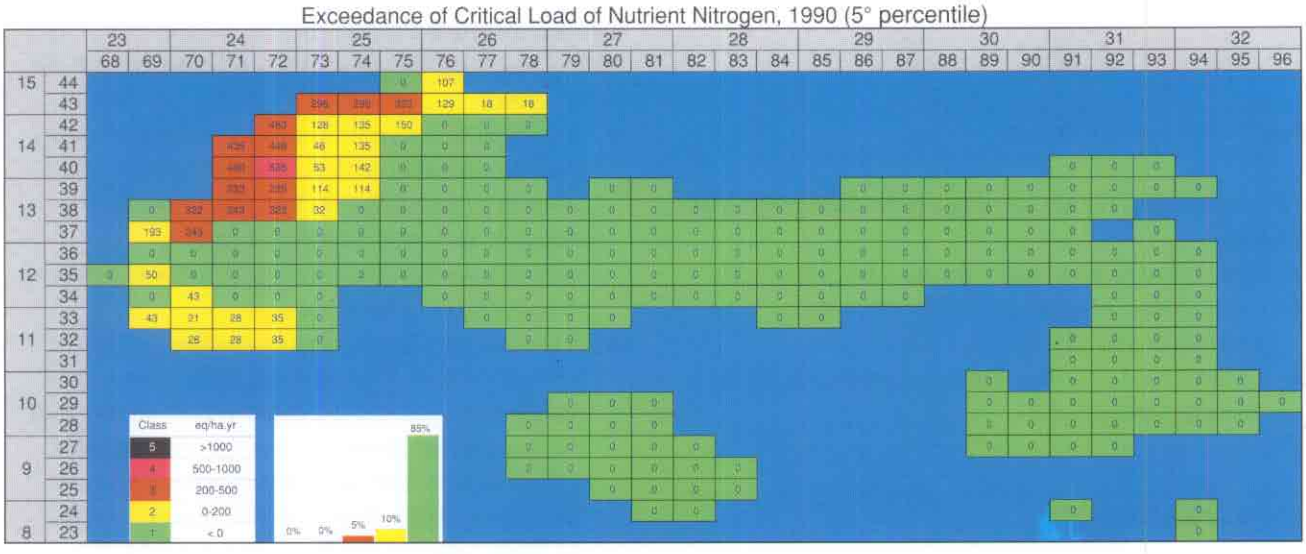

Figure IT-6. Exceedance of the critical load of nutrient nitrogen, 1990 (5th percentile).

NETHERLANDS

National Focal Center/Contact
Jan Willem Erisman
National Institute for Public Health and the Environment (RIVM)
P.O. Box 1
NL-3720 BA Bilthoven
tel: +31-30-274 2824
fax: +31-30-228 7531

Collaborating Institutions/Contact
Wim de Vries
DLO Winand Staring Centre for Integrated Land, Soil and Water Research (SC-DLO)
P.O Box 125
NL-6700 AC Wageningen
tel: +31-317-474353
fax: +31-317-424812
email: w.de.vries @ sc.dlo.nl

National Maps Produced

All maps using the Steady-state Mass Balance (SMB) method:

- Critical load of nutrient nitrogen for forest soils
- Critical load of nitrogen for forest soils: minimum and maximum values
- Critical load of sulfur for forest soils: minimum and maximum values.

Calculation Methods

Critical loads of nitrogen as a nutrient, $CL_{nut}(N)$, and maximum and minimum values for the critical loads of N and S are calculated according to the 1993 CCE Status Report (Downing *et al.* 1993; Eq.4.18; Eq. 4.35; Eq 4.30; Eq. 4.29 and Eq. 4.38):

$$CL_{nut}(N) = N_u + N_{i(crit)} + NO_{3,le(crit)} / (1-f_{de}) \quad (1)$$

$$CL_{max}(N) = N_u + N_{i(crit)} + (BC^*_{dep} + BC_w - BC_u + Ac_{le(crit)}) / (1-f_{de}) \quad (2)$$

$$CL_{min}(N) = N_u + N_{i(crit)} \quad (3)$$

$$CL_{max}(S) = BC^*_{dep} + BC_w - BC_u + Ac_{le(crit)} \quad (4)$$

BC^*_{dep} = the seasalt-corrected total deposition flux of base cations
BC_w = base cation weathering flux
BC_u = are the growth uptake fluxes (net uptake needed for forest growth of base cations and nitrogen respectively
N_u = growth uptake fluxes (net uptake needed for forest growth of base cations and nitrogen respectively
$N_{i(crit)}$ = critical long-term nitrogen immobilization flux
$Ac_{le(crit)}$ = critical leaching flux of acidity ($= -ANC_{le(crit)}$)
f_{de} = denitrification fraction
$NO_{3,le(crit)}$ = critical NO_3 leaching flux

Since the calculation of the critical loads presented in the 1995 CCE Status Report, various changes have been made to calculate critical loads of acidity and nitrogen for Dutch forests soils. These changes are mainly related to the criteria used to calculate a critical leaching flux of acidity and nitrogen (cf. de Vries, 1996):

- A critical Al concentration has no longer been used to calculate critical loads of acidity, since laboratory experiments for correlative field research and model results do not unambiguously show a critical value in relation to root and/or shoot damage.
- A critical Al/Ca ratio has been changed into a critical Al/(Ca+Mg+K) ratio, since a review of results from laboratory experiments shows that this parameter gives the best correlation with root and/or shoot damage (Sverdrup and Warfvinge 1993). Based on this review, critical Al/base cation ratios have no longer been applied uniformly, but are assigned as a function of tree species.
- A critical NO_3 concentration in leaching water related to the occurrence of vegetation changes has no longer been applied, since such changes may already occur at nearly natural low NO_3 leaching fluxes. Such a low flux (100 mol_c ha^{-1} yr^{-1}) has now been used instead in the calculation.

The critical acidity leaching flux, $Ac_{le(crit)}$, was calculated as the sum of Al leaching and H leaching. Two options were now used for the calculation of the critical Al leaching flux, $Al_{le(crit)}$, (de Vries 1996):

1) a criterion for the molar Al/(Ca+Mg+K) ratio in the root zone:

$$Al_{le(crit)} = RAlBC_{(crit)} \cdot (BC_{dep} + BC_w - BC_u) \quad (6)$$

2) a negligible depletion of Al hydroxides:

$$Al_{le(crit)} = 3 \cdot Ca_w + 0.6 \cdot Mg_w + 3.0 \cdot K_w + 3.0 \cdot Na_w \quad (7)$$

where $RAlBC_{(crit)}$ is a critical equivalent Al/(Ca+Mg+K) ratio ($mol_c\ mol_c^{-1}$), Ca_w, Mg_w, K_w and Na_w are the weathering rates of Ca, Mg, K and Na respectively, and the factors (3, 0.6, 3 and 3) refer to the stoichiometric equivalent ratio of Al to Ca, Mg, K and Na respectively. These stoichiometric ratios are based on Microcline (K), Albite (Na), Anorthite (Ca) and Chlorite (Mg).

The value of $Al_{le(crit)}$ used for the critical load calculation was the minimum value calculated by Eqs. 6 and 7. The critical H leaching flux, $H_{le(crit)}$, was calculated as:

$$H_{le(crit)} = PS \cdot [H]_{(crit)} \quad (8)$$

where PS is the precipitation surplus leaving the rootzone ($m^3\ ha^{-1}\ yr^{-1}$) and $[H]_{(crit)}$ is a critical H concentration, which is related to the critical Al concentration according to:

$$[H]_{(crit)} = ([Al]_{(crit)} / KAl_{ox})^{0.33} \quad (9)$$

where KAl_{ox} is the Al hydroxide equilibrium constant ($108\ mol^{-2}\ l^2$). The value of the critical Al concentration is determined by the critical Al leaching flux divided by the water flux (precipitation surplus).

The critical nitrate leaching flux was set at a nearly natural value of 100 $mol_c\ ha^{-1}\ yr^{-1}$.

Data Sources

Application methodology: Critical loads were calculated for all major combinations of tree species (12) and soil types (23) in grid cells of 1 km × 1 km , instead of the 10 km × 10 km grids used in previous applications, as deposition estimates now exist at this finer scale (Erisman *et al.* 1995). Tree species included (with percentage of area) were: *Pinus sylvestris* (Scots pine; 38.2%), *Pinus nigra* (black pine; 5.9%), *Pseudotsuga menziesii* (Douglas fir; 5.5%), *Picea abies* (Norway spruce; 5.1%), *Larix leptolepis* (Japanese larch; 5.7%), *Quercus robur* (oak; 17.4%), *Fagus sylvatica* (beech; 4.1%), *Populus spec* (poplar; 4.6%), *Salix spec* (willow; 2.4%), *Betula pendula* (birch; 7.4%), *Fraxinus excelsior* (ash; 1.9%) and *Alnus glutinosa* (black alder; 1.9%). Soil types were differentiated in 18 non-calcareous sandy soils, calcareous sandy soils, loess soils, non-calcareous clay soils, calcareous clay soils and peat soils on the basis of a recent 1: 250,000 soil map of the Netherlands.

Information on the area (distribution) of each specific forest-soil combination in each grid cell containing forest was derived by overlaying the digitized 1: 250,000 soil map with a spatial resolution of 100 m × 100 m, and a data base with tree species information, with a spatial resolution of 500 m × 500 m. The total number of forest soil combinations for all 1km × 1km grids, i.e. the total number of SMB calculations totals 122,847. The number of forest/soil combinations (calculations) in a grid varied between 1 and 47.

Assessment of input data: Input data for the SMB model can be divided in system inputs and parameters. These data were derived as a function of location (deposition area) and receptor (the combination of tree species and soil type) as shown in Table NL-1.

Table NL-1. Influence of location, tree species and soil type accounted for in the assessment of input data for the SMB model.

Data on:	Location	Tree Species	Soil Type
BC weathering	–	–	x
Growth uptake	–	x	x
Denitrification	–	–	x
Precipitation	x	–	–
Evapotranspiration	x	x	x

"–" means that an influence does exist but the effect was either considered negligible or information was too scarce to include the effect.

Data for all forest/soil combinations within each grid cell were derived by using (or deriving) relationships (transfer functions) with basic land characteristics such as tree species and soil type, that were available in geographic information systems.

Base cation deposition: Bulk deposition data for base cations for a 1km × 1km grid were interpolated from 14 monitoring stations for 1993. However, bulk deposition only includes wet deposition (and a very small part of dry deposition). Dry deposition

was calculated by multiplying base cations concentrations in the bulk (wet) deposition by a scavenging ratio to estimate air concentration fields. These air concentrations were in turn multiplied by a deposition velocity, depending (inter alia) on meteorology and land use, using the model DEADM (Erisman and Bleeker 1995). An estimate of seasalt inputs of Cl and SO_4 was made by assuming an equivalent Cl/Na and SO_4/Na ratio in both bulk deposition and dry deposition equal to these ratios in seawater, namely 1.165 for Cl and 0.116 for SO_4. Both Cl and seasalt SO_4 were subtracted from the total base cation deposition values to derive seasalt-corrected base cation inputs. In the previous application, dry deposition had been calculated by multiplying the bulk (wet) deposition by a dry deposition factor.

Weathering rates: Mineral weathering rates of base cations have been related to the root zone, which has a thickness between 60 and 80 cm depending upon soil type. Values for non-calcareous sandy soils included in the regional application were derived from one-year batch experiments that were scaled to field data by dividing them by a factor of 50. This value is based on a comparison of laboratory and field weathering rates, estimated by the depletion of base cations in the soil profile (Hootsmans and Van Uffelen 1991). For loess, clay and peat soils, an indicative value has been derived from literature.

Uptake: In deriving critical acid loads, the uptake of nitrogen (N_u) and base cations (BC_u) was calculated based on the concept of nutrient-limited uptake, which is defined as that uptake that can be balanced by a long-term supply of base cations. This amount, referred to as the critical base cation uptake, $BC_{u(crit)}$, is calculated from mass balances for each base cation (Ca, Mg and K) separately, as total deposition and weathering minus a minimum leaching of BC. We used a minimum leaching of 50 mol_c ha^{-1} yr^{-1} for Ca and Mg and 0 mol_c ha^{-1} yr^{-1} for K. From the critical base cation uptake, the corresponding critical N uptake ($N_{u(crit)}$) is calculated from the ratio between each cation and nitrogen in the biomass (cf. Posch *et al.* 1993, Eqs. 4.7 and 4.8).

In deriving critical nitrogen loads related to vegetation changes, N_u was calculated according to the concept of growth-limited uptake. Growth-limited uptake is calculated by multiplying the stem growth rate (m^3 ha^{-1} yr^{-1}) by the stem density (kg m^{-3}) and the element contents in stems (mol_c kg^{-1}). Forest growth estimates for all relevant combinations of forest and soil types and the content of N, K, Ca and Mg in stems are based on a literature survey for all tree species considered. The reasons for using different concepts in deriving nutrient uptake are explained in more detail in de Vries (1996).

Nitrogen immobilization: The critical N immobilization rate is calculated by accepting a change of 0.2% of nitrogen in organic matter in the upper soil layer (0–30 cm) during one rotation period (100 years). The pool of organic matter (OM_{pool} in kg ha^{-1}) in this layer is calculated by multiplying the thickness of the soil layer (0.3 m), with the bulk density of the soil layer (kg m^{-3}) and the fraction of organic matter. Bulk density is calculated as a function of organic matter and clay content (cf. van der Salm *et al.* 1993). Data for the contents of clay and organic matter are based on field surveys of 250 forest soils (150 sandy soils, 40 loess, 30 clay and 30 peat). Immobilization rates increase with higher organic matter contents, and generally range between 100 and 350 mol_c ha^{-1} yr^{-1}. These values correspond well with a range of between 2 and 5 kg ha^{-1} yr^{-1} mentioned by Posch *et al.* (1993).

Denitrification: Denitrification fractions were derived for each soil type based on data in Breeuwsma *et al.* (1991) for agricultural soils. These data were corrected for the more acidic forest soils. Values thus derived varied between 0.1 for well-drained sandy soils to 0.8 for peat soils (cf. de Vries *et al.* 1994, de Vries 1996).

Precipitation and evapotranspiration: Precipitation estimates have been derived from 280 weather stations in the Netherlands, using interpolation techniques to obtain values for each grid. Interception fractions, relating interception to precipitation, have been derived form literature data for all tree species considered. Data for evaporation and transpiration have been calculated for all combinations of tree species and soil types with a separate hydrological model (cf. de Vries *et al.* 1994, de Vries 1996).

Comments and Conclusions

Figures NL-1 to NL-3 contains 5 percentile and median (50 percentile) maps of the following critical loads for forest soils in the Netherlands (for 1 km x 1 km grid cells):

- nitrogen as a nutrient
- nitrogen as an acidifying pollutant (minimum)
- sulfur as an acidifying pollutant (maximum)

Maximum critical loads of nitrogen as an acidifying pollutant nearly always exceeded those for nitrogen as a nutrient, and thus has not been included in the present report.

Values vary as a function of soil type as shown in Table NL-2. Relatively low critical loads of both nitrogen as a nutrient and sulfur are calculated for forests on non-calcareous sandy soils, which mainly occur in the central, eastern and southern part of the country. Intermediate values for the critical loads of N and S were calculated for the loess soils in the southernmost part of the Netherlands and the clay soils in the western part of the country. High critical loads of N and low critical loads of S were calculated for the peat soils in the western part of the country. More information on the cause of the differences is given in de Vries (1996).
Compared to the national maps presented in the CCE Status Report 1995, the present critical loads are changed in that:

- The critical loads were calculated on a 1km × 1km scale instead of the 10km × 10km used previously.
- A different approach was used for to calculate N uptake in relation to critical acid loads and to critical nitrogen loads.
- A critical Al concentration has no longer been used to calculate critical loads of acidity since laboratory experiments for correlative field research and model results do not unambiguously show a critical value in relation to root and/or shoot damage.
- A critical Al/Ca ratio has been changed into a critical Al/(Ca+Mg+K) ratio, since a review of results form laboratory experiments shows that this parameter gives the best correlation with root and/or shoot damage (Sverdrup and Warfvinge 1993). Based on this review, critical Al:base cation ratios have no longer been applied uniformly, but are assigned as a function of tree species.
- The total deposition of base cations has now been based on results of the DEADM model. In the former application, these values were based on bulk deposition of data for base cations from 14 monitoring stations during the period 1978–1985, multiplied by a dry deposition factor.
- A critical NO_3 concentration in leaching water related to the occurrence of vegetation changes has no longer been applied, since such changes may already occur at nearly natural low NO_3 leaching fluxes. Such a low flux (100 $mol_c\ ha^{-1}\ yr^{-1}$) has now been used instead in the calculation.

References

de Vries, W., J. Kros and J.C.H. Voogd, 1994. Assessment of critical loads and their exceedance on Dutch forests using a multi-layer steady state model. *Water Air Soil Pollut.* 76: 407-448.

de Vries, W., 1996. Critical loads for acidity and nitrogen for Dutch forests on a 1 km x 1 km grid. DLO Winand Staring Centre for Integrated Land Soil and Water Research, Rep.113, 44pp.

Erisman, J.W. and A. Bleeker, 1995. Emissie, concentrate en depositie van verzurende stoffen. *In*: Heij, G.J. and T. Schneider (eds.), Eindrapport Additioneel Programma Verzurings onderzoek, derde fase (1991-1994), RIVM Rep. 300-05: 9-62.

Hootsmans, R.M. and J.G. van Uffelen, 1991. Assessment of input data for a simple mass balance model to map critical acid loads for Dutch forest soils. Interne mededeling Nr. 133, Winand Staring Centre, Wageningen, Netherlands. 98 pp.

Posch, M., J.P. Hettelingh, H.U. Sverdrup, K. Bull and W. de Vries, 1993. Guidelines for the computation and mapping of critical loads and exceedances of sulfur and nitrogen in Europe. *In*: R.J. Downing, J.-P. Hettelingh and P.A.M. de Smet (eds.), 1993. Calculation and Mapping of Critical Loads in Europe: CCE Status Report 1993. National Institute of Public Health and Environmental Protection Rep. No. 259101003, Bilthoven, Netherlands, pp. 21-37.

Sverdrup, H. and P. Warfvinge, 1993. The effect of soil acidification on the growth of trees, grass and herbs as expressed by the (Ca+Mg+K)/Al ratio. Reports in Ecology and Environmental Engineering 1993: 2, Lund University, Dept. of Chemical Engineering II, 108 pp.

van der Salm, C., J.C.H. Voogd and W. de Vries, 1993. SMB - a Simple Mass Balance model to calculate critical loads: Model description and user manual. DLO Winand Staring Centre for Integrated Land Soil and Water Research, Technical Document 11.

Table NL-2. 5, 50 and 95 percentile values of critical loads (molc $ha^{-1}\ yr^{-1}$) for nitrogen and sulfur for Dutch forests on non-calcareous soils.

	$CL_{nut}(N)$			$CL_{min}(N)$			$CL_{max}(S)$		
Soil type	**5%**	**50%**	**95%**	**5%**	**50%**	**95%**	**5%**	**50%**	**95%**
Sand	448	669	903	338	553	779	803	1377	1910
Loess	637	915	1254	526	806	1144	967	1910	2279
Clay	653	955	1657	319	622	1325	1336	2689	3878
Peat	1127	1323	1875	627	823	1375	352	1049	1295

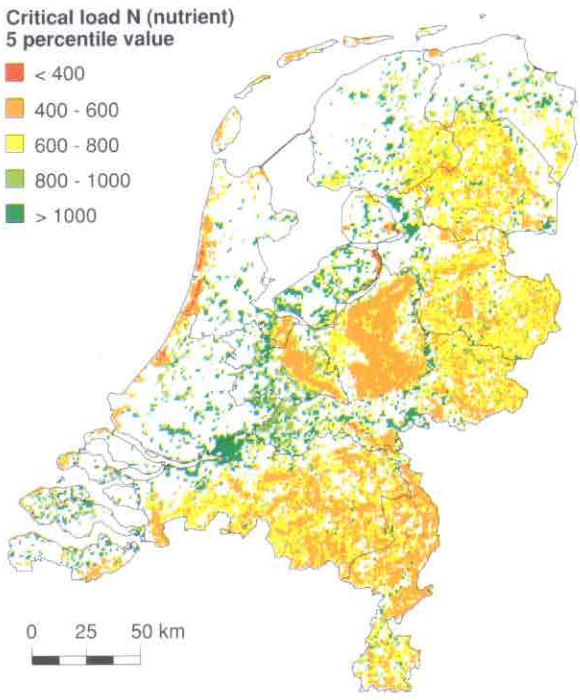

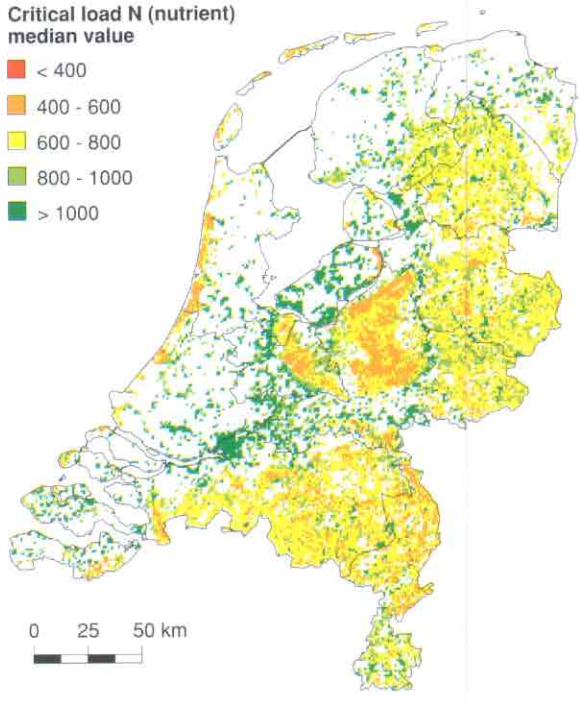

Fig NL-1. Critical load of nitrogen as a nutrient (5 percentile and median).

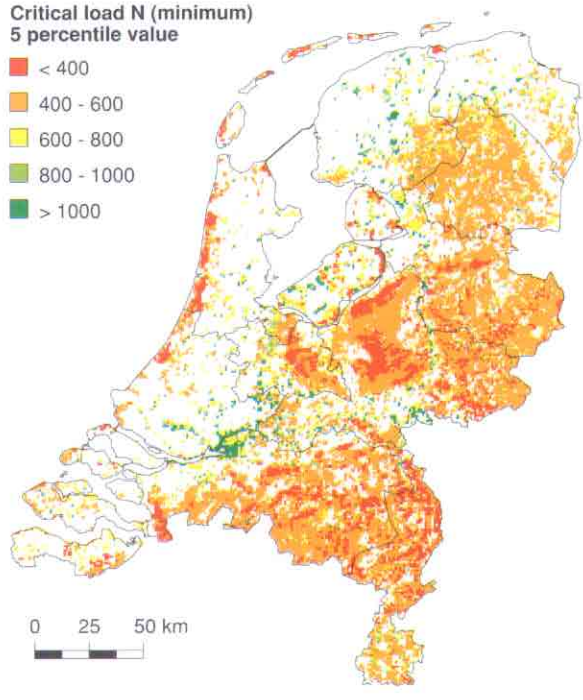

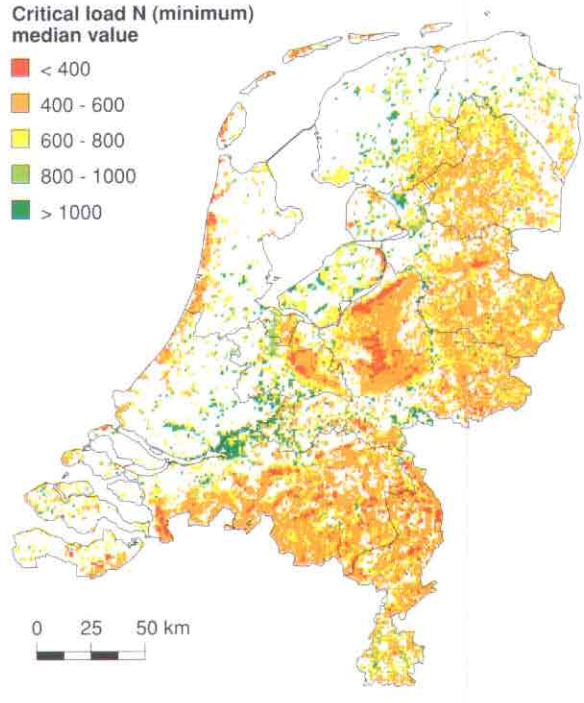

Fig NL-2. Critical load of nitrogen as an acidifying pollutant (minimum) (5 percentile and median).

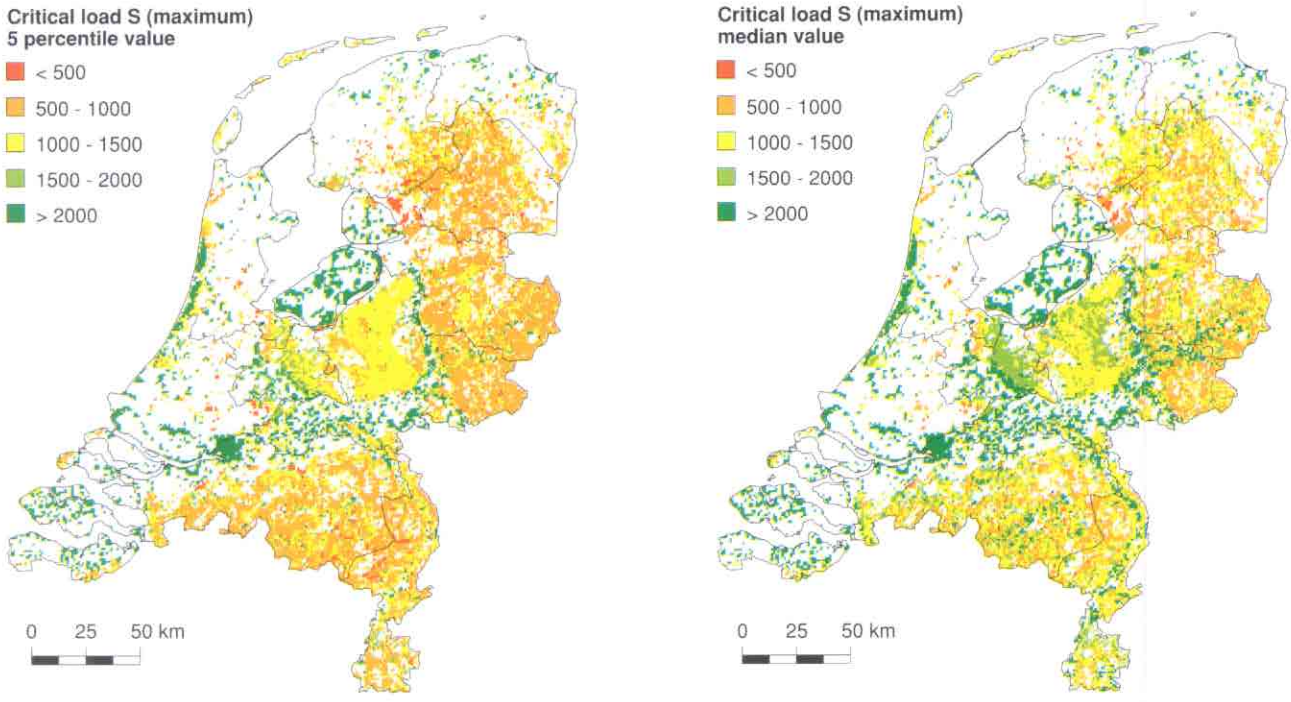

Fig NL-3. Critical load of sulfur as an acidifying pollutant (maximum) (5 percentile and median).

NORWAY

National Focal Center/Contact
Arne Henriksen
Norwegian Institute for Water Research
P.O.Box 173 Kjelsås
N-0411 Oslo
tel: +47-22-185116
fax: +47-22-185200
email: arne.henriksen@niva.no

Collaborating Institutions/Contacts
Kjetil Tørseth
Norwegian Institute for Air Research
P.O. Box 100
N-2007 Kjeller
tel: +47-63-898 158
fax: +47-63-898 050
email: kjetil@nilu.no

Jan Mulder
Norwegian Forest Research Institute
Høgskolev. 12
N-1432 Ås
tel: +47-64-94 91 59
fax: +47-64-94 29 80
email: jan.mulder@nisk.nlh.no

Egil Støren
Norwegian Meteorological Institute
P.O. Box 43 Blindern
N-0313 Oslo
tel: +47-22-96 30 00
fax: +47-22-96 30 50
e-mail: egil.storen@dnmi.no

National Maps Produced

Surface waters, forest soils, vegetation.

A. Surface Waters

Calculation methods

1. The Steady State Water Chemistry (SSWC) method (UBA 1996) was used to calculate critical loads of acidity, using a variable ANC_{limit} (Henriksen *et al.* 1995).
2. The critical load function (the FAB model) (Posch *et al.* 1997) has been used for a preliminary calculation of the required reduction requirements for S and N for each of the Norwegian grids at present deposition and according to current reduction plans for sulfur in 2010 (see Posch *et al.* 1995).

Grid Size: Each 1° longitude by 0.5° latitude grid was divided into 4 x 4 subgrids, each covering about 12 x 12 km^2 in southern Norway (with decreasing grid width at higher latitudes). The land area covered by each of the 2315 grids has been calculated.

Data sources

National regional lake surveys and monitoring programs.

Precipitation: A weighted average total deposition value for each EMEP50 grid cell has been calculated from ambient air concentrations and wet deposition, taking land use data (coverage of different receptors) into account (Tørseth and Pedersen 1994). Weighted means for the period 1988–1992 were used. The deposition values for each of the surface water grids (see above) was estimated from the NILU data base.

Water: The chemistry of surface water within a subgrid was estimated by comparing available water chemistry data for lakes and rivers within each grid. The chemistry of the lake that was judged to be the most typical was chosen to represent the grid. If there were wide variations within a subgrid, the most sensitive area was selected if it amounted to more than 25% of the grid's area. Sensitivity was evaluated on the basis of water chemistry, topography and bedrock geology. Geology was determined from the geological map of Norway (1:1,000,000) prepared by the Norwegian Geological Survey. Mean annual runoff data is from runoff maps prepared by the Norwegian Water and Energy Works. The database was revised in February 1995 and in October 1996.

B. Forest Soils

Calculation methods

The MAGIC dynamic model (Model of Acidification of Groundwater in Catchments, Cosby *et al.* 1985a,b) was used to produce maps for critical loads of acidity and exceedance for sulfur and nitrogen to forest soils. The criterion used was an Ca/Al molar ratio of 1.0 in the upper 60 cm of soil.

Grid size: The same grid system as for surface waters was used. Of these 706 grids are in productive forests, both coniferous (spruce, pine) and deciduous (birch). The remaining grids cover unproductive forests and non-forested areas, for which critical loads for forest soils cannot be calculated.

Data Sources

National monitoring data.

Precipitation: The same data as for surface waters was used.

Soil: The calculations are based on data from the NIJOS (Norwegian Institute of Land Inventory) forest monitoring plots on a 9 × 9 km grid and on the surface water data base referred to above. All input data are aggregated to the 12 × 12 km grid net. The NIJOS soils data are from areas in productive spruce and pine forests. A soil pit was objectively located within the representative vegetation type five meters frm the plot center in the 9 × 9 km grid. The soil pit was dug to at least 50 cm where possible. Soil profile samples were taken and analyzed according to standard procedures.

C. Critical Loads For Nutrient Nitrogen - Vegetation

Calculation Methods

Critical loads of nutrient nitrogen for vegetation has been estimated for Norway using empirically derived values for vegetation types. The vegetation types are taken from a 3 × 3 km^2 network of forest sample plots as recorded by the National Forest Inventory. The same grid system as for water and soil (see above) was used. The data base was updated in 1996; at present 74% of the country has been mapped.

The following critical load values for the vegetation types have been used:

Vegetation type	Critical load value (in kg N ha^{-1} yr^{-1})
Ombrotrophic bog	5
Coniferous forest	7
Deciduous forest	10
Calluna heath	15
Others	20

D. Critical Levels of Ozone

Exceedances of critical levels for ozone have been mapped according to the recommendations from the 1993 UN/ECE workshop in Bern, by a working group supported by the Nordic Council of Ministers (NMR). Maps showing calculated AOT40 values for agricultural crops and for forests in Scandinavia are reported (Lövblad *et al.* 1996).

Ongoing Work

Regional lake surveys

The Nordic countries have carried out several national lake surveys during the 1980's, and one of the major uses of these data has been the assessment of critical loads for surface waters (see Henriksen *et al.* 1996, Posch *et al.* 1997). In the fall of 1995 the Nordic countries decided to carry out a joint Nordic Lake Survey, and an integrated approach was adopted for providing additional data. The Nordic Council of Ministers (NMR), which has supported projects dealing with critical loads since 1985, established a working group which concluded that any integrated program of sampling would be greatly enhanced if adjacent countries with similar lake properties were included. With financial support from Norway and Finland, Russian Kola, Russian Karelia, Scotland and Wales joined Norway, Sweden and Finland in the common lake survey.

The lakes were statistically selected in such a way that they should represent the total lake population in each country (Henriksen *et al.* 1996). Sampling was carried out between September 1995 and January 1996 using the identical statistical lake selection criteria and harmonized sampling procedures. To complete the Nordic area, a subset of lakes in Denmark (not statistically selected) was sampled in the fall of 1996. The samples were

analysed for all major components, total nitrogen, total phosphorus and a selection of heavy metals and trace elements.

The main objectives of this integrated lake survey were to:

- assess general water quality,
- document the occurrence and regional variation in acidification,
- establish a new baseline of chemical data to follow up future effects of the 1994 Sulfur Protocol,
- establish the effects of nitrogen deposition on lake water chemistry in connection with the development of critical loads of nitrogen; and
- assess eutrophication status and the levels of heavy metals.

Major results from the survey have already been published (Henriksen *et al.* 1997). It is planned to evaluate heavy metals and trace elements for all countries in 1998. Figures NO-4 and NO-5 show the concentrations of Cd and Pb in Norwegian lakes.

In addition to water chemistry, the following information for all Nordic lakes has been collected: lake location, elevation and surface area, as well as catchment characteristics such as catchment area, size of upstream lakes, coniferous and deciduous forest area, peatland area, agricultural area, open area, municipalities, point sources (categories, load), liming (yes/no) and runoff (long-term annual mean value). For forests, net growth uptake of N by forests (annual mean value) and deposition of S, NO_3, NH_4, Ca, Mg, Na, K (annual mean values) were also included. This information will be used to derive the critical load function for each lake (Posch *et al.* 1997), and to calculate the required reduction requirements for S and N for the Nordic lakes at present deposition and according to current reduction plans for sulfur in 2010.

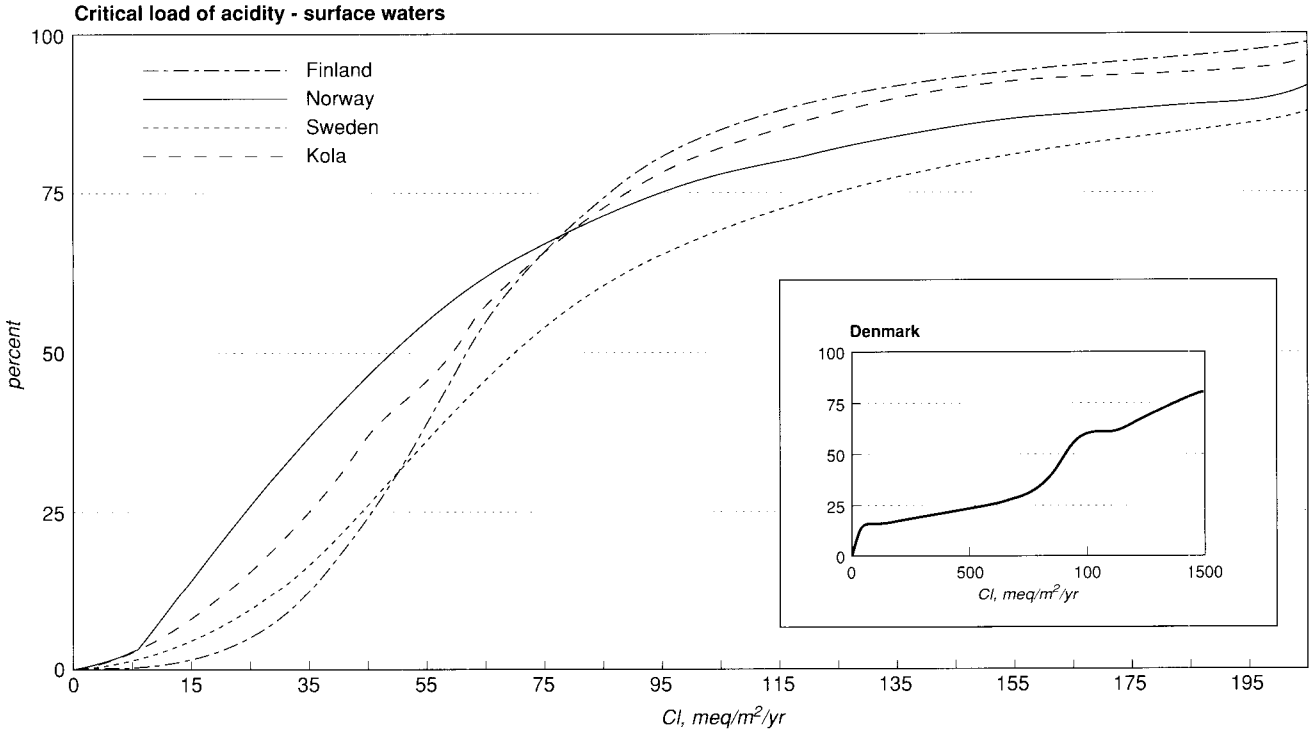

Figure NO-1. Frequency distributions of critical loads of acidity for the Nordic countries. (The Danish lakes were not statistically selected.)

Critical loads and exceedances in the Nordic countries: Critical loads of acidity have been calculated for the lakes in Finland, Norway, Sweden, Russian Kola and Denmark using the SSWC method. Figure NO-1 illustrates the frequency distributions of critical loads for the five regions.

The critical load exceedances for sulfur are illustrated below, using national depostion data (see Henriksen *et al.* 1997 for further details). The Danish lakes were not statistically selected.

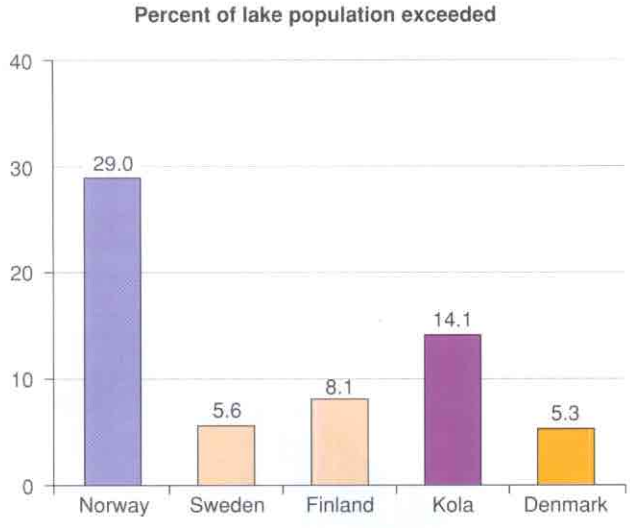

References

Cosby, B.J., G.M. Hornberger, J.N. Galloway and R.F. Wright, 1985a. Modelling the effects of acid deposition: assessment of a lumped-parameter model of soil water and streamwater chemistry. *Water Resour. Res.* 21: 51-63.

Cosby, B.J., R.F. Wright, G.M. Hornberger and J.N. Galloway, 1985b. Modelling the effects of acid deposition: estimation of long-term water quality responses in a small forested catchment. *Water Resour. Res.* 21: 1591-1601.

Henriksen, A, M. Posch, H. Hultberg and L. Lien, 1995. Critical loads of acidity for surface waters: Can the ANC_{limit} be considered variable? *Water Air Soil Pollut.* 85: 2419-2424.

Henriksen, A, B.L. Skjelkvåle, L. Lien, T.S. Traaen, J. Mannio, M. Forsius, J. Kämäri, I. Mäkinen, A. Berntell, T. Wiederhom, A. Wilander, T. Moiseenko, P. Lozovik, N. Filatov, R. Niinioja, R. Harriman and J.P. Jensen, 1996. Regional Lake Surveys in Finland, Norway, Sweden, Northern Kola, Russian Karelia, Scotland, Wales 1995: Coordination and Design. Acid Rain Research Rep. 40/1996, Norwegian Institute for Water Research, Oslo, Norway. 30 pp.

Henriksen, A., B.L. Skjelkvåle, A. Wilander, J. Mannio, T. Moiseenko, J.P. Jensen, J. Harriman, E. Fjeld, J. Vuorenmaa, T.S. Traaen, R. Harriman and P. Kortelainen., 1997. Regional Lake Surveys 1995 in Finland, Norway, Sweden, Denmark, Russian Kola, Russian Karelia, Scotland and Wales - Results. Acid Rain Research Rep. 46/1997. Norwegian Institute for Water Research, Oslo, Norway. (In press).

Lövblad, G., P. Grennfelt, L. Kärenlampi, T. Laurila, L. Mortensen, K. Ojanperä, H. Pleijel, A. Semb, D. Simpson, L. Skärby, J.P. Tuovinen and K. Tørseth, 1996. Ozone Exposure Mapping in the Nordic Countries, Nordic Council of Ministers (TemaNord 1996:522), Copenhagen, Denmark.

Posch, M., P.A.M. de Smet, J.-P. Hettelingh and R.J. Downing (eds.), 1995. Calculation and Mapping of Critical Thresholds in Europe: CCE Status Report 1995. National Institute of Public Health and the Environment Rep. 259101004, Bilthoven, Netherlands.

Posch, M., J. Kämäri, M. Forsius, A. Henriksen and A. Wilander, 1997. Exceedance of critical loads for lakes in Finland, Norway and Sweden: Reduction requirements for acidifying nitrogen and sulfur deposition. *Environ. Manage.* 21(2): 291-304.

Tomter, S.M. and J.M. Esser, 1995. Mapping critical loads for nitrogen, based on an empirical method. Naturens Tålegrenser, Report no. 70 (in Norwegian). National Forest Inventory (NIJOS), 1430 Ås, Norway.

Tørseth, K. and U. Pedersen, 1994. Deposition of sulfur and nitrogen components in Norway: 1988-1992. Norwegian Institute for Air Research (NILU) Rep. OR 16/94.

UBA, 1996. Manual on Methodologies and Criteria for Mapping Critical Levels/Loads and geographical areas where they are exceeded. UN/ECE Convention on Long-range Transboundary Air Pollution. Federal Environmental Agency (Umweltbundesamt), Texte 71/96, Berlin.

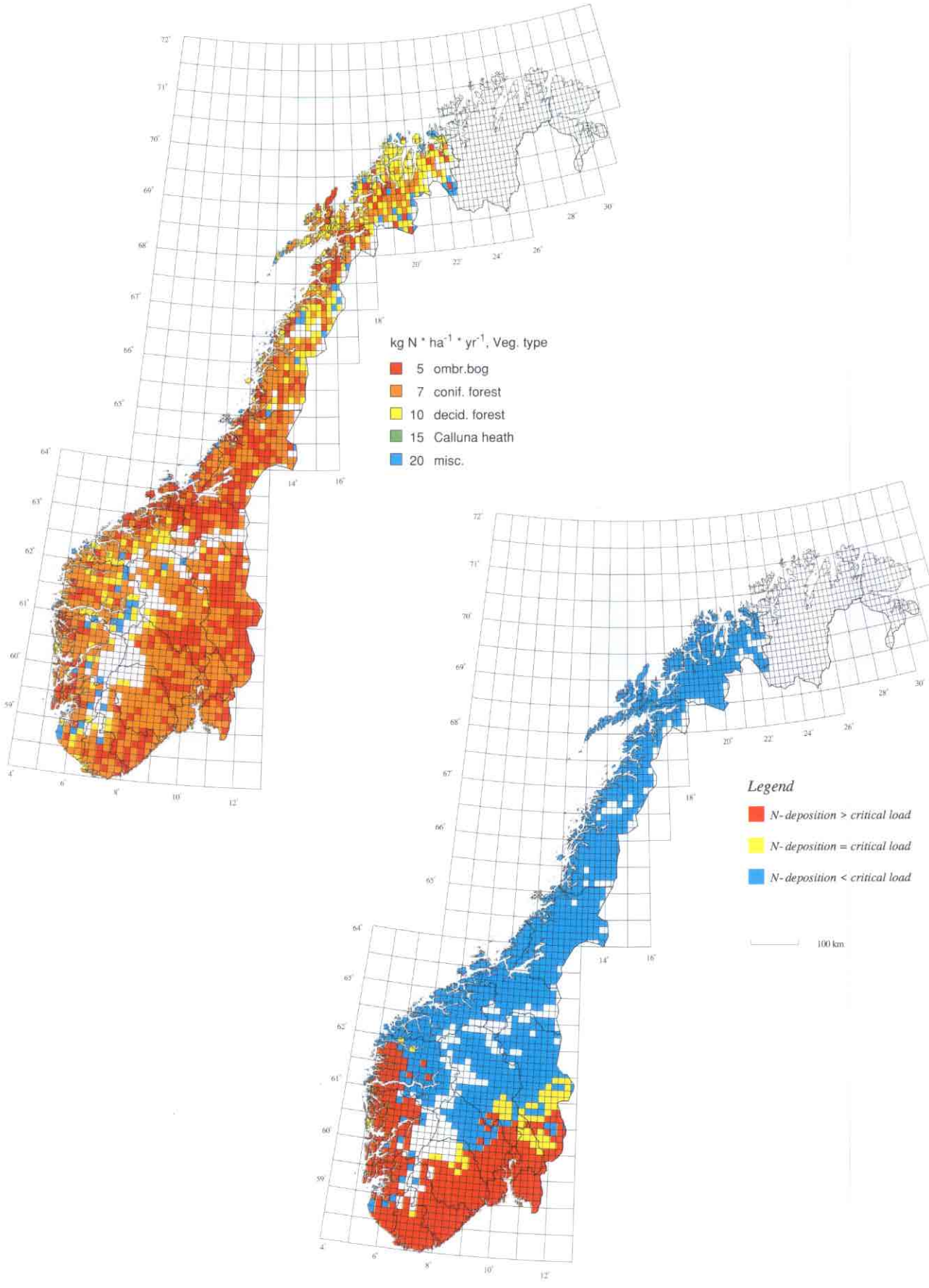

Figure NO-2. (left) Critical loads of nutrient nitrogen, based on vegetation types (updated 1996).
Figure NO-3. (right) Exceedance of critical loads of nutrient nitrogen based on weighted mean deposition data for 1988–1992.

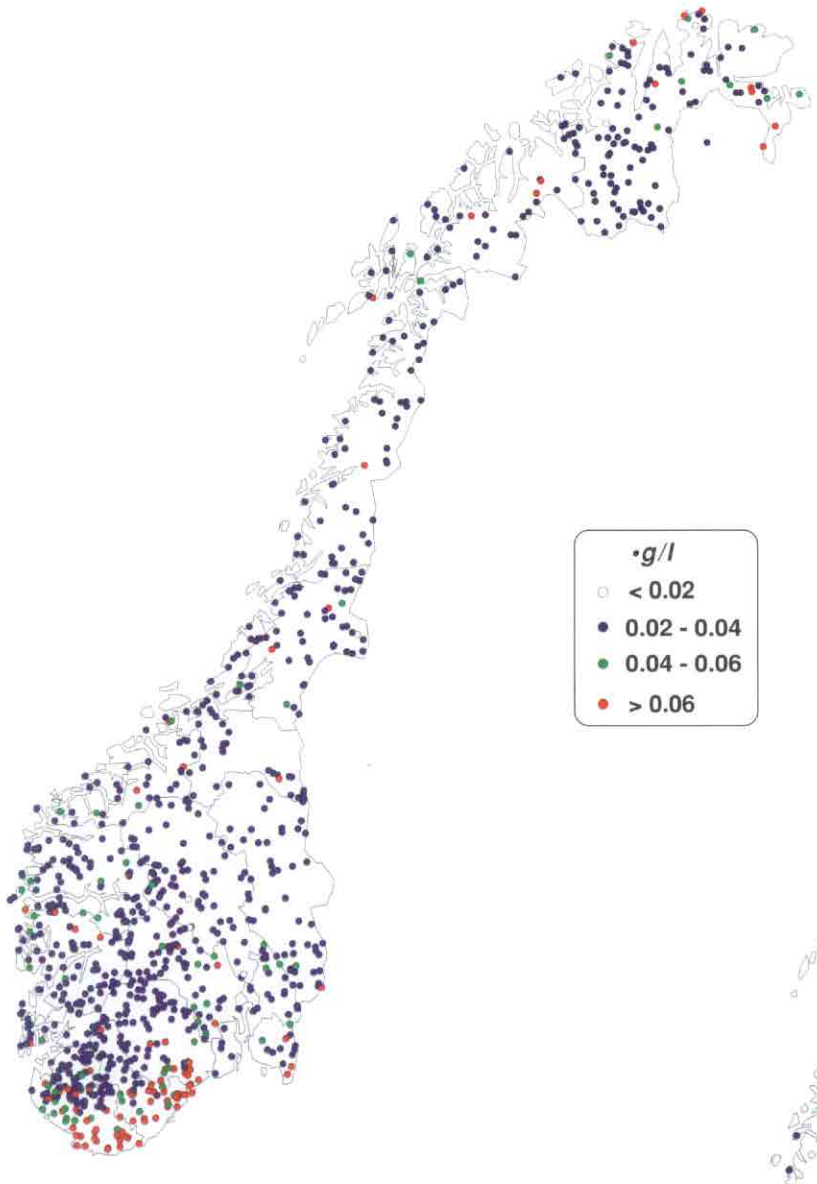

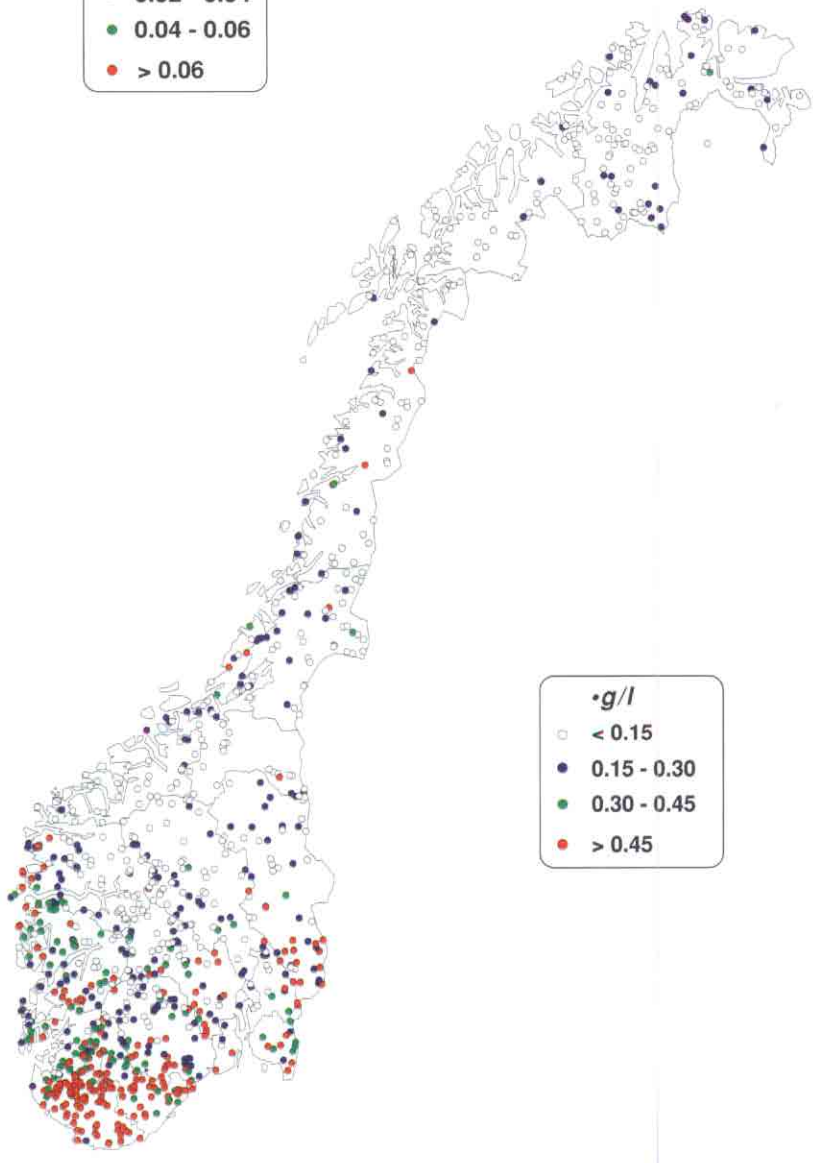

Figure NO-4. (left) Concentrations of cadmium (Cd) in Norwegian lakes, 1995.
Figure NO-5. (right) Concentrations of lead (Pb) in Norwegian lakes, 1995.

POLAND

National Focal Center/Contact
Wojciech A. Mill
Institute for Ecology of Industrial Areas
ul. Kossutha 6
PL-40-832 Katowice
tel: +48-32-154 6031
fax: +48-32-541717
email: mill@ietu.katowice.pl

Collaborating Institutions/Contacts
Jerzy Wawrzoniak
Forest Research Institute
ul. Bitwy Warszawskiej 3
PL-00-973 Warsaw
tel: +48-22-464623
fax: +48-22-224935

Forest Management and Geodesy Office
ul. Wawelska 52/54
Warsaw

Institute of Environmental Engineering
Warsaw University of Technology
ul. Nowowiejska 20
Warsaw

Calculation Methods

The following critical loads for forest soils have been calculated using the SSMB method outlined in the CCE 1995 Status Report (Posch *et al.* 1995):

- Maximum critical loads of sulfur
- Minimum critical loads of nitrogen
- Maximum critical loads of nitrogen
- Critical loads of nutrient nitrogen

For high-elevation areas, the relevant modification of the SSMB method was applied (UBA Vienna 1993). The maps were produced for grids of 0.20° × 0.10° long/lat (nearly 10 × 10 km^2). 1958 receptor points covered by forests divided into coniferous and deciduous species.

Data Sources

Most of the input data used to determine the critical loads values was taken or generated from national data sources as reported in Mill and Wojcik (1996).

Soils: The dominating types of soil in particular grids were adopted on the basis of data from the Polish Soil Atlas (1:300,000). Forty types of predominant soils in Poland were included in the calculations, and adequate values of base cation weathering were attributed to them according to the Mapping Vademecum procedure.

Meteorology: The data concerning precipitation, runoff and average annual temperature was obtained from the Hydrological Atlas of Poland published by the Institute of Meteorology and Water Management.

Forests: The data concerning the spatial location of forests was based on the Forest Map of Poland, edited by the Forest Management and Geodesy Office. Data concerning forest resources, growth and age of trees was obtained from the data bank of the Forest Management and Geodesy Office. For calculating critical loads, all grids in which the percentage of forest area in the grid was greater than zero were considered to be forested.

Uptake: The uptake of base cations and nitrogen was calculated as the minimum of growth-limited uptake and nutrient-limited uptake. The stem growth rate, the stem density and the elements content in stems were obtained from the data bank of the Forest Management and Geodesy Office.

Critical nitrogen leaching: The limiting concentrations of nitrogen for coniferous and deciduous trees suggested in the CCE Status Report 1993 (Downing *et al.* 1993) were taken for calculations.

Nitrogen immobilization: The long-term immobilization factor was set to 214 eq ha^{-1} yr^{-1} as a representative value for Polish conditions.

Denitrification: The constant denitrification fraction was used to estimate the denitrification rate, which is below 1 kg N ha^{-1} yr^{-1} for most forest sites.

Comments and Conclusions

The growing interest of Polish policy makers in the critical loads concept as a tool for environmental policy development and planning, as well as the

recent development of forest monitoring, has uncovered new perspectives for the application of more advanced methods for critical loads estimation than those used to date. This refinements include a substitution of the one-layer Simple Mass Balance method by the use of multi-layer models, and later, dynamic models. The so-called "intensive" monitoring system for forests will produce most of the empirical parameters necessary for critical loads calculations by the use of these more sophisticated methods. This kind of monitoring system has been launched in November 1995 by the Forest Research Institute and the State Inspectorate of Environmental Protection, and the first officially submitted results for 1996 are expected in the middle of 1997.

References

Downing, R.J., J.-P. Hettelingh and P.A.M. de Smet (eds.), 1993. Calculation and Mapping of Critical Loads in Europe: CCE Status Report 1993. National Institute of Public Health and Environmental Protection Rep. No. 259101003, Bilthoven, Netherlands.

Mill, W. and A. Wojcik, 1996. The contribution of selected economy sectors in acidification of terrestrial ecosystems in Poland. Institute for Ecology of Industrial Areas, Report Series, Katowice, Poland

Posch, M., P.A.M. de Smet, J.-P. Hettelingh and R.J. Downing (eds.), 1995. Calculation and Mapping of Critical Thresholds in Europe: CCE Status Report 1995. National Institute of Public Health and the Environment Rep. 259101004, Bilthoven, Netherlands.

UBA Vienna, 1993. Critical loads of acidity for high precipitation areas. Results from a workshop held in Vienna, March 9-10, 1992. Umweltbundesamt Wien.

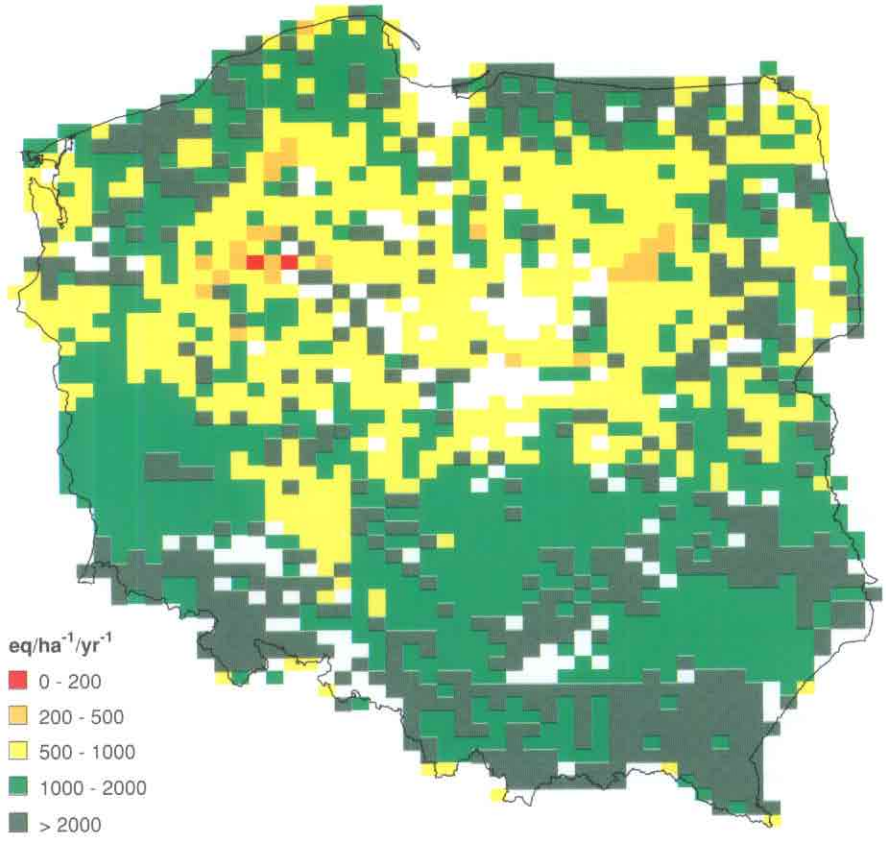

Figure PL-1. Maximum critical loads of sulfur.

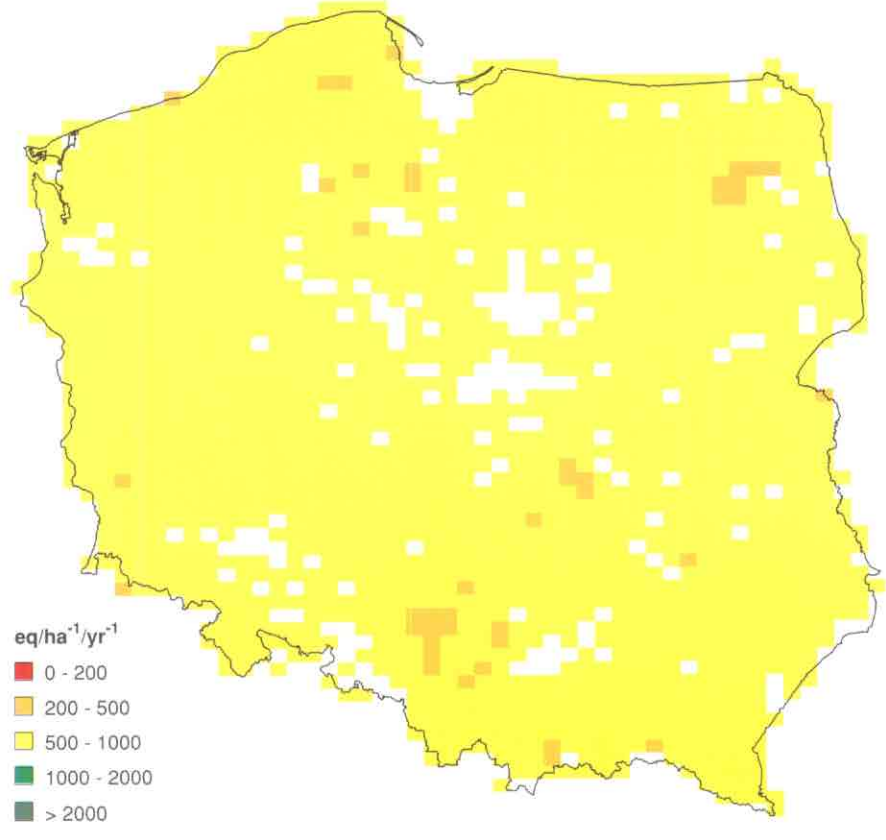

Figure PL-2. Minimum critical loads of nitrogen.

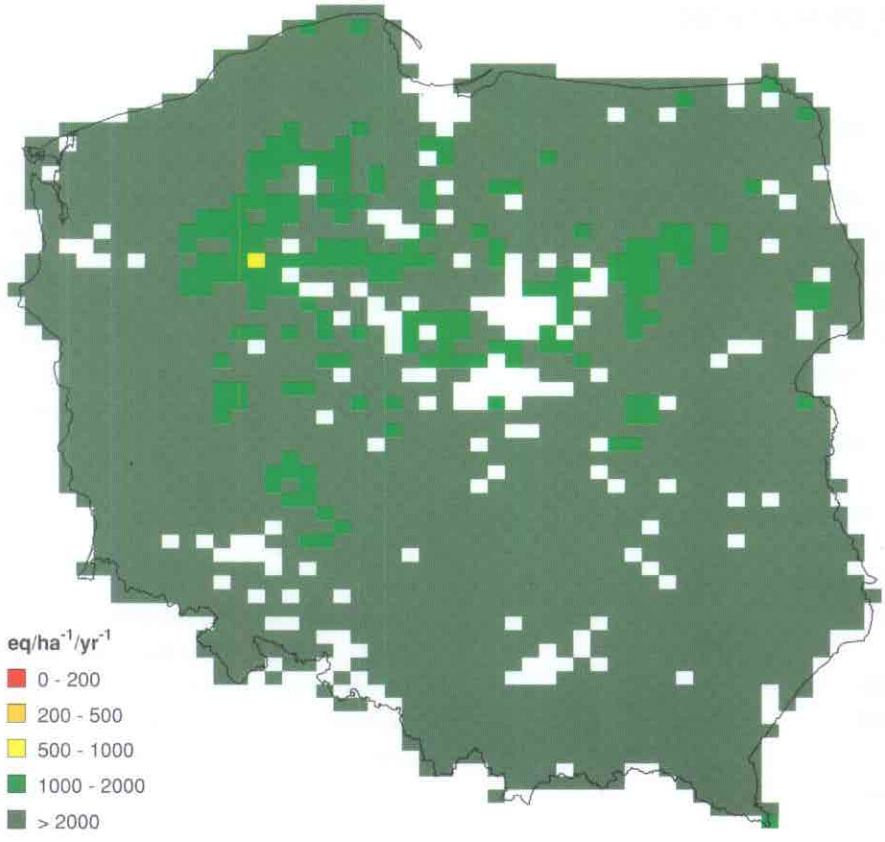

Figure PL-3. Maximum critical loads of nitrogen.

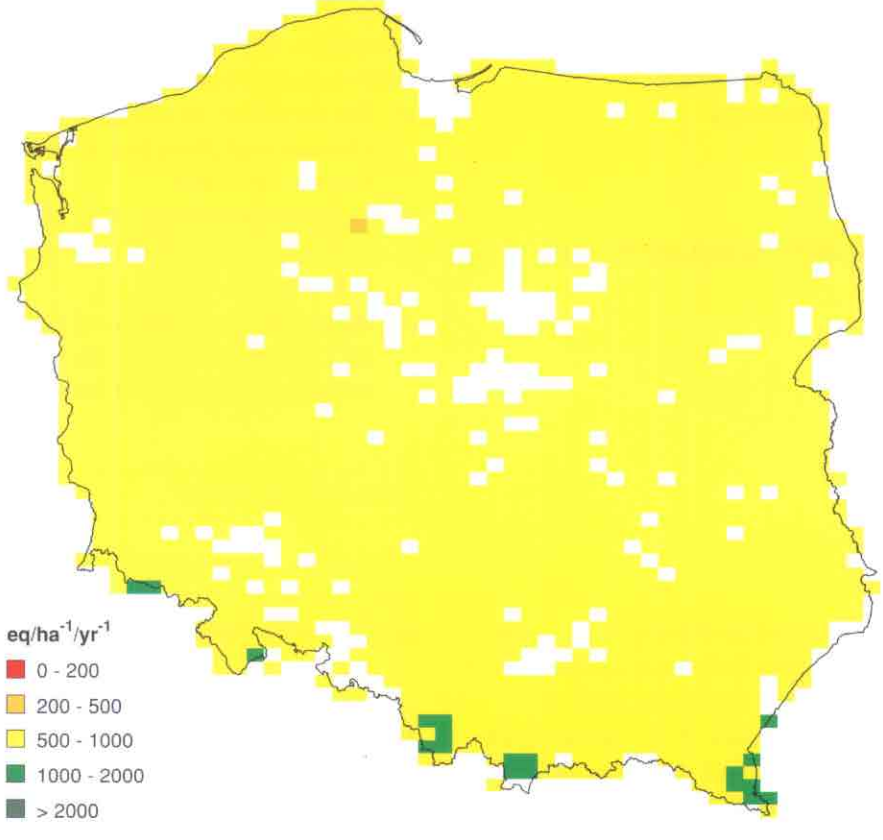

Figure PL-4. Critical loads of nutrient nitrogen.

RUSSIAN FEDERATION

National Focal Center/Contact
Vladimir N. Bashkin
Institute of Soil Science and Photosynthesis
Russian Academy of Sciences
Pushchino, Moscow region, 142292
tel: +7-0967-733845
fax: +7-095-923 3602, +7-0967-790532
email: bashkin@issp.serpukhov.su

Collaborating Institutions/Contacts
Andrei S. Peshkov
Head of Russian Federation NFC
Pavel P. Krechetov
Institute of Nature Protection
Sadki-Znamenskoe
113628 Moscow
tel: +7-095-423 0233
fax: +7-095-423 0233

Alex Yu. Abramychev
Irina V. Priputina
Arina V. Tankanag
Irina N. Chekhina
Institute of Soil Science and Photosynthesis
Russian Academy of Sciences
Pushchino, Moscow region, 142292
tel: +7-0967-733845
fax: +7-095-923 3602, +7-0967-790532
email: bashkin@issp.serpukhov.su

Valentin G. Sokolovsky
Natalya A. Karpova
Ministry of Environmental Protection and Natural Resources
Gruzinskya str. 4/6
123812 Moscow
tel: +095-254 6074
fax: +095-254 8283

Calculation Methods

Critical loads of nutrient and acidifying nitrogen as well as for sulfur and acidity have been calculated for various ecosystems in the European part of Russia based on modified steady-state mass balance (SMB) equations. Due to the large dimensions of the area, all calculations and mapping procedures have been carried out using geoinformation system with elements of a simplified expert-modeling system (Bashkin *et al.* 1995a,b, 1996a,b; Kozlov *et al.* 1995). The initial information consisted of regionalized geological, geochemical, geobotanic, landscape, soil, hydrochemical, biogeochemical, hydrological, and other data. For each elemental taxon, the main links of biogeochemical cycles of N, S and base cations (BC) have been quantitatively characterized based on available case studies. The grid cells were 2′ × 2′. Figures RU-1 through RU-4 present the 5-percentile data.

Data Sources

Geographical: The information on soil cover has been extracted from the digitized FAO Soil Map on a scale of 2′ × 2′ (FAO 1989). Calculations have been carried out for every soil type and subtype and corresponding terrestrial ecosystems. The land use information has been extracted from CORINAIR. Data for 14,251 points has been provided to the CCE.

The quantitative assessment and mapping of sulfur and nitrogen critical loads was carried out on the basis of number of regional parameters for a given ecosystem. For the European part of Russia the following data bases were identified:

- The inventory of values of surface runoff of nitrogen and phosphorus (Kondratjev and Koplan-Dix 1988)
- Biogeochemical regionalization of terrestrial and freshwater ecosystems (Kovalsky 1974, Bashkin *et al.* 1993)
- Annual biomass uptake (Bazilevich and Rodin 1971, Manakov 1972, Bashkin 1987, Bashkin *et al.* 1992, Gundersen and Bashkin 1994).

Acknowledgments

The authors wish to thank the Russian Fund of Basic Research for financial support of the scientific activity of the National Focal Center for Effects.

References

Bashkin, V.N., 1987. Nitrogen agrogeochemistry. Pushchino, 270pp.
Bashkin, V.N., V.P. Uchvatov, A.Y. Kudeyarova *et al.*, 1992. Ecological-agrogeochemical regionalization of the Moscow region. Pushchino: ONTI, 170pp.

Bashkin V.N., E.V. Evstafjeva, V.V. Snakin *et al.*, 1993. Biogeochemical fundamentals of ecological standardization. Moscow, Nauka Publ. House, 312pp.

Bashkin V.N. *et al.*, 1995a. Russian Federation NFC Report. *In*: M. Posch, P.A.M. de Smet, J.-P. Hettelingh and R.J. Downing (eds.), 1995. Calculation and Mapping of Critical Thresholds in Europe: CCE Status Report 1995. National Institute of Public Health and the Environment Rep. 259101004, Bilthoven, Netherlands.

Bashkin V.N., M.Y. Kozlov, I.V. Priputina, A.Yu. Abramychev and I.S. Dedkova, 1995b. Calculation and mapping of critical loads of S, N and acidity on the ecosystems of Northern Asia. *Water Air Soil Pollut.* 85:2395-2400.

Bashkin V.N., M.Y. Kozlov, A. Yu. Abramychev and I.S. Nikiforova, 1996a. Regional and Global Consequences of Transboundary Acidification in the Northern and Northern-East Asia. Proceedings of the International Conference on Acid Deposition in East Asia, Taipei, Taiwan, May 28-30, 1996, pp. 225-231.

Bashkin V.N., M.Y. Kozlov and O.M. Golinets, 1996b. Risk Assessment of Ecosystem Sensitivity to Acid Forming Compounds in the North-Eastern Asia. Proceedings of the International Conference on Acid Deposition in East Asia, Taipei, Taiwan, May 28-30, 1996, 347-56.

Bazilevich, N. and L. Rodin, 1971. Productivity and element cycle in natural and cultural plant communities of the USSR. *In*: N. Bazilevich (ed.), Biological Productivity and Chemical Element Cycle in Plant Communities. Leningrad: Nauka, 5-32.

Gundersen P. and V. Bashkin, 1994. Nitrogen cycling. *In*: B. Moldan and J.Cerny (eds.), Biogeochemistry of Small Catchments. SCOPE 51, J. Wiley and Sons, pp. 255-277.

Kondratjev, K.Ya. and I.S. Koplan-Dix, 1988. Evolution of phosphorus cycle and natural waters eutrophication. Leningrad: Nauka, 206 pp.

Kozlov M.Y., V.N. Bashkin and O.M. Golinets, 1995. Uncertainty analysis of critical loads for terrestrial ecosystems in Russia. *Water Air Soil Pollut.* 85:2569-2564.

Kovalsky, V.V., 1974. Geochemical ecology. Moscow, Nauka Publ. House, 299 pp.

Manakov, K.N., 1972. Productivity and biological turnover in tundra biogeocenoses. Leningrad, Nauka Publ. House, 150 pp.

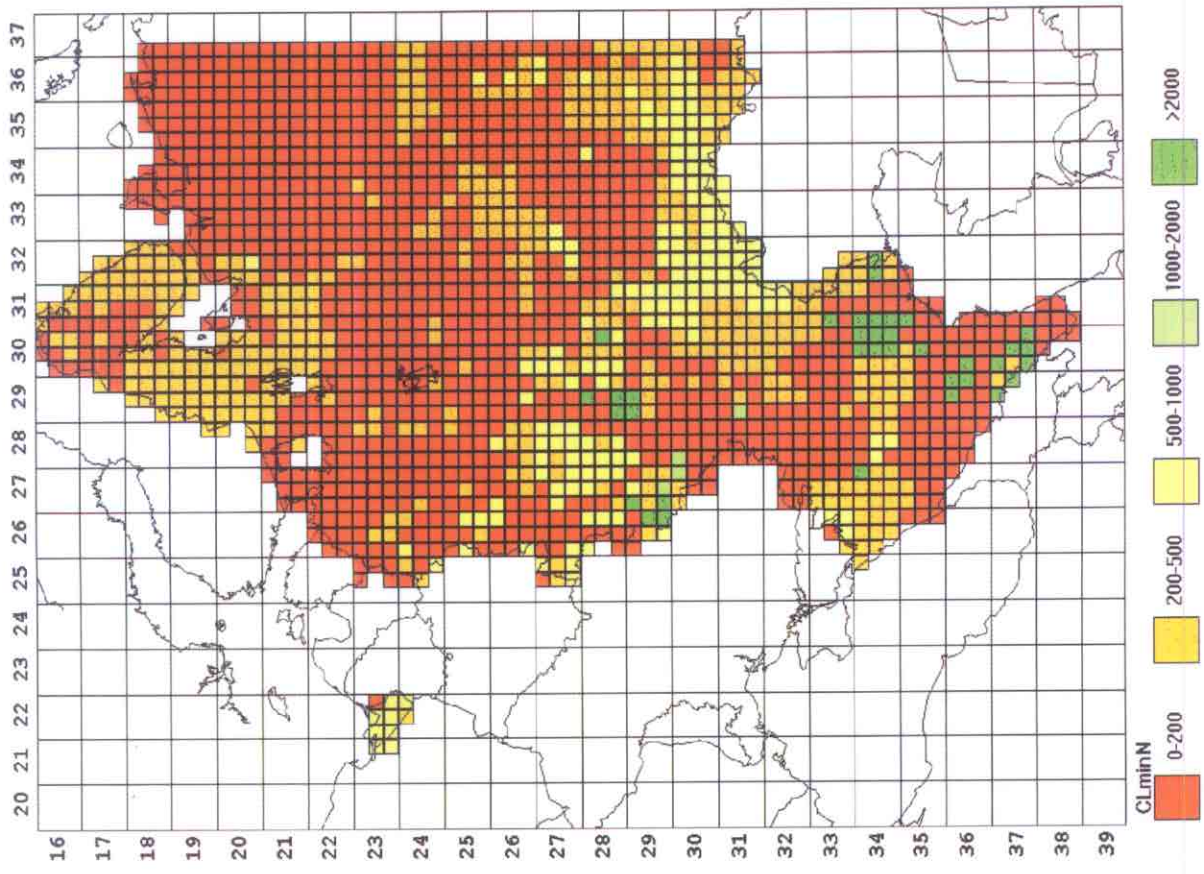

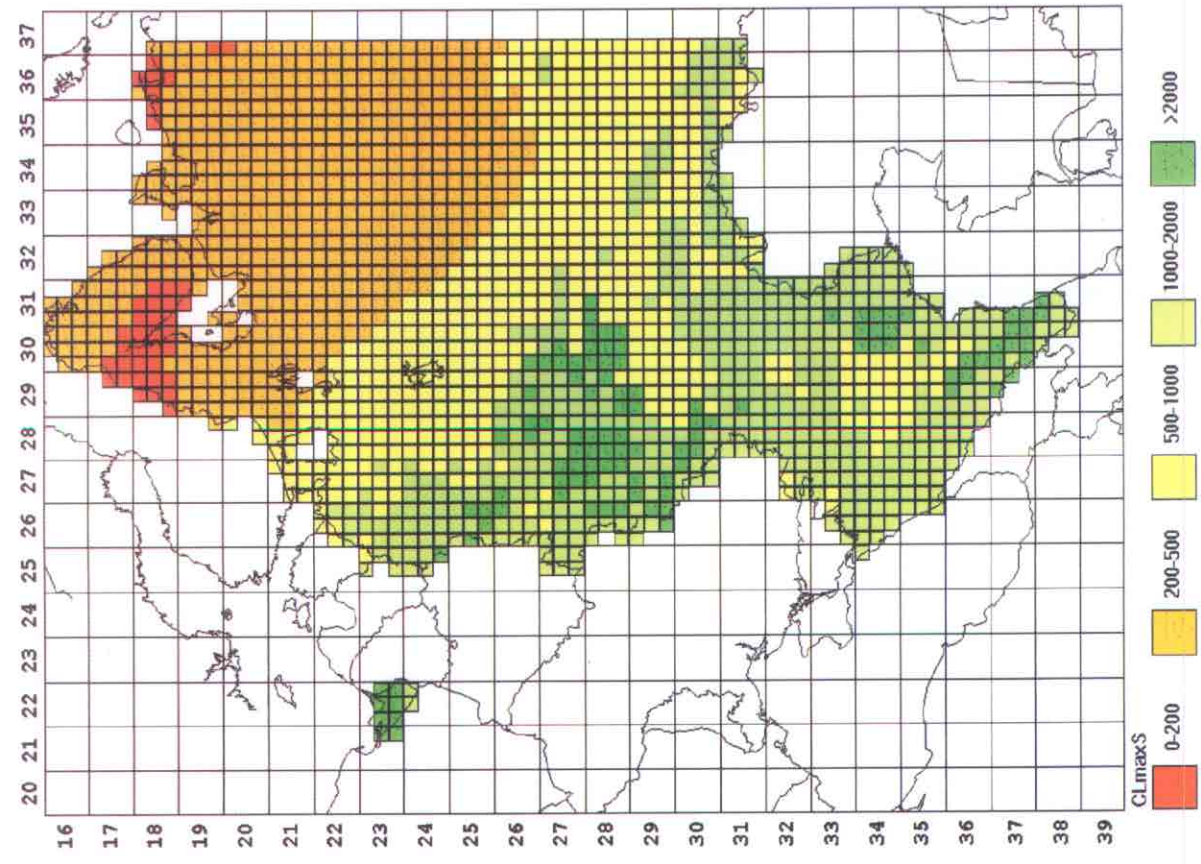

Figure RU-1. (left) Critical loads of maximum sulfur for terrestrial ecosystems in the European part of Russia.
Figure RU-2. (right) Critical loads of minimum nitrogen for terrestrial ecosystems in the European part of Russia.

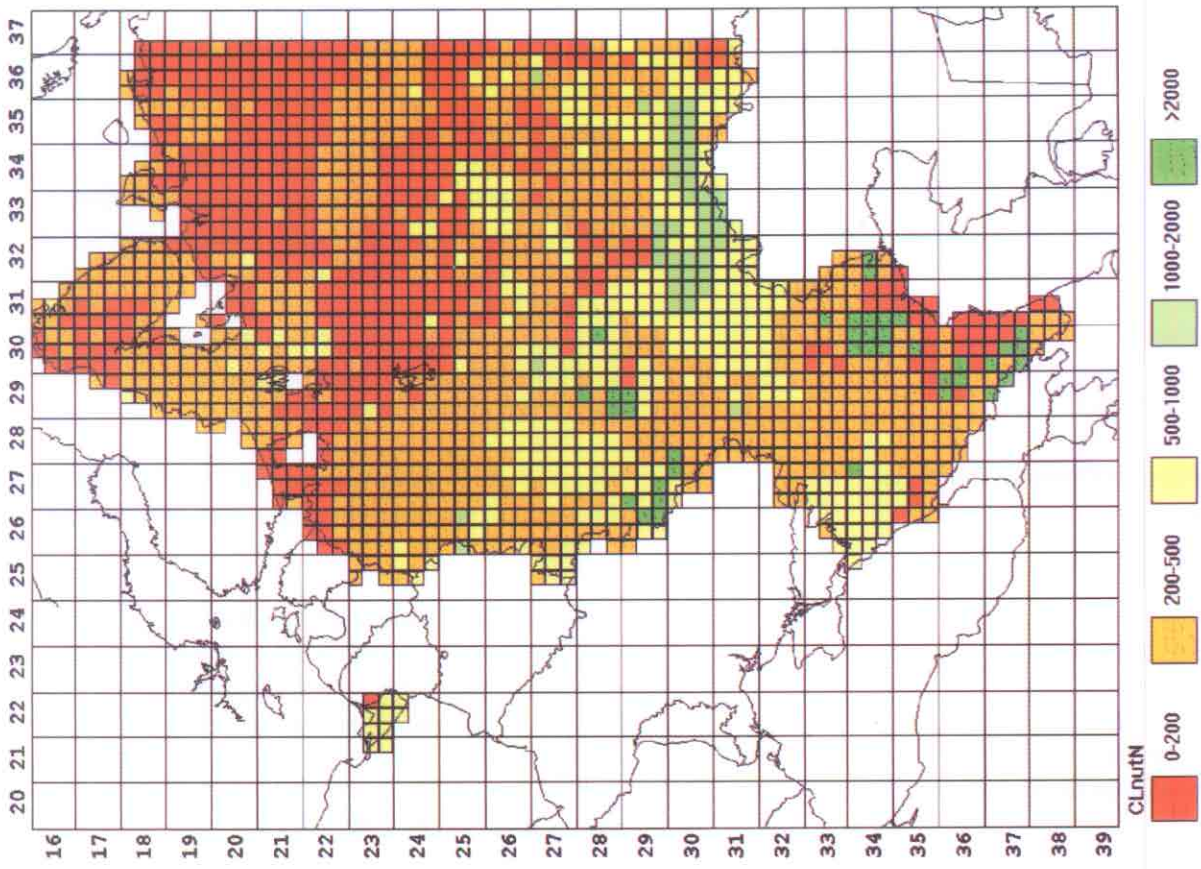

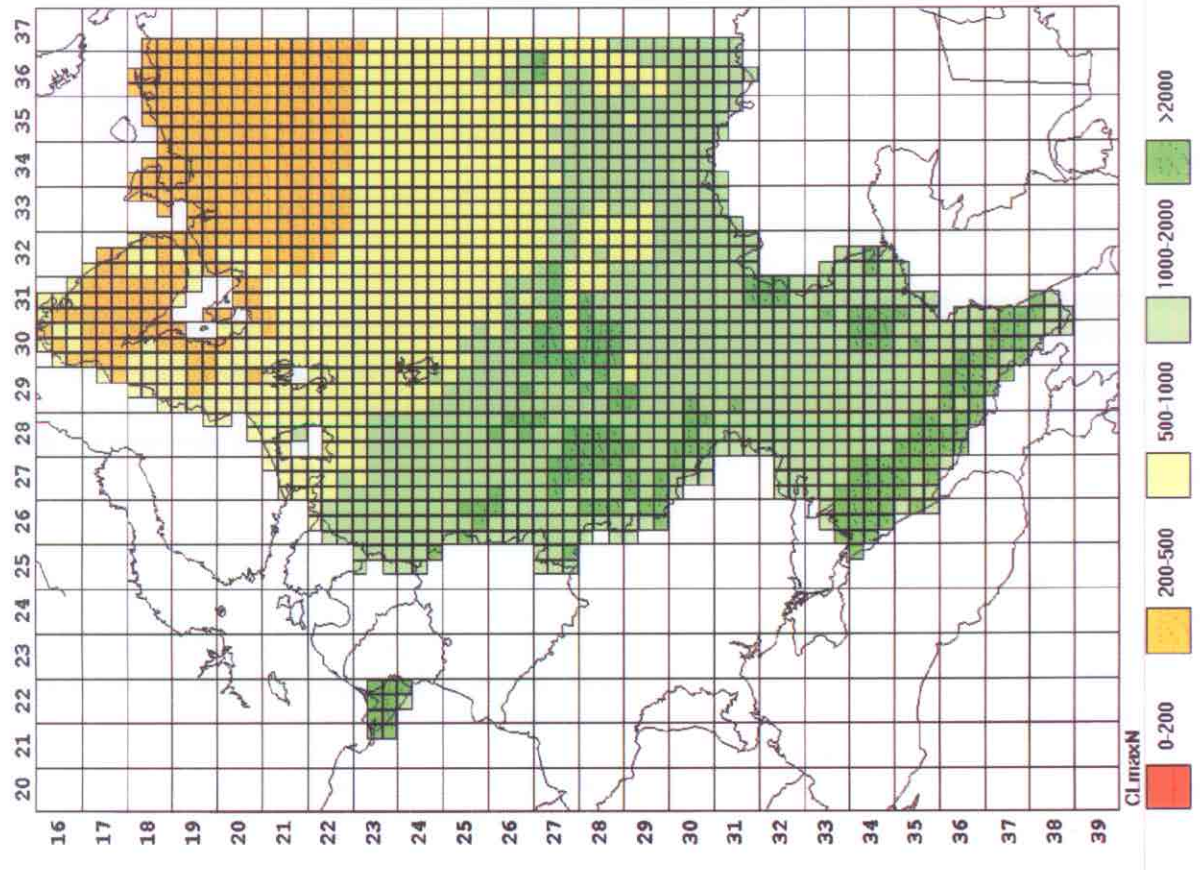

Figure RU-3. (left) Critical loads of maximum nitrogen for terrestrial ecosystems in the European part of Russia.
Figure RU-4. (right) Critical loads of nutrient nitrogen for terrestrial ecosystems in the European part of Russia.

SPAIN

National Focal Center/Contact
Angel Rascón Caballero
Ministerio de Medio Ambiente
Subdirección General de Calidad Ambiental
Pza. San Juan de la Cruz, s/n
Planta 4ª
E-28071 Madrid
tel: +34-1-597 6545
fax: +34-1-597 5857

Collaborating Institutions/Contacts
Isaura Rábago
Matilde Sousa
Thomas Schmid
CIEMAT
Avda. Complutense n° 22
E-28040 Madrid
tel: +34-1-346 6268
fax: +34-1-346 6121
email: isaura@ciemat.es

Cristina Rivero
UNESA
Francisco Gervás n° 3
E-28020 Madrid
tel: +34-1-567 4840
fax: +34-1-567 4982

Marisol Lorente
ASINEL
Carretera de Villaviciosa de Odón a Móstoles, km. 1,700
Apartado 233-28930 Móstoles (Madrid)
tel: +34-1-616 0018
fax: +34-1-616 2372
email: asin0004@tsai.es

Felipe Macías
Dept. Edafología
Facultad de Biología
Universidad de Santiago de Compostela
La Coruña
tel: +34-81-563100
fax: +34-81-596904
email: edfmac@uscmail.usc.es

Calculation Methods

A simple mass balance model has been applied to calculate the following critical loads for forest soils:

1. Critical loads of acidity
2. Maximum critical loads of sulfur
3. Minimum critical loads of nitrogen
4. Maximum critical loads of nitrogen
5. Critical loads of nutrient nitrogen

The grid used has a resolution of 5 x 5 km^2 covering all of Spain, totaling 3409 grid cells which contain forest soils.

The critical loads related to acidity ($CL_{max}(S)$, $CL_{min}(N)$ and $CL_{max}(N)$) and the critical load of nutrient nitrogen ($CL_{nut}(N)$), measured in eq ha^{-1} yr^{-1}, have been calculated as follows (Downing *et al.* 1993):

$$CL_{max}(S) = CL(A) + BC_{dep} - BC_{u}$$

$$CL_{min}(N) = N_{u} + N_{i}$$

$$CL_{max}(N) = N_{u} + N_{i} + CL_{max}(S) \,/\, (1 - f_{de})$$

f_{de} values have been related to the soil according to the method proposed by de Vries *et al.* (1993).

$$CL_{nut}(N) = N_{u} + N_{i} + N_{le(crit)} \,/\, (1 - f_{de})$$

Data Sources

The mapping and data management have been carried out using a geographic information system. A summary of the data sources is presented in Table ES-1.

Vegetation: Data have been obtained from the CORINE land cover data base (European Commission, 1985). This data base contains 64 different types of land cover from which seven have been selected and grouped as coniferous, deciduous and mixed forest.

Soils: The data for the dominant parent material have been obtained from the lithology map (Macías, *in press*) and the texture class from the FAO-UNESCO soil map (1981).

Table ES-1. Summary of data sources.

Data	Parameters	Sources
Soils	Parent material	Lithology Map (1995)
	Texture	FAO (1995)
	Weathering rate	Calculated
Forests	Cartography	CORINE
	Growth rate	Calculated (CORINE, ICONA)
	Nutrient uptake	Calculated
	Element content	de Vries *et al.* (1993)
Climatology	Precipitation	National Climatology Atlas (1992)
	Temperature	National Climatology Atlas (1992)
Hydrology	Evapotranspiration	Calculated (Turc Method)
	Runoff	Calculated
Nitrogen	N immobilization	Downing *et al.* (1993)
	Denitrification factor	de Vries *et al.* (1993)
	Critical uptake	Calculated
	Critical leaching	Calculated
Base Cation Deposition	Ca^{2+}, Mg^{2+}	Calculated from EMEP stations

Climatological data: Temperature and precipitation data have been obtained from the National Climatological Atlas (MOPT 1992).

Nutrient uptake: Base cation and nitrogen uptake have been calculated considering the growth rate and the element contents according to de Vries *et al.* (1993). Forest growth estimates are based on the National Forest Inventory (Instituto para la Conservación de la Naturaleza), which presents the annual biomass increment for each type of forest in the different Spanish provinces.

The combination of this data with the seven CORINE classes allows a growth rate value to be assigned to each type of forest. The forest biomass increment has been obtained from the First National Forest Inventory (1965–1974, for 14 provinces), the Second National Forest Inventory (1986–1995, for 31 provinces) and the Forest Inventory for the Basque Country (1988, 3 provinces).

Base cation uptake has been determined as the minimum of the nutrient-limited uptake and the uptake estimated from growth data according to Posch *et al.* (1995).

Nitrogen uptake has been calculated depending on the base cation uptake. In the first case, if the minimum base cation level depends on the availability of the base cations in soil solution, nitrogen uptake has been estimated as:

$$N_u^{(n)} = \frac{BC_u^{(n)}}{x_{BC:N}}$$

where $x_{BC:N}$ = the base cation to nitrogen ratio for the vegetation type. The $x_{BC:N}$ value for the various ecosystems has been extracted from Downing *et al.* (1993). In the second case, the minimum base cation uptake has been estimated depending on the growth rate (gr):

$$N_u^{(g)} = gr \cdot ctN$$

where ctN = nitrogen content in the vegetation (in eq ha^{-1} yr^{-1}). The data on the nitrogen content in trees have been extracted from de Vries *et al.* (1993) for coniferous and deciduous forests.

Weathering rate: The weathering rate for forest soils is based on the dominant parent material and the texture class (de Vries *et al.* 1993). The dominant parent material is obtained from the lithology map of Spain and the texture class is taken from the FAO soil map for Europe.

The lithology map of Spain contains fourteen substrate classes which were grouped into the five main classes described in the methodology according to Hettelingh and de Vries (1991). Acidic rocks cover some 17%, intermediate rocks 14%, basic rocks 1% and ultrabasic rocks 67%. The remaining area consists of water surfaces.

The texture classes defined in the FAO soil map for Europe have been converted as proposed by Hettelingh and de Vries (1991). Furthermore, the proposed conversion between parent material class, texture class and weathering rate is according to de Vries *et al.* (1993).

The proposed weathering rates have therefore been corrected incorporating the effect of temperature (Sverdrup, 1990). The value for the weathering rate has been calculated assuming a standard soil depth for forests of 0.5 m. The relative distribution of the weathering rates for forest ecosystems is concentrated within certain weathering rate classes, as shown below.

Weathering Rate Range (eq ha^{-1} yr^{-1})	Frequency (%)
0–250	0.09
250–500	0.50
500–750	18.72
750–1000	16.69
1000–1250	2.20
1250–1500	0.18
1500–1750	0.18
1750–2000	0.09
10,000	61.35

Precipitation surplus: Has been calculated as the precipitation minus the actual evapotranspiration:

$$Q = P - ETa$$

where *ETa* has been estimated according to the Turc method.

Base cation deposition: Total base cation deposition is determined according to the assumption that the chloride neutralizes potassium and sodium deposition (de Vries *et al.* 1993). Therefore the total deposition accounts for the calcium and magnesium. Wet deposition of calcium and magnesium has been calculated using the average of the mean annual values (1989–1992) from existing EMEP stations in Spain and neighboring countries. Grid values have been derived by interpolating the EMEP station data. To obtain total deposition, wet deposition values have been corrected with a dry deposition factor according to the type of vegetation. All calculations have been done according to de Vries *et al.* (1993).

Comments and Conclusions

The maps of critical loads are shown in Figures ES-1 through ES-4, and the frequency distribution of the values is shown in Table ES-2.

Table ES-2. Distribution of critical load values in Spain (in percent).

eq ha^{-1} yr^{-1}	$CL(A)$	$CL_{max}(S)$	$CL_{min}(N)$	$CL_{max}(N)$	$CL_{nut}(N)$
<200	0.00	0.00	0.00	0.00	0.00
200–500	0.00	0.18	73.34	0.00	57.32
500–1000	0.06	0.23	25.23	0.00	32.06
1000–2000	1.47	1.03	1.32	0.03	10.03
> 2000	98.47	98.56	0.12	99.97	0.56

References

de Vries, W., M. Posch, G.J. Reinds and J. Kämäri, 1993. Critical loads and their exceedance on forest soils in Europe. Report 58, DLO. The Winand Staring Center, Wageningen, Netherlands.

Downing, R.J., J.-P. Hettelingh and P.A.M. de Smet (eds.), 1993. Calculation and Mapping of Critical Loads in Europe: CCE Status Report 1993. National Institute of Public Health and Environmental Protection Rep. No. 259101003, Bilthoven, Netherlands.

FAO-UNESCO, 1981. Soil Map of World, Vol V: Europe (1:5,000,000). UNESCO, Paris, France.

Hettelingh, J.P. and W. de Vries, 1991. Mapping Vademecum. RIVM, Bilthoven, Netherlands.

Macías, F., 1997. Departamento de Edafología, Facultad de Biología, Universidad de Santiago de Compostela, La Coruña, España, In Press.

MOPT, Ministerio de Obras Públicas y Transportes, Dirección General del Instituto Geográfico Nacional. Atlas Nacional de España. Sección II. Grupo 9. Climatología. 1992.

Posch, M., P.A.M. de Smet, J.-P. Hettelingh and R.J. Downing (eds.), 1995. Calculation and Mapping of Critical Thresholds in Europe: CCE Status Report 1995. National Institute of Public Health and the Environment Rep. 259101004, Bilthoven, Netherlands.

Rivero, C., I. Rábago, M. Sousa, M. Lorente and T. Schmid, 1996. Cálculo y cartografía de cargas críticas para España. Aplicación del modelo SMB. Colección Documentos CIEMAT.

Sverdrup, H., 1990. The kinetics of base cation release due to chemical weathering. Lund University Press.

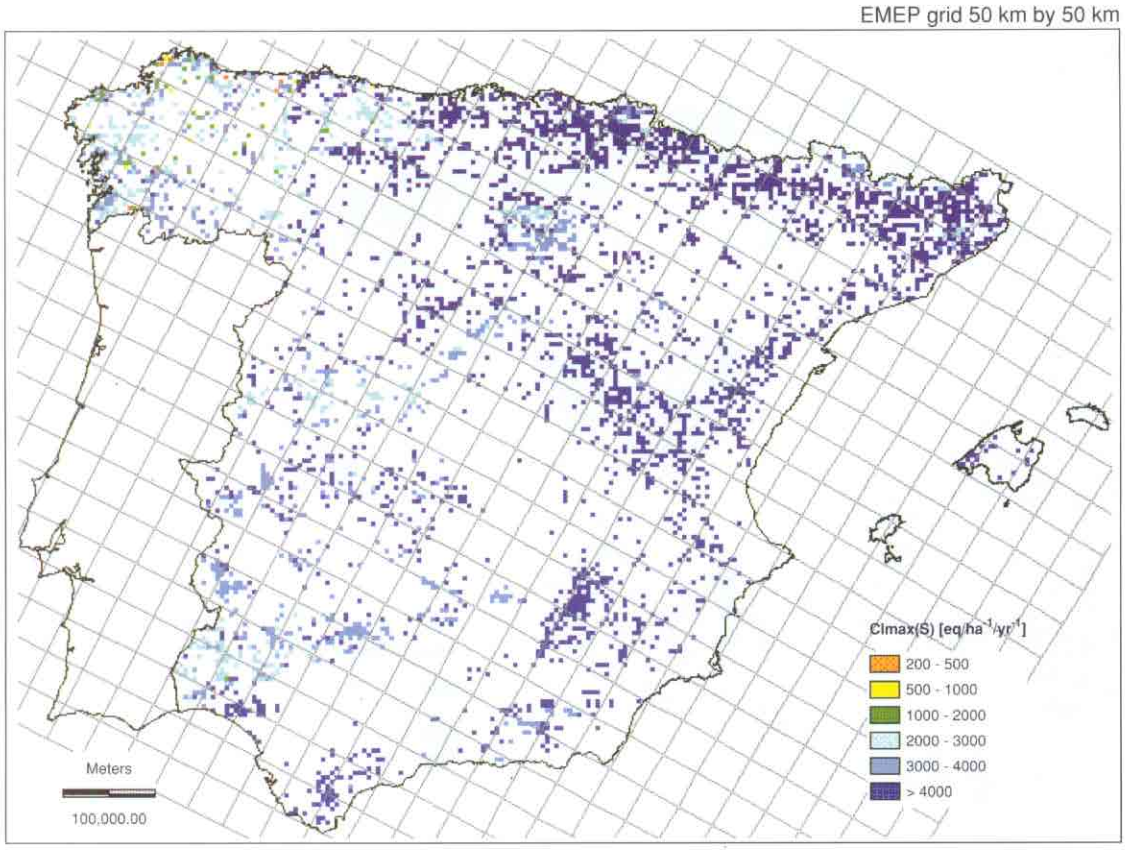

Figure ES-1. Maximum critical loads of sulfur for forest ecosystems.

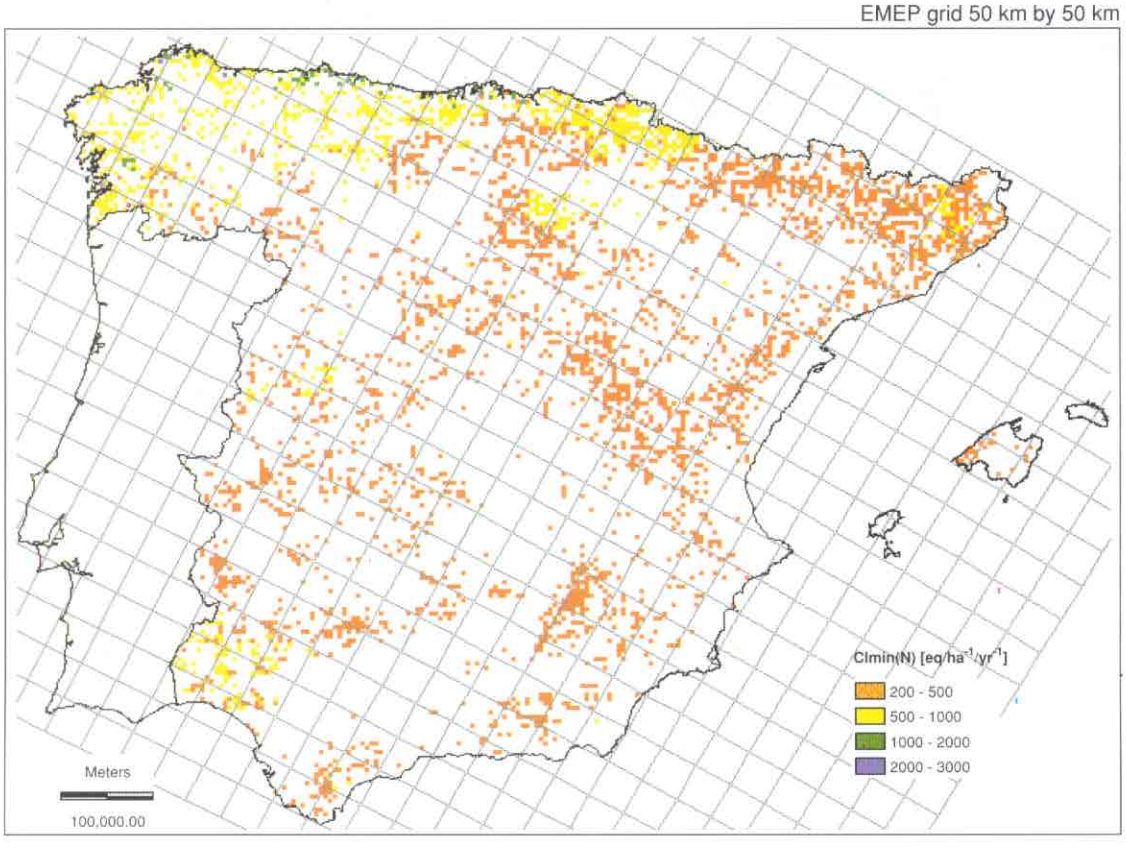

Figure ES-2. Minimum critical loads of nitrogen for forest ecosystems.

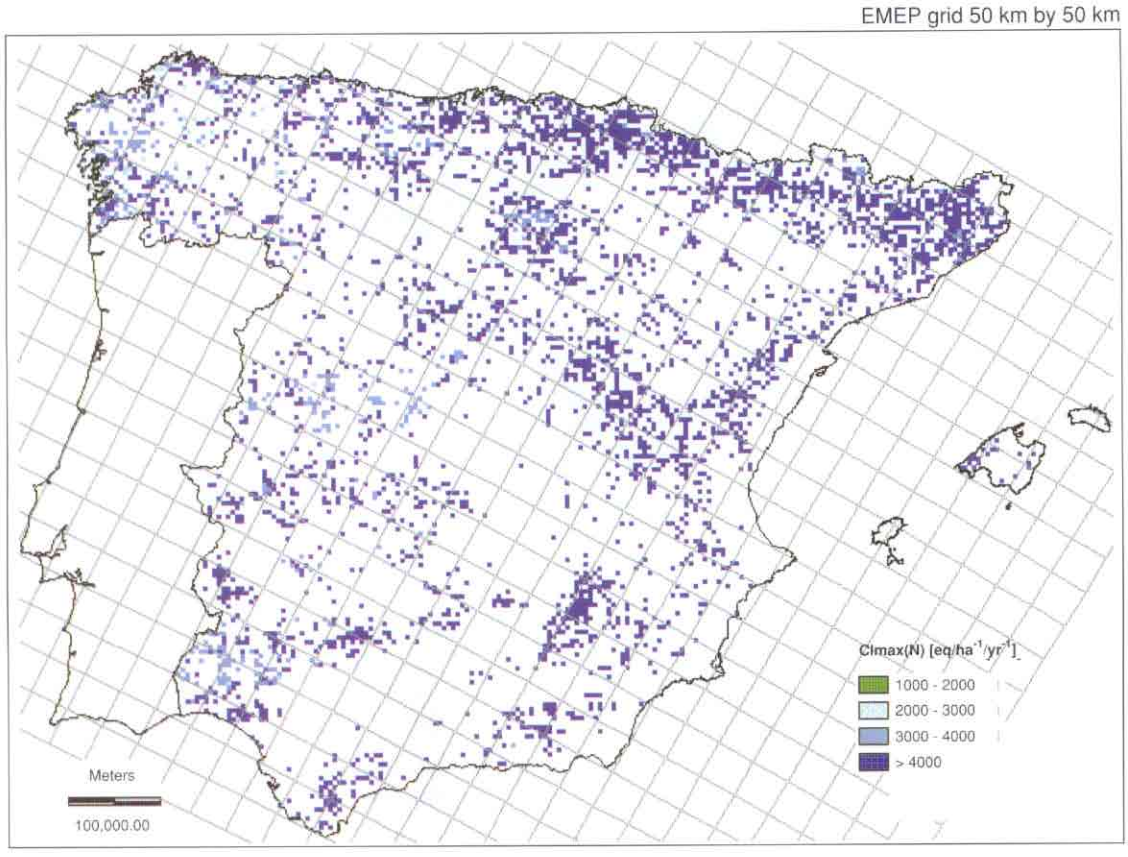

Figure ES-3. Maximum critical loads of nitrogen for forest ecosystems.

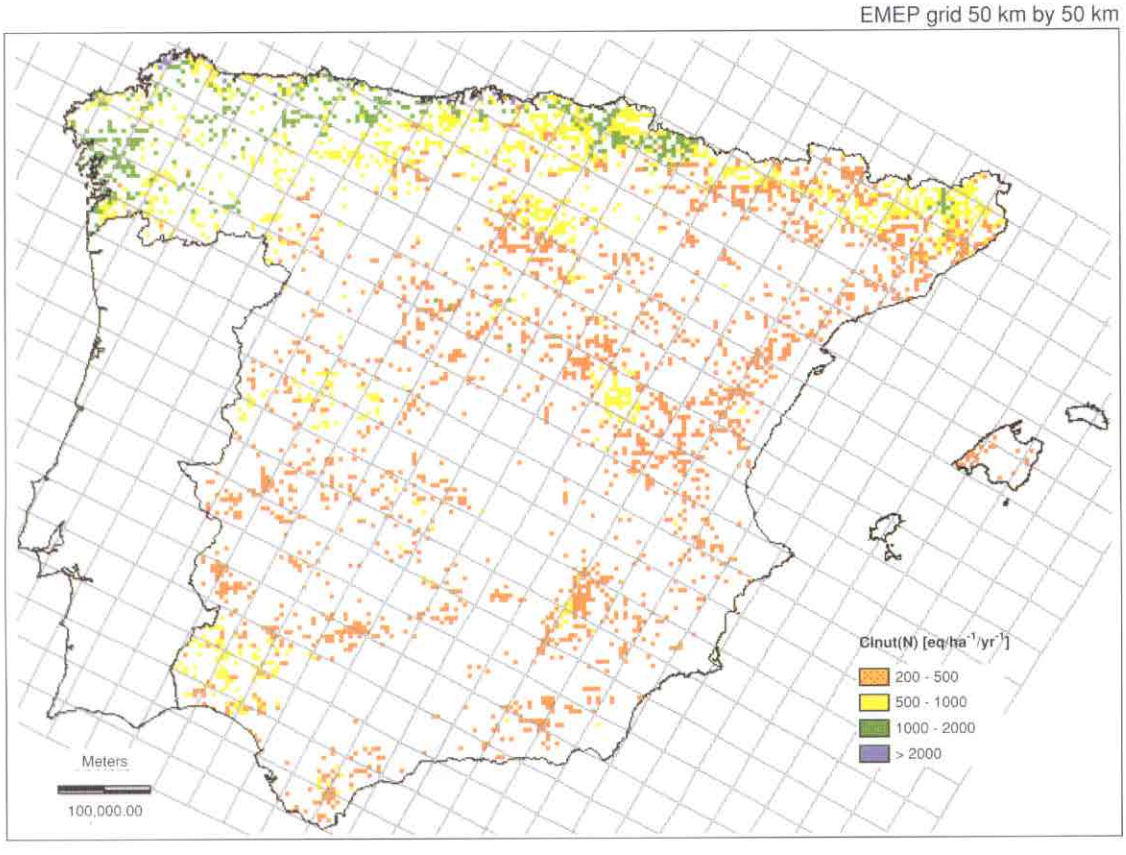

Figure ES-4. Critical loads of nutrient nitrogen for forest ecosystems.

SWEDEN

National Focal Center/Contact
Håkan Staaf
Swedish Environmental Protection Agency
S-106 48 Stockholm
tel: +46-8-698 1442
fax: + 46-8-698 1664
email: hakan.staaf@environ.se

Collaborating Institutions/Contacts
Harald Sverdrup
Department of Chemical Engineering
University of Lund
P.O. Box 124
S-22101 Lund
tel: +46-46-108274
fax: + 46-46-146030
email: harald.sverdrup@chemeng.lth.se

Kevin Bishop
Lars Rapp
Swedish University of Agricultural Sciences
Department of Forest Ecology
S-901 83 Umeå
tel: +46-90-166625
fax: +46-90-167750
email: kevin.bishop@sek.slu.se; lars.rapp@sek.slu.se

Gun Lövblad
Swedish Environmental Research Institute
P.O. Box 47 086
S-40258 Göteborg
tel: +46-31-460080
fax: +46-31-482180
email: gun.lovblad@ivl.se

Calculation Methods

Deposition: Wet deposition of sulfur and nitrogen was estimated using data from the national precipitation network. Dry deposition was calculated from air chemistry concentration fields obtained from the air chemistry network, multiplied by dry deposition velocities. These velocities were derived from throughfall data for sulfur and from the literature for nitrogen. Base cation deposition was estimated as total deposition. Data on sodium and chloride was derived from throughfall measurements. For the other base cations, data were taken from wet deposition measurements using the same ratio between throughfall and wet depositon as for sodium and/or chloride. Deposition was mapped to different types of ecosystems: Norway spruce forest, Scots pine/deciduous forest and open land/lakes. Land-use-weighted deposition was calculated for EMEP50 grids, added to the 150 × 150 km^2 EMEP grid level and compared with the deposition calculated by the EMEP model.

Critical loads of acidity, sulfur and acidifying nitrogen for forest ecosystems: were calculated using the Steady-state Mass Balance approach implemented in the PROFILE model, which allows for an iterative consideration of feedback between soil processes and soil chemistry. The soil profile is divided into four layers using input data for the thickness of each soil layer (O, A/E, B, C). A critical base cation to Al molar ratio of one (1) in the soil solution was used as the chemical criterion in each soil horizon, and used to determine the critical ANC leaching. The PROFILE model contains the following chemical subsystems: deposition, leaching, accumulation of dissolved chemical components, weathering kinetics, adsoption/desorption of inorganic nitrogen and base cations, nitrification, denitrification, canopy exchange, litterfall, immobilization and N mineralization.

Chemical feedback on weathering, uptake, nitrification and denitrification is included in the model, as are soil solution equlibrium reactions involving the carbonate system as well as speciation and complexing of Al and organic acids.

Critical loads of sulfur and acidifying nitrogen for freshwater ecosystems: were calculated using the First-order Acidity Balance (FAB) model as described in Henriksen *et al.* (1993) and Posch (1995). The net base cation leaching was computed using a variable ANC_{limit} according to Henriksen *et al.* (1995). All the catchment-specific parameters were selected according to Henriksen *et al.* (1993) and Posch (1995).

The critical load of nutrient nitrogen: for forest soils, $CL_{nut}(N)$, was calculated using the steady-state mass balance approach according to the equation:

$$CL(N) = N_u + N_i + N_{de} + N_{le(crit)}$$

The long-term uptake of N was calculated as the net uptake in forest biomass balanced by the supply of

base cations and phosphorus from weathering and deposition. This criterion is introduced to avoid long-term nutrient imbalances in forest trees. The supply of different cations from weathering was calculated using the PROFILE model.

N immobilization was determined by a semi-empirical approach. Immobilization + leaching is assumed to be linearly related to N deposition, and was set to a maximum of 12 kg N ha^{-1} yr^{-1} and a mean of 8 kg N ha^{-1} yr^{-1} for southern Sweden at present deposition levels. These values are based on results from N mass balance studies performed in a range of Swedish coniferous forests. For pre-industrial conditions, a long-term immobilization + leaching rate of 0.5–1.5 kg N ha^{-1} yr^{-1} was used. This level was derived from chronosequence studies of Swedish forest soil (Rosén *et al.* 1992). The immobilization rate for each site was then scaled down from present levels to the one pertaining at critical N deposition using an iterative procedure. Denitrification was calculated using the Sverdrup-Ineson equation as given in the UN/ECE mapping manual (UBA 1996).

Mapping: When calculating protection isolines for a grid cell, forest and lake ecosystems were given equal weight, i.e. the weight assigned to each lake or forest site measured within a grid cell was adjusted so that the total weight of lake ecosystems was equal to that of forest ecosystems in that grid cell. This was done by assigning each lake a weight (km^2) equal to half the cell ecosystem area divided by the number of lakes in that cell. For the forest sites, the weights based on the Swedish Forest Inventory were rescaled up to half the cell ecosystem area. To account for cell areas not at risk from acid deposition, 10% of each cell area was subtracted when calculating the cell ecosystem area.

Data sources

Deposition: Data used to calculate deposition of sulfur, nitrogen and base cations include:

- Wet deposition monitoring data from the national monitoring network from 30 stations for precipitation chemistry and 700 stations for precipitation amount.
- Throughfall monitoring data from regional forests surveys from approximately 100 sites.
- Air concentrations from six EMEP air chemistry stations in Sweden.
- Air concentrations from approximately 30 sites with passive sampling of SO_2 and NO_2.
- Land use data from the Swedish University of Agricultural Sciences.

Forest soils: The forest soil data used is based on samplings made within the Swedish Forest Inventory between 1983-1987 (Kempe *et al.* 1992). This inventory consists of a network of stations evenly spread over Sweden. Soil samples down to ca. 60 cm depth were collected at 1804 sites. Absolute soil mineralogy for 124 sites was measured by the Swedish Geological Survey in Uppsala, and 15 samples by the Czech Geological Survey, Prague. Total element analyses was determined for all 1804 sites, using wet chemistry methods for Ca, Mg, Na, K, Al, Si, Fe, Ti and trace elements. The UPPSALA model was then used to reconstruct mineralogy from total analyses (Sverdrup and Warfvinge 1995). The calculations were checked by calculating the amount of quartz in the soil samples and adding all components, accepting all samples where the estimated total content fell within 95–110%.

Texture was measured by granulometry and BET/adsorption analysis on subsamples from 124 sites. The texture for all 1804 sites were then read from an empirically derived relationship between field classification of soil texture and laboratory measurements.

Forest growth, soil type and moisture class were measured on all forest sites. The long-term net uptake was calculated from measurements of base cations and nitrogen concentrations in stem and branches combined with estimates of production over a the life span of a tree.

Several other parameters such as CO_2 pressure, dissolved organic carbon (DOC), evaporation, gibbsite coefficients and distribution of uptake were entered as standard values taken from the literature. These parameters generally stayed constant between runs and sites. Annual average air temperature, precipitation and runoff were taken from the official statistics of the Swedish Meteorological Institute (SMHI).

Freshwaters: Water chemistry data for 3174 unlimed lakes were taken from the 1990 Swedish Lake Survey. A long- term average (1961–90) of runoff data from the Swedish Meterological Institute (SMHI) was used. Land use data were based on the

Swedish Forest Inventory, 1983–92. The long-term average of nutrient uptake was derived as for forest soils.

Comments and Conclusions

Mapping of ozone exposure over Nordic countries has been performed in cooperation between Denmark, Norway, Finland and Sweden (Lövblad *et al.* 1996). Nordic maps of AOT40 for crops and forest trees, made in accordance with the procedure recommended by the Bern workshop, were presented in the 1995 CCE Status Report (Posch *et al.* 1995). No update of ozone exposure maps for Sweden has been performed since then.

Different methods for estimating surface water critcal loads have been tested against paleolimnological data on pre-industrial lake chemistry for 58 lakes in northern Sweden, and a smaller set of lakes in southern Sweden. The comparisons showed that the F-factor model, augmented by an organic acid subroutine, predicted pH values well in northern Sweden when the pre-industrial pH was above pH 6.5, but less well at lower pH's, and in lakes from southern Sweden. Predictions of surface water critical load values using the PROFILE model were dependent on the estimates of catchment soil depths and flow pathways.

References

Henriksen, A., M. Forsius, J. Kämäri, M. Posch and A. Wilander, 1993. Exceedance of Critical Loads for lakes in Finland, Norway and Sweden: Norwegian Institute for Water Research, REPORT 32/1993.

Henriksen, A., M. Posch, H. Hultberg and L. Lien , 1995. Critical loads of acidity for surface waters: Can the ANC_{limit} be considered variable? *Water Air Soil Pollut.* 85:3419-2424.

Kempe *et al.* 1992. The Swedish National Forest Inventory. Swedish Univ. Agricultural Sciences, Umeå. Dept. of Forest Survey. Report 51.

Lövblad, G. *et al.*, 1996. Ozone exposure mapping in the Nordic Countries. Nordic Council of Ministers. TemaNord 1996:528.

Posch, M., 1995. Critical Loads for Aquatic Ecosystems. *In*: Hornung, M., M.A. Sutton and R.B. Wilson (eds.), 1995. Mapping and modelling of critical loads for nitrogen: Proceedings of the Grange-Over-Sands Workshop. Institute of Terrestrial Ecology (UK), 207 pp.

Posch, M., P.A.M. de Smet, J.-P. Hettelingh and R.J. Downing (eds.), 1995. Calculation and Mapping of Critical Thresholds in Europe: CCE Status Report 1995. National Institute of Public Health and the Environment Rep. 259101004, Bilthoven, Netherlands.

Rosén, K. *et al.*, 1992. Nitrogen enrichment of Nordic forest ecosystems. *Ambio* 21: 364-368.

Sverdrup. H. and P. Warfvinge, 1995. Critical loads of acidity for Swedish forest soils. *Ecol. Bull.* 44:75-89.

UBA, 1996. Manual on Methodologies and Criteria for Mapping Critical Levels/Loads and geographical areas where they are exceeded. UN/ECE Convention on Long-range Transboundary Air Pollution. Federal Environmental Agency (Umweltbundesamt), Texte 71/96, Berlin.

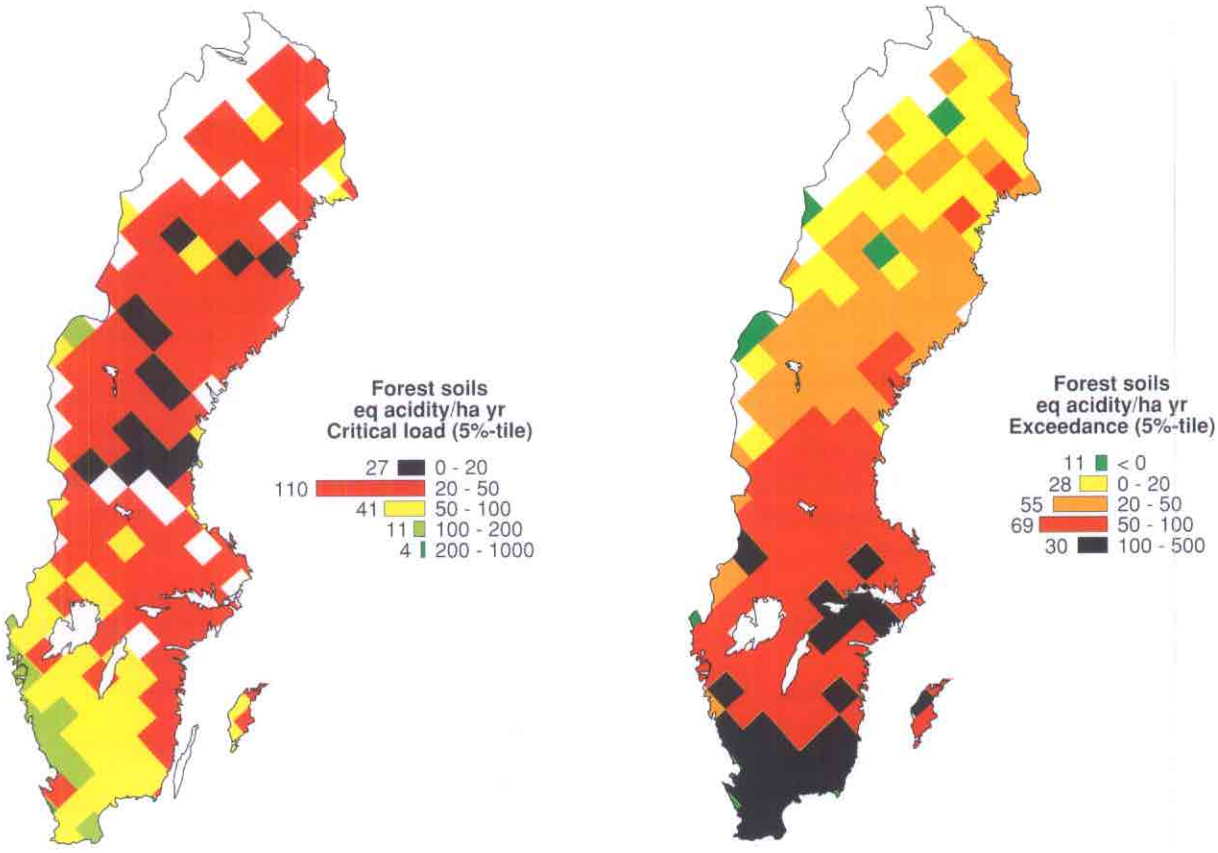

Figure SE-1. 5-percentile critical load of acidity (left) and exceedances (right) for forest ecosystems.

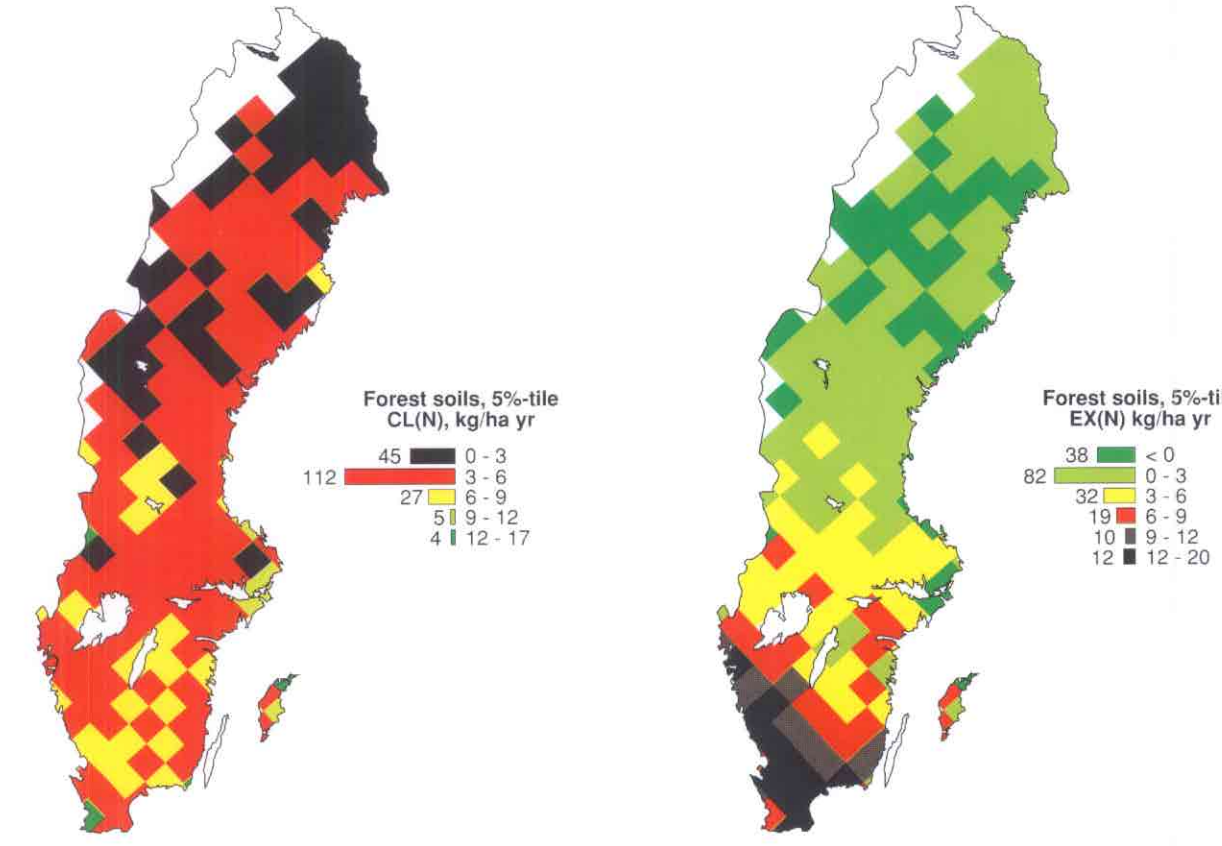

Figure SE-2. 5-percentile critical load of nutrient nitrogen (left) and exceedances (right) for forest ecosystems.

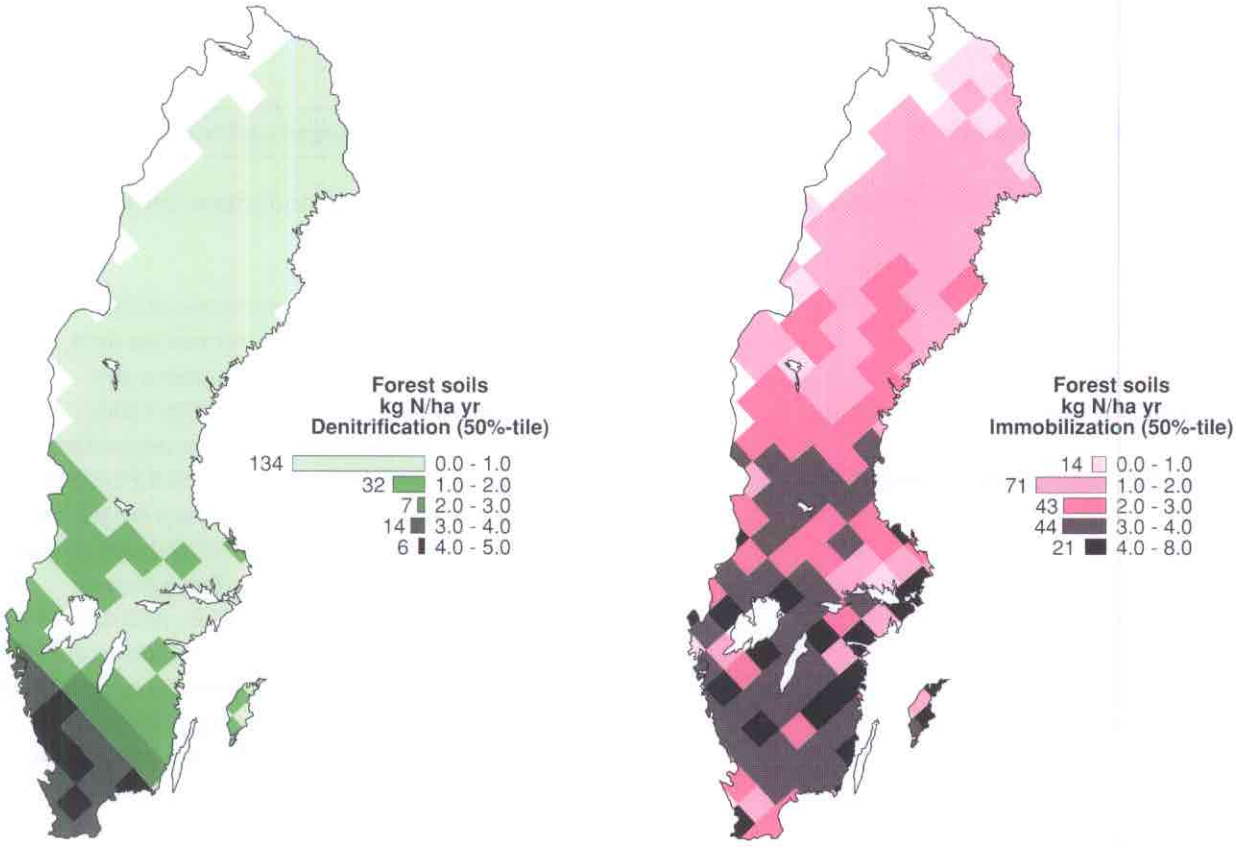

Figure SE-3. 50-percentile values for denitrification (left) and nitrogen immobilization (right) for forest soils.

SWITZERLAND

National Focal Center/Contact
Beat Achermann
Federal Office of Environment, Forests and Landscape (FOEFL)
Air Pollution Control Division
CH - 3003 Bern
tel: +41-31-322 9978
fax: +41-31-324 0137
email: beat.achermann@buwal.admin.ch

Collaborating Institutions/Contacts
Beat Rihm
Meteotest
Fabrikstrasse 14
CH - 3012 Bern
tel: +41-31-307 2626
fax: +41-31-307 2610
email: rihm@meteotest.ch

Critical Loads of Acidity

Receptors: Forest soils and sensitive alpine lakes.
Method: Steady-state mass balance (SMB), ca. 12,300 points.
Remarks: $CL_{min}(N)$ for alpine lake catchments, which are mainly covered by grassland, has been set to 3 kg N ha^{-1} yr^{-1} (instead of 2) in order to take into account N_i and N_u. National data have been submitted for all EMEP cells that are (at least) partially covered by Switzerland.
Reference: FOEFL (1994).

Critical Loads of Nutrient Nitrogen

Receptors: Forests and (semi-)natural ecosystems.
Methods: SMB for forests (ca. 11,000 points), empirical method for natural and semi-natural ecosystems (ca. 14,000 points).
Remarks: For the Swiss input to the European map, the results of the SMB and the empirical method were merged by choosing the lowest value on an individual grid cell basis (1 × 1 km^2 grid). National data have been submitted for all EMEP cells (partially) covered by Switzerland.
Reference: FOEFL (1996).

Present Loads of Nitrogen and Sulfur

Receptors: Forest, grassland, crops, settlements, lakes, rocks/glaciers.
Resolution: 1 × 1 km^2 grid.
Pollutants: Nutrient N compounds, sulfur
Methods: Concentration and deposition data, dispersion models, resistance analogue dry deposition models and spatial interpolation.
References: The sulfur and nitrogen deposition for the period 1986–90 is described in FOEFL (1994). An updated nitrogen deposition map for the period 1993–95 can be found in FOEFL (1996). An intensive monitoring exercise, including deposition of ammonia and other N components, was carried out at a nature reserve site in the Swiss Plateau (BUWAL 1994a). Several cantonal authorities have permanent or temporary monitoring sites, e.g. Ticino (wet deposition) and Zurich (wet and dry deposition, Krieg *et al.* 1996). The national network NABEL measures the wet deposition at two sites.

Critical Levels of Ozone and Their Exceedances

Definitions: The critical levels for the following receptors were considered: agricultural crops, forests and humans (health). The critical level for **crops** is expressed as Accumulated exposure Over a Threshold (AOT) of 40 ppb, calculated for daylight hours during a 3-month period ($AOT40_c$). In general, the period from May to July is used. The critical value was set at 3000 ppb·h (=3 ppm·h) at the Kuopio Workshop (see Kärenlampi and Skärby 1996, UBA 1996).

The critical level for **forests** is expressed as an AOT of 40 ppb, calculated for daylight hours from April to September ($AOT40_f$). The critical value is 10 ppm·h (see Kärenlampi and Skärby 1996, UBA 1996).

A **health**-related critical level was discussed at the UN/ECE-WHO workshop held at Eastbourne in June 1996 (UN/ECE-WHO 1997). It is based on the redefined WHO Air Quality Guideline for Europe (WHO 1996). WHO recommends an 8-hour mean ozone concentration of 120 μg m^3 (ca. 60 ppb). Thus, the critical level can be expressed as the number of moving non-overlapping 8-hour means exceeding 60 ppb (*N8h60*), with a critical value of 0.
A surrogate health parameter to be used for

integrated assessment modelling is $AOT60_h$, which is the AOT of 60 ppb, calculated for daylight hours from April to September. $AOT60_h$ can be modelled by EMEP (Simpson 1997) and is a good indicator for exceedances of the N8h60 critical level (Achermann *et al.* 1997).

General Mapping Procedure: The general procedure used for mapping present levels of ozone in Switzerland is given below (according to Künzle and Rihm 1996). The procedure is a spatial interpolation of ozone indices ($AOT40_c$, $AOT40_f$ and *N8h60*) computed from monitored data. The raw data are first checked for plausibility, as they come from different institutes and authorities. Because the AOT40 is an accumuated dose, missing hourly means must be supplied. This can be done by deriving the missing data from other nearby monitoring stations, or by calculating from the existing values of the same station, under the assumption that the missing and the existing values have the same frequency distribution.

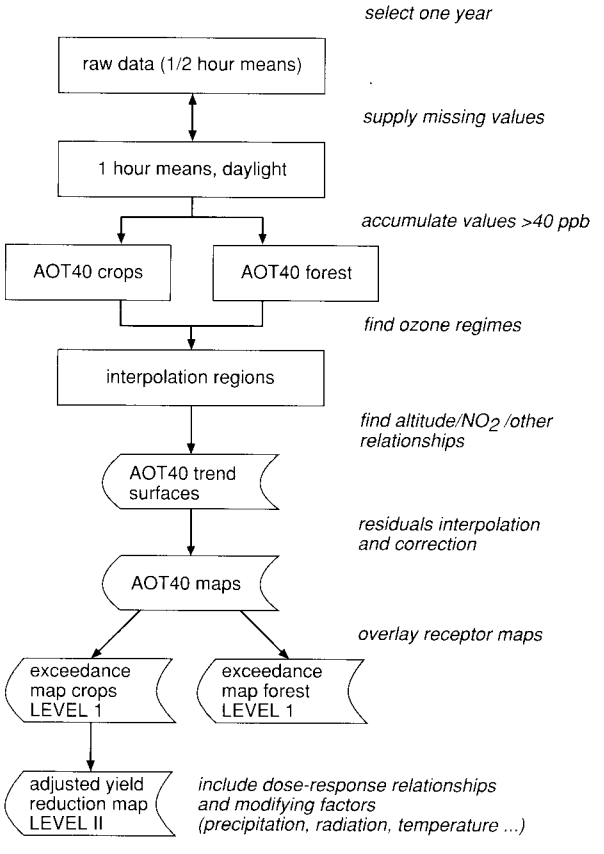

After those preparations it is easy to calculate the AOT40 for crops and forests, as well as the health-related N8h60. For the definition of the daylight hours it is best to use monitored values of global solar radiation (>50 W m^{-2}).

For the spatial interpolation of AOT40 and N8h60 values, it must be decided whether data from all monitoring stations can be used at the same time or if the study area must be divided into subregions, which have a more or less homogeneous ozone regime. The following criteria might be used to delimit such interpolation regions: topographic elements, climatic conditions, or the distribution of emitters of NO_x and VOC.

Within each subregion, monitored AOT40 and N8h60 values are correlated with altitude, NO_2 levels or other environmental parameters that can explain the spatial distribution of ozone and are available at an adequate spatial resolution for the whole study area. If it is possible to find satisfying relationships, a trend surface of the ozone values can be calculated as a function of those explanatory parameters. We suggest setting lower and upper limits to the results of those functions in order to avoid interpolated ozone values that are outside the range of monitored values. Of course, this procedure is not practicable if the number of monitoring stations per subregion is too small, nor is it applicable for peak values of ozone (at least in Switzerland).

The residuals for each monitoring station are calculated as the difference between the monitored value and the value of the trend surface at that location. They are then spatially interpolated by methods such as kriging or inverse-distance weighting. The resulting "residual surface" is then added to the trend surface; thus the final AOT40 and N8h60 maps also show spatial variations that are unrelated to the explanatory parameters, and match exactly the monitored values at the locations of the monitoring stations.

In the last stage of Level I mapping, the ozone maps are overlaid and intersected by a receptor map. The resulting maps may be called exceedance map for crops, exceedance map for forests, and population exposure map, respectively. This step is important if the receptors are not evenly distributed within the study area, e.g., in Switzerland forests are generally situated at higher altitudes and therefore have AOT40s that are above the average of the whole country.

Ozone levels in summer can vary enormously from one year to another. For exceedance mapping, the mean of the AOT40 over a period of 5 years should be used (see UBA 1996). Ozone maps for Switzerland have so far only been produced for single years.

Production of Ozone Maps for 1994: For the Swiss mapping exercise, monitored data from 1992, 1993 and 1994 are available from more than 80 monitoring stations, including 16 stations from the national monitoring network (NABEL), many cantonal stations, a few stations from research institutes and one Italian station. Half of those stations represent rural sites. This section describes the computation of ozone maps, based on monitoring data from 1994 only.

In order to supply missing values, some efforts were made to derive them from neighboring stations. However that method is time-consuming and complicated, as the monitoring results must be correlated to the results of several other stations in order to find a substitute station, which is not always possible. Therefore we applied the following method: first, raw AOT40 for forests and crops are calculated without the missing values, on a month by month basis. In a second step, the monthly AOT40 were updated as follows:

$$AOT40_m = RAOT40_m \cdot N_{tot,m} / (N_{tot,m} - N_{miss,m})$$

where:

$AOT40_m$ = corrected AOT40 for month m
$RAOT40_m$ = raw AOT40 (without missing values) for month m
$N_{tot,m}$ = total number of daylight hours for month m
$N_{miss,m}$ = number of missing hours for month m

Finally, $AOT40_c$ and $AOT40_f$ were calculated as the sum of the appropriate $AOT40_m$. For the calculation of *N8h60*, missing values were not supplemented.

For determining daylight hours (>50W m^{-2}) global radiation data were used from 15 stations of the national monitoring network (NABEL), which provides good cover for the various regions in Switzerland.

While looking for relationships between AOT40, N8h60 and the explanatory parameters, it became evident that it would be useful to divide Switzerland into several different interpolation regions. Four subregions were defined as follows:

1. *"North"*: This region includes the northern and western parts of Switzerland. The Jura mountains and the Alps mark the northern and southern boundaries of the area. In the eastern part of this region the topography is open.
2. *"Alps"*: This includes the alpine regions, and central and northeastern Switzerland. In this area, the ozone levels are generally lower than in the North region at sites with comparable topographic exposure. Those differences might arise from lower temperature and radiation in eastern Switzerland and from clouds that are formed mainly at altitudes between 1000 and 2000 meters in summer.
3. *"Valais"*: This region covers more or less the canton of Valais, and is is an inner-alpine valley with little cloud cover and high global radiation. The emissions of ozone precursors are relatively high compared to other valleys (e.g., the Engadin in the canton of Grisons).
4. *"Ticino"*: This region covers the canton of Ticino and the Italian-speaking valleys of the Grisons. The Alps form the northern boundaries of this area, while it is open to the south. Its regime is partially influenced by ozone that is formed over the Po lowlands (Milano) and transported northwards (BUWAL 1994b).

Within each interpolation region, relative height (H_{rel} in meters) and NO_2 concentration (in µg m^{-3}, annual mean) turn out to be the most evident explanatory parameters. H_{rel} is defined as the elevation above the lowest site within a radius of 5 km. In the Ticino region, AOT40 values also depend on latitude, i.e., they decrease from south to north. Latitude is in the range from 75,000 to 135,000 meters (national system). Several regression functions and parameter combinations were tested before finally selecting the following "trend surfaces" for forests (units in ppb·h):

- trend for North and Alps regions: ($R^2 = 0.56$)
  $AOT40_f = \min\{23440 + 3.90 \cdot H_{rel} - 332 \cdot [NO_2], 26100\}$
  26100 ppb·h is the highest value measured in these regions.
- trend for Valais region: ($R^2 = 0.61$)
  $AOT40_f = 17650 - 249 \cdot [NO_2]$
- trend for Ticino region: ($R^2 = 0.91$)
  $AOT40_f = \min\{95600 - 0.53 \cdot latitude - 403 \cdot [NO_2], 37800\}$
  37800 ppb·h is the highest value measured in this region.

There is a close linear relationship between $AOT40_f$ and $AOT40_c$ for monitoring data in 1994 (also in 1992 and 1993). Therefore the trend surface for crops can be calculated from the trend for forest according to the following regression ($R^2 = 0.98$):

$$AOT40_c = 0.643 \cdot AOT40_f$$

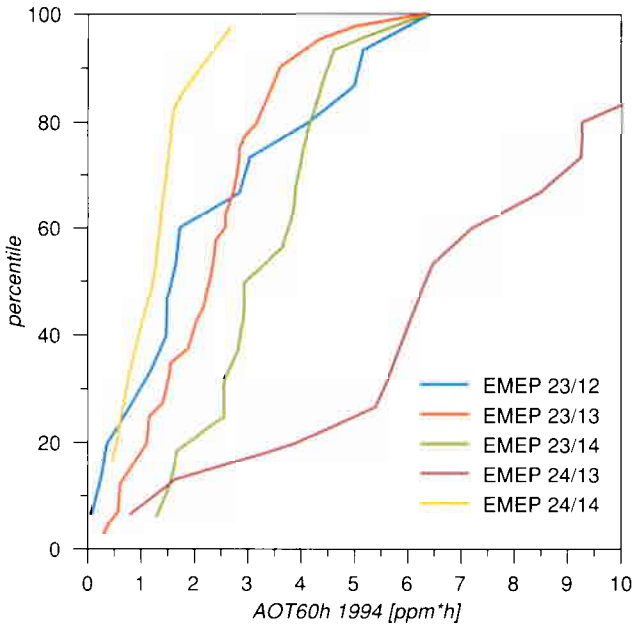

Figure CH-1. Cumulative frequency distributions for $AOT60_h$ values from 84 Swiss monitoring stations in 1994 for each EMEP grid cell.

For $AOT60_h$, no trend regression function could be found, as the spatial distribution of this parameter is very inhomogeneous, at least in 1994. Therefore $AOT60_h$ values are not presented as a map but as cumulative frequency distribution functions for each EMEP grid (Figure CH-1).

N8h60 has been mapped on the basis of a N1h60 map. The parameter *N1h60* is defined as the number of 1-hour mean values above 60 ppb (air quality standard of the Swiss Ordinance on Air Pollution Control). N8h60 can be derived from N1h60 by the following regression function ($R^2 = 0.98$):

$$N8h60 = \max\{0.159 \cdot N1h60 - 4\ ,\ 0\}$$

The trend surface for N1h60 is calculated as follows:

- trend for North region: ($R^2 = 0.75$)

$N1h60 = 525 + 0.429 \cdot H_{rel} - 8.8 \cdot [NO_2]$

- trend for Alps region: ($R^2 = 0.82$)

$N1h60 = 352 + 0.763 \cdot H_{rel} - 4.77 \cdot [NO_2]$

- trend for Valais region: ($R^2 = 0.77$)

$N1h60 = 436 - 9.99 \cdot [NO_2]$

- trend for Ticino region: ($R^2 = 0.66$)

$N1h60 = 1418 + 0.093 \cdot H_{rel} - 8.4 \cdot [NO_2] - 0.005 \cdot \text{latitude}$

The next step is the calculation and spatial interpolation of the residuals. The interpolation is made for all regions combined (in some cases this may not be the best solution) by applying an inverse-distance-weighting algorithm.

Results

Figures CH-2 and CH-3 show the maps for ozone AOT40 values in 1994 for forests and crops, respectively. The critical level of 10 ppm·h (forests) is exceeded in almost the entire country. The highest values (up to 35 ppm·h) occur in the Ticino region.

The critical level for crops (3 ppm·h) is exceeded in the whole country. It is important to note that this is Level I mapping, where it is not possible to indicate an exact amount of yield loss. The highest AOT40 values occur in the Valais and Ticino regions (18 ppm·h), but one station in the Jura region is also at that level. For crops, only monitoring stations below 1200m altitude are selected in interpolating residuals. The final maps of AOT40 for crops are cut off at 1200m, as there are very few crops above that altitude.

The map of the health-related parameter N8h60 (Figure CH-4) shows that in the center of larger cities the number of exceedances of the 8-hour mean of 60 ppb is relatively low, because the NO2 level is high. An assessment of the populationìs exposure to N8h60 has shown that about 50% of the Swiss population (3.4 million people) live in areas where more than 40 non-overlapping exceedances of the 8-hour mean of 60 ppb were recorded from April to September 1994 (Achermann *et al.* 1997).

First attempts to implement a Level II approach to assess realistically assess crop yield losses have already been made by Fuhrer (1995). The potential yield reduction is corrected by a factor taking into account the soil water availability during the growth period. The correction factor is calculated as a function of the mean temperature, the mean solar radiation and the precipitation sum in June and July of the specified year. The meteorological parameters needed to calculate the soil water availability are mapped on the basis of 64 monitoring stations of the Swiss Meteorological Institute. For the spatial interpolation, specific methods developed for Meteonorm (BEW 1995) have been applied. They include altitude dependencies for different climatic regions, as well as local temperature variations due to large lakes, exposition, etc.

Further Activities in Switzerland

This section describes some of the further studies on critical levels/loads, damage and risk assessment in Switzerland.

Critical loads of acidity for forests have been calculated for ca. 700 points with the regionalized PROFILE model. The results of the SMB and PROFILE were compared (FOEFL 1997a).

The dynamics of soil acidification were modelled at ca. 620 points using the regionalized SAFE model (FOEFL 1997b). A specific case study was carried out at the "Copera" forest site in southern Switzerland, using the dynamic model SAFE (Zysset *et al.* 1997).

Fertilizer experiments in plantations, together with field observations of Norway spruce and beech trees during a period of over ten years, indicate a high probability for an increase of nutrient imbalances, soil acidification, sensitivity to drought and disease as a result of excess N deposition (Flückiger *et al.* 1997).

As part of the NITREX program, the nitrogen budgets in two small catchments at the Alptal site are investigated. One of them is being fertilized (Schleppi and Bucher 1997). First results are available, and are in line with results of other NITREX sites in Europe.

A statistically significant relationship between stem growth reduction and ozone levels (AOT40) was found as a result of a multivariate analysis based on data of 60 beech observation plots in different areas of Switzerland, taking into account stand age, humus form, site fertility, relative forest cover, soil wetness, water regime, crown size, social position, altitude, exposition, inclination, ozone, deposition of acidity and nitrogen (Braun and Flückiger 1997). These growth reduction data suggest a slightly higher sensitivity of mature trees than of young trees in chamber experiments.

A multi-stress risk assessment, including critical loads of acidity, critical loads of nitrogen, critical levels for ozone and their exceedances, was performed for some alpine forest sites in the Reusstal region in the canton of Uri (BUWAL 1996).

References

Achermann B., B. Rihm and T. Künzle, 1997. Ozone: Mapping Exceedances of Air Quality Guidelines and Assessment of Population Exposure in Switzerland. *In*: UN/ECE-WHO 1997, *op. cit.*

Braun, S. and W. Flückiger, 1997. Epidemiological indication of ozone effects in mature beech (fagus sylvatica L.). Poster presented at the Fourth Internat. Symp. on Responses of Plant Metabolism to Air Pollution and Global Change, 1-5 April 1997, Egmond aan Zee, Netherlands.

BEW (ed.), 1995. METEONORM, Meteorologische Grundlagen für die Sonnenenergienutzung. Bundesamt für Energiewirtschaft, Bern. 186pp.

BUWAL (ed.), 1994a. Stickstoffeintrag aus der Luft in ein Naturschutzgebiet. Bundesamt für Umwelt, Wald und Landschaft, Umwelt-Materialien Nr. 28. Bern. 135pp.

BUWAL (ed.), 1994b. Sommersmog-Messflüge 1990 bis 1992. Bundesamt für Umwelt, Wald und Landschaft, Umwelt-Materialien Nr. 24. Bern. 138pp.

BUWAL (ed.), 1996. Belastungen des Gebirgswaldes, Ansätze einer Risikobeurteilung - Fallstudie im Urner Reusstal. Bundesamt für Umwelt, Wald und Landschaft, Umwelt-Materialien Nr. 59. Bern. 237pp.

Eidgenössische Forschungsanstalt für Wald, Schnee und Landschaft (ed.), 1997. Säure- und Stickstoffbelastungen - ein Risiko für den Schweizer Wald? Forum für Wissen 1997, 100 pp.

Flückiger W., S. Braun, and R. Quiring, 1997. Wieviel Stickstoff ertragen unsere Wälder? Untersuchungen über Wirkungszusammenhänge. *In*: Eidgenössische Forschungsanstalt für Wald, Schnee und Landschaft 1997, *op. cit.* pp. 59-72.

FOEFL (ed.), 1994. Critical Loads of Acidity for Forest Soils and Alpine Lakes - Steady State Mass Balance Method. Environmental Series No. 234, Federal Office of Environment, Forests and Landscape, Bern, 68 pp.

FOEFL (ed.), 1996. Critical Loads of Nitrogen and their Exceedances - Eutrophying Atmospheric Deposition. Environmental Series No. 275, Federal Office of Environment, Forests and Landscape, Bern, 74 pp.

FOEFL (ed.), 1997a. Critical Loads of acidity for forest soils - regionalized PROFILE model. Environmental Series Air, Federal Office of Environment, Forests and Landscape, Bern, in press.

FOEFL (ed.), 1997b. Regional Dynamic Assessment of Acidification of Swiss Forest Soils. Environmental Series Air, Federal Office of Environment, Forests and Landscape, Bern, in press.

Fuhrer, J., 1995. Critical levels for ozone to protect agricultural crops: interaction with water availability. *Water Air Soil Pollut.* 1355-1360.

Kärenlampi, L. and L. Skärby (eds.), 1996. Critical Levels for Ozone in Europe: Testing and Finalizing the Concepts. UN-ECE Workshop Report. Univ. of Kuopio, Dept. of Ecology and Environmental Science.

Krieg F., E. Peier E. and H. Müller, 1996. Depositionsuntersuchungen in Wallisellen und auf dem Bachtel, Resultate 1995. Im Auftrag des Amtes für technische Anlagen und Lufthygiene des Kantons Zürich, Forschungsstelle für Umweltbeobachtung, Egg.

Künzle T. and B. Rihm, 1996. Ozone Mapping in Alpine Regions - Experiences and Data Analysis Regarding Ozone Modelling by EMEP. *In*: Proceedings of EMEP Workshop on the Control of Photochemical Oxidants over Europe, St. Gall, Switzerland 24-27 Oct. 1995. Federal Office of Environment, Forests and Landscape. Environmental Documentation No. 47, Bern, 1996, pp. 89-96.

Schleppi, P. and J.B. Bucher, 1997. Kritische Stickstoffbelastung im Alptal (SZ) - Ergebnisse einer Fallstudie. *In*: Eidgenössische Forschungsanstalt für Wald, Schnee und Landschaft, 1997, *op. cit.* pp. 43-49.

Simpson, D., 1997. Modelled ozone concentrations in relation to health issues. *In*: WHO-UN/ECE, 1997, *op. cit.* pp. 53-55.

UBA, 1996. Manual on Methodologies and Criteria for Mapping Critical Levels/Loads and geographical areas where they are exceeded. UN/ECE Convention on Long-range Transboundary Air Pollution. Federal Environmental Agency (Umweltbundesamt), Texte 71/96, Berlin.

UN/ECE-WHO, 1997. Health Effects of Ozone and Nitrogen Oxides in an Integrated Assessment of Air Pollution. Proceedings of a UN/ECE-WHO Workshop, Eastbourne, UK, 11-12 June 1996. Institute for Environment and Health, Univ. Leicester, Special Report 3.

WHO, 1996. Update and Revision of the WHO Air Quality Guidelines for Europe, Volume 6, Classical Air Pollutants. Final consultation, Bilthoven, Netherlands, 28-31 October 1996. WHO Regional Office for Europe.

Zysset M., P. Blaser and J. Luster, 1997. Kritische Säurebelastung im Tessin - Ergebnisse einer Fallstudie am Standort Copera. *In*: Eidgenössische Forschungsanstalt für Wald, Schnee und Landschaft 1997, *op. cit.* pp. 37-42.

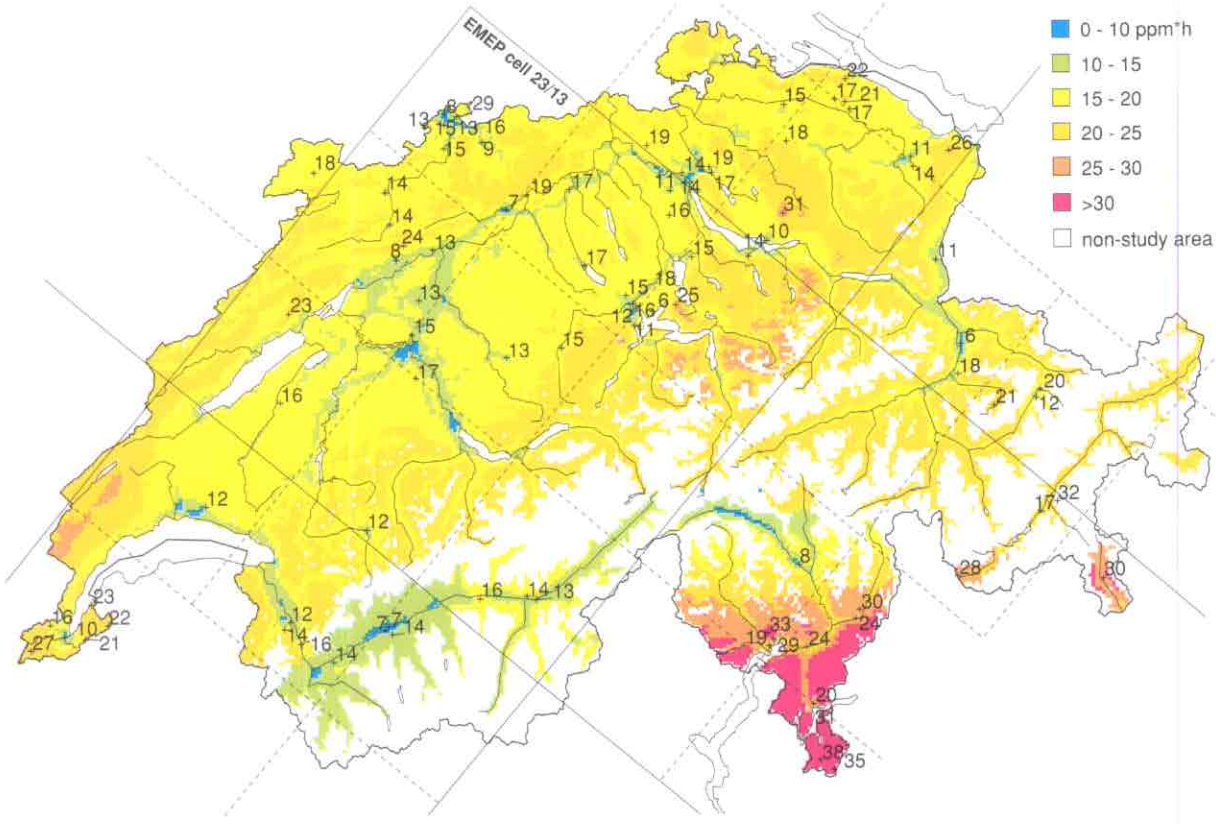

Figure CH-2. Interpolated ozone levels for forests in 1994: accumulated exposure over a threshold of 40ppb for daylight hours from April to September ($AOT40_f$). (The critical level is 10ppm·h; the study area is below 2000m altitude.)

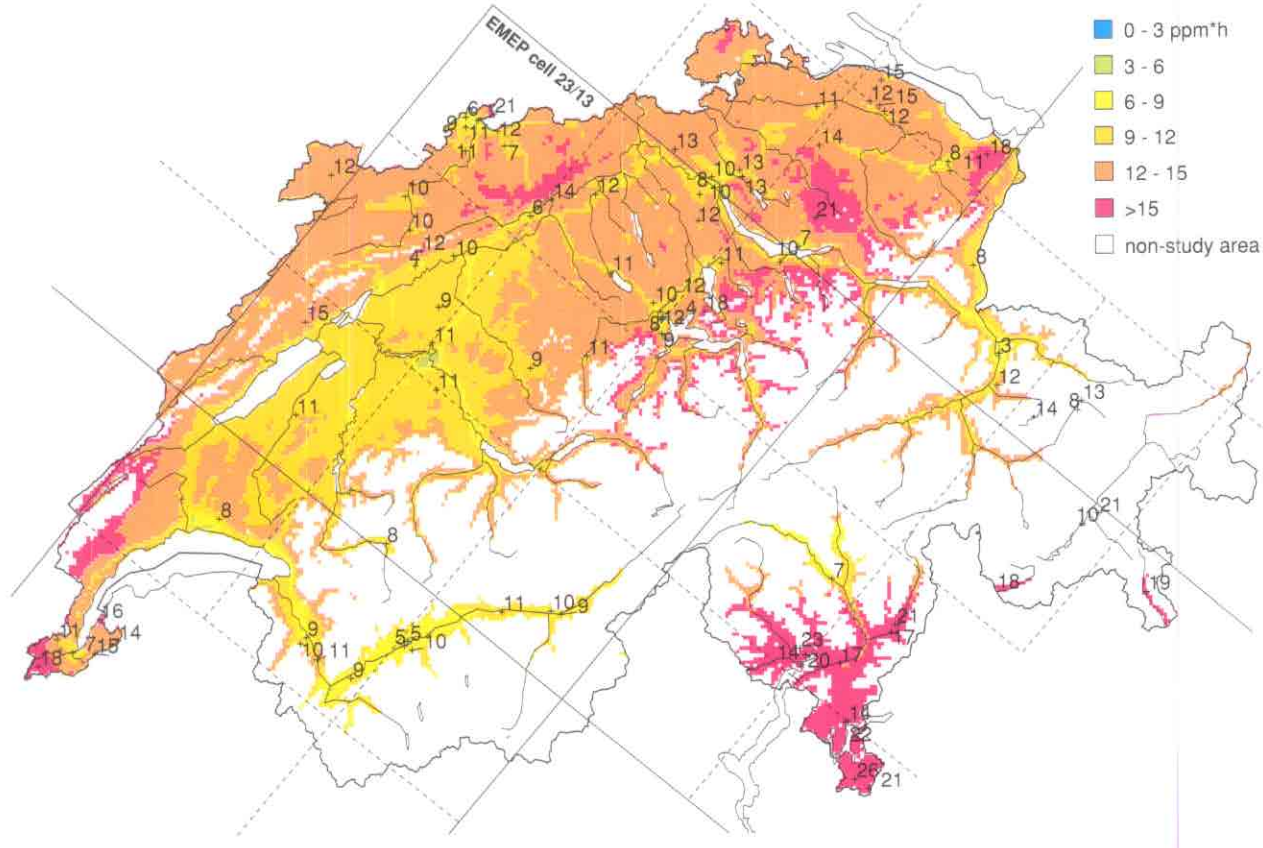

Figure CH-3. Interpolated ozone levels for crops in 1994: accumulated exposure over a threshold of 40ppb for daylight hours from May to July ($AOT40_c$). (The critical level is 3ppm·h; the study area is below 1200m altitude.)

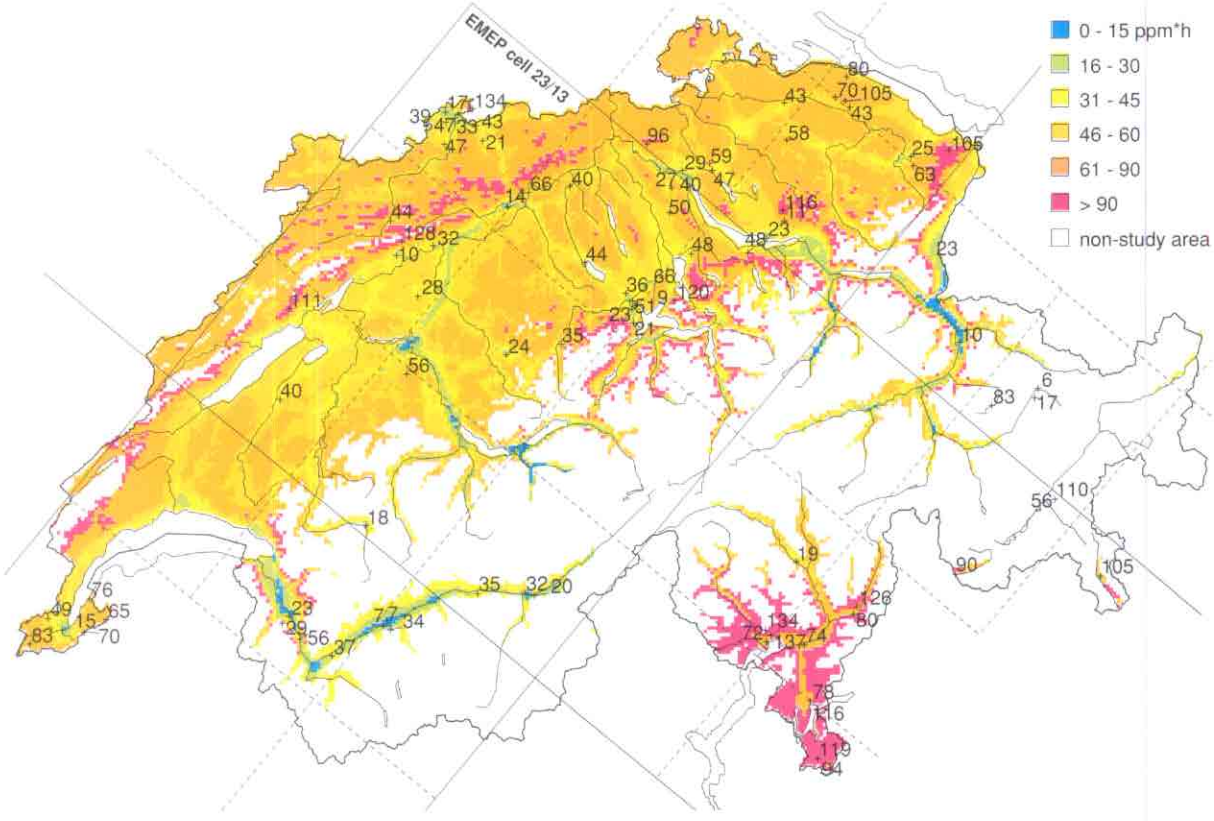

Figure CH-4. Interpolated ozone levels related to health in 1994: number of non overlapping 8h-means exceeding 60ppb from April to September (*N8h60*). (The critical level is set to 0.)

UNITED KINGDOM

National Focal Center/Contact
Jane Hall
Environmental Information Centre
Institute of Terrestrial Ecology
Monks Wood
Abbots Ripton
Huntingdon PE17 2LS
tel: +44-1487-773381
fax: + 44-1487-773467
email: j.hall@ite.ac.uk

Collaborating Institutions/Contacts
Prof. Michael Hornung (Soils)
Institute of Terrestrial Ecology
Merlewood
Windermere Road
Grange-over-Sands
Cumbria LA11 6JU
tel: +44-15395-32264
fax: +44-15395-35226
email: m.hornung@ite.ac.uk

Prof. Rick Battarbee (Freshwaters)
Environmental Change Research Centre
Department of Geography
University College London
26 Bedford Way
London WC1H 0AP
tel: +44-171-380 7582
fax: +44-171-380 7565
email: rbattarb@geography.ucl.ac.uk

Michael Ashmore (Vegetation/Levels)
Centre of Environmental Technology
Imperial College London
48 Prince's Gardens
London SW7 2PE
tel: +44-171-594 9291
fax: +44-171-581 0245
email: m.ashmore@ic.ac.uk

Prof. David Fowler (Deposition)
Institute of Terrestrial Ecology
Bush Estate
Penicuik
Midlothian EH26 0QB
tel: +44-131-445 4343
fax: +44-131-445 3943
email: d.fowler@ite.ac.uk

Sarah Metcalfe (Modelled deposition)
Department of Geography
University of Edinburgh
Drummond Street
Edinburgh EH8 9XP
tel: +44-131-650 8162
fax: +44-131-650 2524
email: sem@ossian.geo.ed.ac.uk

Alan Jenkins (Dynamic modelling)
Institute of Hydrology
Maclean Building
Crowmarsh Gifford
Wallingford
Oxfordshire OX10 8BB
tel: +44-1491-838800
fax: +44-1491-692424
email: a.jenkins@ioh.ac.uk

National Maps Produced

Acidity critical loads and exceedances:
- Empirical critical loads for three non-woodland terrestrial ecosystems
- Simple Mass Balance critical loads for woodland ecosystems
- Steady-State Water Chemistry model, Diatom model and First-order Acidity Balance model for freshwater ecosystems critical loads
- Exceedance maps, and exceedance class maps for the critical loads function

Sulfur critical loads and exceedances:
- Minimum and maximum critical loads of sulfur for all ecosystems
- Exceedance maps

Nitrogen (acidity) critical loads and exceedances:
- Minimum and maximum critical loads of nitrogen for all ecosystems
- Exceedance maps

Nitrogen (nutrient) critical loads and exceedances:
- Empirical critical loads for 14 terrestrial ecosystems
- Mass Balance critical loads for coniferous and deciduous woodland ecosystems
- Exceedance maps

Critical levels and exceedances:

- Receptor maps: agriculture, arable, forestry, semi-natural vegetation, heathland, herbaceous semi-natural vegetation, all grasslands, green lichens, cyanobacterial lichens and bryophyte *Pleurozium schreberi*
- Exceedance of critical levels of SO_2
- Exceedance of critical levels of NO_x
- Exceedance of critical levels of O_3

Calculation Methods

1. Empirical critical loads of acidity: Empirical critical loads of acidity for soils have been assigned to each 1km grid square of the UK based upon the mineralogy of the dominant soil series present in the square (Hornung *et al.* 1995). The data are mapped in five classes representing the "Skokloster" ranges of critical loads values. The mid-range critical load values (0.1, 0.35, 0.75, 1.5, 2.0, 4.0 keq H^+ ha^{-1} yr^{-1}) have been assigned to three soil-vegetation ecosystems: acid grassland, calcareous grassland and heathland, where the ecosystem occupies more than 5% of the total area (Hall *et al.* 1997). This approach is consistent with the calculation of weathering rates for different soil types using the PROFILE model, which has shown that in most cases the weathering rate falls within these class ranges (Langan *et al.* 1995).

2. Simple mass balance critical loads of acidity: The simple mass balance (SMB) model has been used to calculate acidity critical loads for coniferous and deciduous woodland ecosystems (Hall *et al.* 1997). The chemical criterion often used in the SMB is the base cation (calcium + magnesium) to aluminum (BC:Al) ratio. This assumes that magnesium affords the same protection to plant roots as calcium. This assumption needs checking experimentally, particularly when considering areas like parts of the UK which receive high inputs of base cation deposition through sea salt. Therefore, in the UK, a decision was made to use a calcium to aluminum (Ca:Al) ratio in the SMB equation, together with total (wet plus dry, non-marine plus marine) calcium deposition and estimates of calcium weathering and uptake.

Calcium losses by uptake and removal in harvesting of woodlands is calculated from the average volume increment (i.e. a measurement of yield) achieved by each species in Britain. Average volume increments are converted to amount removed in harvesting using species-specific wood densities and the calcium concentrations of timber from published studies. Area-weighted average volume increments and wood densities are calculated from the average values for each species, with each species contributing to the average depending on the proportion of UK coniferous or deciduous woodland they represent. Calcium concentrations for oak are used for deciduous woodland and Sitka spruce for coniferous woodland. The values used in the SMB represent the theoretical maximum, assuming potential yields at harvest are achieved.

The uptake values for deciduous woodland have been calculated for oak on calcium-rich soils. However, in some areas of southern Britain deciduous trees grow on calcium-poor podozolic soils, where such uptake values would be overestimates of removal. Two different sets of uptake values were therefore calculated for deciduous woodland, one for calcium-rich soils and the other for calcium-poor soils. These soil types were then identified from a 1 × 1 km^2 map and the appropriate uptake values applied. The table below shows the uptake values for calcium, base cations (used for calculating maximum critical load of sulfur) and nitrogen (used for calculating critical loads of nutrient nitrogen).

Woodland & soil type	Uptake values in keq ha^{-1} yr^{-1}		
	Ca	BC	N
Conifers	0.117	0.253	0.279
Deciduous Ca-rich soils	0.516	0.613	0.278
Deciduous Ca-poor soils	0.076	0.171	0.278

When the SMB uses the Ca:Al ratio, the weathering component of $ANC_{le(crit)}$ (critical leaching of base cations) needs to be re-calculated for calcium weathering only. To achieve this, "calcium correction" values have been assigned to each soil series previously used to determine empirical critical loads. These were assigned to each 1km square of Britain where that soil series dominates. Calcium weathering (Ca_w) values were then calculated as:

$Ca_w = ANC_w$·calcium correction value

where the ANC_w equals the "mid-range" empirical critical loads value, except for 1km grid squares dominated by peat soils, which were set to zero weathering.

The calculated SMB critical load values for woodland 1km squares dominated by peat soils were zero. Alternative approaches were tested and the decision made to replace them with the original empirical critical load estimates.

3. Critical loads of acidity: all terrestrial ecosystems: The national map of critical loads of acidity combines both empirical and mass balance values for the five terrestrial soil-vegetation ecosystems: acid grassland, calcareous grassland, heathland, coniferous and deciduous woodland.

The 5-percentile critical load of acidity was determined by first calculating critical loads at 1km resolution for each individual ecosystem as described above. Values and areas were then compared for each 1km grid and the critical load associated with the most sensitive 5% of the total ecosystem area in this grid used in a 1km 5-percentile map for all ecosystems.

4. Critical loads of acidity for freshwaters: In the UK, critical loads of sulfur and of acidity have been calculated for approximately 1500 freshwaters using the Steady-State Water Chemistry model and the Diatom model. In addition, the First-order Acidity Balance (FAB) model has been applied to 527 of these catchments. The methods have been described in detail by Posch *et al.* (1995), CLAG (1995) and Battarbee *et al.* (1996).

Work is continuing at the UK NFC with colleagues at University College London to collate the necessary catchment information and apply FAB to all 1500 sites.

5. Empirical critical loads of nutrient nitrogen: A range of nutrient nitrogen critical load values have been defined for 14 terrestrial ecosystems (UBA 1996) comprising of tree and forest ecosystems, heathlands, species-rich grasslands and wetlands. Experts in the UK have identified a single value within each range to be used for mapping. The methods for identifying the geographic distribution of the 14 different ecosystems in the UK have been described in Posch *et al.* (1995).

6. Mass balance critical loads of nutrient nitrogen: The UK has applied the mass balance method of calculating critical loads of nutrient nitrogen to coniferous and deciduous woodland ecosystems. The equation used is reported in Posch *et al.* (1995). Values of nitrogen uptake for coniferous and deciduous woodland have been calculated using the same method as described in the table above for calcium uptake.

7. Critical loads of nutrient nitrogen - all terrestrial ecosystems: In the UK methods have been developed to use the data from empirical, mass balance or both of these approaches to calculate nutrient nitrogen critical loads for the same terrestrial ecosystems for which acidity critical loads have been derived (Hall *et al.* 1997). The method uses the ITE Land Cover Map, together with the National Vegetation Classification and Biological Records Centre data; it is a sequential process such that the lowest critical loads value for any appropriate ecosystem present in a 1km square is used. For each ecosystem, critical loads were only applied where the ecosystem occupies more than 5% of the total area. For coniferous woodland ecosystems, mass balance critical loads have been used, and for deciduous woodland ecosystems the lowest critical load values, empirical or mass balance, were applied.

From the five sets of values (acid grassland, calcareous grassland, heathland, coniferous woodland, deciduous woodland), a 5-percentile critical load was determined by selecting the lowest critical load value for each 1 km square.

8. The Critical Loads Function (CLF): In the UK the CLF is being used to examine exceedances in three ways:
(i) to map the seven regions of exceedance (identified by the CLF graph) using current or future estimates of sulfur and nitrogen deposition. This identifies the acidifying pollutant(s) in any grid square that need to be reduced.
(ii) to calculate the minimum deposition (sulfur + nitrogen) reduction required to reach the envelope of protection. This allows actual values of deposition reduction required to be assigned to grid squares.
(iii) to consider the effects of maximising reductions of sulfur or nitrogen deposition. This highlights the possible "trade-off" between reducing one pollutant or another.

9. Critical levels: The methods for defining the geographic distribution of critical level receptors in the UK is described in Posch *et al.* (1995). Exceedance maps based on the revised critical level values (UBA 1996) have been prepared for the UK and will be published in 1997 in the UK

Critical Loads Advisory Group, Critical Levels sub-group report.

Data Sources

Information on the data sources for empirical critical loads of soils, land use and land cover data, species distribution data, measured and modelled deposition and concentration data and runoff data is given in Posch *et al.* (1995).

The methodology used for determining empirical and simple mass balance critical loads of acidity for soil-vegetation ecosystems has been described by Hall *et al.* (1997). The report describes in detail the data submitted to the CCE in December 1996 and a sub-set of the maps are presented here.

Comments and Conclusions

The NFC is continuing to develop methods to calculate and map critical loads (acidity and nutrient nitrogen), critical levels and exceedances in collaboration with members of the UK Critical Loads Advisory Group, the CCE and the UN/ECE Task Force on Mapping.

Northern Ireland data are not included in critical loads maps at present. Data for the calculation of calcium weathering rates and nitrogen critical loads are being collated in the UK and will shortly be made available to the NFC.

Simple Mass Balance calculations of acidity critical loads have previously been carried out using the ARC/INFO geographic information system (GIS). A menu-driven user-friendly interface has now been developed to run or modify the model, draw the maps on screen, calculate exceedances and give a statistical breakdown of the maps into critical load or exceedance classes. The NFC is currently developing procedures to implement the First-order Acidity Balance model in the GIS and build a user-friendly interface.

The NFC has begun collaboration with organizations in the UK and Europe to develop methods for the calculation of critical loads of heavy metals.

Acknowledgements for maps and data

Maps and data are compiled by the UK NFC at ITE Monks Wood.

Critical loads data are provided by the Critical Loads Advisory Group sub-groups for soils, vegetation and freshwaters.

Other data are provided by the Institute of Terrestrial Ecology Monks Wood (ITE Land Cover, BRC species distributions), Institute of Terrestrial Ecology Merlewood (ITE Land Classification), Institute of Terrestrial Ecology Bush Estate (deposition), AEA Technology (deposition and concentrations), Hull and Edinburgh Universities (modelled deposition), Institute of Hydrology (runoff), Lancaster University (National Vegetation Classification), Ministry of Agriculture, Fisheries and Food (agricultural statistics), and CORINE (land cover for Northern Ireland).

References

Battarbee, R.W., T.E.H. Allott, S. Juggins, A.M. Kreiser, C. Curtis and R. Harriman, 1996. Critical loads of acidity to surface waters: an empirical diatom-based palaeolimnological model. *Ambio* 25:366-369.

CLAG, 1995. Critical loads of acid deposition for United Kingdom freshwaters: Sub-group report on Freshwaters. Report prepared at the request of the Department of Environment.

Hall, J., M. Hornung, P. Freer-Smith, P. Loveland, I. Bradley, S. Langan, H. Dyke, J. Gascoigne and K.R. Bull, 1997. Current status of UK critical loads data - December 1996. Report to the Department of Environment.

Hornung, M., K.R. Bull, M. Cresser, J. Hall, S.J. Langan, P. Loveland and C. Smith, 1995. An empirical map of critical loads of acidity for soils in Great Britain. *Environ. Pollut.* 90:301-310.

Langan, S.J., H.U. Sverdrup and M. Coull, 1995. The calculation of base cation release from the chemical weathering of Scottish soils using the PROFILE model. *Water Air Soil Pollut.* 85:2497-2502.

Posch, M., P.A.M. de Smet, J.-P. Hettelingh and R.J. Downing (eds.), 1995. Calculation and Mapping of Critical Thresholds in Europe: CCE Status Report 1995. National Institute of Public Health and the Environment Rep. 259101004, Bilthoven, Netherlands.

UBA, 1996. Manual on Methodologies and Criteria for Mapping Critical Levels/Loads and geographical areas where they are exceeded. UN/ECE Convention on Long-range Transboundary Air Pollution. Federal Environmental Agency (Umweltbundesamt), Texte 71/96, Berlin.

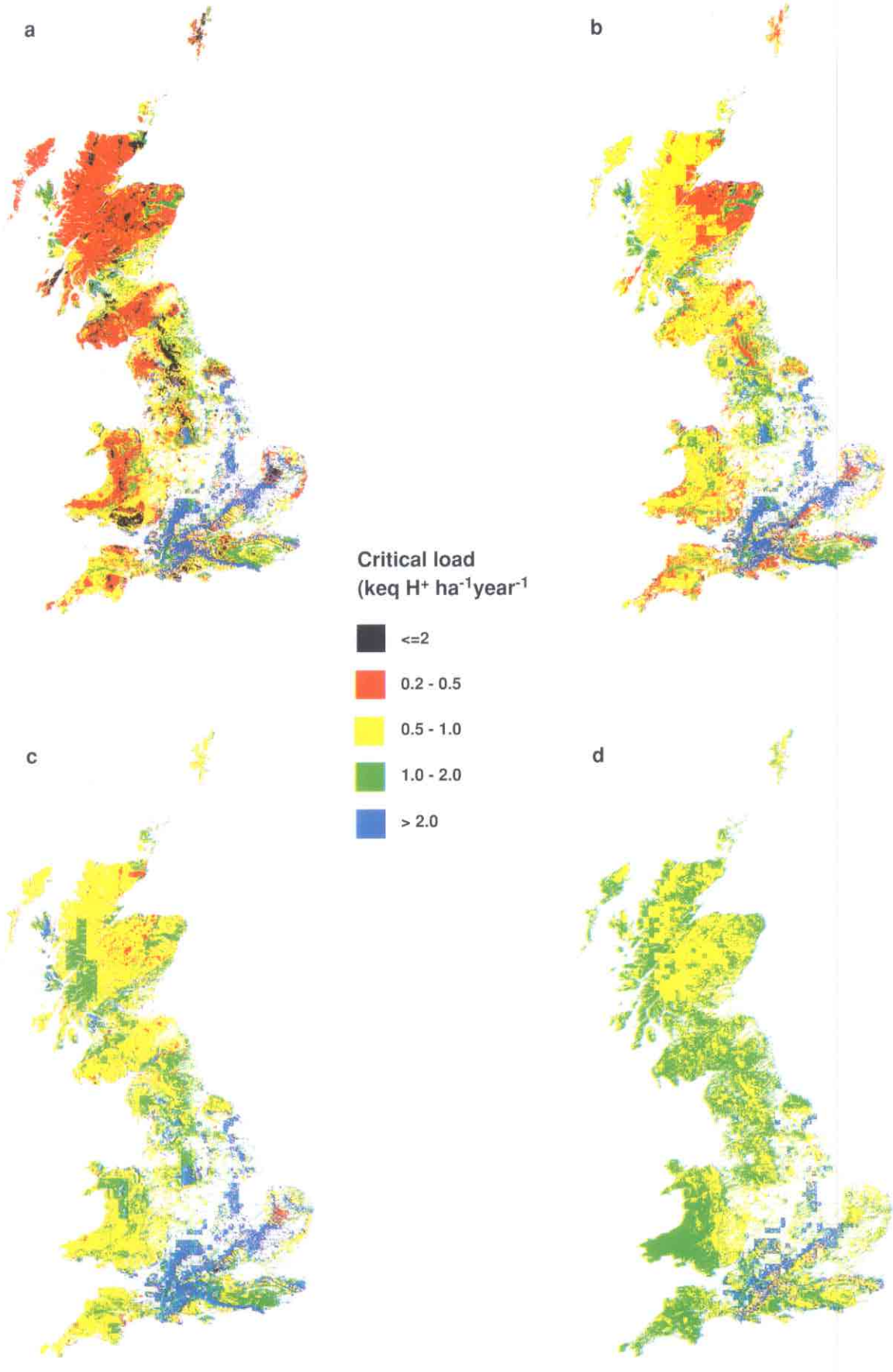

Figure UK-1. 5-percentile critical load maps for (a) acidity, (b) maximum sulfur ($CL_{max}(S)$), (c) maximum nitrogen ($CL_{max}(N)$), (d) nutrient nitrogen. The maps are based on 1 x 1 km^2 data for acid grassland, calcareous grassland, heathland, coniferous woodland and deciduous woodland ecosystems.

Appendix A: The polar stereographic projection (EMEP grid)

To make critical loads useful for pan-European negotiations on emission reductions one has to be able to compare them to deposition estimates. Deposition of sulfur and nitrogen compounds have up to now been reported by EMEP on a 150 km × 150 km grid covering (most of) Europe, but recently depositions have also become available on a 50 km × 50 km subgrid. These grid systems are based on the so-called polar stereographic projection. This projection and how to calculate the area of a grid cell is described in this Appendix.

The polar stereographic projection

In the polar stereographic projection each point on the Earth's sphere is projected from the South Pole onto a plane perpendicular to the Earth's axis and intersecting the Earth at a fixed latitude ϕ_0 (see Figure A-1, top). Consequently, the coordinates x and y are obtained from the geographical longitude λ and latitude ϕ (in radians) by the following equations (see Figure A-1, bottom):

$$x = x_p + M \tan\left(\frac{\pi}{4} - \frac{\phi}{2}\right) \sin(\lambda - \lambda_0) \tag{A.1}$$

and

$$y = y_p - M \tan\left(\frac{\pi}{4} - \frac{\phi}{2}\right) \cos(\lambda - \lambda_0) \tag{A.2}$$

where (x_p, y_p) are the coordinates of the North Pole; λ_0 is a rotation angle, i.e. the longitude parallel to the y-axis; and M is the scaling of the x-y coordinates. In the above definition the x-values increase and the y-values decrease when moving towards the equator. For a given M, the unit length (grid size) d in the x-y-plane is given by

$$d = \frac{R}{M}(1 + \sin\phi_0) \tag{A.3}$$

where R (= 6370km) is the radius of the Earth. The inverse transformation, i.e. longitude and latitude as function of x and y, is given by

$$\lambda = \lambda_0 + \arctan\left(\frac{x - x_p}{y_p - y}\right) \tag{A.4}$$

and

$$\phi = \frac{\pi}{2} - 2\arctan\left(\frac{\sqrt{(x - x_p)^2 + (y - y_p)^2}}{M}\right) \tag{A.5}$$

The *arctan* in Eq. A.5 gives the correct longitude for quadrant 4 ($x>x_p$ and $y<y_p$) and quadrant 3 ($x<x_p$ and $y<y_p$); π (=180°) has to be added for quadrant 1 ($x>x_p$ and $y>y_p$) and subtracted for quadrant 2 ($x<x_p$ and $y>y_p$). Note that quadrant 4 is the one covering (most of) Europe.

Every stereographic projection is a so-called conformal projection, i.e. an angle on the sphere remains the same in the projection plane, and vice versa. However, the stereographic projection distorts areas (even locally), i.e. it is not an equal-area projection (in fact, it can be shown that a projection cannot be both conformal and equal-area).

A **grid cell** (i, j) is defined as a square in the x-y-plane with side length d (see Eq. A.3) and its center point is given by the integral part of x and y, i.e.

$$i = \text{nint}(x) \quad \text{and} \quad j = \text{nint}(y) \tag{A.6}$$

where 'nint' is the nearest integer (rounding function). Consequently, the corners of the grid cell have the coordinates $(i \pm 1/2, j \pm 1/2)$.

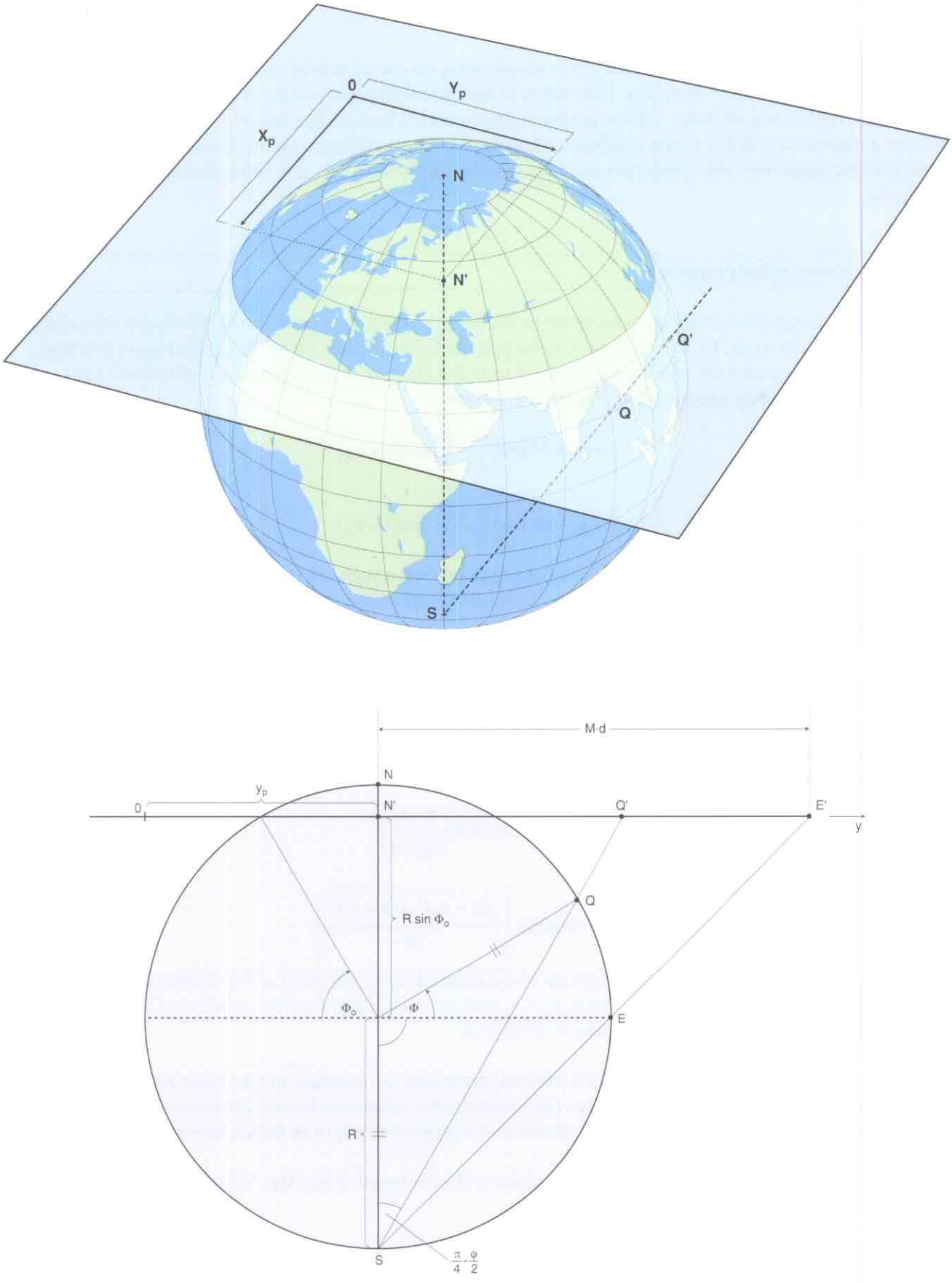

Figure A-1. Polar stereographic projection from the South Pole onto a plane cutting the Earth at a given latitude (top). Geometric relationships in a plane cutting the Earth vertically at a given longitude used to derive the projection equations (bottom).

The 150 km × 150 km grid (EMEP150 grid)

The coordinate system used by EMEP/MSC-W for the Lagrangian long-range transport model (and still by the CCE for mapping critical loads) is defined by the following parameters:

$$\phi_0 = \frac{\pi}{3} = 60°\text{N}, \quad \lambda_0 = -32°(\text{i.e. } 32°W), \quad (x_p, y_p) = (3,37), \quad d = 150 \text{ km} \tag{A.7}$$

which yields M=79.2438...

The 50 km × 50 km grid (EMEP50 grid)

In the future, deposition and concentration fields will also become available on a 50km × 50km grid, the EMEP50 grid. This grid is a subdivision of the EMEP150 grid into 3×3=9 subgrids, and its parameters are given by

$$\phi_0 = \frac{\pi}{3} = 60°\text{N}, \quad \lambda_0 = -32°(\text{i.e. } 32°W), \quad (x_p, y_p) = (8,110), \quad d = 50 \text{ km} \tag{A.8}$$

yielding M=237.7314...

Consequently, calling these EMEP50 coordinates p and q, they are obtained from the EMEP150 coordinates x and y via

$$p = 3x - 1 \text{ and } q = 3y - 1 \tag{A.9}$$

An EMEP150 grid cell (i, j) contains 9 EMEP50 grid cells (m, n) with indices m=3i–2,3i–1,3i and n=3j–2,3j–1,3j. The part of the two EMEP grid systems covering (most of) Europe is shown in Figure A-2.

To convert a point (*xlon, ylat*), given in degrees of longitude and latitude, into EMEP150 coordinates (*emepi, emepj*) the following FORTRAN subroutine can be used:

```
c
      subroutine llemep (xlon,ylat,emepi,emepj)
c
c     Returns for a point (xlon,ylat), where xlon is the longitude and ylat
c     is the latitude in degrees, its EMEP150 coordinates (emepi,emepj).
c
      real               xlon, ylat, emepi, emepj
c
      data xp, yp /3.,37./       ! EMEP150 coordinates of the North Pole
      data xlon0 /-32./          ! = lambda_0
      data em /79.24387880/      ! = M=(R/d)*(1+sin(pi/3)); R=6370km, d=150km
      data pi180 /57.2957795/    ! = 180/pi
      data pi360 /114.591559/    ! = 360/pi
c
      tp = tan((90.-ylat)*pi360)
      rlamp = (xlon-xlon0)*pi180
      emepi = xp+em*tp*sin(rlamp)
      emepj = yp-em*tp*cos(rlamp)
                                        return
      end
```

The EMEP50 coordinates can then be obtained with the aid of Eq. A.9.

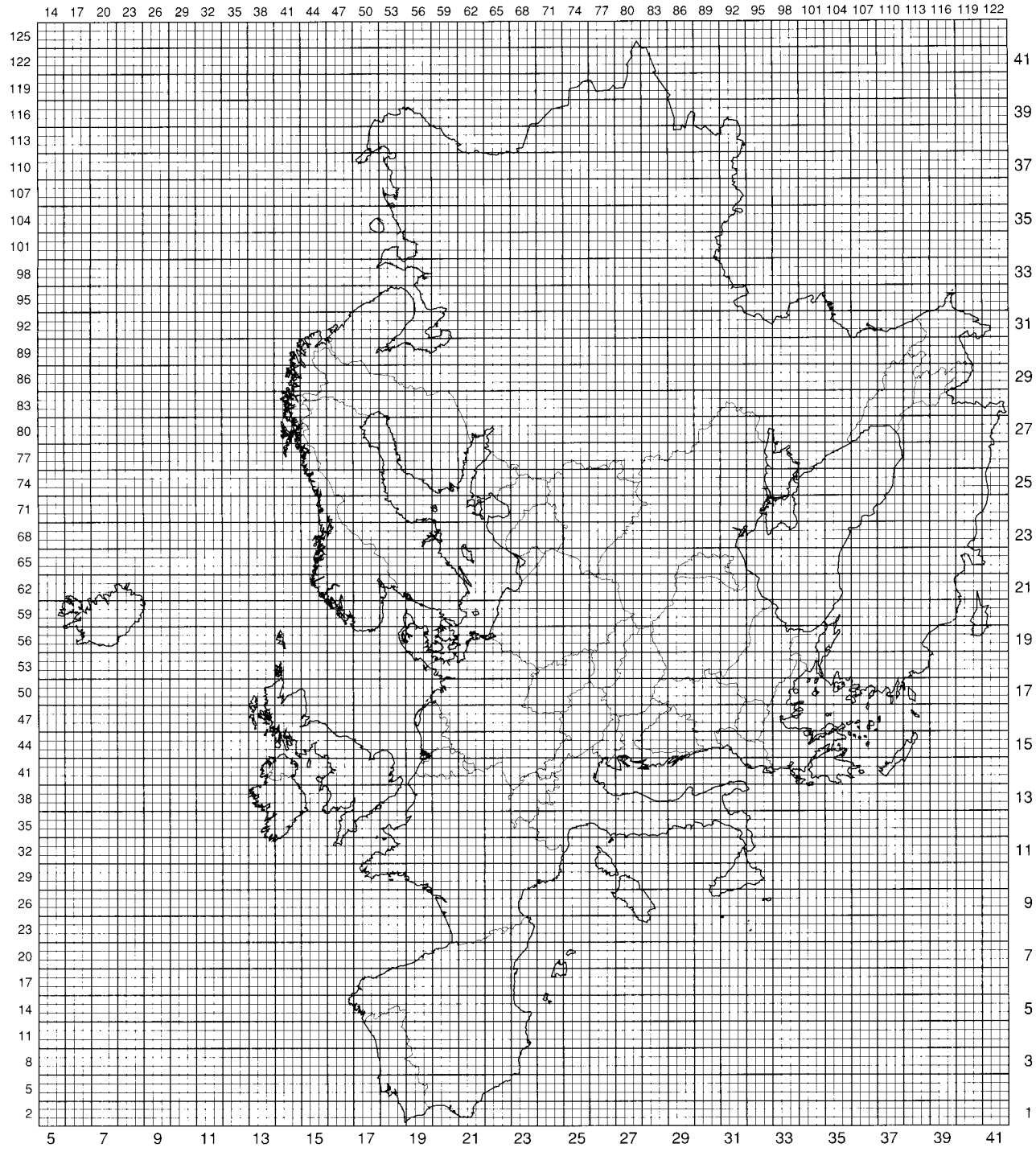

Figure A-2. The EMEP150 grid (thick lines) and the EMEP50 grid (thin lines). The labels at the bottom and right are the EMEP150 grid indices (every second), and the labels at the top and left are the EMEP50 grid indices (every third).

Conversely, given the EMEP150 coordinates of a point, its longitude and latitude can be computed with the following subroutine:

```
c
      subroutine emepll (emepi,emepj,xlon,ylat)
c
c     Returns for a point (emepi,emepj), given in the EMEP150
c     coordinate system, its longitude xlon and latitude ylat in degrees.
c
      data xp, yp /3.,37./        ! EMEP150 coordinates of the North Pole
      data xlon0 /-32./           ! = lambda_0
      data em /79.24387880/       ! = M=(R/d)*(1+sin(pi/3)); R=6370km,d=150km
      data pi180 /0.017453293/    ! = pi/180
      data pi360 /0.008726646/    ! = pi/360
c
      ex = emepi-xp
      ey = yp-emepj
      if (ex .eq. 0. .and. ey .eq. 0.) then ! North Pole
        xlon = xlon0 ! or whatever
      else
        xlon = xlon0+pi180*atan2(ex,ey)
      endif
      r = sqrt(ex*ex+ey*ey)
      ylat = 90.-pi360*atan(r/em)
                                          return
     end
```

To convert the EMEP50 coordinates (p,q) of a point to longitude and latitude, call the above subroutine with *emepi*=$(p+1)/3$ and *emepj*=$(q+1)/3$.

The area of an EMEP grid cell

As mentioned above, the stereographic projection does not preserve areas, e.g. a 150 km × 150 km EMEP grid cell is 22500 km^2 only in the projection plane, but never on the globe. Here we want to derive the formula for computing the area on the Earth of an arbitrarily located EMEP grid cell. To this end we first recapitulate the basic formulae for computing curved surface areas in three dimensions.

The area S of a surface in three dimensions is given by

$$S = \iint |\boldsymbol{x}_u \times \boldsymbol{x}_v| du dv \tag{A.10}$$

where $\boldsymbol{x}=\boldsymbol{x}(u,v)$ is the equation of the surface with parameters u and v, $\boldsymbol{x}_u$ is the vector of partial derivatives with respect to u and '×' denotes the vector product. For example, the surface of a sphere with radius R (the Earth) can be represented by longitude λ and latitude ϕ as:

$$\boldsymbol{x}(\lambda,\phi) = R\begin{pmatrix}\cos\phi\cos\lambda\\ \cos\phi\sin\lambda\\ \sin\phi\end{pmatrix}, \quad 0 \le \lambda < 2\pi, \quad -\frac{\pi}{2} \le \phi \le \frac{\pi}{2} \tag{A.11}$$

and a straightforward calculation yields

$$\boldsymbol{x}_\lambda \times \boldsymbol{x}_\varphi = R^2 \begin{pmatrix} \cos^2\phi\cos\lambda \\ \cos^2\phi\sin\lambda \\ \sin\phi\cos\phi \end{pmatrix} \quad \text{and} \quad \left|\boldsymbol{x}_\lambda \times \boldsymbol{x}_\varphi\right| = R^2\cos\phi \tag{A.12}$$

which gives, e.g., for the area of a longitude-latitude grid cell:

$$S_{\lambda\phi} = R^2 \int_{\lambda_1}^{\lambda_2} \int_{\phi_1}^{\phi_2} \cos\phi \, d\phi d\lambda = R^2(\lambda_2 - \lambda_1)(\sin\phi_2 - \sin\phi_1) \tag{A.13}$$

Now we want to compute the area of an EMEP grid cell on the surface of the Earth, i.e. its "real" area. To this end we have to express longitude and latitude in terms of the EMEP coordinates x and y (see Eqs. A.4, A.5):

$$\lambda = \lambda_0 - \arctan(t) \quad \text{and} \quad \phi = \frac{\pi}{2} - 2\arctan(r/M) \tag{A.14}$$

with the abbreviations

$$t = \frac{x - x_p}{y - y_p} \quad \text{and} \quad r = \sqrt{(x - x_p)^2 + (y - y_p)^2} \tag{A.15}$$

The area of an EMEP grid cell with lower left corner (x_1,y_1) and upper right corner (x_2,y_2) is then given by making the coordinate transformation in Eq. A.10 (see also Eq. A.13):

$$S_{xy} = R^2 \int_{y_1}^{y_2} \int_{x_1}^{x_2} \cos\left(\frac{\pi}{2} - 2\arctan(r/M)\right) \left|\frac{\partial(\lambda,\phi)}{\partial(x,y)}\right| dxdy \tag{A.16}$$

For the partial derivatives we obtain from Eqs. A.14, A.15:

$$\begin{aligned} \frac{\partial\lambda}{\partial x} &= \frac{-1}{1+t^2} \cdot \frac{1}{y - y_p}, \quad \frac{\partial\lambda}{\partial y} = \frac{1}{1+t^2} \cdot \frac{t}{y - y_p}, \\ \frac{\partial\phi}{\partial x} &= \frac{-2}{1+(r/M)^2} \cdot \frac{x - x_p}{Mr}, \quad \frac{\partial\phi}{\partial y} = \frac{-2}{1+(r/M)^2} \cdot \frac{y - y_p}{Mr} \end{aligned} \tag{A.17}$$

which yields for absolute value of the Jacobi determinant:

$$\left|\frac{\partial(\lambda,\phi)}{\partial(x,y)}\right| = \frac{2}{Mr} \cdot \frac{1}{1+(r/M)^2} \tag{A.18}$$

Considering further that

$$\cos\left(\frac{\pi}{2} - 2\arctan(r/M)\right) = \frac{2(r/M)}{1+(r/M)^2} \tag{A.19}$$

and making the coordinate transformation $u=(x-x_p)/M$ and $v=(y-y_p)/M$ we arrive at the following double integral for the area of an EMEP grid cell

$$S_{xy} = 2R^2\left\{I(u_2,v_2) - I(u_1,v_2) - I(u_2,v_1) + I(u_1,v_1)\right\} \quad \text{with} \quad I(u,v) = \iint \frac{2dudv}{(1+u^2+v^2)^2} \tag{A.20}$$

where $u_1=(x_1-x_p)/M$, etc. With the substitution $x=u/(1+v^2)^{1/2}$, a partial integration and back-substituting one obtains

$$\int \frac{2du}{(1+u^2+v^2)^2} = \frac{u}{(1+v^2)(1+u^2+v^2)} + \frac{1}{(1+v^2)^{3/2}} \arctan\frac{u}{\sqrt{1+v^2}} \tag{A.21}$$

Substituting $x=u/(1+v^2)^{1/2}$ in the second term on the right-hand side of Eq. A.21, partial integration and back-substituting yield

$$\int \frac{1}{(1+v^2)^{3/2}} \arctan\frac{u}{\sqrt{1+v^2}} dv = \frac{v}{\sqrt{1+v^2}} \arctan\frac{u}{\sqrt{1+v^2}} + \int \frac{uv^2 dv}{(1+v^2)(1+u^2+v^2)} \tag{A.22}$$

Combining Eqs. A.21 and A.22 results in

$$\iint \frac{2dudv}{(1+u^2+v^2)^2} = \frac{v}{\sqrt{1+v^2}}\arctan\frac{u}{\sqrt{1+v^2}} + \int \frac{udv}{1+u^2+v^2} \tag{A.23}$$

Carrying out the last integration finally yields

$$I(u,v) = \iint \frac{2dudv}{(1+u^2+v^2)^2} = \frac{v}{\sqrt{1+v^2}}\arctan\frac{u}{\sqrt{1+v^2}} + \frac{u}{\sqrt{1+u^2}}\arctan\frac{v}{\sqrt{1+u^2}} \tag{A.24}$$

which, after insertion into Eq. A.20, allows the calculation of the area of any EMEP grid cell by inserting ($i-1/2$, $j-1/2$) for (x_1,y_1) and ($i+1/2$,$j+1/2$) for (x_2,y_2).

The following FORTRAN functions compute the area of an EMEP grid cell for arbitrary grid indices (i,j), for the EMEP50 or the EMEP150 grid, depending on the parameter *iopt*:

```
c
      real function aremep (iopt,i,j)
c
c     Returns the area (in km2) of an EMEP grid cell with
c     centerpoint (i,j); iopt=1: EMEP150 grid, iopt=2: EMEP50 grid.
c
      integer             iopt, i, j
      real                dd(2), xp(2), yp(2)
      external            femep
c
      data rearth /6370./             ! radius of the Earth (km)
      data dd(1), dd(2) /150.,50./    ! size of EMEP150/50 grid cell (km2)
      data xp(1), yp(1) /3.,37./      ! EMEP150 coordinates of the North Pole
      data xp(2), yp(2) /8.,110./     ! EMEP50 coordinates of the North Pole
      data drm /1.8660254/            ! = 1+sin(pi/3) = 1+sqrt(3)/2
c
      x1 = real(i)-0.5
      y1 = real(j)-0.5
      emi = dd(iopt)/(rearth*drm) ! = 1/M
      u1 = (x1-xp(iopt))*emi
      v1 = (y1-yp(iopt))*emi
      u2 = u1+emi
      v2 = v1+emi
      ar0 = 2.*rearth*rearth
      aremep = ar0*(femep(u2,v2)-femep(u1,v2)-femep(u2,v1)+femep(u1,v1))
                                          return
      end
c
      real function femep (u,v)
c
c     Function used in computing the area of an EMEP grid cell.
c
      real                u, v
c
      ui = 1./sqrt(1.+u*u)
      vi = 1./sqrt(1.+v*v)
      femep = v*vi*atan(u*vi)+u*ui*atan(v*ui)
                                          return
    end
```

In Figure A-3 isolines of the area of the EMEP50 grid cells over Europe are displayed. It shows that only the grids at 60°N have an area of (approximately) 50 × 50=2500 km^2.

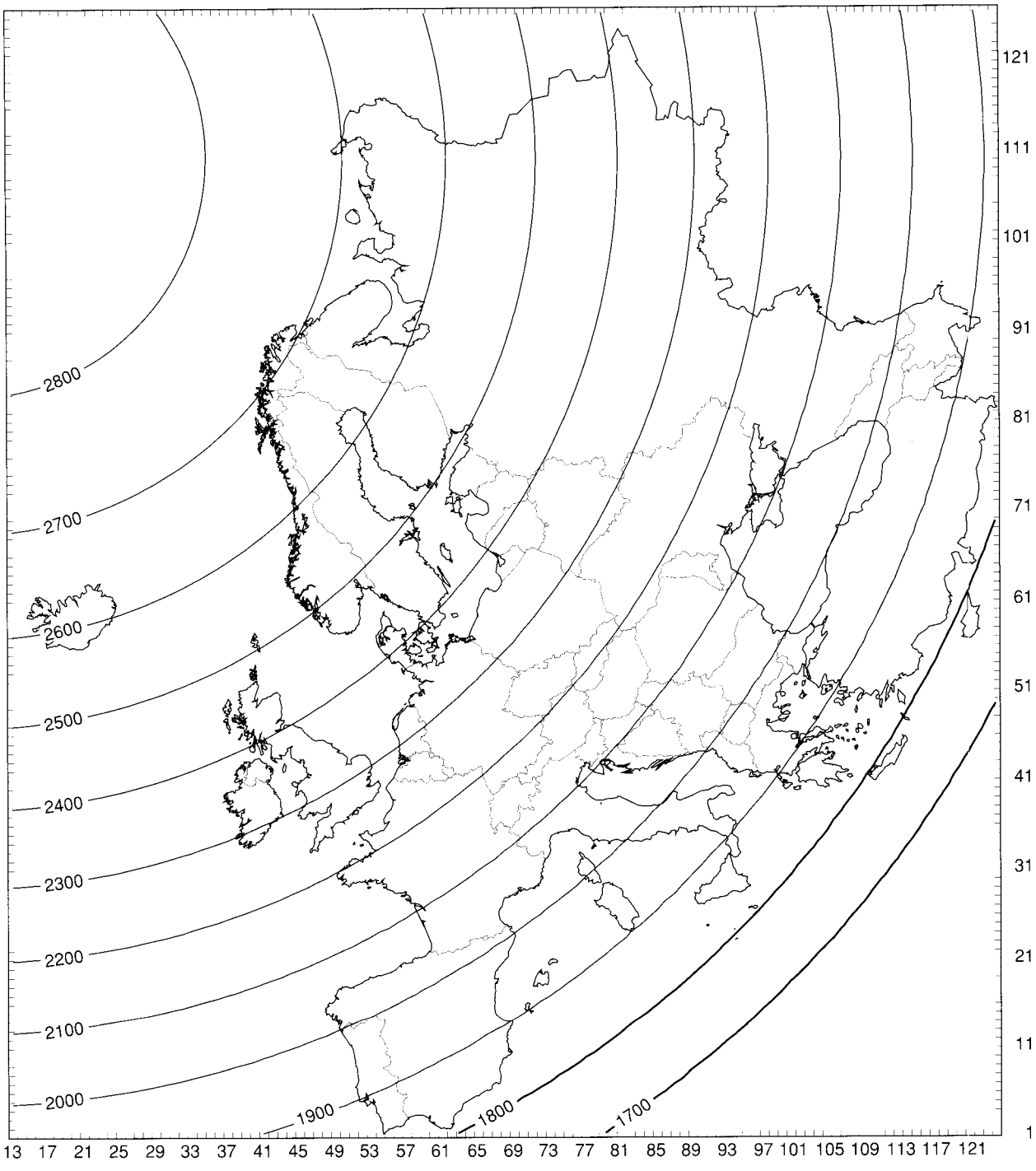

Figure A-3. Isolines of the EMEP50 grid cell areas over Europe in km^2.

Appendix B. Some FORTRAN routines

FORTRAN subroutines are provided here for the computation of certain statistics of distribution functions (weighted mean, variance and percentiles) and the computation of protection isolines and protection percentages. These subroutines are provided on an "as is" basis, and no guarantee is given for their correctness. The subroutines contain non-standard features of FORTRAN, but they work under Microsoft FORTRAN. It should not be a problem for the experienced user to convert these subroutines into another programming language.

Computing weighted mean and variance

Let x_i, i=1,...,n, be a set of (critical load) values and w_i their respective weights. Then their weighted arithmetic mean is given by:

$$\mu_n = \frac{1}{W_n}\sum_{i=1}^{n} w_i x_i \quad \text{with} \quad W_n = \sum_{i=1}^{n} w_i \tag{B.1}$$

and the variance is defined as:

$$\sigma_n^2 = \frac{1}{W_n}\sum_{i=1}^{n} w_i (x_i - \mu_n)^2 = \frac{1}{W_n}\sum_{i=1}^{n} w_i x_i^2 - \mu_n^2 \tag{B.2}$$

The computation of these quantities is seemingly straightforward:

```
....
wsum = 0.
xave = 0.
sig2 = 0.
do i = 1,n
   wsum = wsum+wv(i)
   xave = xave+wv(i)*xv(i)
   sig2 = sig2+wv(i)*xv(i)**2
enddo
xave = xave/wsum
sig2 = sig2/wsum-xave**2
.....
```

where the vectors *xv( )* and *wv( )* contain the values and weights, respectively. However, this is not a proper way for calculating the variance, especially when there are a large number of values or when the values differ by several orders of magnitude, since roundoff errors might occur in the last equation. The proper way is to compute first the mean and sum of weights (as above), and then the variance in a second loop:

```
....
sig2 = 0.
do i = 1,n
   sig2 = sig2+wv(i)*(xv(i)-xave)**2
enddo
sig2 = sig2/wsum
.....
```

Occasionally, when n is very large, it might be impossible to store the values and weights in vectors, and the only way is to compute mean and variance recursively (while reading in the data). From Eqs. B.1 and B.2 one easily derives the following recurrence relations:

$$W_n = W_{n-1} + W_n \tag{B.3}$$

$$\mu_n = \frac{W_{n-1}}{W_n}\mu_{n-1} + \frac{w_n}{W_n}x_n$$

$$\sigma_n^2 = \frac{W_{n-1}}{W_n}\sigma_{n-1}^2 + \frac{w_n W_{n-1}}{W_n^2}(\mu_{n-1} - x_n)^2$$

and the computation can be done with the following program fragment:

```
.....
wold = 0.
xave = 0.
sig2 = 0.
do while (.not.EOF(1))
   read (1,*) xi,wi
   wsum = wold+wi
   sig2 = wold*(sig2+wi*(xave-xi)**2/wsum)/wsum
   xave = (wold*xave+wi*xi)/wsum
   wold = wsum
enddo
.....
```

Computing quantiles (percentiles)

A prerequisite for computing quantiles is the sorting of the critical load values, not forgetting the corresponding rearrangement of the weights. Routines to do that are easily available, for example the routine *sort2* in Press *et al.* (1992, p. 326). In the following we assume that the vectors of critical loads are sorted in ascending order; however, the weights don't have to be normalized to one (e.g., they can be the original ecosystem areas).

A subroutine for computing an arbitrary quantile is then given by:

```
c
      subroutine qantilcw (q,num,vec,wei,xq)
c
c     Computes the q-quantile xq of the num values in vec()
c     - sorted in ascending order - with corresponding weights wei()
c     from the empirical distribution function.
c
      integer               num
      real                  q, vec(*), wei(*), xq
c
      if (num .eq. 0) stop ' Quantile of nothing?!'
      if (q .lt. 0. .or. q .gt. 1.) stop ' q outside [0,1]!'
c
      wsum = wei(1)
      do k = 2,num
         wsum = wsum+wei(k)
      enddo
```

```
c
      qw = q*wsum
      sum = 0.
      do k = 1,num
         sum = sum+wei(k)
         if (qw .lt. sum) then
            xq = vec(k)
                                              return
         endif
      enddo
      xq = vec(num) ! if q=1
                                              return
      end
```

Often one has to compute many percentiles of the same cumulative distribution function. This can be done either by calling the above subroutine repeatedly, or — more efficiently — by calling the following routine:

```
c
      subroutine qvecsngl (nq,qv,num,vec,wei,xqv)
c
c     Computes the nq quantiles xqv() given in qv() of num values in
c     vec() - sorted in ascending order - with corresponding weights
c     wei() from the empirical distribution function, using that
c     qv(1) <= qv(2) <= ... <= qv(nq).
c
      integer             nq, num
      real                qv(*), vec(*), wei(*), xqv(*)
c
      if (num .eq. 0) stop ' Quantile of nothing?!'
      if (qv(1) .lt. 0.) stop ' qv(1) < 0!'
      if (qv(nq) .gt. 1.) stop ' qv(nq) > 1!'
      do n = 1,nq-1
         if (qv(n) .gt. qv(n+1)) stop ' q-values not sorted!'
      enddo
c
      wsum = wei(1)
      do k = 2,num
         wsum = wsum+wei(k)
      enddo
c
      n = 1
      qw = qv(1)*wsum
      sum = 0.
      do k = 1,num
         sum = sum+wei(k)
10       continue
         if (qw .lt. sum) then
            xqv(n) = vec(k)
            if (n .eq. nq)                    return
            n = n+1
            qw = qv(n)*wsum
                                              goto 10
         endif
      enddo
```

```
      do m = n,nq  ! if qv(n)=...=qv(nq)=1
        xqv(m) = vec(num)
      enddo
                                          return
      end
```

Computing a protection isoline

For computing the points in the x-y plane defining a protection isoline the distance of the intersection of a ray with a given angle with a polygon (critical load function) is needed (see Chapter 3 in Part I). This is accomplished by the following subroutine:

```
c
      subroutine isectang (xv,yv,npnt,ang,dist)
c
c     Computes the distance 'dist' from the origin of the intersection
c     point of a ray with angle 'ang' (in radian, measured from the x-axis)
c     with a polygon of 'npnt' points stored in xv() and yv().
c     Assumption:  polygon monotonically decreasing in 1st quadrant:
c                  0=xv(1)<=...<=xv(npnt) and yv(1)>=...>=yv(npnt)=0
c
      integer             npnt
      real                xv(*), yv(*), ang, dist
c
      data pihalf /1.5707/ ! = pi/2
c
      if (ang .le. 0.) then
        dist = xv(npnt)
                                          return
      endif
      if (ang .ge. pihalf) then
        dist = yv(1)
                                          return
      endif
      ta = tan(ang)
      tg = 1.e+30
      do n = 1,npnt
        if (xv(n) .gt. 0.) tg = yv(n)/xv(n)
        if (tg .le. ta) then
          xi = (yo*xv(n)-xo*yv(n))/(ta*(xv(n)-xo)-(yv(n)-yo))
          dist = sqrt(1.+ta*ta)*xi
                                          return
        endif
        xo = xv(n)
        yo = yv(n)
      enddo
      end
```

The distances to all critical load functions in a grid for a given angle are then stored in a vector, sorted in ascending order (together with their weights), and the desired percentile computed with the routine *qantilcw* given above. The projections of the percentiles onto the x- and y-axes yield the coordinates of the desired protection isoline.

In order to determine the percentage of ecosystem area protected in a grid cell, one must be able to decide whether a given pair of deposition (N_{dep}, S_{dep}) lies inside or outside a given protection isoline. In other words, one needs a routine that determines if a point is inside a polygon or not.

Let $\boldsymbol{x}_1,...,\boldsymbol{x}_n$ with $\boldsymbol{x}_i=(x_i,y_i)$ (i=1,..,n) be n points defining a closed polygon P_n, i.e., the polygon is obtained by connecting $\boldsymbol{x}_1$ with $\boldsymbol{x}_2$, ..., $\boldsymbol{x}_{n-1}$ with $\boldsymbol{x}_n$ and $\boldsymbol{x}_n$ with $\boldsymbol{x}_1$. For an arbitrary point $\boldsymbol{x}_0=(x_0, y_0)$ (inside or outside P_n) we define the angle ϕ_i by

$$\phi_i = \arccos\frac{(\boldsymbol{x}_i - \boldsymbol{x}_0)\cdot(\boldsymbol{x}_{i+1} - \boldsymbol{x}_0)}{|\boldsymbol{x}_i - \boldsymbol{x}_0|\cdot|\boldsymbol{x}_{i+1} - \boldsymbol{x}_0|}, \qquad i = 1, \ldots, n \qquad (\boldsymbol{x}_{n+1} \equiv \boldsymbol{x}_1) \tag{B.4}$$

We order to determine the orientation of the angle ϕ_i, we multiply it by the sign of the external product of the defining vectors, i.e. by the sign of the expression $(x_i-x_0)(y_{i+1}-y_0)-(y_i-y_0)(x_{i+1}-x_0)$. The sum of the n oriented angles determines then, whether the point x_0 lies outside, on, or inside P_n:

$$\left|\sum_{i=1}^{n}\phi_i\right| = \begin{cases} 0 & \text{if } x_0 \text{ outside } P_n \\ \pi & \text{if } x_0 \text{ on } P_n \\ 2\pi & \text{if } x_0 \text{ inside } P_n \end{cases} \tag{B.5}$$

and the following subroutine *inside* does exactly this:

```
c
      subroutine inside (x,y,xv,yv,nbeg,nend,angle)
c
c     Computes the cumulative 'angle' (in radian) of a point (x,y)
c     with the nodes of the (closed) polygon (xv(n),yv(n),n=nbeg,nend).
c     If |angle|=2*pi, (x,y) is inside the polygon, if angle=0, outside.
c     [if |angle|=pi, then the point is ON the polygon]
c     Note: angle is <0 or >0, depending on the Umlaufsinn!
c
      integer             nbeg,nend
      real                x, y, xv(*), yv(*), angle
c
      data pi /3.14159265/
c
      x2 = xv(nend)-x
      y2 = yv(nend)-y
      b = x2*x2+y2*y2
      if (b .eq. 0.) then
        angle = pi
                                          return
      endif
      angle = 0.
      do m = nbeg,nend
        x1 = x2
        y1 = y2
        x2 = xv(m)-x
        y2 = yv(m)-y
        a = b
        b = x2*x2+y2*y2
        if (b .eq. 0.) then
          angle = pi
                                          return
        endif
```

```
      arg = (x1*x2+y1*y2)/sqrt(a*b)
      if (arg .gt. 1.) arg = 1.
      if (arg .lt. -1.) arg = -1.
      sgn = sign(1.,x1*y2-x2*y1)
      angle = angle+sgn*acos(arg)
    enddo
                                        return
    end
```

This subroutine, together with the routine *isectang* given above, can be used to compute the percent of ecosystems protected in a grid cell for a given pair of deposition (*depn, deps*); and the following program fragment does exactly that:

```
    .....
    do m = 1,miso
      read (1,*) npnt,(xv(n),yv(n),n=1,npnt)
      xv(npnt+1) = 0.  ! close polygon by
      yv(npnt+1) = 0.  ! adding origin (0,0)
      call inside (depn,deps,xv,yv,1,npnt+1,angle)
      if (abs(angle) .gt. 5.) then ! inside
        if (m .eq. 1) then ! 100% protection
          protper = 100.
        else ! interpolate
          z = sqrt(deps*deps+depn*depn)
          ang = atan2(deps,depn)
          call isectang (xv,yv,npnt,ang,dist)
          call isectang (xold,yold,npnto,ang,disto)
          per = vy(m)-(vy(m)-vy(m-1))*(dist-z)/(dist-disto)
          protper = amax1(100.-per,0.)
        endif
                                        goto 99 ! done for that grid
      else ! store isoline
        npnto = npnt
        do n = 1,npnt
          xold(n) = xv(n)
          yold(n) = yv(n)
        enddo
      endif
    enddo ! go and read next isoline
    protper = 0. ! outside all percentile isolines
99  continue
    .....
```

The do-loop runs over *miso* percentile functions read from a file. The corresponding percentages are stored in the vector *vy*: *vy(1)=0,...,vy(miso)*=100. As soon as two consecutive pre-computed percentile functions are found so that the given point lies inside one and outside the other, the protection percentage is estimated by linearly interpolating between the two *vy*-values using the distances (computed with *isectang*) to the two percentile functions. The program fragment has to be embedded into loops which run over the desired grid cells and do the necessary writing to an output file.

Reference

Press, W.H., S.A. Teukolsky, W.T. Vetterling and B.P. Flannery, 1992. Numerical Recipes in FORTRAN: The Art of Scientific Computing. Second Edition, Cambridge University Press, 963 pp.

Appendix C. *DEIMOS*: CCE's anonymous FTP server

The CCE has an extensive international network of collaborating institutions, and to fulfil its mandate efficient communication is essential. To support this communication the CCE has set up an anonymous FTP server named **deimos.rivm.nl.** It is possible to connect to deimos.rivm.nl from any suitable computer via internet with the File Transfer Protocol (FTP).

To ensure the confidentiality of data bases on the **deimos** server, the CCE has created a directory structure with restricted read and write permissions for every directory (see Figure C-1). For example, a National Focal Center can send revised or updated national critical loads data to the CCE by transferring it to a specific directory created for that country under */pub/cce/incoming*, with restricted read and write permissions (e.g. the Finnish NFC sends its data to */pub/cce/incoming/fi*). The CCE makes its calculation results (files) derived from national contributions available to the NFC on a specific directory for the country branching under */pub/cce/outgoing*, with restricted read and write permissions (e.g. data for the Finnish NFC is on */pub/cce/outgoing/fi*).

Authorized users are given instructions for the use of a "key" that allows for transfer of files from **deimos.rivm.nl** to their site. The server contains one directory (*/pub/cce/world*) without read and write restrictions, which is intended to serve as a "bulletin board" for general information exchange. Announcements, publications, data bases, requests, etc. can be put on it by both the CCE and other users.

Accessing deimos.rivm.nl

Accessing the CCE server requires FTP software and an Internet connection. The section below describes in further detail how to access the server. The style conventions used are the following:

Italics	User-issued commands are in *italics*.
[...]	Optional parts of commands are between square brackets.
< ... >	File-related naming in commands is between angular brackets.
`Courier`	Responses from the CCE server are in `Courier typeface`.

Connecting to deimos.rivm.nl:

To connect to the server, type:

	ftp deimos.rivm.nl	(starts an ftp session and connects with **deimos.rivm.nl**),
or	*ftp* and	(starts an ftp session on your system and establishes a
	open deimos.rivm.nl	connection with deimos.rivm.nl).

If a connection is established, you get a message reading something like:

```
Connected to deimos.rivm.nl.
220 deimos FTP server (Version wu-2.4(3) .............) ready.
```

To log in you will be asked for a name and a password:

`Name:` type *ftp* or *anonymous*

```
331 Guest login ok, send your complete e-mail address as password.
```

`Password:` type your full e-mail address.

Now you will be logged to the root directory of deimos.rivm.nl. It is ready to execute transfers in binary mode:

```
230 Guest login ok, access restrictions apply.
Remote system type is UNIX.
Using binary mode to transfer files.
ftp>
```

/		= Home and root directory.
|		Active: *ls*. Not active: *put*, *get*, etc.
|_pub		= General top directory for RIVM public purposes.
|		Active: *ls*. Not active: *put*, *get*, etc.
|_cce		= Top-level directory of the CCE tree.
|		Active: –. Not active: *put*, *get*, *ls*, etc.
|_world		= Public directory that serves as a "bulletin board".
|		Active: *put*, *get*, *ls*, etc. Not active: –
|_incoming		= Has one subdirectory per nation for incoming NFC files.
| |		Active: –. Not active: *put*, *get*, *ls*, etc.
| |_al	Albania	= National subdirectory where NFC can put confidential national
| |_at	Austria	contributions to the CCE.
| |_ba	Bosnia-Herzegovina	For each country exists one directory with a 2-character code (see below)
| |_be	Belgium	Active: *put*. Not active: *get*, *ls*, etc.
| |		
| *etc.*		
|		
|_outgoing		= Has one subdirectory per nation for outgoing CCE files addressed to
|		a specific NFC (name refers to a 2-character ISO country code)
|		Active: –. Not active: *get*, *put*, *ls*, etc.
|_al		= National subdirectories where NFCs can get confidential
|_at		data from the CCE.
|		Active: *get*. Not active: *put*, *ls*, etc.
etc.		

Figure C-1. Directory structure on the anonymous FTP server deimos.rivm.nl under the directory */pub/cce*. Permission settings for every subdirectory are also indicated.

The 2-character ISO country code names (in lower case) of the subdirectories are:

al = Albania
at = Austria
ba = Bosnia-Herzegovina
be = Belgium
bg = Bulgaria
by = Belarus
ch = Switzerland
cz = Czech Republic
de = Germany
dk = Denmark
ee = Estonia
es = Spain
fi = Finland
fr = France
gr = Greece
hr = Croatia
hu = Hungary
ie = Ireland
it = Italy
li = Liechtenstein
lt = Lithuania
lv = Latvia
md = Republic of Moldova
nl = Netherlands
no = Norway
pl = Poland
pt = Portugal
ro = Romania
ru = Russian Federation
se = Sweden
si = Slovenia
sk = Slovakia
ua = Ukraine
yu = Yugoslavia
uk = United Kingdom

File transfer to deimos.rivm.nl:
To send files with national (confidential) information to the server deimos.rivm.nl, select the relevant national subdirectory under */pub/cce/incoming*, e.g., a Finnish NFC representative would type:
cd pub/cce/incoming/fi (cd= change directory)

The server will return with:
`250 CWD command successful.`
(With the command *pwd* (= present working directory) you can always check the current directory of the FTP server you are in.)

Now the Finnish user can send files to subdirectory */pub/cce/incoming/fi* with the command:
put <file name> [*<file name at deimos.rivm.nl>*]

The server will inform you about the success of the file transfer, with something like:

```
200 PORT command successful.
150 Opening BINARY mode data connection for <file name>.
226 Transfer complete.
15 bytes sent in 0.01 seconds (1.70 Kbytes/s)
```

For security purposes, certain functions have been disabled. For example, no *ls* (list files) and no file transfers from the subdirectories branching under */pub/cce/incoming* is possible. The server does not display the files presently in each directory, and thus prevents the files from unauthorized access. If a *put* command was not executed successfully (e.g. when the file name already exists, due to sending a file with the same name earlier) a new attempt should be made with another file name. Overwriting of an existing file is not possible.

Information intended for all to read should be copied in the same way to */pub/cce/world*, which has no read or write restrictions.)

File transfer from deimos.rivm.nl:
To retrieve files created by the CCE from deimos.rivm.nl, one must select the relevant national subdirectory of */pub/cce/outgoing* with the correct two-character (lower case) country code. For example, a Finnish user would type: *cd pub/cce/outgoing/fi*

To transfer files from the CCE server to your site you use the *get* command. An e-mail message from the CCE will inform the authorized user about the exact names of the files which can be retrieved from the server. In this way, the file name serves as the "key" necessary to retrieve the file from the CCE server with the command:
get <file name at deimos.rivm.nl> [*<file name at your system>*]

The server will inform you about the success of the file transfer:

```
200 PORT command successful.
150 Opening BINARY mode data connection for <file name>.
226 Transfer complete.
15 bytes sent in 0.01 seconds (1.70 Kbytes/s)
```

Terminating the connection with deimos.rivm.nl:
To terminate a connection with the server deimos.rivm.nl type:
close (disconnects from the deimos.rivm.nl server)

To terminate the FTP session on your system use:
bye or *quit* (terminates ftp session)

If you are still connected to the server and type *bye* or *quit*, then both the connection to deimos.rivm.nl and the ftp session will be terminated.

Appendix D: Conversion factors

In this Appendix tables of the most commonly used conversion factors for sulfur and nitrogen deposition as well as for different concentrations are presented.

For convenience we use the term "equivalents" (eq) instead of "moles of charge" (mol_c). If X is an ion with molecular weight M and charge z, then one has:

$$1\ g\ X = \frac{1}{M} molX = \frac{z}{M} eqX \tag{D.1}$$

Obviously, moles and equivalents are the same for z=1. Conversion factors for sulfur and nitrogen deposition are given in the following tables:

Table D-1. Conversion factors for sulfur deposition (g stands for grams of S; M=32, z=2). For conversion multiply by the factors given in the table.

From: / To:	mg/m²	g/m²	kg/ha	mol/m²	eq/m²	eq/ha
mg/m²	1	0.001	0.01	0.00003125	0.0000625	0.625
g/m²	1000	1	10	0.03125	0.0625	625
kg/ha	100	0.1	1	0.003125	0.00625	62.5
mol/m²	32000	32	320	1	2	20000
eq/m²	16000	16	160	0.5	1	10000
eq/ha	1.6	0.0016	0.016	0.00005	0.0001	1

Table D-2. Conversion factors for nitrogen deposition (g stands for grams of N; M=14, z=1). For conversion multiply by the factors given in the table.

From: / To:	mg/m²	g/m²	kg/ha	mol/m²	eq/m²	eq/ha
mg/m²	1	0.001	0.01	0.0000714..	0.0000714..	0.71428..
g/m²	1000	1	10	0.0714..	0.0714..	714.28..
kg/ha	100	0.1	1	0.00714..	0.00714..	71.428..
mol/m²	14000	14	140	1	1	10000
eq/m²	14000	14	140	1	1	10000
eq/ha	1.4	0.0014	0.014	0.0001	0.0001	1

Next, we provide conversion factors for concentrations, more specifically between $\mu g/m^3$ and ppb (parts per billion). One ppb is one particle of a pollutant in one billion ($=10^9$) particles of the air-pollutant mixture. How many (and which mass) of them can be found in one m^3 depends on the density of the air, i.e. on its temperature and pressure; the conversion formula is

$$1\ ppb = \frac{V_0}{M} \mu g/m^3 \tag{D.2}$$

where M is the molecular weight and V_0=0.022414 m^3/mol is the molar volume, i.e. the volume occupied by one mole, at the standard temperature of T_0=273.15K (≈0°C) and the standard pressure of p_0=101.325 kPa (=1 atm). Assuming ideal gas conditions, the conversion for other temperatures and/or pressures can be accomplished by replacing V_0 in Eq. D.2 by

$$V_1 = V_0 \frac{T_1}{T_0} \cdot \frac{p_0}{p_1} \tag{D.3}$$

For example, for T_1=298K (=25°C) and $p_1=p_0$ the molar volume V_1 is 0.024453 m^3/mol.

Table D-3. Conversion factors for concentrations of common pollutants at two different temperatures (1 ppm=1000 ppb).

		From ppb to μg/m³, multiply by:		From μg/m³ to ppb, multiply by:	
	M	*T*=0°C	*T*=25°C	*T*=0°C	*T*=25°C
SO_2	64	2.855..	2.617..	0.350..	0.382..
NO_2	46	2.052..	1.881..	0.487..	0.532..
NH_3	17	0.758..	0.695..	1.318..	1.438..
O_3	48	2.141..	1.963..	0.467..	0.509..

A publication of:

RIVM, NATIONAL INSTITUTE OF PUBLIC HEALTH AND THE ENVIRONMENT
P.O. Box 1, 3720 BA Bilthoven, The Netherlands

1997